SEDIMENTARY PROCESSES AND ENVIRONMENTS IN THE COLUMBIA RIVER ESTUARY

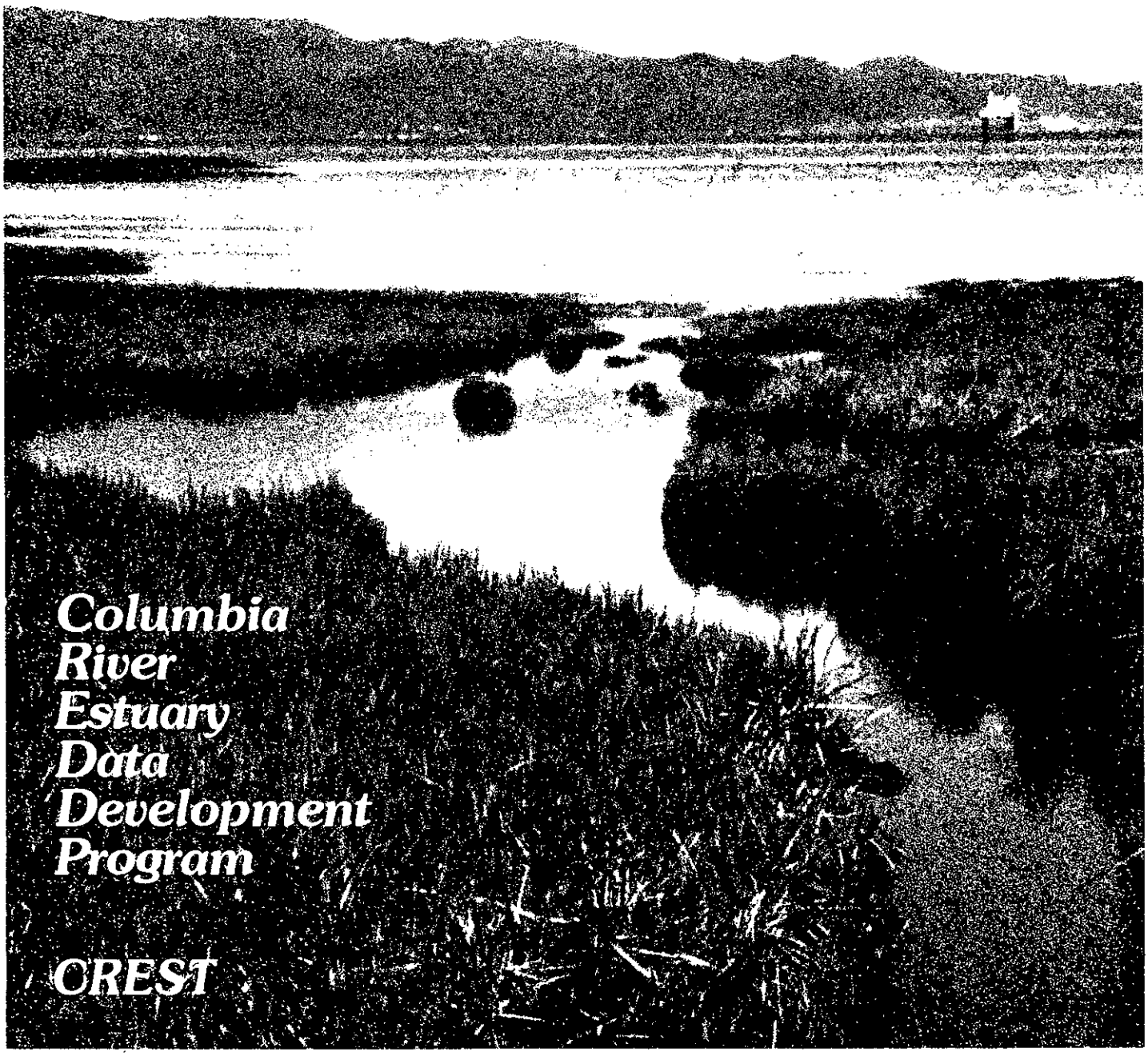

Final Report on the Sedimentation and Shoaling Work Unit

of the Columbia River Estuary Data Development Program

SEDIMENTARY PROCESSES AND ENVIRONMENTS

IN THE

COLUMBIA RIVER ESTUARY

Contractor:

School of Oceanography
University of Washington
Seattle, Washington 98195

Principal Investigator:

Dr. Joe S. Creager
School of Oceanography, WB-10
University of Washington
Seattle, Washington 98195
(206) 543-5099

June 1984

Authors

Christopher R. Sherwood

Joe S. Creager

Edward H. Roy

Guy Gelfenbaum

Thomas Dempsey

PREFACE

The Columbia River Estuary Data Development Program

This document is one of a set of publications and other materials produced by the Columbia River Estuary Data Development Program (CREDDP). CREDDP has two purposes: to increase understanding of the ecology of the Columbia River Estuary and to provide information useful in making land and water use decisions. The program was initiated by local governments and citizens who saw a need for a better information base for use in managing natural resources and in planning for development. In response to these concerns, the Governors of the states of Oregon and Washington requested in 1974 that the Pacific Northwest River Basins Commission (PNRBC) undertake an interdisciplinary ecological study of the estuary. At approximately the same time, local governments and port districts formed the Columbia River Estuary Study Taskforce (CREST) to develop a regional management plan for the estuary.

PNRBC produced a Plan of Study for a six-year, $6.2 million program which was authorized by the U.S. Congress in October 1978. For the next three years PNRBC administered CREDDP and $3.3 million was appropriated for the program. However, PNRBC was abolished as of October 1981, leaving CREDDP in abeyance. At that point, much of the field work had been carried out, but most of the data were not yet analyzed and few of the planned publications had been completed. To avoid wasting the effort that had already been expended, in December 1981 Congress included $1.5 million in the U.S. Water Resources Council (WRC) budget for the orderly completion of CREDDP. The WRC contracted with CREST to evaluate the status of the program and prepare a revised Plan of Study, which was submitted to the WRC in July 1982. In September, after a hiatus of almost one year, CREDDP work was resumed when a cooperative agreement was signed by CREST and the WRC to administer the restructured program and oversee its completion by June 1984. With the dissolution of the WRC in October 1982, the National Oceanic and Atmospheric Administration (NOAA) assumed the role of the WRC as the federal representative in this cooperative agreement.

CREDDP was designed to meet the needs of those groups who were expected to be the principal users of the information being developed. One such group consists of local government officials, planning commissions, CREST, state and federal agencies, permit applicants, and others involved in planning and permitting activities. The other major anticipated user group includes research scientists and educational institutions. For planning purposes, an understanding of the ecology of the estuary is particularly important, and CREDDP has been designed with this in mind. Ecological research focuses on the linkages among different elements in the food web and the influence on the food web of such physical processes as currents, sediment transport and salinity intrusion. Such an ecosystem view of the estuary is necessary to

predict the effects of estuarine alterations on natural resources.

Research was divided into thirteen projects, called work units. Three work units, Emergent Plant Primary Production, Benthic Primary Production, and Water Column Primary Production, dealt with the plant life which, through photosynthesis and uptake of chemical nutrients, forms the base of the estuarine food web. The goals of these work units were to describe and map the productivity and biomass patterns of the estuary's primary producers and to describe the relationship of physical factors to primary producers and their productivity levels.

The higher trophic levels in the estuarine food web were the focus of seven CREDDP work units: Zooplankton and Larval Fish, Benthic Infauna, Epibenthic Organisms, Fish, Avifauna, Wildlife, and Marine Mammals. The goals of these work units were to describe and map the abundance patterns of the invertebrate and vertebrate species and to describe these species' relationships to relevant physical factors.

The other three work units, Sedimentation and Shoaling, Currents, and Simulation, dealt with physical processes. The work unit goals were to characterize and map bottom sediment distribution, to characterize sediment transport, to determine the causes of bathymetric change, and to determine and model circulation patterns, vertical mixing and salinity patterns.

Final reports on all of these thirteen work units have been published. In addition, these results are integrated in a comprehensive synthesis entitled The Dynamics of the Columbia River Estuarine Ecosystem, the purpose of which is to develop a description of the estuary at the ecosystem level of organization. In this document, the physical setting and processes of the estuary are described first. Next, a conceptual model of biological processes is presented, with particular attention to the connections among the components represented by the work unit categories. This model provides the basis for a discussion of relationships between physical and biological processes and among the functional groups of organisms in the estuary. Finally, the estuary is divided into regions according to physical criteria, and selected biological and physical characteristics of the habitat types within each region are described. Historical changes in physical processes are also discussed, as are the ecological consequences of such changes.

Much of the raw data developed by the work unit researchers is collected in a magnetic tape archive established by CREDDP at the U.S. Army Corps of Engineers North Pacific Division Data Processing Center in Portland, Oregon. These data files, which are structured for convenient user access, are described in an Index to CREDDP Data. The index also describes and locates several data sets which were not adaptable to computer storage.

The work unit reports, the synthesis, and the data archive are intended primarily for scientists and for resource managers with a scientific background. However, to fulfill its purposes, CREDDP has developed a set of related materials designed to be useful to a wide

range of people.

Guide to the Use of CREDDP Information highlights the principal findings of the program and demonstrates how this information can be used to assess the consequences of alterations in the estuary. It is intended for citizens, local government officials, and those planners and other professionals whose training is in fields other than the estuary-related sciences. Its purpose is to help nonspecialists use CREDDP information in the planning and permitting processes.

A detailed portrait of the estuary, but one still oriented toward a general readership, is presented in The Columbia River Estuary: Atlas of Physical and Biological Characteristics, about half of which consists of text and illustrations. The other half contains color maps of the estuary interpreting the results of the work units and the ecological synthesis. A separate Bathymetric Atlas of the Columbia River Estuary contains color bathymetric contour maps of three surveys dating from 1935 to 1982 and includes differencing maps illustrating the changes between surveys. CREDDP has also produced unbound maps of the estuary designed to be useful to resource managers, planners and citizens. These black-and-white maps illustrate the most recent (1982) bathymetric data as contours and show intertidal vegetation types as well as important cultural features. They are available in two segments at a scale of 1:50,000 and in nine segments at 1:12,000.

Two historical analyses have been produced. Changes in Columbia River Estuary Habitat Types over the Past Century compares information on the extent and distribution of swamps, marshes, flats, and various water depth regimes a hundred years ago with corresponding recent information and discusses the causes and significance of the changes measured. Columbia's Gateway is a two-volume set of which the first volume is a cultural history of the estuary to 1920 in narrative form with accompanying photographs. The second volume is an unbound, boxed set of maps including 39 reproductions of maps originally published between 1792 and 1915 and six original maps illustrating aspects of the estuary's cultural history.

A two-volume Literature Survey of the Columbia River Estuary (1980) is also available. Organized according to the same categories as the work units, Volume I provides a summary overview of the literature available before CREDDP while Volume II is a complete annotated bibliography.

All of these materials are described more completely in Abstracts of Major CREDDP Publications. This document serves as a quick reference for determining whether and where any particular kind of information can be located among the program's publications and archives. In addition to the abstracts, it includes an annotated bibliography of all annual and interim CREDDP reports, certain CREST documents and maps, and other related materials.

To order any of the above documents or to obtain further information about CREDDP, its publications or its archives, write to CREST, P.O. Box 175, Astoria, Oregon 97103, or call (503) 325-0435.

FOREWORD

The work presented in this report was conducted over several years by personnel of the School of Oceanography at the University of Washington. Many of the conclusions are based on data and ideas generated by graduate students and investigators associated with the program at earlier stages. Much credit is due to Jeff Borgeld and Steve Walter, who made major contributions to the understanding of the sedimentary processes in the estuary, and to Jeannie Barnett and Dick Stewart, who studied the mineralogy.

The field program benefited from the enthusiasm of several graduate students, including Bobbie Rice and Jan Johnson, and could not have been completed without the help and the cooperation of the CREDDP field staff, the Astoria Field Office of the Corps of Engineers, the skippers and mates of the research vessels, and local fishermen and charter skippers. Thanks also to Gary Muelberg of Clatsop Community College and the energetic field assistants he provided. The patience and help of numerous individuals who allowed us to place navigation equipment on their property and/or allowed us temporary mooring facilities is especially appreciated.

Scientific help and advice from several sources is gratefully acknowledged: the U.S. Geological Survey, especially Drs. Hubbell and Glenn; Dr. Mark L. Holmes, Dr. J. D. Smith, and David Jay, all of the University of Washington; and Dave Askren of the Corps of Engineers, Portland District.

Dean McManus provided impetus, guidance, and field assistance. Special recognition is due the technicians who analyzed the sediment samples, including Marcia Campbell, Lee Sims, and Ginger White. Many thanks to Shirley Patterson and Lin Sylwester for assistance in preparing the manuscript.

The manuscript was greatly improved by critical comments of several reviewers, including Mr. Richard Morse of NOAA, Dr. Richard Sternberg of the University of Washington, Dr. Kenneth Schieddegger of Oregon State University, and the CREDDP editorial staff.

In addition to funding provided by the various phases of CREDDP, support for this research was provided by the Corps of Engineers, Portland District, the School of Oceanography, University of Washington, and the TEXACO Fellowship Program.

This research is dedicated to the memory of David Nils Major and the spirit of scientific curiosity that he exemplified.

TABLE OF CONTENTS

		Page
LIST OF FIGURES		xiii
LIST OF TABLES		ixx
EXECUTIVE SUMMARY		ES-1
1.	INTRODUCTION	1
1.1	INTRODUCTION TO THE FINAL REPORT	1
1.1.1	Objectives of the Study	1
1.1.2	Purpose of the Report	2
1.1.3	Structure of the Report	2
1.2	SETTING OF THE COLUMBIA RIVER ESTUARY	3
1.2.1	Plate Tectonics	3
1.2.2	Sea Level	4
1.2.3	Sediment Supply	4
1.2.4	Hydrography	11
1.2.5	Physical Oceanography	12
1.3	PREVIOUS STUDIES	15
2.	METHODS	17
2.1	BOTTOM SEDIMENTS	17
2.1.1	Sampling Plan	17
2.1.2	Grain Size Analysis	18
2.1.3	Mineralogy	22
2.1.4	Statistical Techniques	22
2.2	BEDFORMS AND BOTTOM TOPOGRAPHY	46
2.2.1	Side-scan Sonar	46
2.2.2	Bathymetry	49
2.2.3	Aerial Photographs	50
2.3	SUSPENDED SEDIMENTS	50
2.3.1	Field Measurements	50
2.3.2	Laboratory Analysis	52
3.	RESULTS	53
3.1	BOTTOM SEDIMENTS	53
3.1.1	Factor Analysis	53
3.1.2	R-mode Cluster Analysis	57
3.1.3	Q-mode Cluster Analysis	59
3.1.4	Relationships Among Sediment Parameters	65
3.1.5	Spatial Variability of Grain Size	74

3.2 SUSPENDED SEDIMENTS 94
3.2.1 Texture 94
3.2.2 Transmissivity 94
3.2.3 Nephelometry 97

3.3 BEDFORMS 105
3.3.1 Data Coverage 105
3.3.2 General Bottom Characteristics 105
3.3.3 Seasonal Changes 120

4. DISCUSSION 123

4.1 RELATION OF SEDIMENT TRANSPORT TO FLOW PROPERTIES 123

4.2 SEDIMENT DISTRIBUTION 128
4.2.1 Grain Size Distributions 128
4.2.2 Exploratory Statistics 131
4.2.3 Characterisics of the Overall Grain Size Distributions 133

4.3 SUSPENDED SEDIMENT TRANSPORT 137

4.4 BEDLOAD SEDIMENT TRANSPORT 139
4.4.1 Site-Specific Discussions 141
4.4.2 General Patterns of Bedform Sediment Transport 144

4.5 SYNTHESIS OF OBSERVATIONS 145
4.5.1 Friction Effects 145
4.5.2 Deposition of Fine Sediment 147
4.5.3 Deposition of Coarse Sediments 148
4.5.4 Shoaling Patterns 150
4.5.5 Sedimentary Environments 154

5. CONCLUSION 161

5.1 SUMMARY OF CONCLUSIONS 161

5.2 RECOMMENDATIONS FOR FUTURE WORK 165

LITERATURE CITED 169

APPENDIX A: Bottom Samples in the Columbia River Estuary and Adjacent Continental Shelf 185

APPENDIX B: Summary of Computer Programs Modified or Developed for the CREDDP Program 255

APPENDIX C: Analysis of Historical Changes in the Columbia River Estuary 267

LIST OF FIGURES

		Page
1.	The Columbia River Estuary (commonly mentioned locations)	5
2.	Bathymetry of the Columbia River Estuary	8
3.	Drainage basin of the Columbia River	10
4.	Discharge of the Columbia River Estuary and study periods	14
5.	Transects sampled during the baseline and seasonal sampling schemes	19
6.	Size class distributions of unrotated theoretical factors	26
7.	Size class distribution of rotated theoretical factors	27
8.	Size class distributions of final factors (end-members) after oblique rotation	28
9.	Dendrogram (a) and grain size distributions of clusters (b), Set 1, October 1979	32 33
10.	Dendrogram (a) and grain size distributions of clusters (b), Set 2, October 1979	34 35
11.	Dendrogram (a) and grain size distributions of clusters (b), Set 3, October 1979	36 37
12.	Dendrogram (a) and grain size distributions of clusters (b), Set 1, February 1980	38 39
13.	Dendrogram (a) and grain size distributions of clusters (b), Set 2, February 1980	40 41
14.	Dendrogram (a) and grain size distributions of clusters (b), Set 1, June, 1980	42 43
15.	Dendrogram (a) and grain size distributions of clusters (b), Set 2, June 1980	44 45
16.	Tracklines run with side-scan sonar	47
17.	Locations of nephelometer stations and bridge-mounted transmissometer	51

18. Relative importance of each of 6, 8, and 10 factors in explaining 125 samples collected in October 1979 from between Harrington Point and the Astoria-Megler Bridge 56

19. Relative importance of each of the standard clusters (from all three seasons) 58

20. Cumulative sediment distribution curves of standard clusters (1 to 6) for the three seasons plotted separately (a, b, and c) and together (d) 60

21. Generalized distribution of standard clusters in October 1979 62

22. Generalized distribution of standard clusters in June 1980 63

23. Relationship between standard deviation and mean grain size for three seasons 66

24. Plots of skewness and kurtosis versus mean (a and b), and standard deviation and kurtosis versus skewness (c and d) for all October 1979 samples 67

25. Plots of skewness and kurtosis versus mean (a and b), and standard deviation and kurtosis versus skewness (c and d) for all February 1980 samples 68

26. Plots of skewness and kurtosis versus mean (a and b), and standard deviation and kurtosis versus skewness (c and d) for all June 1980 samples 69

27. Passega diagrams 72

28. Passega diagrams and C-M fields associated with river mile location of samples 73

29. Mean and standard deviation (sorting) versus depth for all three seasons 75

30. Variation of mean grain size with depth for four river mile intervals and three seasons 78

31. Mean and standard deviation (sorting) versus river mile for all samples from three seasons 79

32. Mean grain size and standard deviation (sorting) versus river mile for channel samples (>30 ft) during three seasons 80

33a. Average mean grain size of samples from four river mile intervals and three seasons 82

33b. Average phi size of the coarsest one-percentile from four river mile intervals and three seasons 82

34. Variation of average mean grain size with river mile, for four depth intervals and three seasons 84

35. Generalized sediment distribution map for October 1979 and seasonal fall samples 88

36. Generalized sediment distribution map for February 1980 and seasonal winter samples 89

37. Generalized sediment distribution map for June 1980 and seasonal spring samples 90

38. Generalized silt plus clay distribution including all samples 93

39. Size frequency of two suspended sediment samples from station 11 95

40. Time series of depth-averaged suspended sediment concentrations obtained from profiling nephelometer station 2N, the farthest seaward station, and for station 11, the farthest landward station 96

41. Time series of speed, salinity, and transmissivity obtained from the bridge-mounted instrument array between 4 July and 23 August 1980 98

42. Time series of depth-averaged suspended sediment concentrations for stations 6S and 4S; the central part of the estuary 99

43. Schematic representation of semidiurnal tidal excursion of the turbidity maximum 100

44. Time series of bottom salinity and depth-averaged suspended sediment concentrations for station 6S during a spring tide 103

45. Time series of bottom salinity and depth-averaged suspended sediment concentrations for station 6S during a neap tide 104

46. Bedform distribution based on side-scan sonar information obtained in September 1979 and October 1980 107

47. Bedform distribution based on side-scan sonar information obtained in February 1980 108

48. Bedform distribution based on side-scan sonar information obtained in June 1980 109

49. Side-scan sonar and echo-sounder records of large-scale, seaward-oriented bedforms in the fluvially-dominated upper estuary (vicinity of Rice Island) 111

50. Side-scan sonar and echo-sounder records of small-scale, reversing bedforms in the tidally-dominated lower estuary (vicinity of Jetty A) 112

51. Side-scan sonar and echo-sounder records of landward-oriented bedforms generated by estuarine circulation in the North Channel (near Chinook) 114

52. Schematic diagram of depth-related bedform orientation reversals 115

53. Side-scan sonar and echo-sounder records of bedforms whose orientation reverses with depth from the navigation channel (near Flavel Bar) 116

54. Plot of bedform orientation reversal depth against River Mile 118

55. Side-scan sonar and echo-sounder records of dredge furrows in the navigation channel (Flavel Bar) 119

56. Schematic representation of the seasonal variation in the landward limit of landward-oriented bedforms for the high discharge season (June) and the low discharge season (October) 121

57. Side-scan sonar and echo-sounder records of differential erosion of exposed strata along the south flank of the North Channel 136

58. Sedimentation patterns based on bedform sediment transport 143

59. Comparative morphology of shoals and islands
a) Components of the Hayes (1975) model of a mesotidal flood-tidal delta 152

b) Schematic of Desdemona Sands and components of a flood-tidal delta 152

c) Schematic of Taylor Sands and components of a flood-tidal delta with fluvial influence 153

d) Schematic of a vegetated fluvial island and components 153

60a. Overview of sedimentary environments in the Columbia River Estuary 156

60b. Dominant influences on sedimentation and erosion 157

61. CREDDP bottom sample locations, October 1979 191

62. CREDDP bottom sample locations, October 1979 192

63. CREDDP bottom sample locations, February 1980 205

64. CREDDP bottom sample locations, February 1980 206

65. CREDDP bottom sample location, June 1980 216

66. CREDDP bottom sample location, June 1980 217

67. Seasonal fall bottom sample locations 227

68. Seasonal winter bottom sample locations 233

69. Seasonal spring bottom sample locations 237

70. CREDDP bottom sample locations, October 1980 (not analyzed) 243

71. CREDDP bottom sample locations, October 1980 (not analyzed) 244

72. System flowchart of computer programs used in the CREDDP study 258

73. Map of the Columbia River Estuary showing 13 subareas used in volume and area calculations 279

74. Map of the Columbia River Estuary showing the "normal" surveyed area (m^2 10^6) in each of the 13 subareas during the 1958 survey period 285

75. Hypsometric curve relating cumulative surface area with depth in the entrance region for 1868, 1935, and 1958 300

76. Hypsometric curve relating cumulative surface area with depth in the South Channel in 1868, 1935, and 1958 301

77. Hypsometric curve relating cumulative surface area to depth for the estuary as a whole and several subareas in 1868 and 1958 304

78. Hypsometric curve relating cumulative surface area to depth in the upper river channel in 1868, 1935, and 1958 305

79. Hypsometric curve relating cumulative surface area to depth in Cathlamet Bay in 1868, 1935, 1958 306

80a. Map of the Columbia River Estuary showing the rates of shoaling (+) or erosion (-) (cm/yr) in each of the 13 subareas for 1868-1935. Rates are normalized by the 1958 area 312

80b. Map of the Columbia River Estuary showing the rates of shoaling (+) or erosion (-) (cm yr^{-1}) in each of the 13 subareas for 1935-1958 313

80c. Map of the Columbia River Estuary showing the rates of shoaling (+) or erosion (-) (cm yr^{-1}) in each of the 13 subareas for the entire period (1868-1958) 314

LIST OF TABLES

		Page
1.	River discharge summary for the study period and the preceding ten years	13
2.	Summary of sediment grain size descriptions	20
3.	Collection periods for CREDDP side-scan sonar data and freshwater discharge at Astoria	48
4.	Summary of seasonal factor analysis results	54
5.	Standard clusters chosen to represent 7 sets of 200 samples	59
6.	Summary of results of sediment grain size differences between crests and troughs of large-scale bedforms	110
7.	Man's major influences on the Columbia River Estuary	126
8.	Comparison of suspended sediment concentration range over several time scales	138
9.	Summary of bottom sample data collection	189
10.	October 1979 bottom sample locations	193
11.	February 1980 bottom sample locations	207
12.	June 1980 bottom sample locations	218
13.	Seasonal fall bottom sample locations	228
14.	Seasonal winter bottom sample locations	234
15.	Seasonal spring bottom sample locations	238
16.	October 1980 bottom sample locations	245
17.	Chronology of important events affecting the physical evolution of the Columbia River Estuary	271
18.	Depth intervals used in area calculations	281
19.	Areas, volumes, volume changes, and area changes by depth regime for 1868, 1935, and 1958	283
20.	Areas, volumes, volume changes, and area changes by depth regime for 1868, 1935, and 1958	284

21. Area and area changes by depth regime in the Upper River Channel 286

22. Area and area changes by depth regime in the Entrance 287

23. Area and area changes by depth regime in Cathlamet Bay 288

24. Area and area changes by depth regime in Youngs Bay 289

25. Area and area changes by depth regime in Baker Bay 290

26. Area and area changes by depth regime in Brix Bay 291

27. Area and area changes by depth regime in the South Channel 292

28. Area and area changes by depth regime in the Lower River Channel 293

29. Area and area changes by depth regime in Desdemona Sands 294

30. Area and area changes by depth regime in Grays Bay 295

31. Area and area changes by depth regime in the North Channel 296

32. Area and area changes by depth regime in the Mid-Estuary Shoals 297

33. Area and area changes by depth regime in Trestle Bay 298

34. Volumes, volume changes, and sedimentation by subarea 307

35. Shoaling rates 311

36. Comparison of shoaling rates and estimated time required to fill the estuary 317

EXECUTIVE SUMMARY

This report summarizes the results of several years of research into the sedimentology of the Columbia River Estuary. Two major objectives were attained during the study: 1) the sedimentology of the estuary was investigated and described, and 2) some understanding was gained of the processes important to sedimentation.

As an introduction to the present study, background information on the tectonic, geologic, and oceanographic settings of the estuary are provided, as well as a brief listing of previous sedimentological studies performed in the estuary. The changes in relative sea level, the hydrography of the Columbia River, and the sources of sediments available to the system are considered because of their influence on the sedimentology of the estuary.

Several methods were utilized in the investigations of both processes and distributions in the estuary. A very large suite of sediment samples was obtained over the entire estuary during three distinct river discharge seasons (fall, winter, and spring). These samples were analyzed to determine their grain size distributions and some aspects of their mineralogy. Several approaches, both statistical and graphical, were taken in an effort to interpret the distributions. Information on the morphology of the estuary bottom was obtained using a side-scan sonar over various tidal stages during all three seasons. Suspended sediment processes were monitored with both fixed transmissometers and profiling nephelometers which were calibrated with physical samples of suspended sediments. An analysis of the historical changes in bathymetry of the estuary, including volumes and rates of sediment accumulation were performed using digitized bathymetry data provided by Northwest Cartography, Inc. (CREDDP, 1983). Several other sources of data were incorporated into the final interpretations, including recent bathymetry and aerial photographs.

The data served to emphasize the spatial and temporal variability of processes and sedimentary environments in the estuary. The tidal current, ocean waves, and river currents are energetic compared to most well-studied estuaries. Although the ultimate source of most of the sediment found in the estuary is the Columbia River, much of the sediment has been reworked within the estuary and on the adjacent continental shelf, resulting in a range of grain-size distributions within the estuary. Overall, the estuary floor is comprised of fine sand; deposits of gravel are rare and restricted to areas of extreme scour, while deposits of silt and clay are mostly confined to peripheral bays and inactive channels. Much of the sediment is of a size that is tranported intermittently as suspended sediment under high tidal currents but moves regularly as bedload. As a

result, the grain size distributions in the estuary depend on daily, spring-neap, seasonal, and catastrophic current events as well as sediment supply.

In general, the sediments in the estuary show a greater variance among samples and are finer and more poorly sorted than the river sediments. Sediments on the continental shelf immediately seaward of the entrance are much better sorted than the estuary sediments and slightly finer. The variance among estuary sediments is attributed to the variety of sedimentary environments and range of active processes within the estuary.

The importance of bedload and intermittently suspended load transport in the estuary is emphasized by the ubiquitous bedforms. The bedform distribution allows the integrated effect of variable transport rates to be observed. Bedform distributions in the Columbia River estuary indicate that tidally-reversing bedload transport occurs at depth in the entrance region, but that density-driven circulation influences the tidal transport sufficiently to cause net landward transport as far upstream as the Port of Astoria in the major channels. Bedform studies also indicate that fluvial processes dominate landward of Tongue Point, and that sediment transport rates and pathways vary with neap-spring and seasonal circulation changes.

The study of suspended sediment processes and the distribution of fine sediment suggest that a turbidity maximum exists in the Columbia River Estuary; the turbidity maximum contains high concentrations of suspended sediment, it is advected with diurnal tidal currents, and it changes character in response to neap-spring and seasonal current changes. Much of the sediment suspended in the turbidity maximum is re-suspended bottom material. Ephemeral fine deposits are the result of deposition beneath the turbidity maximum during the waning phases of a spring tide, but most of the suspended sediment in the estuary is either flushed out into the Pacific Ocean or transported to and deposited in one of the peripheral bays. As a result, silt and clay are volumetrically less important than sand in the estuary sediments, and estuarine sedimentation is most closely associated with deposition of bedload material. Thus the long-term shoaling of the estuary is a result of horizontal accretion of bedform and point-bar deposits during channel migration, rather than vertical accretion of fine sediment deposited from suspension.

The construction of jetties has had a profound effect on the sedimentology of the estuary, resulting in rapid accumulation of sediments in the estuary and a temporarily increased supply of sediment to the longshore transport system. The estuary is shoaling at an average rate of

0.5 cm yr^{-1}. Various lines of evidence indicate that it effectively traps the entire fluvial supply of bedload sediment but retains less than 20% of the suspended sediment.

The CREDDP studies have provided a substantial data base for this highly dynamic system, and valuable insight into the processes and their implications has resulted. Future work will be able to draw on these data and expand on these conclusions.

1. INTRODUCTION

1.1 INTRODUCTION TO THE FINAL REPORT

1.1.1 Objectives of the Study

The primary objective of this study was to attain an understanding of the processes of sediment erosion, transportation, and deposition in the Columbia River Estuary and of their importance relative to the variety of temporal and spatial scales found in the estuary. To accomplish this objective, data collected during the initial phases of the Columbia River Estuary Data Development Program (CREDDP) have been analyzed and interpeted. The field data contain: 1) a spectrum of information pertaining to the physical parameters that influence sedimentological processes, 2) measurements of the processes themselves over various space and time scales, and 3) measurements of the resultant products and their distributions. The latter data, which include sediment grain size analyses and patterns of bedform distribution, are used to evaluate the importance of sedimentation processes and their time scales.

Additional sediment size analyses were carried out to provide a higher sample density in the most complex reach of the estuary. A number of exploratory statistical techniques were developed and applied to the interpretation of the sediment size information, and the results of these approaches were integrated with the results obtained from detailed examination of the distribution of the sediment size and sediment size parameters. Conclusions and hypotheses regarding the behavior of bedforms and suspended sediment, developed during earlier stages of the study, were then incorporated with morphological evidence in such a way as to obtain a complete synthesis linking the sediment transport processes with products. Areas in which particular processes are dominant were identified as sedimentary environments and mapped, providing users some qualitative predictions regarding the physical parameters and dynamics occurring in these sub-areas. Examination of historical bathymetric changes provided a longer-term perspective on the importance of the various processes and on the distribution of their products.

A second important objective of the study was to provide a characterization of the present geological conditions in the estuary. It was intended that this goal be met by presenting the original data as well as several levels of interpretation.

Finally, this study, in conjunction with those provided by the CREDDP physical oceanography researchers, is intended to provide a data base and some overall understanding of the

physical processes operating in this and similar estuaries to aid in the development of research and management proposals in the future.

1.1.2 Purpose of the Report

The purpose of this report is to disseminate the findings of these studies and discuss their implications relative to the understanding the Columbia River Estuary. Furthermore, this report is intended to provide access to the data collected during the CREDDP studies as well as a scientific interpretation of the data. It is hoped that, in addition to providing the reader with more detailed knowledge regarding the sedimentology of the Columbia River Estuary, this report will allow comparisons to be made between this estuary and other estuaries that have been studied around the world.

1.1.3 Structure of the Report

The remainder of the Introduction provides a physical background in which to examine the sedimentology of the estuary. The geologic setting is described, and the important sources of sediment and energy for the estuarine processes are briefly discussed. The final part of the Introduction discusses the work accomplished by previous researchers in this estuary.

The Methods section presents the procedures used in the collection, analysis, and, to some extent, the interpretation of the data. The techniques used to detect errors and/or estimations of the error involved with each step of the procedures are included when appropriate. When standard techniques and procedures are used, reference to the acknowledged source is provided. The Methods section is organized according to the phenomenon being investigated; it includes the procedures used in collection and analyses of data of the following phenomena: 1) bottom sediments, including aspects of their grain size and mineralogy, 2) bedforms and large-scale bottom topography, and 3) suspended sediments.

The data obtained using these procedures are presented in the Results section, which is organized to correspond with the Methods section. Some results are introduced that were not obtained from data collected during this study, but were provided by earlier workers or other CREDDP work unit researchers. These data are referenced to enable the reader to access the data directly.

The Discussion draws together the evidence found as results and follows the evolution of a general model of sedimentary processes in the Columbia River Estuary. The Conclusion reiterates the important findings of the study

and summarizes the processes and time scales that dominate sedimentation in the estuary.

Three appendices contain additional data and results. Appendix A is a listing of the location, depth and mean grain size of the sediment samples obtained during this and previous studies in the estuary. Appendix B presents a brief description of the computer programs developed during the CREDDP work for the determination of grain-size statistics and analysis of the data. Appendix C relates the methods, results, and conclusions of an analysis of the historical shoaling trends in the estuary. The data base used for this work was a digital compilation of the bathymetric data from several surveys conducted over several years around 1868, 1935, and 1982 (CREDDP 1983; Northwest Cartography, Inc. 1984). The three appendices contain data, methods, and discussions that are important to the overall conclusions drawn in the main body of the report, but are separated from the main report due to their length and detail.

1.2 SETTING OF THE COLUMBIA RIVER ESTUARY

1.2.1 Plate Tectonics

The Pacific coast of the northwestern United States is located on an active continental margin. The North American plate of continental crust is overriding the Juan de Fuca plate, a portion of relatively young ocean floor that is currently forming along the Gorda and Juan de Fuca ocean ridges (Atwater 1970; McKee 1972). The subduction of the seafloor is associated with the eruptions of the andesite volcanoes of the Cascade Range, the emplacement of dioritic plutons, and with a tilting of the continental crust. The result is an uplift of the continental shelf and coastal regions of Oregon and Washington and a downwarp of interior regions along a linear lowland trough, which includes Puget Sound, parts of the Chehalis Valley, and the Willamette Valley. Minor, deep-focus earthquakes occur along the subduction zone, but these are notably less severe than those found along similar structures elsewhere in the world (Ando and Balazas 1979).

Repeated cycles of plate collision, subduction, uplift, and erosion have produced the complex and rugged terrain of the Cordillera (McKee 1972). This relatively young tectonic province contains a wide variety of geologic terranes and has changed rapidly in the last several million years. The tectonic regime exerts both direct and indirect influences on the physical processes within the estuary, and exerts ultimate control over estuarine sedimentation on a geologic

time scale. The interaction of the subducting ocean plate and the continental margin have determined the large scale topography of the ocean basin, continental slope and shelf, and the continental uplands. This topography influences oceanographic, atmospheric, and hydrologic processes in and around the estuary. More directly, tectonic control of uplift and volcanism regulates sediment supply to the estuary, and crustal movements determine, in part, changes in local sea level.

1.2.2 Sea Level

Average sea level around the United States, as measured from tide gauges, has been rising at a rate of approximately 1.5 mm yr^{-1} since 1940 (Hicks 1978). Apparently this is a continuation of a trend associated with the melting of glaciers following the last Pleistocene glaciation which ended about 9,000 years ago. Geologic evidence suggests that since then, sea level rose worldwide at a relatively rapid rate of 5 to 7 mm yr^{-1}, but subsequently slowed to the present rate of 1 to 2 mm yr^{-1} about 5000 years ago (Kraft 1971). Glenn (1978) reports radiocarbon dates in a core from Tillamook Bay that suggest similar rates for coastal Oregon. The Columbia River Estuary (Figures 1 and 2) occupies a river valley incised into Tertiary bedrock during a previous episode of lowered sea level which has since been inundated by the sea level rise.

However, sea level has not continued to rise along the Oregon-Washington coast adjacent to the estuary in recent times. The tectonic uplift of the coastal regions is resulting in a lowering of relative sea level along the western United States north of Cape Mendocino (Hicks 1972). Geodetic leveling data from 1904 to 1974 and tide gauge data from 1946 to 1974 both suggest that relative sea level in Astoria has been falling since the turn of the century at rates of 2 to 5 mm yr^{-1} (Ando and Balazas 1979; Chelton and Davis 1982).

1.2.3 Sediment Supply

The Columbia River is responsible for almost all of the sediment supplied to the estuarine system. The river drains 667,000 square kilometers of geologically varied terrain which includes igneous, sedimentary, and metamorphic rocks and extensive alluvial and eolian surficial deposits (Whetten et al. 1969; Figure 3). Estimates of the total suspended load of the river vary from 7 to 30 million tons per year (Van Winkle 1914a,b; Judson and Ritter 1964; Haushild et al. 1966) and a generally accepted value is 10 million tons per year. Bedload supply is estimated at about 10% of this value, or one million tons per year (Whetten et al. 1969).

Columbia River Estuary

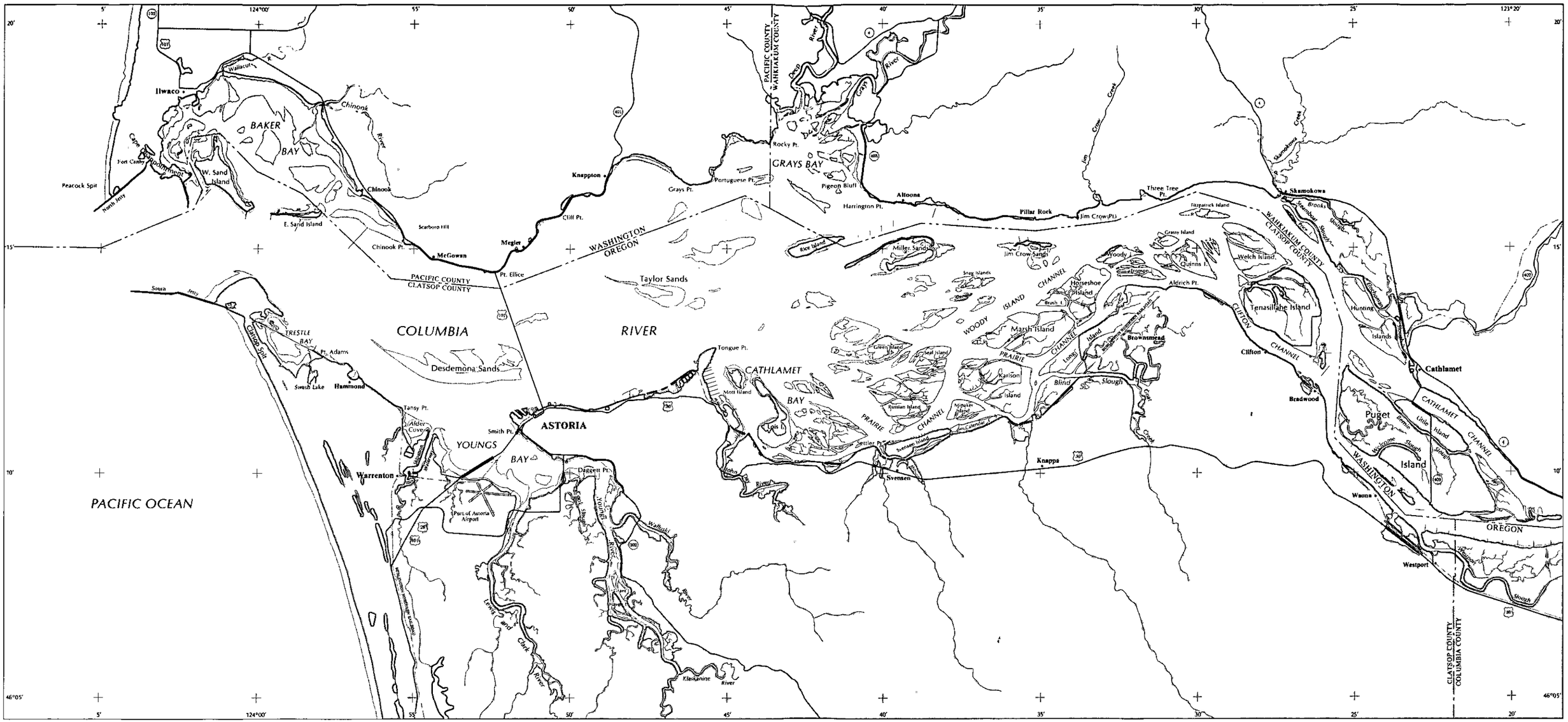

Scale 1:160,000

0 1 2 3 4 5 6 7 8 9 10 Kilometers

0 1 2 3 4 5 6 Miles

Map produced in 1983 by Northwest Cartography, Inc.
for the Columbia River Estuary Data Development Program

- Shoreline (limit of non-aquatic vegetation)
- Intertidal vegetation
- Shoals and flats
- Lakes, rivers, other non-tidal water features
- Major highways
- Megler Cities, towns
- Railroads
- Other cultural features

Figure 1. Columbia River Estuary

The sediments trapped behind upriver reservoirs reflect the plutonic, volcanic, and metamorphic source rocks and the extensive loess deposits found in eastern Washington and the drainage basin of the Snake River (a major tributary). The dominant minerals in these sediments are quartz and feldspars; the dominant heavy mineral is hornblende. Metamorphic and plutonic rock fragments are also common. The sediments in the lower reaches of the Columbia River reflect the contribution of andesite volcanic materials from the tributaries draining the western slopes of the Cascades. Downriver, the sediments contain increasing amounts of plagioclase and volcanic rock fragments and decreasing percentages of quartz and potassium. Hypersthene becomes the dominant heavy mineral in the lower reaches (Kelley and Whetten 1969; Whetten et al. 1969). The overall composition of the sediment in the lower Columbia River resembles graywacke, and may provide a modern example of the source of ancient graywackes (Whetten 1966).

Volcanism in the Cascade Range may be responsible for an important fraction of the sediment input. The 1980 eruption of Mt. St. Helens and the subsequent debris flow down the Toutle-Cowlitz Rivers and into the Columbia River at Longview provide models for the intermittent and substantial supply of sediment to the estuary. In the absence of human interaction, an eruption of Mt. St. Helens, Mt. Hood, Mt. Adams, or other andesite volcano might be expected to provide airborne ash, an almost immediate influx of suspended sediment, and a longer term supply of coarser material. Although cataclysmic in human terms, over geologic time these major eruptions represent a relatively constant supply of sediment to the Columbia River system. The mineralogy of the estuarine sediments, and especially the volcanic rock fragments, pumice, and glass-mantled grains found in the estuary subsequent to the Mt. St. Helens eruption (Roy et al., 1982) point to the importance of the volcanic contribution to the estuarine sediments.

Marine sediments found adjacent to the Columbia River are similar in composition to the river sediments. Two reasons for this similarity exist: 1) most of the sediments found on the beaches of Washington and the continental shelves of northern Oregon and Washington are derived from the Columbia River drainage system, and 2) the sediment supplied to the Oregon continental shelf from numerous small rivers and coastal erosion is derived from comparable volcanic rocks and sediments (Hodge 1934; Runge 1966; White 1967, 1970; Scheidegger et al. 1971; Nittrouer 1978). Scheidegger et al. (1971) used subtle differences in the composition of the heavy mineral fraction to trace the sediments originating in the Klamath and Siskiyou Mountains, the coast range of Oregon, and the Pleistocene terrace deposits of Oregon on the continental shelf. They reached the conclusion that sediment generally moves northward along

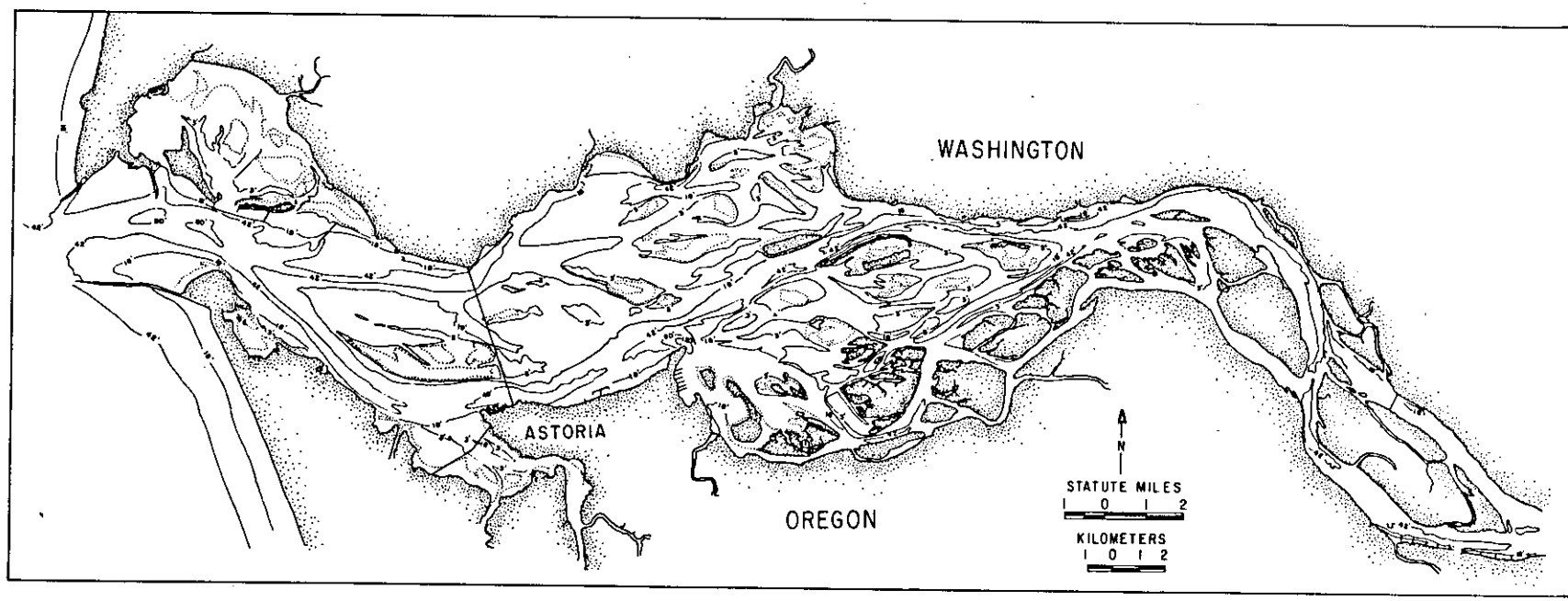

Figure 2. Bathymetry of the Columbia River Estuary (after CREDDP, 1983, and Northwest Cartography, Inc., 1984).

the Oregon shelf and that transport rates may have been higher in the past when sea level was lower. Several other lines of evidence also suggest that although seasonal changes occur, littoral drift and the net transport direction along the beaches and continental shelf of Oregon and Washington is northward (Hopkins 1971; Barnes et al. 1972; Smith and Hopkins 1972; Sternberg and McManus 1972).

Several lines of evidence suggest that some of the sediments in the estuary have been recently transported into the estuary from the adjacent nearshore and shelf regions. Current meter studies have documented landward flow predominance in the deeper portions of the entrance channels (U.S. Army Corps of Engineers 1933; Lockett and Kidby 1961; Jay 1984), and various physical and numerical models indicate net landward bottom flow and sediment transport through the entrance under low and moderate discharge conditions (O'Brien 1936; Herrmann 1968; Hamilton 1983, 1984; McAnally et al. 1983a,b). Morse et al. (1968) used seabed drifters to demonstrate that marine sediments could be transported into the estuary, and Walter (1980; Walter et al. 1979) used a distinctive lamellar pyroxene as a mineral tracer of coastal sediment transported into the estuary. Lockett (1967) used sediment size evidence to argue that positively skewed fine sand has been transported into the estuary.

Additional sediment sources include local tributaries, erosion of older deposits within the estuary, and windblown transport. Cooper (1958, 1959) provides a discussion of the dune development on the prograding beach of Clatsop Spit following jetty construction. Hodge (1934) and O'Brien (1936) were concerned with eolian erosion and transport of beach sand into the estuary. O'Brien argued that wind transport to the NNE occurred at an average rate of 177-402 kg $m^{-1}day^{-1}$ (120-270 lbs $ft^{-1}day^{-1}$) on the exposed and unvegetated portions of Clatsop Spit. Those rates, over a cross-section of 4 km, would provide more than a million cubic meters of sediment to the estuary each year, exceeding the average shoaling rate of Trestle Bay (see Appendix C) by a factor of 8. Roy et al. (1982) examined sand grains from Clatsop Spit dunes with a scanning electron microscope and found that the grains were surprisingly fresh and displayed little of the characteristic pitting commonly associated with dune sands (Krinsly and Donahue 1968). The sand dunes were largely stabilized during revegetation efforts by the Soil Conservation District in 1935 (McLoughlin andBrown 1942) and eolian transport is probably less important now than in the period following jetty construction. Furthermore, eolian supply of volcanic ash occurred following one of the Mt. St. Helens eruptions in 1980, but resulted in an insignificant deposit of sediment over the estuary. Although it is difficult to quantify the importance of eolian transport within the system, it is not believed to be

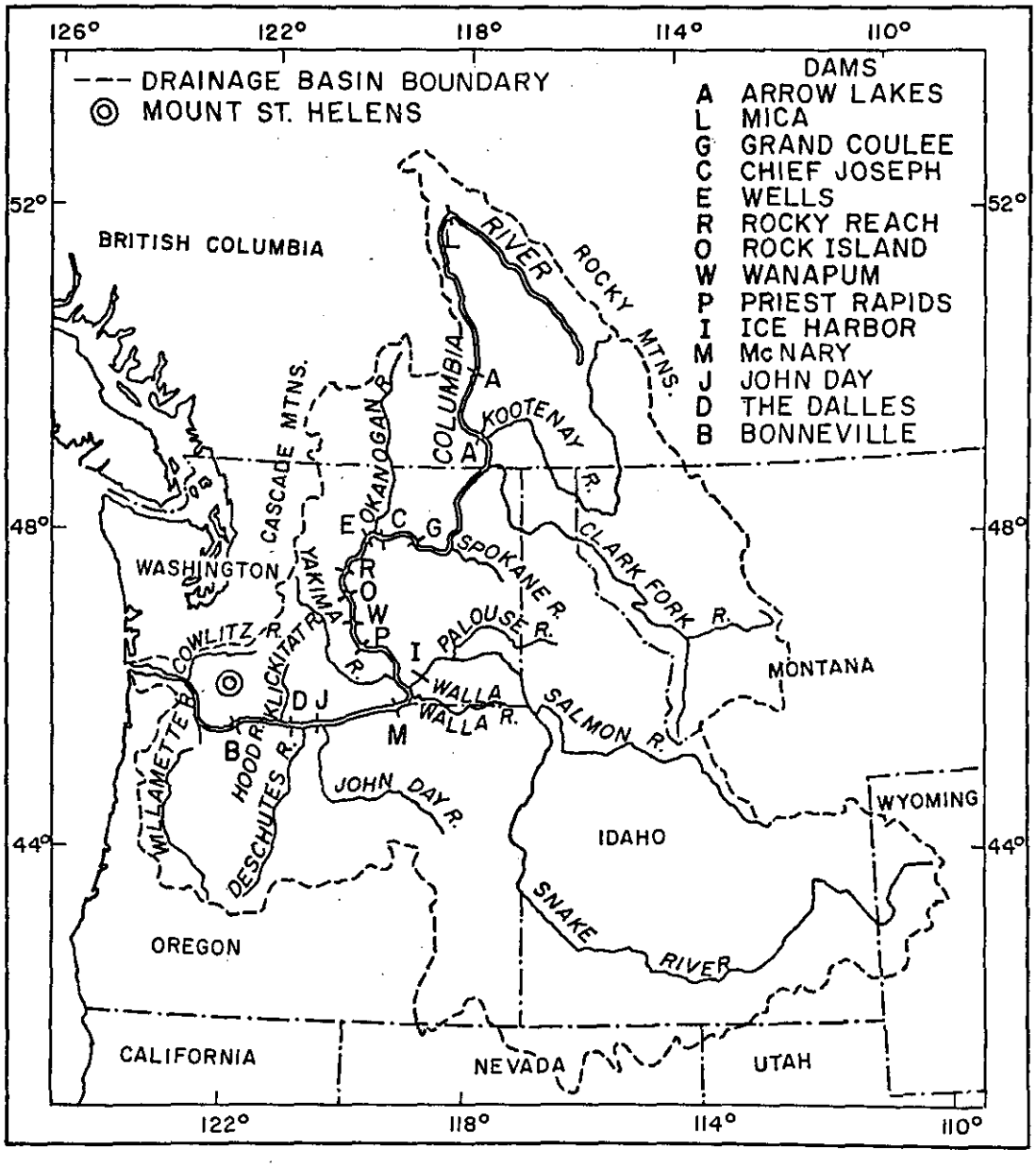

Figure 3. Drainage basin of the Columbia River.

a major process in the redistribution of estuary sediments.

Erosion of the estuarine shoreline has been identified as a sediment source in other northwest estuaries, including Tillamook Bay (Glenn 1978) and Willapa Bay (Clifton 1983), but in both instances it was not considered a primary sediment source. Some of the rocky headlands in the Columbia River estuary are eroding and contributing talus to the estuary, but the Tertiary bedrock does not appear to erode rapidly nor contribute significantly to the volume of estuarine sediments. Erosion of younger (Pleistocene and Holocene) estuarine and fluvial deposits from within the river valley may represent a more important source but is still thought to be minor relative to the upriver fluvial supply. Most of the other estuaries that have been studied along the Oregon-Washington coast have as their sediment sources some combination of either fluvial or marine sediments (Kulm et al. 1968; Boggs and Mones 1976; Scheidegger and Phipps 1976; Glenn 1978; Clifton and Phillips 1980; Peterson et al. 1982; Peterson et al. 1984), and the Colubmia River appears to exhibit similar characteristics.

Sediment from local tributaries may be a locally important source near the entrance to these rivers. Workers at Oregon State University have suggested that most of the sediment in the upper reaches of Youngs Bay are derived from erosion of Oligocene-Miocene sedimentary rocks in the drainages of the Youngs, Walluski, and Lewis and Clark Rivers (Slotta 1975). It is likely that similar situations occur in the lower reaches of the Grays River, Elochoman River, and Skomokawa Creek, but the contribution of these tributaries to the overall sediment budget is expected to be minimal. In summary, sediment sources other than the Columbia River and the adjacent marine environment are believed to be quantitatively much less important to the sedimentology of the estuary.

1.2.4 Hydrography

The Columbia River is the largest river on the Pacific coast of North America and has an average discharge of approximately 260,000 cubic feet per second (cfs), or 7,360 m^3s^{-1} (Jay 1984). Discharge varies seasonally; precipitation in the Cascade and Coast Ranges creates periodic winter freshets from November to March and a spring freshet caused by snowmelt in the upper reaches of the drainage basin occurs from April to July. The hydrographic curve has been damped by the construction of dams along both the main stem of the Columbia River and along many tributaries. Diversion for irrigation and long term climactic changes have historically altered the flow regime in the estuary (Jay 1984; Simenstad et al. 1984). The modern hydrographic curve exhibits attenuated peak discharges and

increased discharge during low-flow periods. Before flow regulation, the highest recorded discharge occurred during the flood of 1894 (1.2 million cfs, 33,980 m^3s^{-1}) and the record low monthly mean flow was 65,000 cfs (1,840 m^3s^{-1}; Neal 1972). Average discharge during a ten-year period beginning in 1970 was 239,000 cfs (6,770 m^3s^{-1}), with an average high discharge of 613,000 cfs (17,360 m^3s^{-1}) and an average low discharge of 89,400 cfs (2,530 m^3s^{-1}) (Table 1). The discharge during this study is shown in Figure 4.

1.2.5 Physical Oceanography

The tides along the Pacific coast are mixed semi-diurnal. The mean tidal range at Astoria is 6.5 ft (2.0 m) and the mean greater diurnal range is 8.5 ft (2.6 m) (Neal 1972). Spring-neap variations during parts of the study period resulted in maximum daily semi-diurnal ranges of 5.6 ft (1.7 m) during neap tides and 11 ft (3.4 m) during spring tides (Gelfenbaum 1983). River discharge acts to suppress the tidal range and raise the water level at upriver tide gauges (Jay 1984). Tidal effects are observed upriver as far as the Bonneville Dam (140 statute miles, 225 km) during low flow periods. Tidal currents can cause flow reversals as far as 53 statute miles (85 km) upriver from the entrance. In the estuary, tidal currents exceed 10 feet per second (fps, 3.3 ms^{-1}) at the surface during some ebb tides, and 6 fps (2 ms^{-1}) during some flood tides (Neal 1972).

Analysis of temperature-salinity plots suggests that three water masses are mixed in the estuary (Jay 1982). River water has zero salinity and a temperature that varies greatly with season. Sub-surface ocean water is the densest water mass, with the lowest temperatures and the highest salinities. Surface ocean water is the warmest water mass with near-oceanic salinities (Conomos et al. 1972). The temperature and salinity vary in response to coastal upwelling and downwelling (Jay 1984). The mixture of the three water masses produces estuarine water which has widely variant properties. The estuary has been classified as partially mixed (Neal 1972, according to the scheme of Pritchard 1955), but the stratification is highly dependent on the fortnightly tides and the river discharge (Jay 1982). The system exhibits behavior ranging from salt wedge to well mixed. For example, during the low-discharge period of October 1980, vertical mixing decreased and stratification increased during neap tides; during spring tides mixing increased and resulted in decreased stratification (Jay 1982). Saline water reaches Harrington Point (23 statute miles, 37 km upriver) and beyond during low discharge events but is generally confined to the region seaward of Tongue Point (18 statute miles, 29 km).

Wave hindcasting studies conducted near the mouth of the Columbia River (National Marine Consultants 1961)

Table 1. River discharge summary for the study period and the preceding ten water years

Water Year	Discharge (x 1000) Maximum cfs	(m^3s^{-1})	Minimum cfs	(m^3s^{-1})	Average cfs	(m^3s^{-1})
1980	398.9	(11.3)	86.9	(2.46)	205.5	(5.82)
1979	458.6	(12.99)	81.4	(2.30)	196.0	(5.55)
1978	582.2	(16.49)	73.9	(2.09)	225.2	(6.38)
1977	285.5	(8.08)	66.6	(1.89)	148.7	(4.21)
1976	680.5	(19.27)	95.3	(2.70)	285.1	(8.07)
1975	616.0	(17.44)	96.9	(2.74)	243.1	(6.88)
1974	932.9	(26.42)	103.5	(2.93)	317.7	(9.00)
1973	381.9	(10.81)	92.1	(2.61)	174.2	(4.93)
1972	941.6	(26.66)	106.0	(3.00)	321.6	(9.11)
1971	813.5	(23.04)	91.1	(2.58)	295.2	(8.36)
1970	651.2	(18.44)	89.3	(2.53)	218.9	(6.20)
Average	613.0	(17.36)	89.4	(2.53)	239.2	(6.77)

Explanation: Discharge data (USGS, 1970-1980) were used to calculate freshwater input to the estuary by adding discharges of the Columbia River at The Dalles, the Willamette River at Salem, Oregon, and the Cowlitz River at Castle Rock, Washington, plus 10 percent of this sum (formula used by U.S. Army Corps of Engineers, Mel Maki, pers. communication). Modified from Roy et al. (1982).

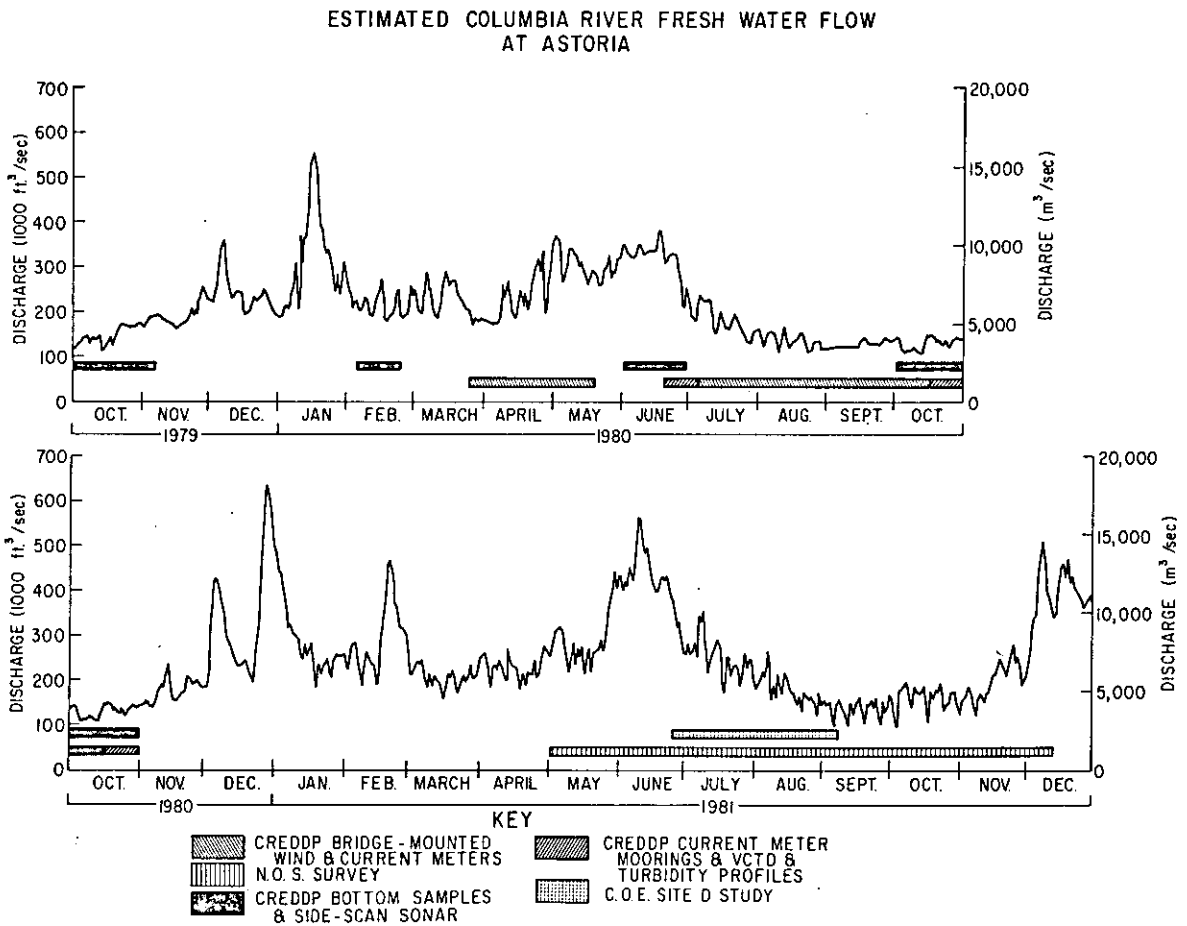

Figure 4. Discharge of the Columbia River Estuary and study periods.

indicate that during major storms significant wave height (H_s) can vary from 23 to 30 ft (7 to 9 m) with periods of 11 to 14 s. The largest storms occur in conjunction with southerly and southwesterly winds associated with low-pressure systems which move eastward across the Oregon-Washington coast. Winds during the winter season blow from the south-southwest at 10 to 22 knots (average) with a maximum of about 55 knots (Barnes et al. 1972).

In the summer the establishment of the North Pacific high-pressure cell generates northerly and northwesterly winds along the Oregon-Washington coast with typical speeds of 5 to 15 knots.

The seasonal reversal of wind and wave patterns results in seasonal changes in continental shelf circulation and generates the littoral drift patterns discussed above. During the summer, northerly winds and a resultant offshore Ekman transport generate upwelling of colder, more saline, and nutrient-rich bottom water (Smith and Hopkins 1972). During the winter, southerly winds and associated Ekman transport pile surface waters against the coast. The resultant downwelling results in well-mixed shelf waters and stronger coupling of the currents within the water column. The net sediment transport on the shelf during the winter, when storm conditions occur most frequently, is northward and slightly offshore. Littoral drift along the beaches and nearshore zones in Oregon and Washington also reverses seasonally, displaying a dominant net northerly component in the winter and a less important southerly component in the summer (Hodge 1934; Ballard 1964; Smith and Hopkins 1971; Sternberg and McManus 1972).

1.3 PREVIOUS STUDIES

The need to satisfy navigational requirements has been the main impetus for sedimentological research in the Columbia River. The reports of Bagnall (1916), Lockett (1959, 1962) and Kidby and Oliver (1965) describe morphologic changes that occurred as a result of jetty construction. Numerous studies have been performed by and for the U. S. Army Corps of Engineers (COE) on sediment transport in the vicinity of dredge disposal areas (U. S. Army Corps of Engineers 1933; Sternberg et al. 1977; Borgeld et al. 1978; Walter et al. 1979; Roy et al. 1979; Roy et al. 1982).

In addition to studies related to navigation, the Atomic Energy Commission (AEC) in conjunction with the U. S. Geological Survey (USGS) has supported several studies related to the fate of radionuclides originating at the Hanford nuclear reactors. Many of the studies were concerned with the bioenvironmental effects of radionuclides

in the estuary, and are summarized in Pruter and Alverson (1972).

Physical and numerical models of aspects of circulation and sedimentation in the estuary have been constructed (Hermann, 1968, 1970; O'Brien, 1971; Callaway, 1971; Lutz et al., 1975; Hamilton, 1981, 1983, 1984; McAnally et al. 1980; McAnally et al., 1983a,b). Studies by Hubbell et al. (1971), Hubbell and Glenn (1973), Glenn (1973) and Stevens et al. (1973) described the presence of a turbidity maximum in the estuary and delineated patterns of sediment size distribution and bedform distribution. Several studies unrelated to either navigation or radionuclide accumulation have provided sedimentological information, including the early studies of the dunes of Clatsop Spit (Cooper 1958), geochemical and physical studies in Youngs Bay (Johnson and Cutshall 1975; Slotta 1975) and studies related to the resource potential of local concentrations of heavy-mineral enriched "black sands" (Norberg 1980; Dearborn Associates 1980). Studies of the mineralogy and beach sands were made by Hodge (1934), Twenhofel (1946) and White (1967). More recent studies of the mineralogy of the Columbia River sediments have been performed by Whetten (1966), Knebel et al. (1968), Kelley and Whetten (1969), Whetten et al. (1969), and Walter (1980).

2. METHODS

2.1 BOTTOM SEDIMENTS

2.1.1 Sampling Plan

Under CREDDP a sampling plan was devised to obtain bottom grab samples on a seasonal basis over the entire estuary. An areal sampling density was adopted that would permit interpretation of grain size and mineralogical distributions on an estuary-wide basis. Transects were chosen perpendicular to the local trend of the estuary and a baseline sampling effort was conducted in October 1979. Samples were taken using a Shipek or Van Veen grab sampler aboard one of several small vessels. When depth changes occurred along the transect, an attempt was made to obtain samples from a range of water depths in proportion to steepness of bottom gradient. In the absence of bathymetric variation, samples were taken at spacings of approximately 1000 ft (300 m).

Positioning data were generally obtained using a Motorola Mini-ranger microwave ranging system, but a few locations were obtained by dead reckoning or horizontal sextant triangulation in October 1979. Although the Mini-ranger system is purported to have a precision of ± 10 ft (3 m), various factors degraded the precision (Creager et al. 1980). Field calibrations established that the system exhibited an average precision of ± 16 ft (5 m) at the operating ranges. Shore station positions were determined using a variety of sources, including Corps of Engineers records, National Oceanic and Atmospheric Administration (NOAA) charts, U. S. Geological Survey maps, air photos, horizontal sextant angles and Mini-ranger triangulation. The accuracy of shore station location control varied accordingly and ranged from ± 0.1 ft to ± 100 ft (0.03 m to 30 m). The accuracy of a final sample station location depended on the range precision, the control on shore transponder location, and the geometry of the fix involved. The accuracy varied from fix to fix, but on the average, positions obtained with the Mini-ranger system are considered accurate to within ± 100 ft (30 m). The roundoff errors that arose in calculating the coordinates of each sample and computer plotting are negligible and, at the commonly used scale of 1:40000, the stations are plotted to within ± 0.03 in (0.008 cm).

Sample depths were recorded on various recording echo-sounder systems with accuracies of ± 1 ft (0.3 m) and corrected to mean lower low water (MLLW) by interpolating predicted tide height data (National Ocean Survey 1978, 1979). Depths are probably accurate to within ± 1.5 ft (0.5 m). A detailed discussion of quality assurance in the

navigational data is available in the CREDDP Procedures Manual (Pacific Northwest River Basins Commission, 1980).

The transects occupied during the baseline sampling effort are shown as hatched lines in Figure 5. The transects shown in solid lines were reoccupied in February, June, and October 1980. During each of these seasonal surveys, an attempt was made to reoccupy a previous sample location, but priority was placed on obtaining a sample from the same corrected depth. The lack of up-to-date bathymetry over much of the estuary was a significant problem, and an effort was made in June 1980 to obtain continuous bathymetric profiles along the transects.

In all, approximately 1850 samples were obtained in October 1979, 450 in February 1980, 400 in June 1980 and 400 in October 1980. Grain size analysis was performed on all seasonal samples from the June and February surveys and on more than 600 of the October 1979 samples collected during the original CREDDP. An additional 274 grain size analyses were performed under the final CREDDP contract. These samples were selected from the remaining October 1979 data pool to provide additional sample density in the central portions of the estuary. The locations of all CREDDP samples chosen for analysis and all of the samples from October 1980 (none of which were analyzed) are presented in Appendix A. This report also discusses data obtained under various contracts with the Corps of Engineers and previously reported in Sternberg et al. (1977), Borgeld et al. (1978), Walter et al. (1979), Roy et al. (1979), and Roy et al. (1982). Most of the samples from these earlier studies are located in the lower estuary, near the entrance and on the continental shelf, and were obtained with grab samplers such as those used for CREDDP work. Some were recovered with a bedload sampling device incorporated in the tripod apparatus described in Walter et al. (1979). Locations of all stations are included in Appendix A. Navigational control for these earlier samples included horizontal sextant fixes, Loran-C, and Mini-ranger, and may have been slightly less accurate than the more recent data.

2.1.2 Grain Size Analysis

Preliminary descriptions of the raw samples were recorded in the boat log, and the sediment was packaged in plastic bags, transported to the University of Washington and stored in a refrigerator until analyzed. An attempt was made to separately bag representative sediment from each layer when obvious stratigraphy was observed in the grab sample, but inevitably some mixing occurred. In the laboratory, each sample was homogenized, quartered to appropriate size and agitated in a 30% solution of hydrogen peroxide to remove organic material. The sample was then wet sieved at 4 phi (64 microns) to remove the fine

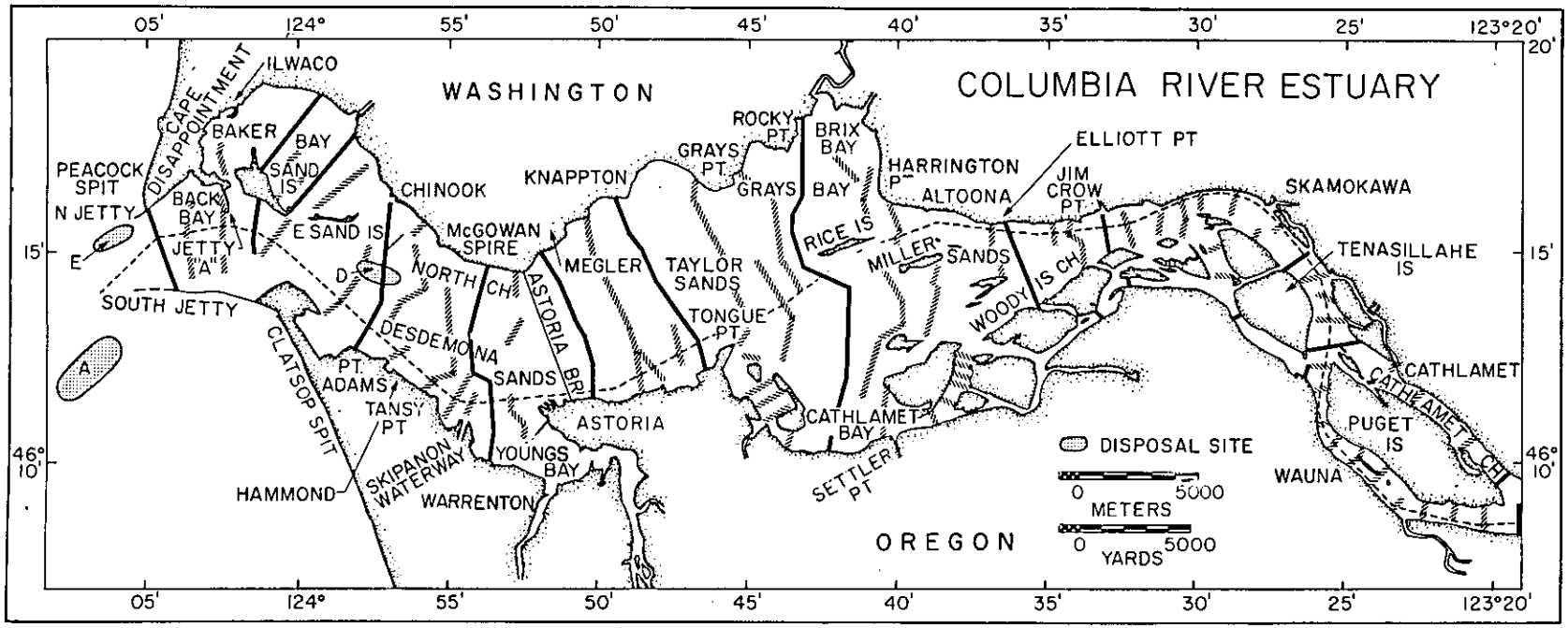

Figure 5. Transects sampled during the baseline (black and hatchured lines) and seasonal (black lines only) sampling schemes.

Table 2. Summary of sediment grain size descriptions (Lang et al. 1947).

CLASS NAME		METRIC UNITS (mm)	ENGLISH UNITS (inch)	MICRONS	PHI UNITS
Boulder	Very large	4096-2048	160-70		-11
	Large	2048-1024	80-40		-10
	Medium	1024-512	40-20		- 9
	Small	512-256	20-10		- 8
Cobble	Large	256-128	10-5		- 7
	Small	128-64	5-2.5		- 6
Gravel	Very coarse	64-32	2.5-1.25		- 5
	Coarse	32-16	1.25-0.625		- 4
	Medium	16-8	0.625-0.31		- 3
	Fine	8-4	0.31-0.16		- 2
	Very fine	4-2	0.16-0.08		- 1
Sand	Very coarse	2.00 -1.00		2000-1000	0
	Coarse	1.000-0.500		1000-500	1
	Medium	0.500-0.250		500-250	2
	Fine	0.250-0.125		250-125	3
	Very fine	0.125-0.062		125-62	4
Silt	Coarse	0.062-0.031		62-31	5
	Medium	0.031-0.016		31-16	6
	Fine	0.016-0.008		16-8	7
	Very fine	0.008-0.004		8-4	8
Clay	Coarse	0.004-0.002		4-2	9
	Medium	0.002-0.001		2-1	10
	Fine	0.0010-0.0005		1-0.5	11
	Very fine	0.0005-0.00024		0.5-0.24	12

fraction. (The phi scale and conversion to metric units is included in Table 2). The coarse fraction retained on the wet sieve was washed with distilled water, dried, and sieved at standard 1/4-phi mesh intervals to 4 phi. The fine pan fraction remaining was added to the fines from the wet sieving and suspended in a 1000-ml cylinder with a known quantity (approximately 0.5 gm) of sodium metahexaphosphate (Calgon) as a dispersing agent. Pipette fractions were drawn from the settling tube at 1/2-phi intervals from 4 phi to 8 phi (silt range) and at 1.0-phi intervals between 8 phi and 12 phi (clay-size range) or until less than 5% of the total sample weight remained. The last was adopted as a time-saving measure after it was determined that termination of the analysis at the 5% level had a negligible effect on the eventual outcome of factor analysis calculations. The fraction weights obtained at each step in the sieve and pipette analyses were recorded on a standard keypunch form, encoded and verified. The resultant raw data were open weight distributions over 47 discrete phi size classes from -4.25 phi to 12 phi. A series of computer programs adapted to the University of Washington Harris-6 computer processed the raw size-class data, produced a printed summary of the commonly used sediment size parameters, and generated a file of the same data for use in statistical and mapping programs. A summary of the system of computer programs developed for this study is included as Appendix B. In most of the ensuing discussion, moment measures of the grain size distribution, which include contributions from all phi classes, will be used rather than graphical measures.

Triple replicates of several samples representing the finest-, average- and coarsest-grained size distributions were analyzed to establish the precision of the laboratory technique. Variations of less than 1% occurred in the weight percents of each phi class. Throughout the program, consistent laboratory techniques were used to ensure data quality. The laboratory techniques for size analysis and quality control are described in the Procedures Manual (Pacific Northwest River Basins Commission 1980) and are based on standard sedimentological routines (Krumbein and Pettijohn 1938; Inman 1952; Shepard 1954; Folk and Ward 1957; Folk 1974).

Similar procedures were utilized in analyzing sediments obtained on earlier Corps of Engineers cruises, except that analyses were carried to 12 phi in all cases (Sternberg et al. 1977; Borgeld et al. 1978; Roy et al. 1979.) The size statistics from those cruises were recalculated during this study as a convenient way to reformat the data, but the algorithms were the same and identical numbers were obtained.

2.1.3 Mineralogy

In order to investigate the mineralogy of the estuary samples, samples from several transects were analyzed for sand-size heavy mineral and magnetic mineral content. Minerals with a specific gravity of > 2.96 g cm^{-3} (heavy fraction) were separated from the sand-sized fraction of the sample using tetrabromoethane and standard separation techniques (Hutton 1950; Creager et al. 1980). Magnetic minerals were separated from the heavy fractions using a hand magnet and cloth after it was determined that this method was more effective than the Franz separator (Creager et al. 1980). The heavy mineral contents and magnetic mineral contents were expressed as a percentage of the total sand-size sample weight. A determination of the precision of the technique was obtained by performing five replicates on a sample (Sample 391 from Cruise Z7910.) The distribution of heavy and magnetic minerals by size was investigated by dry sieving two samples at 1/2-phi intervals and separating those fractions.

The May 1980 eruption of Mt. St. Helens resulted in a large sediment contribution from the Toutle-Cowlitz Rivers into the Columbia River as well as widespread deposition of volcanic ash over the drainage basins of several tributaries to the Columbia River. To permit recognition of sediment originating from Mt. St. Helens and other Cascade volcanoes, airfall ash samples were collected at 12 locations in Washington and Oregon following the major eruptions of 18 May, 25 May and 12 June 1980. The size distributions of two ash samples were determined using standard sieve and pipette techniques. Heavy mineral separations were performed on several samples and the light and heavy mineral fractions were mounted in epoxy on slides. The light fraction was stained to facilitate identification of plagioclase and potassium feldspar, and grain identifications on more than 100 grains were made for each slide. In addition to these petrographic techniques, various bulk ash samples and several estuary samples were photographed with a scanning electron microscope (SEM) to provide information on grain shape and surface texture. Bulk mineralogy of both ash and estuary samples was investigated using x-ray diffraction. Qualitative interpretations of the mineralogical data were used to supplement the other lines of investigation, and captioned photomicrographs summarizing the mineralogy of the estuary are included in Roy et al. (1982).

2.1.4 Statistical Techniques

Q-mode factor analysis

Several statistical approaches to the analyses of the surficial sediment grain size data were used during the course of the present contract. Q-mode factor analysis has

been shown to be a useful technique in both heavy mineral analysis (Imbrie and Van Andel 1964) and grain size analysis (Imbrie and Purdy 1962; Klovan 1966). The approach proved extremely useful as an exploratory technique in earlier studies near the entrance to the estuary and offshore (Sternberg et al. 1977; Borgeld et al. 1978; Roy et al. 1979). However, as suggested by Drapeau (1973), factor analysis is a somewhat subjective technique. It was less satisfactory in providing sample groupings that provided geologic insight when run on batches of the large and variable suite of samples from the entire estuary. At the outset of this project it was hoped that factor analysis could be performed on all of the samples collected throughout the estuary in one run. It is believed that the factor analysis technique is less effective when forced to run in batches and that a single run would have been a useful exploratory tool. An extended effort was made to program around the need for a sample-by-sample matrix in the computer during the eigenvector calculations (see discussion below), but there proved to be no way of avoiding this size-limiting problem. The lengthy section on statistical methods below is included to provide some insight to the internal mechanics of the commonly used techniques. This information will be useful in following the ensuing discussion of the relative merits of factor analysis, cluster analysis, and less sophisticated alternatives.

There are two basic approaches to factor analysis: (1) R-mode analysis, which examines the relationships among variables based upon all of the samples, and (2) Q-mode analysis, which examines the relationships among samples based upon the variables. For example, R-mode factor analysis could be used to build a table of correlations among the depth, mean grain size, deviation, and skewness, and then to determine a factor or two which combine the variables to best explain the information in the correlation matrix. Q-mode factor analysis might build a table of correlations among all samples based upon the variables, and then determine one or more factors that best explained most of the information in the correlation matrix.

In this study, Q-mode analysis was used to compare samples based upon their sediment size distributions. (In contrast, R-mode analysis of size distributions would have described how well a particular phi size class correlates with another phi class. Q-mode factor analysis describes how well sample X correlates with sample Y.) Each sample was composed of 47 grain size classes containing fractional sediment weights. Each size class was a variable which may be thought of as a vector component of a sample's grain size distribution, with the grain size distribution as the resultant vector.

The basic input to factor analysis was a matrix of

similarities between samples. The correlation coefficient, a commonly used index of similarity, could have been used to calculate similarities, but it requires computation of variances across variables, which would have been a statistical anomaly. The cosine-theta coefficient is the most common measure of similarity used in Q-mode factor analysis and is defined as follows:

$$\cos \theta_{ij} = \frac{\Sigma_{k=1} X_{ik} X_{jk}}{\Sigma_{k=1} X_{ik} \Sigma_{k=1} X_{jk}}$$

where X(i,k) is the kth variable of the ith observation and m is the number of variables. For any two samples, i and j, in m-dimensional variable space, this equation gives the cosine of the angle between two sample vectors. For example, if two samples are identical, they have a cosine-theta coefficient of 1.0; if two samples are completely different, they have a cosine-theta coefficient of zero. (There are no negative cosine-theta coefficients for sediment size data because all sample vectors lie in positive space.) A Q-mode cosine-theta coefficient matrix was built with N samples to a side, where N = the number of samples. Available computer resources limited N to less than 220 per program run, thus the data had to be analyzed in parts.

Factor analysis attempts to convey the most information in the similarity matrix with the fewest number of independent dimensions. Mathematically, this is accomplished by extracting the eigenvalues and eigenvectors from the similarity matrix, which can be a significant computational task if the number of samples is large. The resulting principal axes matrix contains eigenvectors (unscaled theoretical factors) in the columns and samples in the rows.

Projection of each sample onto the factor axes yields the factor loadings matrix, which has factors (scaled to the data) in the columns, and samples in the rows. Each element in this matrix is a "factor loading", which indicates the contribution of each factor to each sample. The sum of the squared factor loadings for a sample is called the sample's communality, which indicates how well the sample vector has been described by the factors. A communality of 1.0 shows a complete explanation.

In the Columbia River Estuary sediment data, the first six factors usually accounted for about 96 percent of the variance in the samples. Three separate runs were performed in order to determine the usefulness of more factors: six, eight, and ten theoretical factors were permitted, and the remaining factors were assumed to be unimportant.

To plot the theoretical factors, the factor scores matrix was obtained, specifying the grain size distribution of each theoretical factor. For each factor, the 47 grain size variables were standardized so that the sum of their absolute values was unity, and the factors were then plotted with grain size on the X axis and standardized amplitude on the Y axis. Figure 6 shows that the unrotated theoretical factors resemble peaked sine waves: the first factor resembles the order zero harmonic, the second factor resembles the order one harmonic, the third factor resembles the order two harmonic, and so forth.

Each sample can now be expressed as a superposition of increasing harmonics of sine waves (factors), where the factor loadings express the fractional contribution of each factor. At this point, however, it is difficult to relate the theoretical factors with the actual samples, because the factors contain mixtures of positive and negative phi sizes.

Because the position of the axes of the permitted factors is affected by the axes of the discarded factors, Kaiser's varimax rotation was used to reorient the factors with respect to the samples in 47-dimensional space. The varimax rotation maximized the variance of the sample loadings on the permitted factor axes, causing the absolute value of the loadings to approach either 1.0 or 0.0. In other words, each factor axes was placed so that sample vectors loaded either highly or not much at all. A rotated factor loadings matrix was thus produced which best fit different groups of sample vectors to different factors.

The rotated factor scores matrix was then obtained, and the rotated theoretical factors were plotted (Figure 7). The plots revealed that varimax rotation increased the amplitudes of the major sine wave peaks and decreased the amplitudes of the minor ones. This procedure helped make each factor more completely positive or negative, making it appear less like a sine wave and more like an actual sample. (Note that a negative factor correlates additively with a sample if the sample loads negatively on it, because a negative factor with negative loadings is the same as a positive factor with positive loadings.)

Like the unrotated factors, the rotated theoretical factors are also difficult to interpret because some components lie in negative 47-dimensional space. Because of this mixture of positive and negative elements in the factors, it is necessary to obliquely rotate each factor axis to the nearest actual sample, called an "end-member sample" (Figure 8). This relaxes the restriction of orthogonality maintained previously, which had forced some factors partially into negative space. In essence, one of the samples from the actual data set is chosen as most representative of a particular factor. The factor loadings

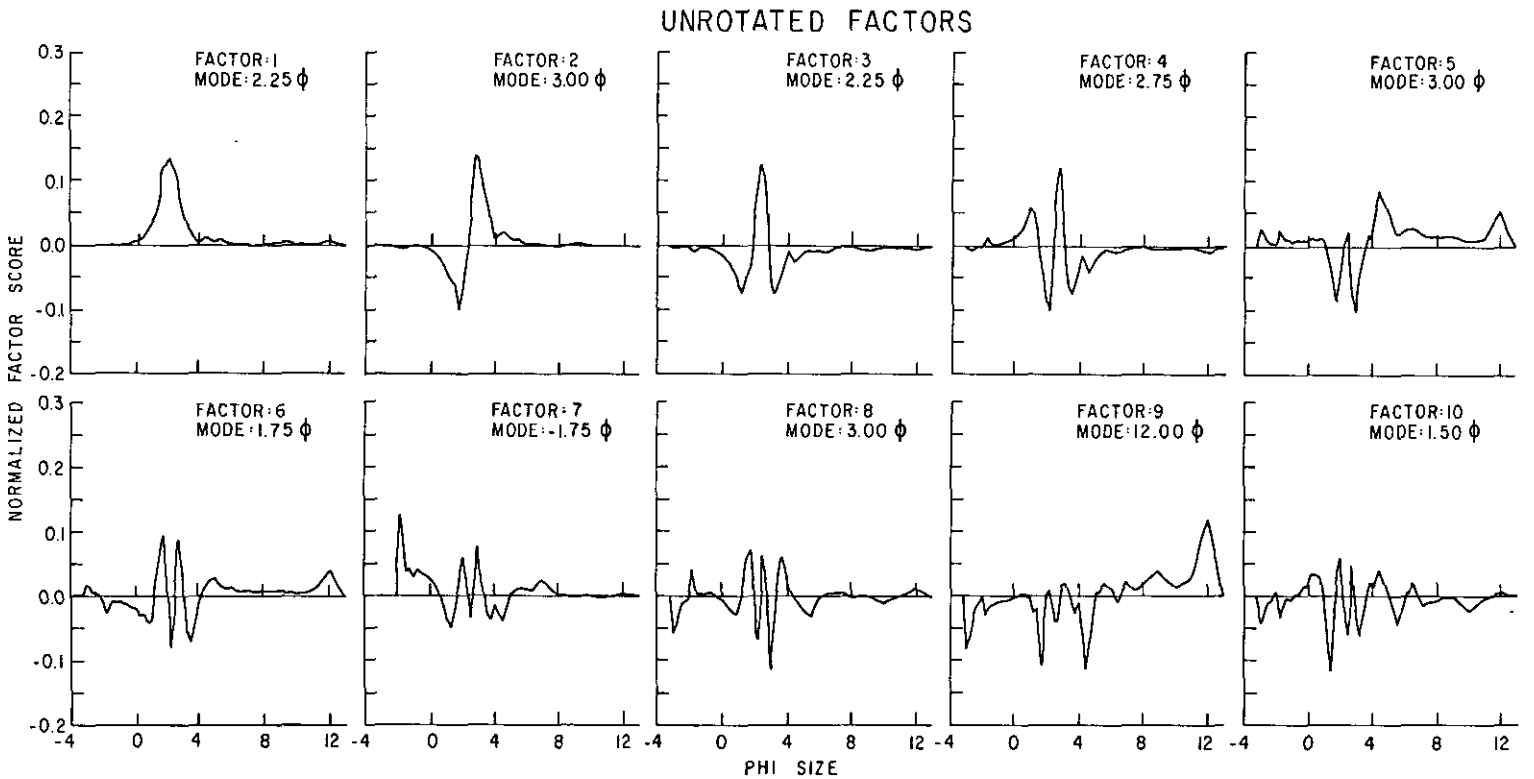

Figure 6. Size class distributions of unrotated theoretical factors.

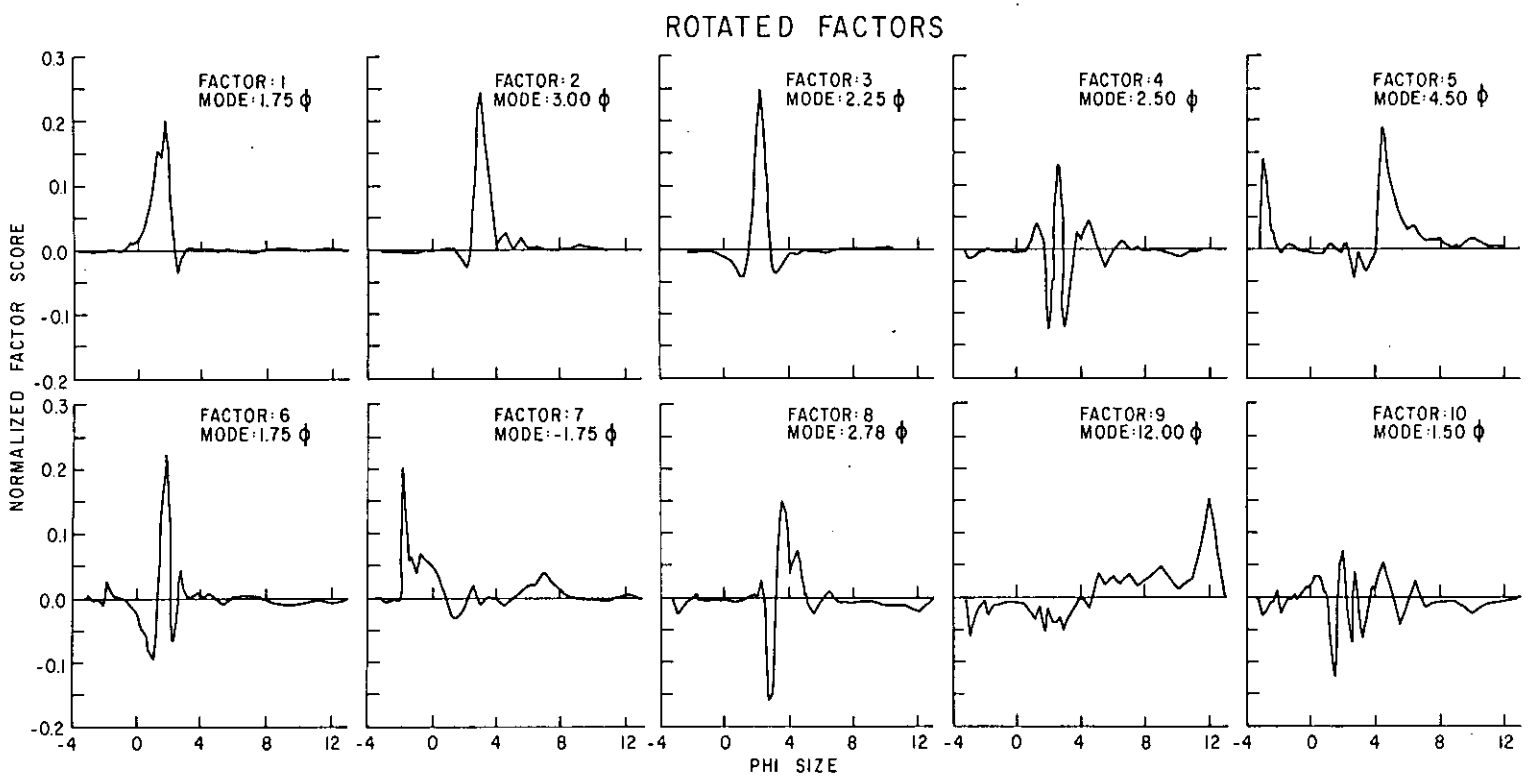

Figure 7. Size class distributions of rotated theoretical factors.

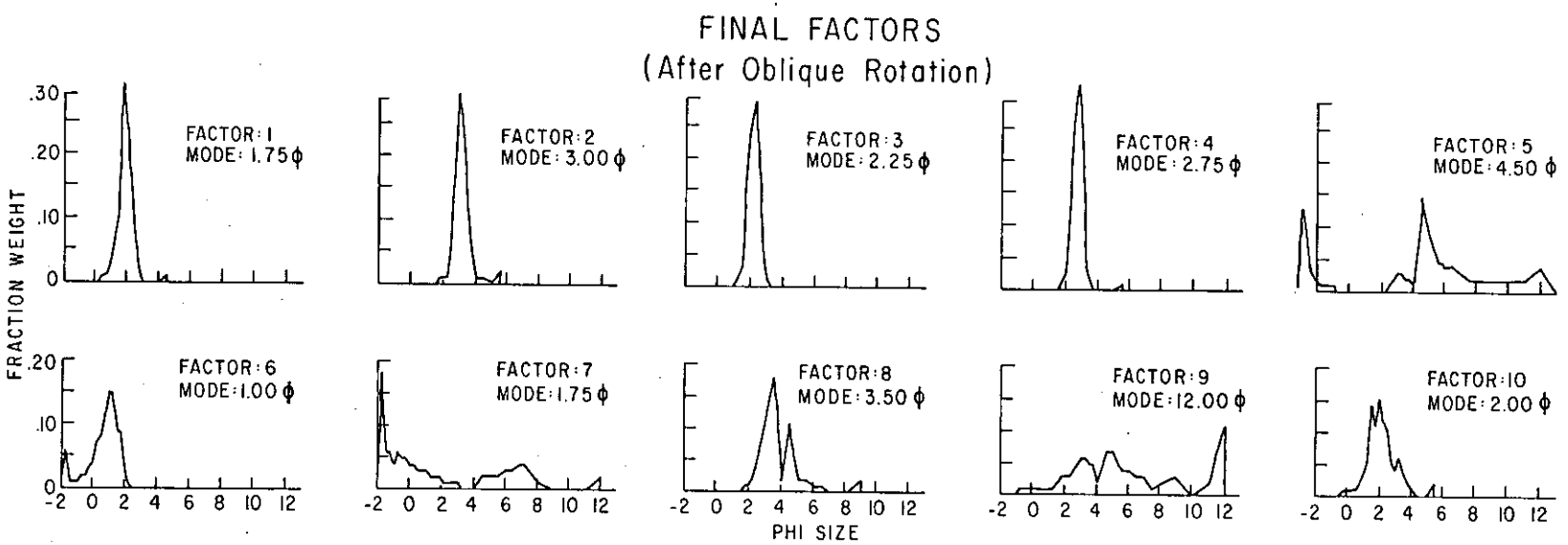

Figure 8. Size class distributions of final factors (end-members) after oblique rotation.

of the other samples on that factor are converted to factor loadings on the end-member sample during the oblique rotation. The advantage to this final rotation is that it clarifies sample associations; the disadvantage is that it allows end-members to be intercorrelated.

As pointed out above, factor analysis with a final oblique rotation was used to examine sediment size distributions during earlier studies in the estuary, including previous CREDDP work (Sternberg et al. 1977; Borgeld et al. 1978; Roy et al. 1979; Walter et al. 1979; Roy et al. 1982). In these studies, the number of samples in each program run was restricted to 100 because of the computer used. In order to run large sample sets, an iterative process was developed that involved increasing the number of factors chosen and transporting extremal factors from batch to batch until runs of all batches chose the same extremal factors.

During this study, the focus has been on interpreting the results of factor analysis and comparing the technique with cluster analysis. A random subset of 125 samples was chosen from the 287 October 1979 samples located between Astoria and Harrington Point. Factor analysis was run on this subset and permitted to choose 6, 8, and 10 factors. Intermediate plots of the theoretical factors and the factors after the varimax and final oblique rotations were generated for use in interpretation of the technique and for comparison with cluster analysis results on the same data.

Cluster Analysis

Cluster analysis places samples into relatively homogeneous groups and identifies outlier samples. Like factor analysis, cluster analysis can be run as Q-mode or R-mode. The Q-mode and R-mode similarity matrices are constructed exactly as described in the section on factor analysis. Both Q- and R-mode analyses were employed in this section.

For the Q-mode analysis, an N by N (where N = sample size) matrix was constructed using the cosine-theta correlation coefficient, identical to the matrix used in factor analysis. This matrix was used as input to the weighted pair-group clustering scheme described below.

In addition, an R-mode similarity matrix was built from the correlation coefficients among the following variables: depth, moment mean, moment standard deviation, moment skewness, and moment kurtosis. Before the correlations were calculated, each variable was transformed to standard normal form by subtracting its mean and dividing by its standard deviation. This was done so that the differing magnitudes and ranges of the different variables

would not affect their correlations. The resulting R-mode matrix of correlations between standard normal variables was processed by the cluster analysis scheme described below.

The cluster analysis scheme that was adopted was the weighted pair-group clustering with arithmetic averages (Davis 1973, pp. 456-473). Briefly, this technique seeks the highest similarity in each column of the similarity matrix. By examining all columns, the pairs whose mutual similarities are the highest are picked from the matrix. These are called "mutually high pairs." If sample A is most highly correlated to sample C, but sample C is most highly correlated with some other sample, A and C do not qualify as mutually high pairs. But if both samples are more highly correlated with each other than with any other sample, then they are mutually high pairs.

Once all the mutually high pairs are determined, each pair is linked and displayed on a dendrogram (a "branch diagram") at the appropriate level of similarity (Figures 9-15). The similarity matrix is then recomputed, treating each mutually high pair as one element. Because each pair has two correlations with each of the other elements in the matrix, the two correlations must be averaged to create one correlation. For example, the correlation between pair AB and sample D will be the average of the correlation between D and A and between D and B. The process of: 1) determining mutual high pairs, (2) linking mutually high pairs on the dendrogram, and (3) recomputing the similarity matrix continues until all clusters of samples have been linked on the dendrogram. Note that a "pair" can refer not only to two individual samples but also to two groups (clusters) of samples.

R-mode cluster analysis was performed on two suites of samples to examine the relationships among variables. The variables compared were depth, longitude, and moment measures of mean, standard deviation, skewness and kurtosis. Because the available computer facilities limited the matrix size to 200 x 200 in the cluster analysis program, all of the cluster analysis runs were performed on data subsets of 200 or fewer samples. The R-mode analysis was performed on 200 randomly selected samples from the 435 samples obtained in February and on 200 samples from the 431 collected in June 1980.

In order to compare the results of factor analysis and cluster analysis, a Q-mode cluster analysis was performed on the same set of 125 samples from October 1979 on which the factor analysis had been run. This analysis utilized the same size variables as the R-mode cluster analyses described above.

Once it was established that a Q-mode cluster analysis

approach was more likely to provide useful information than the previous factor analysis approach, the CREDDP samples were submitted to a Q-mode analysis. In the Q-mode analysis, 47 phi classes were considered the variables, and the relationships among the 200 samples were examined. Exclusive sets of 200 were randomly selected from the seasonal sample pool until most of the samples were analyzed. Q-mode cluster analysis was run on the following data sets:

(1) Three exclusive sets of 200 samples randomly selected from 623 October 1979 samples.

(2) Two exclusive sets of 200 samples randomly selected from 435 February 1980 samples.

(3) Two exclusive sets of 200 samples randomly selected from 431 June 1980 samples.

Dendrograms displaying the mutually highest pairs were generated with each run. The volume of information in the seven resulting dendrograms suggested that condensation was in order. A scheme was adopted whereby cluster branches were defined as distinct if they connected with a cosine-theta coefficient of 0.65 or less. For a sample size of 200, this produced from five to nine distinct clusters per dendrogram, which was meant to roughly coincide with the number of factors rotated in factor analysis. The resulting clusters contained between one and ninety-eight samples. To characterize each cluster, the mean fraction weight in each size class was calculated over all of the samples in the cluster, and the resulting means were plotted to create an average fraction and cumulative curve. Statistical parameters were also averaged over all of the samples in the cluster (as opposed to calculating new parameters from the resulting average fraction weight curve) and plotted with their associated curve. The average fraction weight curve for each cluster was then attached to its associated dendrogram (Figures 9-15). A map of the cluster distribution was plotted for each season and used in the later interpretations of sedimentary processes in the estuary.

Graphic Techniques and Maps

Several computer plotting programs were developed for the present study to plot various grain size parameters and to map the distribution of sediment size parameters. A summary of these and other programs developed for data manipulation is included as Appendix B. Maps were plotted with a mercator projection at a scale of 1:40000 for overlaying on the most recent bathymetry, provided by Northwest Cartography, Inc. (CREDDP, 1983). The following sediment parameters were plotted for all three seasons of CREDDP data and for all samples analyzed:

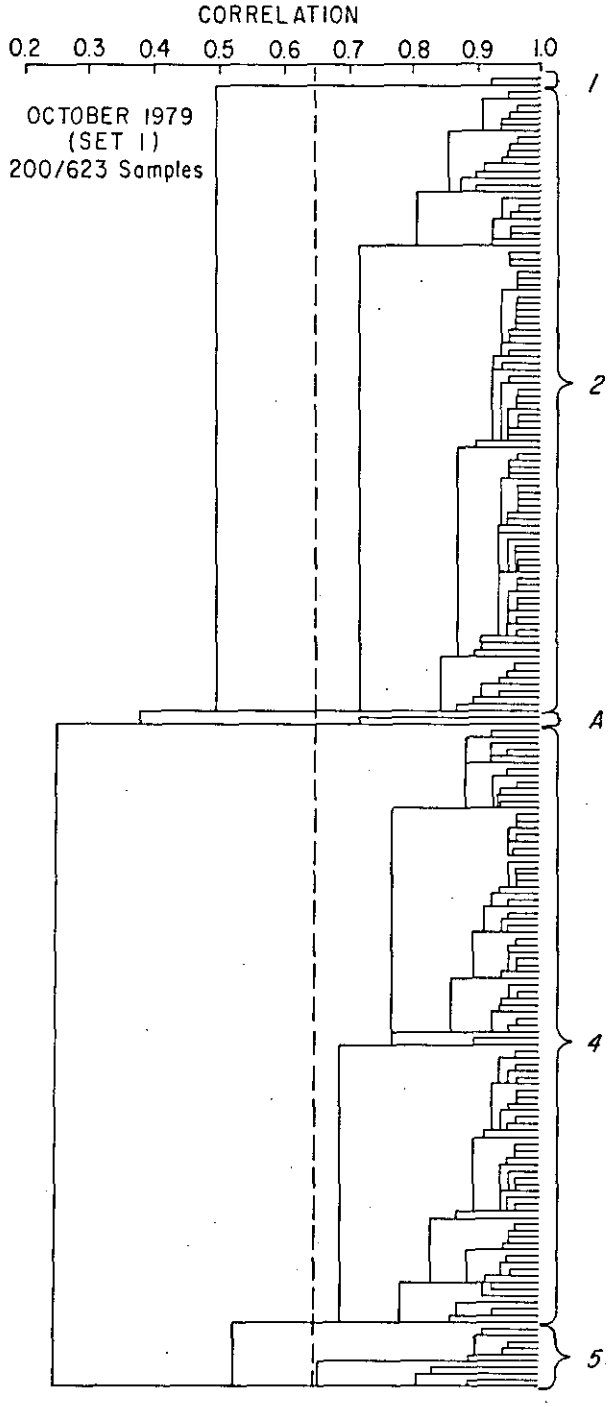

Figure 9a. Dendrogram of clusters, Set 1, October 1979.

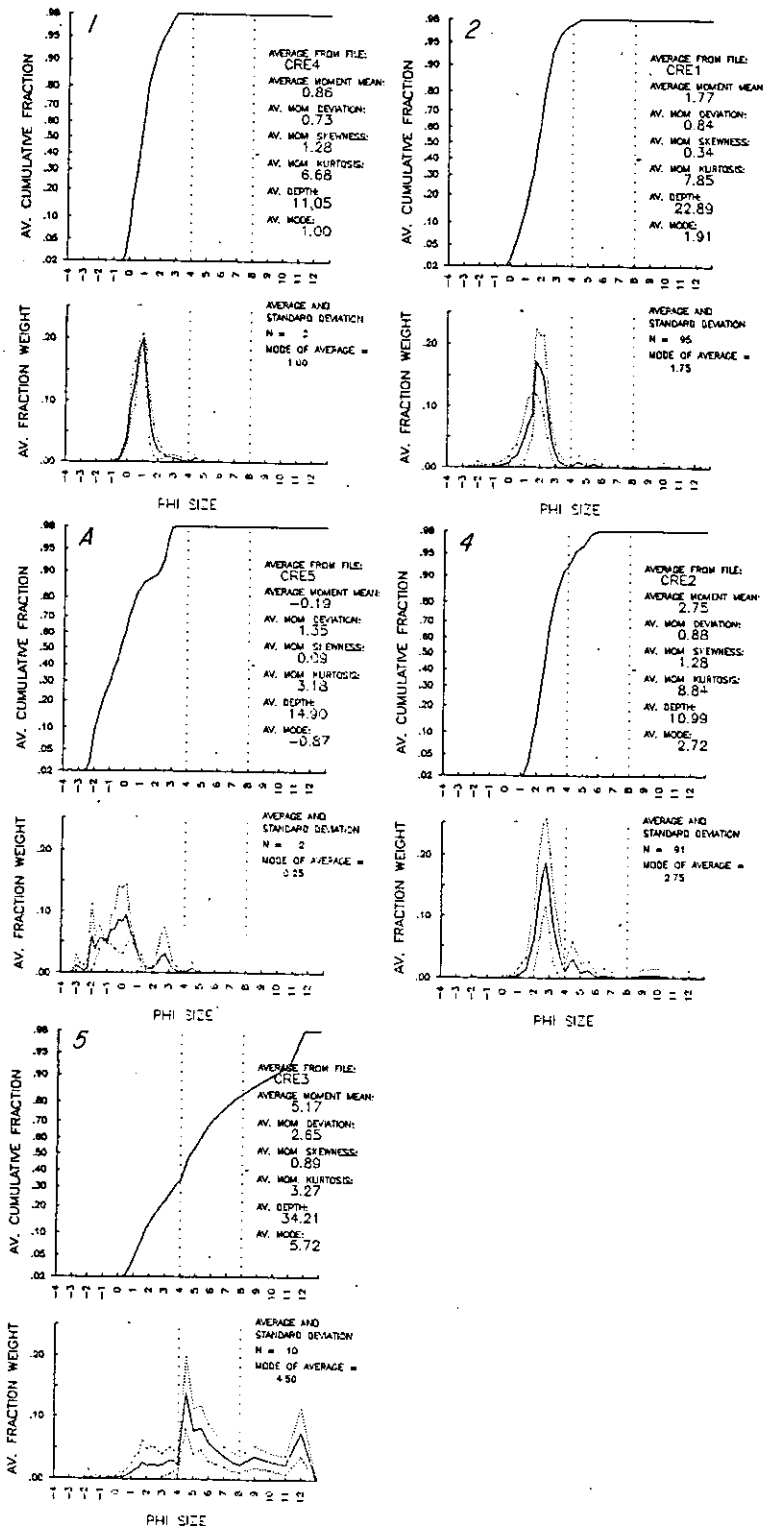

Figure 9b. Grain size distributions of clusters, Set 1, October 1979.

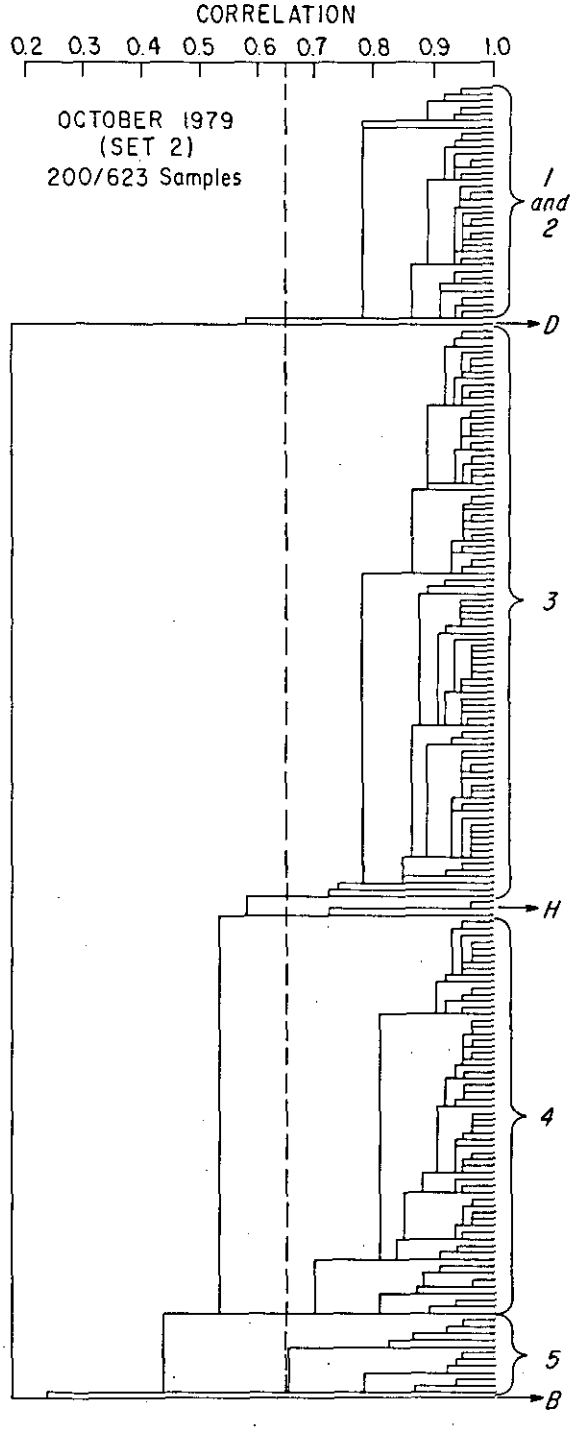

Figure 10a. Dendrogram of clusters, Set 2, October 1979.

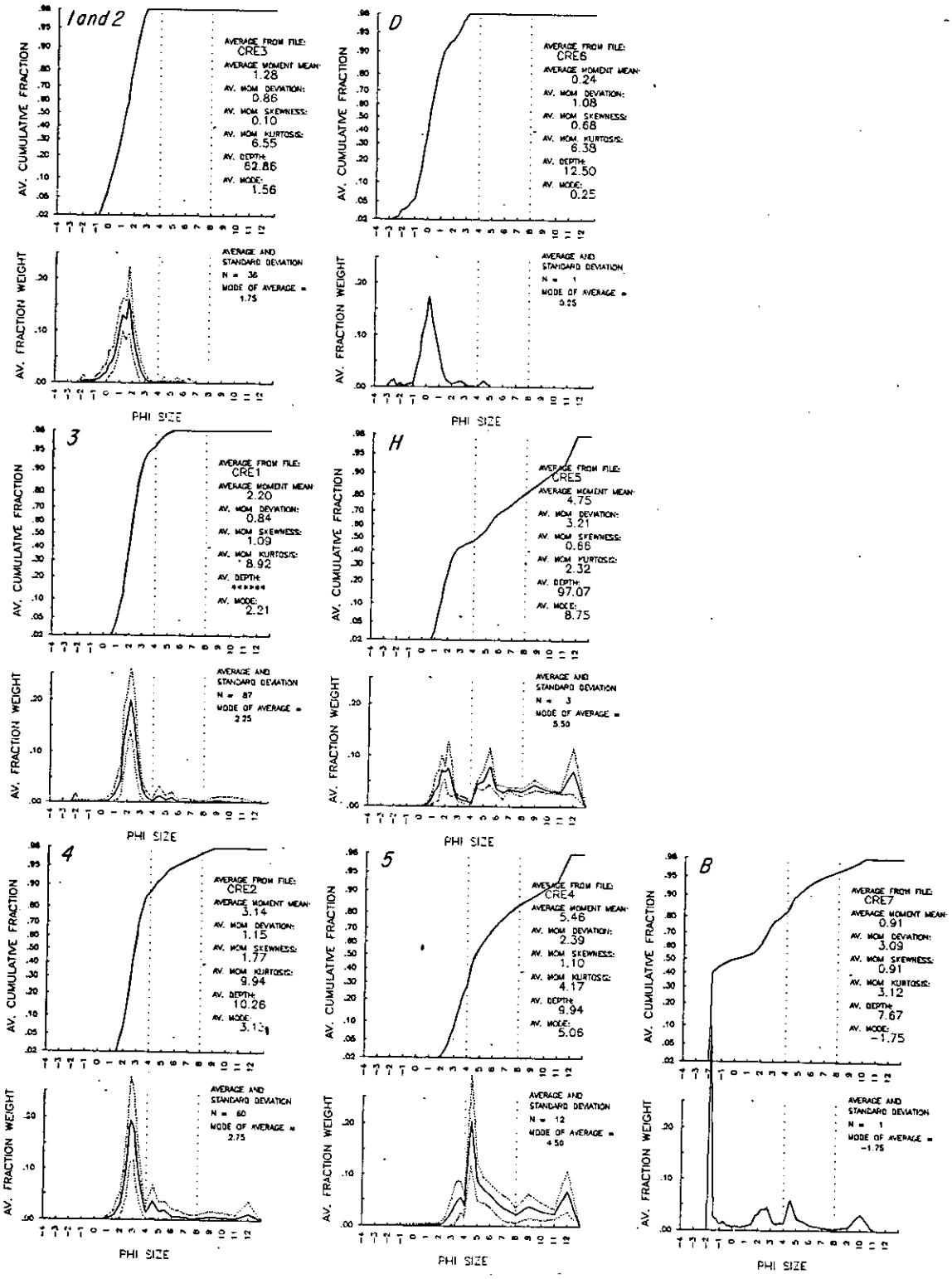

Figure 10b. Grain size distributions of clusters, Set 2, October 1979.

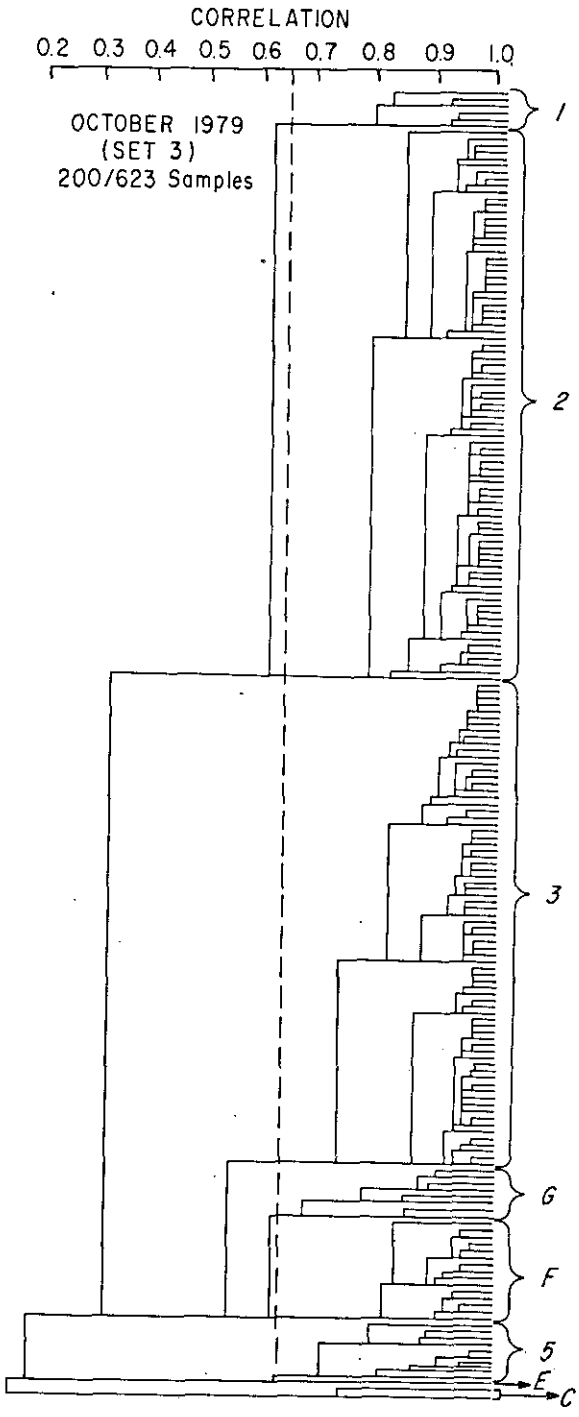

Figure 11a. Dendrogram of clusters, Set 3, October 1979.

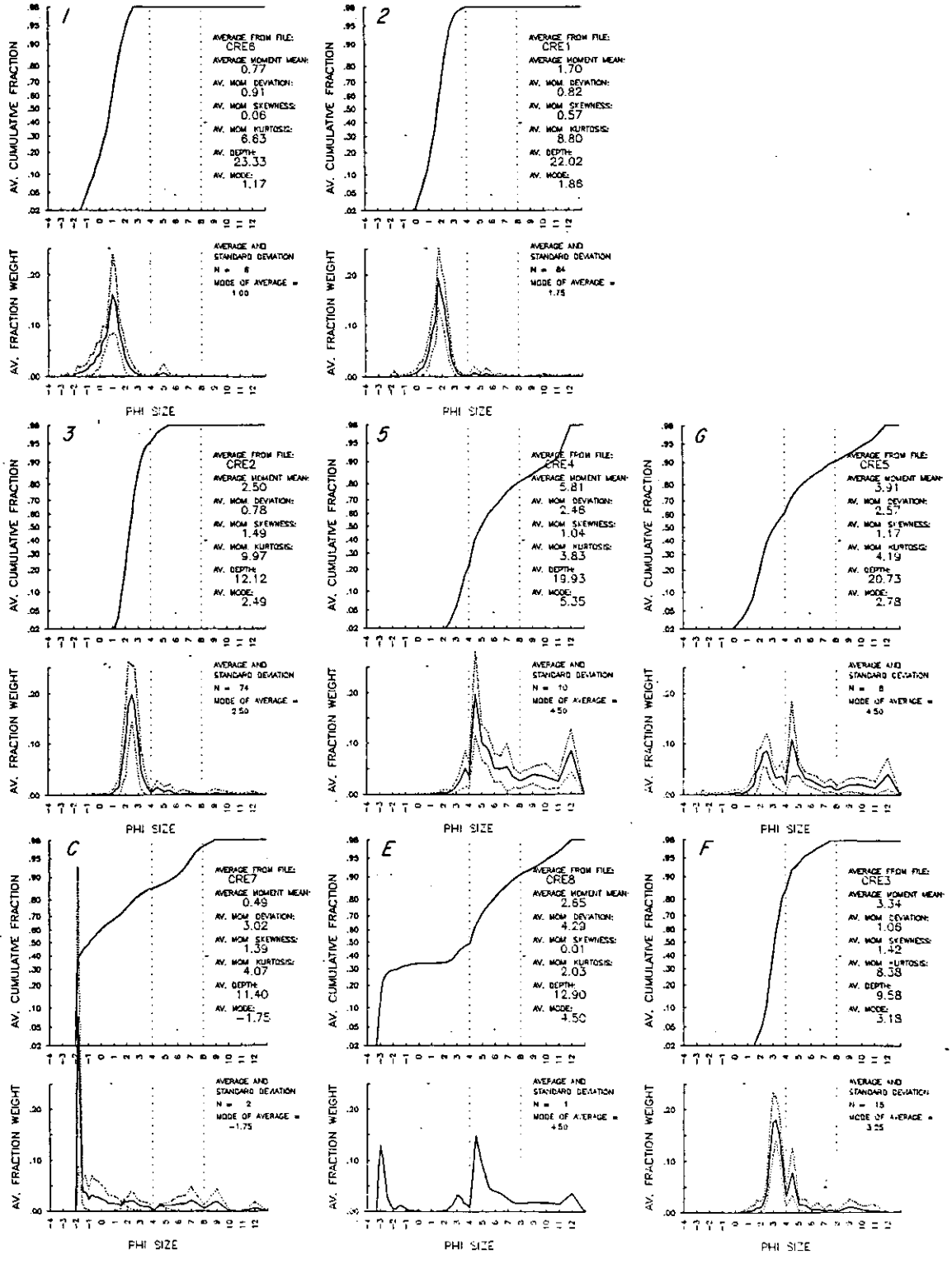

Figure 11b. Grain size distribution of clusters, Set 3, October 1979.

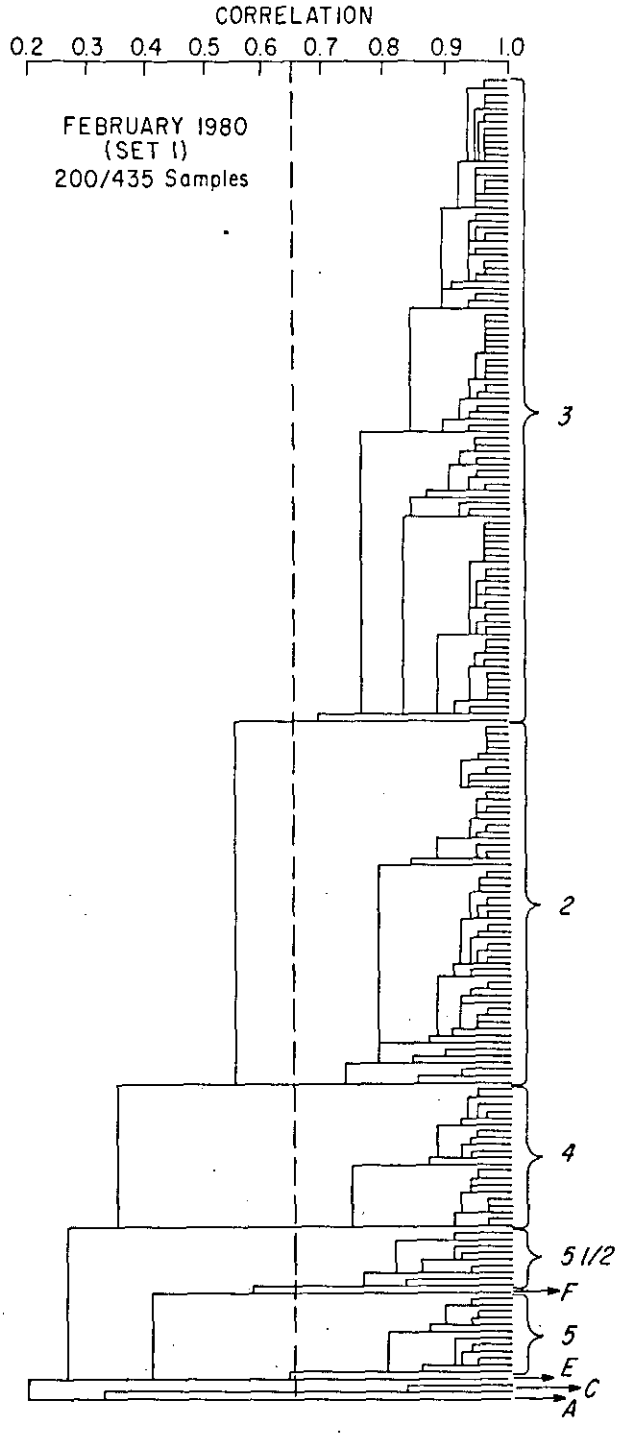

Figure 12a. Dendrogram of clusters, Set 1, February 1980.

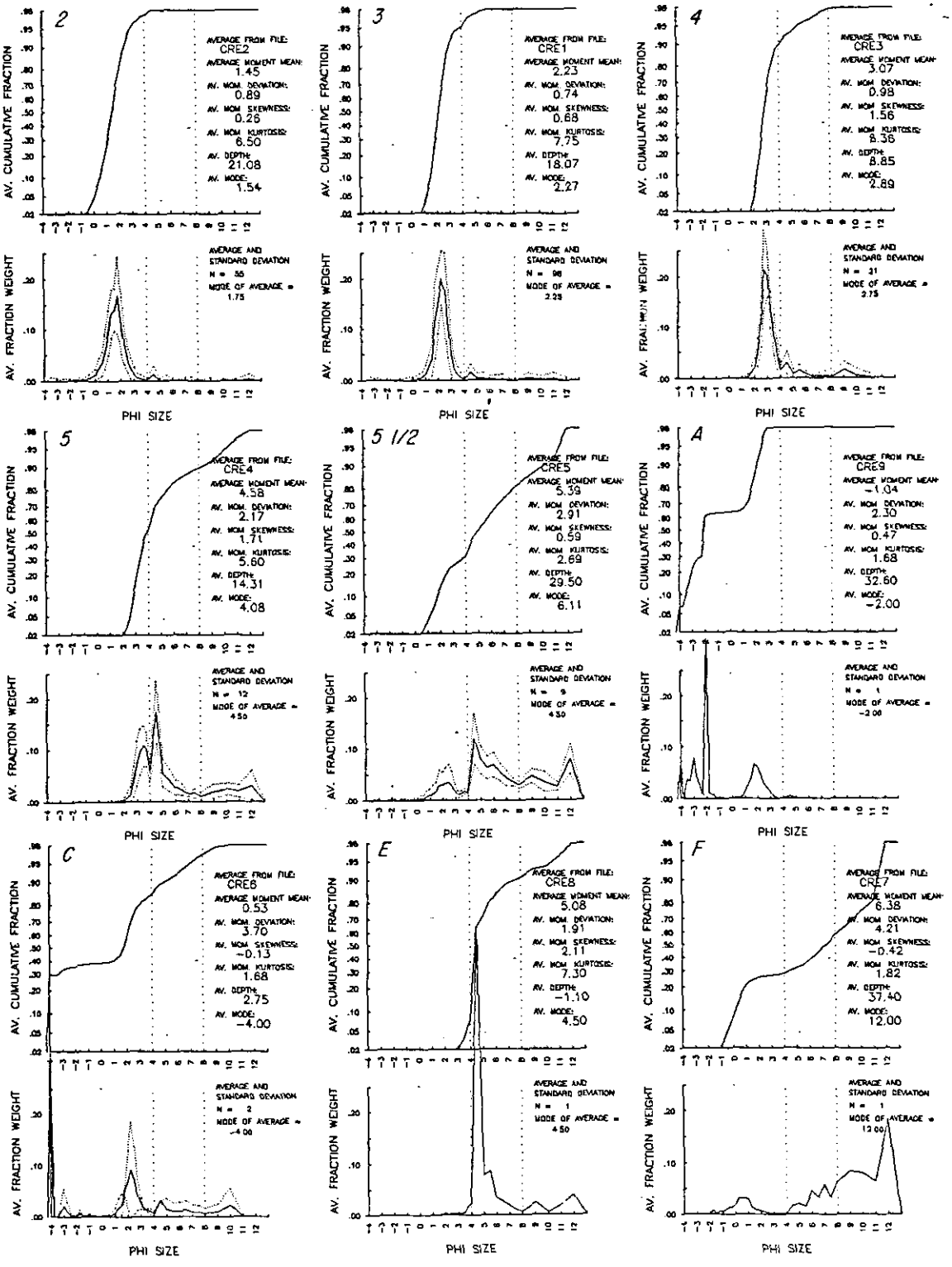

Figure 12b. Grain size distribution of clusters, Set 1, February 1980.

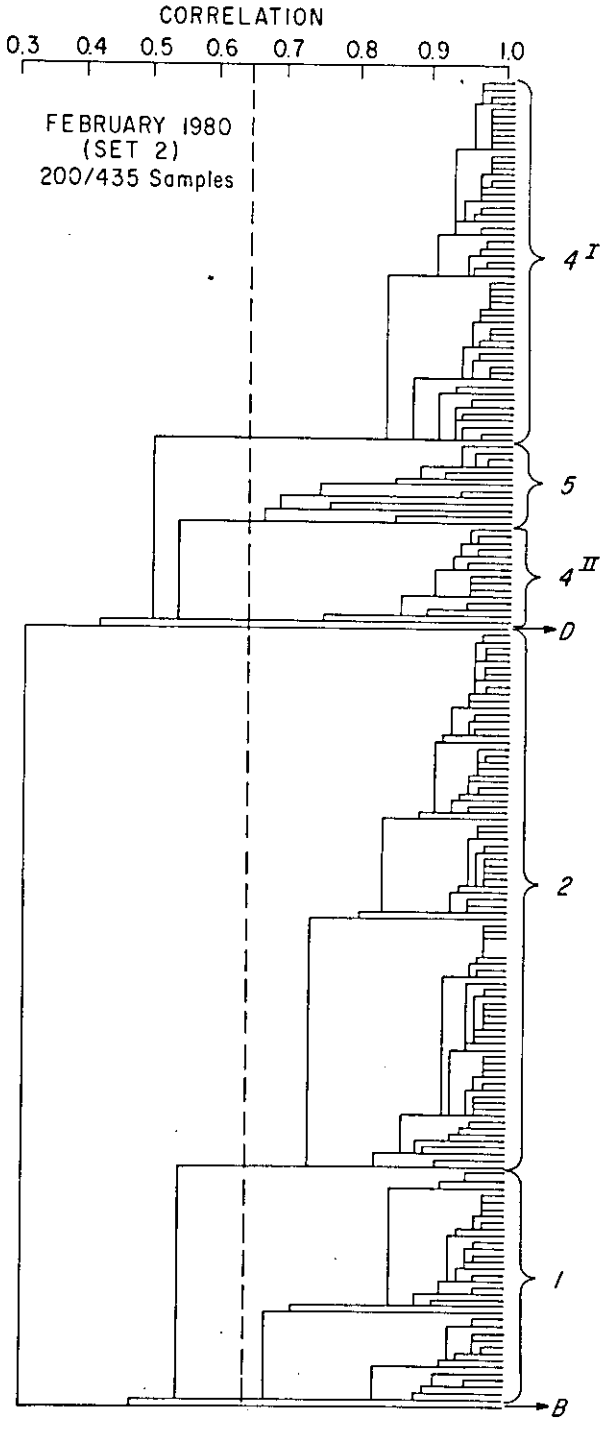

Figure 13a. Dendrogram of clusters, Set 2, February 1980.

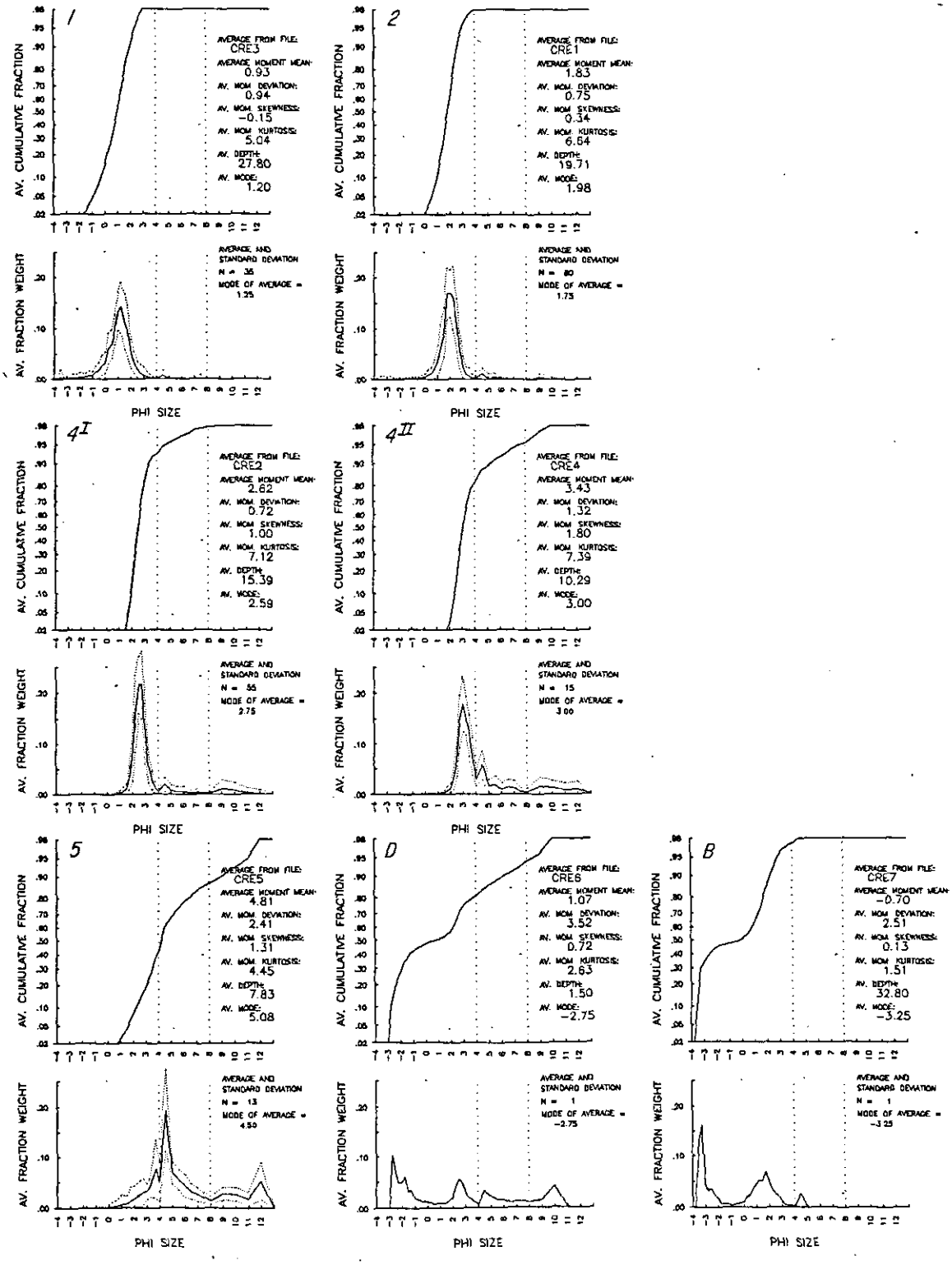

Figure 13b. Grain size distribution of clusters, Set 2, February 1980.

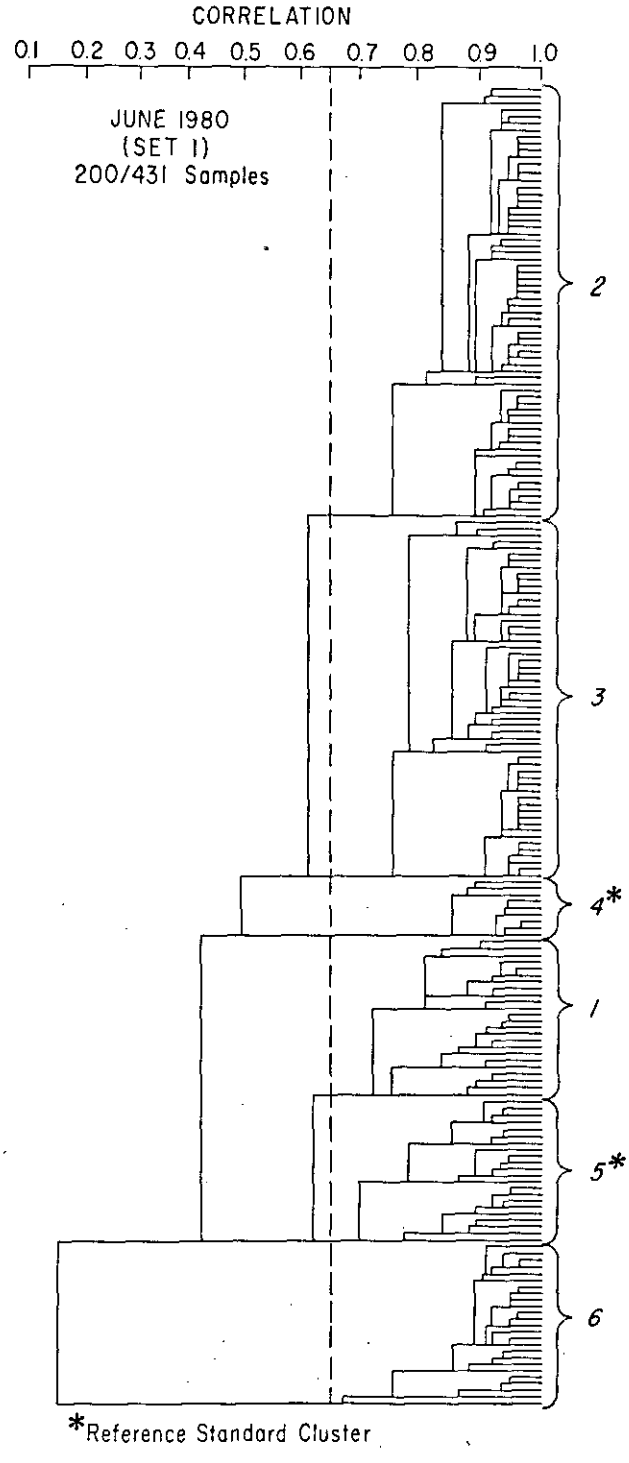

Figure 14a. Dendrogram of clusters, Set 1, June 1980.

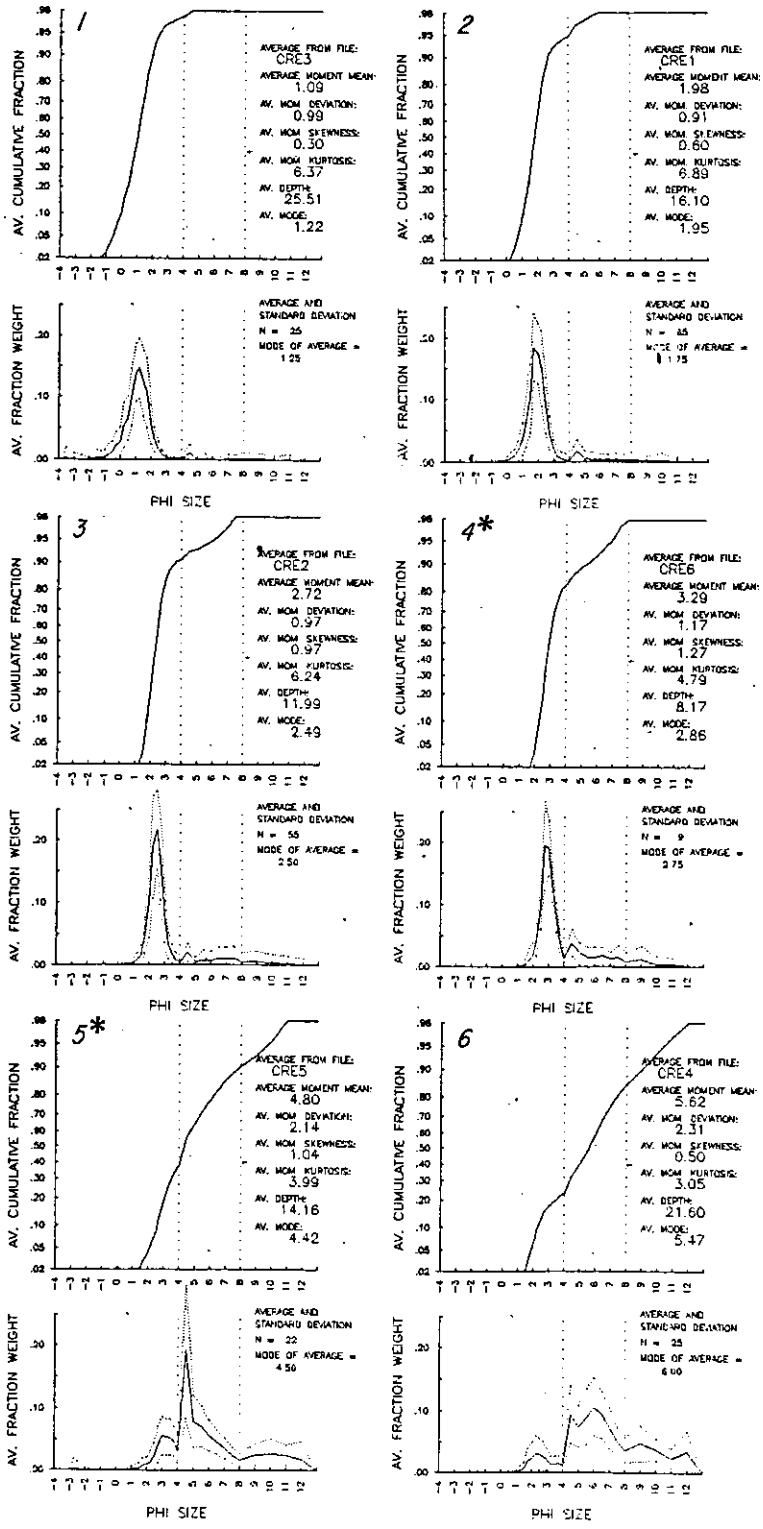

Figure 14b. Grain size distribution of clusters, Set 1, June 1980.

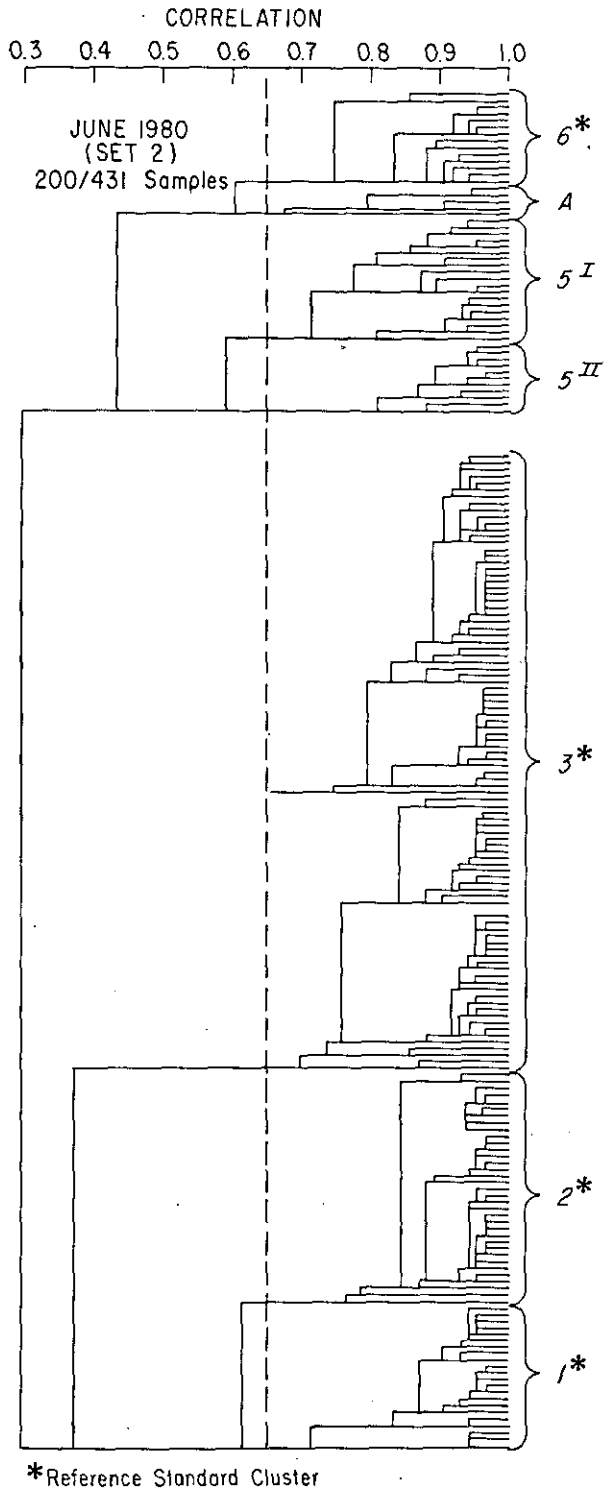

Figure 15a. Dendrogram of clusters, Set 2, June 1980.

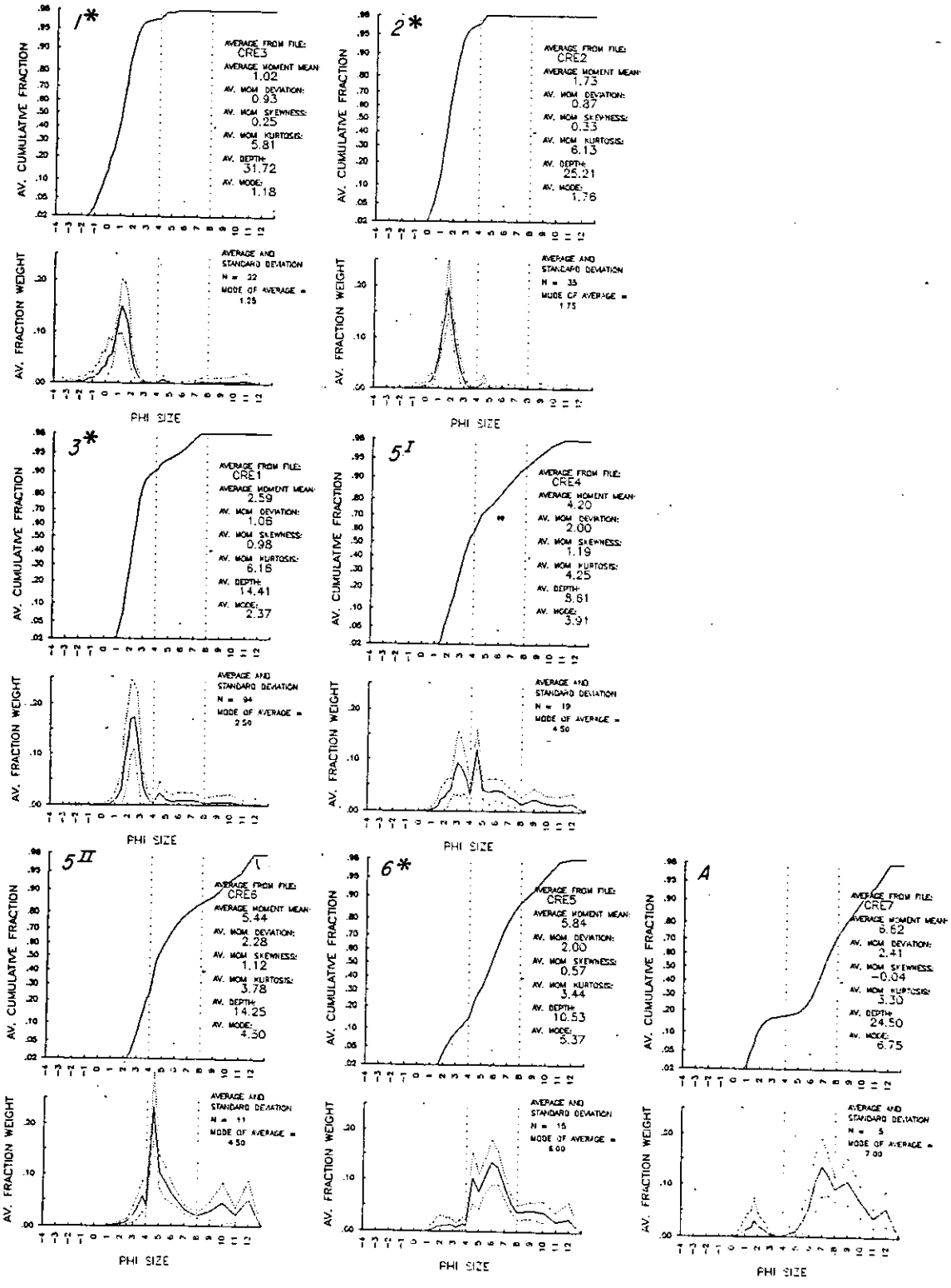

Figure 15b. Grain size distribution of clusters, Set 2, June 1980.

(1) station location

(2) moment mean

(3) moment standard deviation

(4) moment skewness

(5) phi size of the coarsest one-percentile

(6) percent silt plus clay

(7) station depth

(8) location of samples with stratigraphy or "mudballs"

The same parameters were plotted for the composite seasonal data from earlier studies. These composite data files combined all of the data available from the studies conducted for the Corps of Engineers (Sternberg et al. 1977; Borgeld et al. 1978; Roy et al. 1979; Walter et al. 1979) into three seasons based on the collection month. July through October was considered fall, November through March was considered winter, and April through June was considered spring. These assignments were intended to group months with comparable discharge and continental shelf conditions into the appropriate seasons. Summary maps combining several parameters for all of the data, by season, were generated for use in the final interpretations.

Plotting programs were developed and used to plot various combinations of sediment parameters in x-y plots. The range of plots available is listed in Appendix B. In addition to generating x-y plots, these programs provided statistical summaries of the information plotted which were helpful in intepreting the trends in grain size parameters.

2.2 BEDFORMS AND BOTTOM TOPOGRAPHY

2.2.1 Side-Scan Sonar

Seasonal information on the nature of the estuary bed was obtained during several multi-day cruises with a side-scan sonar (Creager et al. 1980; Roy et al. 1982). During each of the cruises an attempt was made to obtain complete coverage of the main channels in the estuary and to examine the entrance and lower portions (west of Tongue Point) at various stages of the tide. Data were obtained during September 1979, February 1980, June 1980, and October 1980 along the tracklines shown in Figure 16. The two fall cruises were conducted under low river discharge conditions, while the winter and spring cruises were conducted during mild freshets (Table 3, Figures 4 and 16). A site-specific

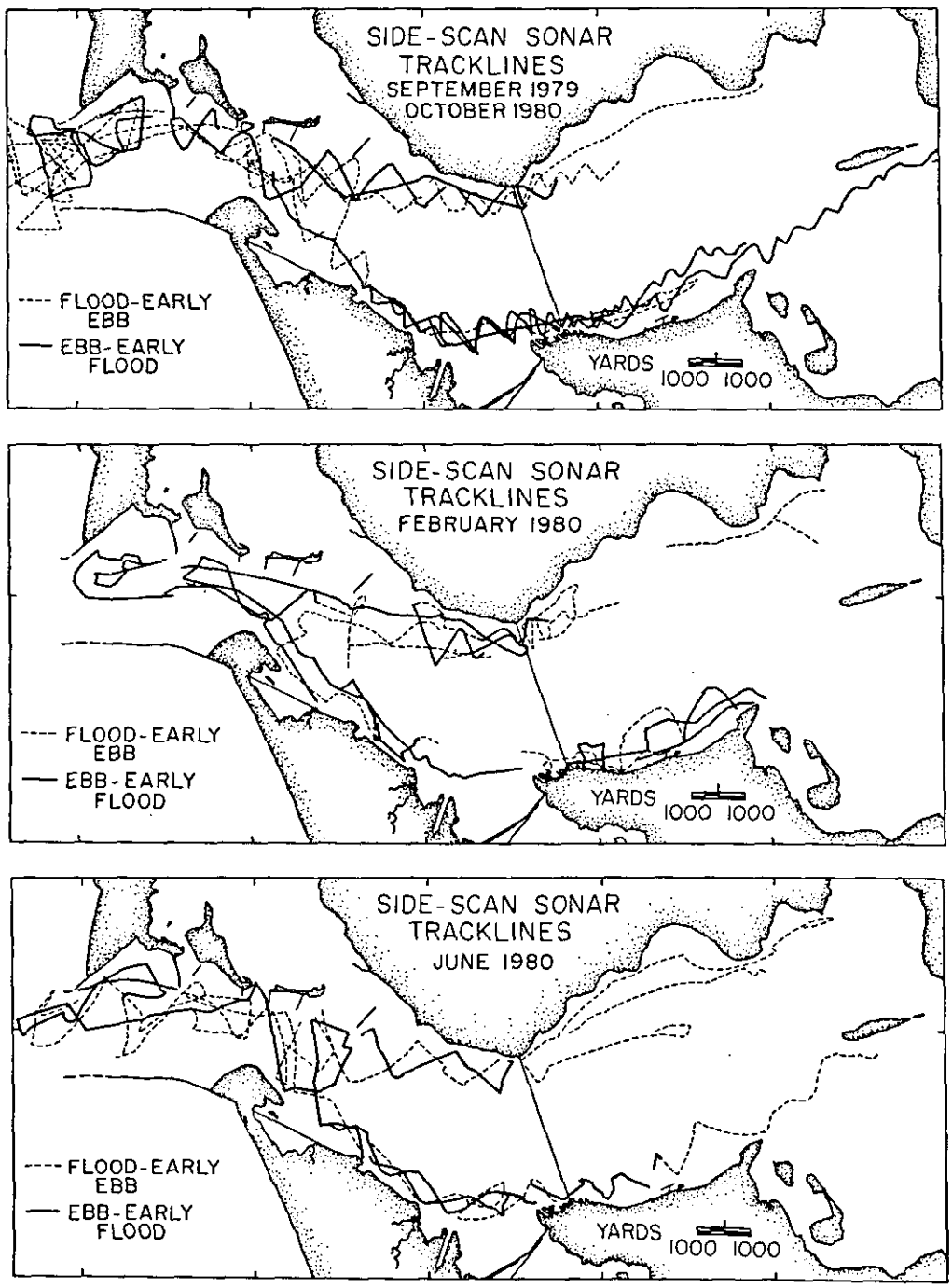

Figure 16. Tracklines run with side-scan sonar.

Table 3. Collection periods for CREDDP side-scan sonar data and freshwater discharge at Astoria

DATE	TIDE	DISCHARGE (cfs)	DISCHARGE (m^3s^{-1})
20 September 1979	Spring flood	134,000	3,794
21	Spring flood	116,000	3,285
22	Spring flood, ebb	120,000	3,398
17 October 1980	Neap ebb	160,105	4,534
21	Mean flood, ebb	140,701	3,984
22	Mean flood	135,102	3,826
25	Spring flood, ebb	132,616	3,755
26	Spring ebb, flood	101,299	2,868
27	Mean flood, ebb	163,878	4,641
29	Neap ebb, flood	150,315	4,256
7 February 1980	Neap flood, ebb	176,440	4,996
9	Neap ebb, flood	191,950	5,435
10	Neap ebb, flood	156,970	4,445
11	Mean ebb	177,760	5,034
1 June 1980	Spring flood	319,803	9,056
3	Mean ebb, flood	341,770	9,678
4	Mean flood	328,702	9,308
5	Mean ebb, flood	305,657	8,655
10	Spring flood, ebb	345,785	9,792
22	Neap ebb	328,900	9,313

study was conducted in the North Channel near dredge disposal site D (Figure 5) during the summer months of 1981. Repeated surveying of this area over 25-hour periods and during several consecutive neap and spring tides was intended to provide information on shorter-term changes in bed characteristics.

The equipment used during these surveys included a Klein 100-kHz towfish (model 422S-001A), a Klein dual channel transceiver (SA-350A), and an EPC 3200 dual channel graphic recorder. The side-scan was normally operated at a sweep rate of 1/8 second, which provided a maximum slant range of about 300 ft (94 m) to each side. Ship speed through the water was kept near 2 knots, but currents resulted in over-the-bottom speeds of 0.5 to 7 knots. Under these conditions resolution of the system varied, but fields of bedforms with heights in the range of 8 to 12 inches (0.3 m) and wavelenths of 6 to 9 ft (2 to 3 m) were generally well resolved. Various recording echo-sounders were used in conjunction with the side-scan. Positioning was determined with the Motorola Mini-ranger described above; the trackline positions are believed accurate to ± 75 ft (25 m). More precise navigation was required for the Site D studies so, in the summer of 1981, an acoustic bottom transponder (Data Sonics model HFT 120) was used to provide a fixed bottom reference point on the side-scan records. During the Site D studies, the Mini-ranger system was replaced by a Del-Norte system provided by the Corps of Engineers which had a nominal precision of ± 10 ft (3 m).

All records collected contained geometric distortions inherent in the technique. These were removed manually with the help of a programmable calculator, and the data were translated onto computer-generated trackline maps. These maps were compiled by season and used in the final interpretation. The data from Site D were treated separately. Detailed bedform maps from each survey were compiled and studied in an effort to measure bedform migration and the behavior of a dredge-disposal mound created for the experiment by the Corps of Engineers.

2.2.2 Bathymetry

Bathymetric profiles were run across the seasonal sampling transects during the June 1980 field season and corrected to MLLW by interpolating predicted tide tables. The Corps of Engineers provided intensive surveys of the Site D area at regular intervals during the summer of 1981. The Corps of Engineers also provided up-to-date condition surveys of the navigable portions of the estuary during the course of the program. Their surveys are generally mapped at large-scales (1:5000, 1:10000, or 1:20000) and have good horizontal and vertical control. The most valuable bathymetry was provided by Northwest

Cartography, Inc. (CREDDP, 1983) in the form of a 1:40000 map of the estuary including natural shorelines, intertidal features and the bathymetry obtained by the Corps of Engineers in 1980 to 1982. This bathymetry was used extensively in the interpretations presented in this report.

2.2.3 Aerial Photographs

A set of overlapping near-vertical photographs were obtained during an overflight conducted for the Corps of Engineers on 24 June 1980. The large-format photos were made with false-color infrared film during a two-hour period centered around a -1.0 ft (-0.3 m) low tide. The color photos and black and white prints enlarged to a scale of 1:40000 were used in the interpretation of sedimentary environments and to delineate intertidal areas.

2.3 SUSPENDED SEDIMENTS

2.3.1 Field Measurements

Approximately 160 turbidity profiles were collected at four stations during the latter part of October 1980 (Figure 17) (Roy et al. 1982; Gelfenbaum 1983). Profiles were obtained from each station at 1/2- to one-hour intervals over periods of 16 to 38 hours using a profiling instrument array. Station 6S was occupied twice, first on 16, 17, and 18 October and again on 22, 23, and 24 October in order to investigate the changes in the suspended sediment field on a fortnightly time scale. At each of these stations x-y recorder plots of turbidity profiles were obtained with an in situ, continuously recording nephelometer (Montedoro-Whitney model TMU-1B). The nephelometer measures the return of light scattered by particles in the water and its output, in volts, is directly proportional to the turbidity of the water.

Suspended sediment samples were collected periodically at various depths using a U. S. P-61 integrating suspended sediment sampler (Tennessee Valley Authority 1941). These samples were collected for use in nephelometer calibration and suspended sediment size analysis. The profiling array also included an Inter-Ocean CTD which included a pressure sensor, thermistor, and induction-conductivity coil and provided salinity and depth information.

Long-term data on the suspended sediment field were collected using a transmissometer mounted on the footing of the Astoria-Megler Bridge (Bartz et al. 1978). The transmissometer measured light attenuation over a 5-cm path length through the water and collected data concurrently with an Aanderaa current meter. Transmission and current information was collected at 15-minute intervals between 4 July and 23 August 1980.

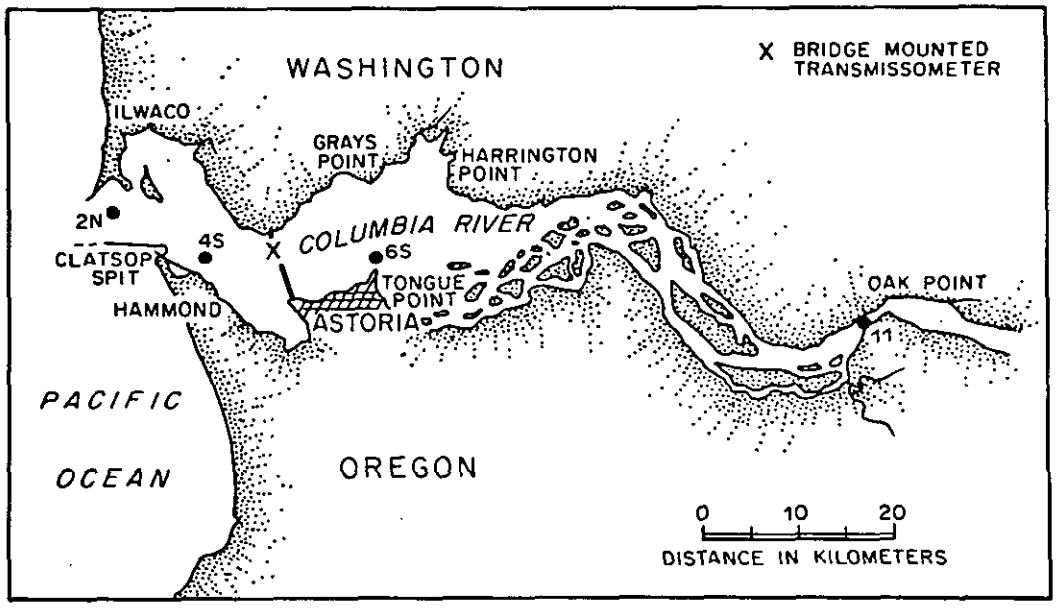

Figure 17. Locations of nephelometer stations and bridge-mounted transmissometer.

2.3.2 Laboratory Analysis

The turbidity profiles were digitized, normalized, and depth-averaged over the top, middle, and bottom thirds of the water column. Time series of depth-averaged suspended sediment concentrations were plotted for interpretation.

Measured aliquots of the suspended sediment samples were filtered and weighed to obtain concentrations, then treated with hydrogen peroxide, washed and re-weighed to determine organic content. Size analyses of the suspended sediment samples were conducted with a Coulter counter (model TA II) using a weak electrolyte as a dispersing agent and aperature sizes of 280 and 50 μm. These procedures are outlined in detail by Gelfenbaum (1983) and based on earlier work by Swift et al.(1972), Walker et al. (1974) and Shideler (1976). Four replicates were run for each sample and the results expressed as mean volume percent per 1/3-phi interval with one standard deviation error bars.

3. RESULTS

3.1 BOTTOM SEDIMENTS

3.1.1 Factor Analysis

Q-mode Factor Analysis

The Q-mode factor program run during the early CREDDP data analysis required between seven and eleven factors to explain more than 97% of the variability in the grain size distributions (Roy et al. 1982). Table 4 summarizes the modal grain size and relative contribution of each of the factor extremals picked in October 1979, February 1980, and June 1980. The modal size of the extremals varies from season to season, as does the number of factor extremals chosen. Furthermore, no easily interpreted areal distributions were perceived from these factor extremals. One of the goals of the present study was to find and apply a statistical technique that would provide consistent and meaningful results.

Plots of Theoretical Factors

As part of the search for a more appropriate statistical approach, Q-mode factor analysis approach was examined step by step to determine to which characteristics of the grain size distribution it was most sensitive. The Q-mode analysis of 125 samples from the most intensively sampled middle portion of the estuary (between Astoria and Harrington Point) was studied at each step in the factor analysis. Figures 6, 7, and 8 depict the grain size distribution associated with each of the ten factors chosen during the program run. By tracing the evolution of these curves at various steps in the analysis, it was possible to gain some insight into which components of the sediment distribution most affected the final end-members chosen. The varimax rotation (Figure 7) resulted in a slight shift in the modal values for each factor and an increase in the amplitudes, relative to the unrotated factors (Figure 6). The final oblique rotation was required to choose one sample from the data set to be represented with a loading of 1.0. A comparision between rotated theoretical factor 4 and its corresponding end-member sample (#4) revealed that both had similar modes (2.50 versus 2.75), and that the sample had zero sediment in the two phi sizes in which the theoretical factor had large negative peaks. Because a negative number loaded on zero is zero, it is clear why the negative portion of the theoretical factor did not contribute to this sample. Similarly, end-member #6 loaded negatively on the negative mode of rotated factor 6, making a positive relationship, and the positive portion of factor 6 (which was negatively related with end-member #6) did not make a contribution because end-member #6 had zero amounts in those

Table 4. Summary of seasonal factor analysis results. Secondary modal phi sizes are in parentheses (Roy et al. 1982).

October 1979		February 1980		June 1980	
Modal Phi Size	% of Loadings >0.5	Modal Phi Size	% of Loadings >0.5	Modal Phi Size	% of Loadings >0.5
		-2.0	1	0.25	1
		(-3.0, 1.75, -4.0)			
0.25	1	0.75	4	1.00	2
1.00	5				
1.75	22	1.50	28	1.50	18
				2.00	28
2.25	33	2.25	35	2.50	20
2.75	23	2.75	20	2.75	11
3.25	8	3.50	6	3.5 (4.5)	5
4.50 (12.50)	8	4.50	4	4.50	5
				4.50 (12.0, -2.75)	2
				6.0 (2.0)	6
		12.50	2	9.0 (12.0)	2

phi sizes. Although these examples demonstrated that the rotated factors corresponded to actual samples by correlation with the positive or negative element and lack of correlation with the opposite element, the association of many of the final factors with the original orthogonal factors was less clear. The choice of final end-members may still have been biased by an unrealistic mixture of positive and negative elements in the orthogonal factors. It should be noted that Clarke (1978) developed a computer program to maintain the theoretical factors in positive space, but the example he presented gave the same results as does the type of oblique rotation used here.

Three characteristics of the factor analysis approach were highlighted by these examinations. First, the construction of orthogonal axes created theoretical factors with negative vector components in some phi classes, which made the theoretical vectors difficult to interpret geologically. Second, the varimax rotation attempted to distribute the factor loadings over as wide a range as possible, but gave no particular information on which factors were most useful in explaining the variability. Third, the oblique rotation chose the representative sample, and one was left with only the size distribution of that sample to characterize a group of sediments. The interpreter had little knowledge of how the samples that loaded at varying levels on that extremal differed from the end-member. Finally, the in-depth examination of factor analysis served to emphasize that only the size distributions were being examined; all of the sources of similarity or difference among samples available to factor analysis were also available to the interpreter in the size-distribution curves.

Comparison of Results from Factor Analysis with Six, Eight, and Ten Factors

A comparison of the end-members chosen in experiments with six, eight, or ten factors permitted showed that the same, or very similar, end-members were chosen. For example, three different samples were chosen for end-member #4 in the three experiments, but these samples were all closely related, with cosine-theta coefficients of between 0.78 and 0.89. In addition, end-members #1, 5, 6 and 7 were the same for all experiments. This was not surprising, because the unrotated and rotated theoretical factors are virtually identical in the three experiments, and one would have expected similar end-member samples to be chosen.

In general, the importance of each successive factor declined, but higher-ordinal factors were occasionally important (Figure 18). In three cases, the ordinal of the end-member in one experiment was different in another experiment: end-member #3 in the six- and ten-factor

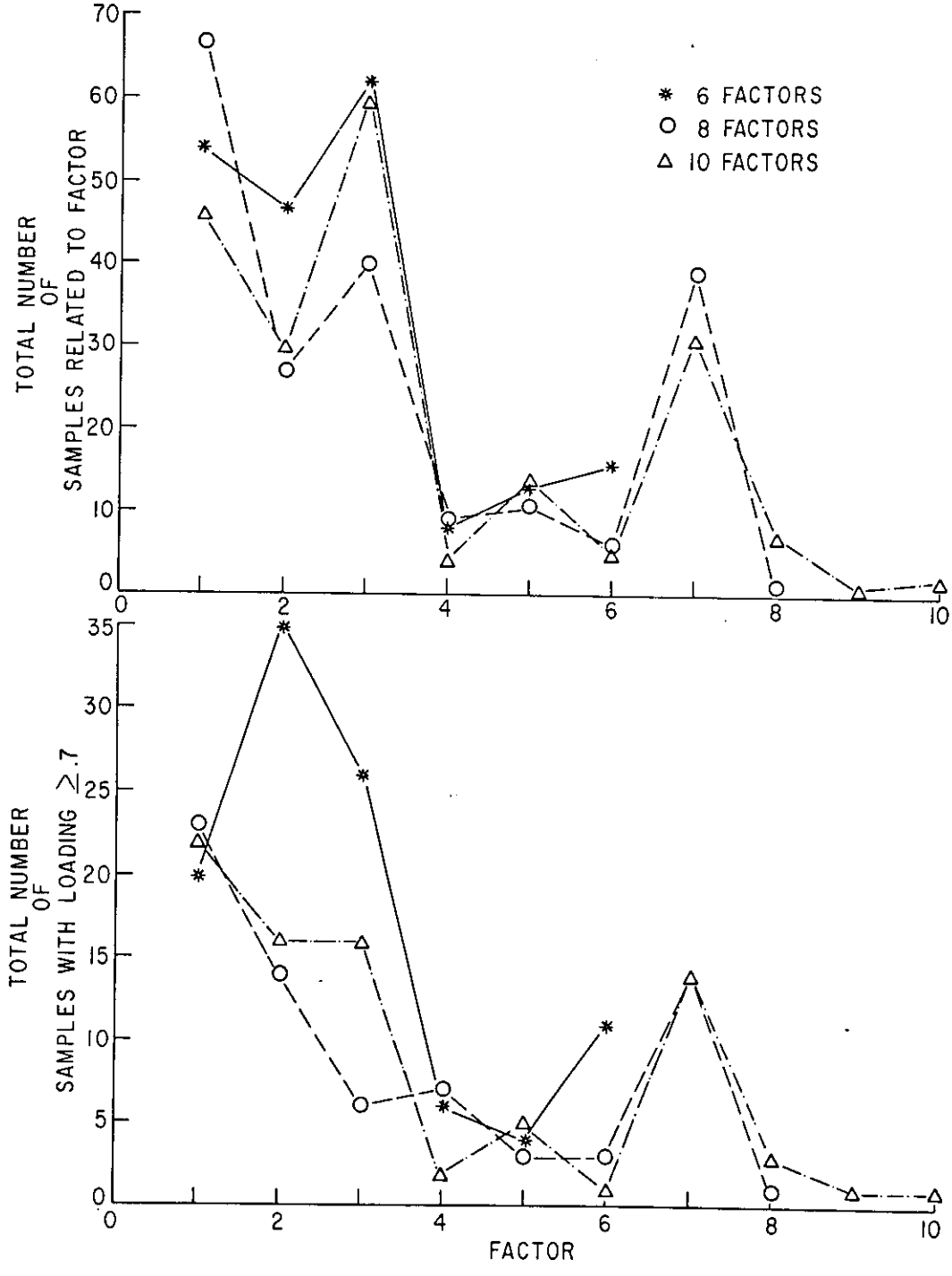

Figure 18. Relative importance of each of 6, 8, and 10 factors in explaining 125 samples collected in October 1979 from between Harrington Point and the Astoria-Megler Bridge.

experiments was the same as end-member #9 of eight permitted, and end-member #3 of eight was the same as end-member #10 of ten permitted. This suggested that higher-ordinal end-members (like #8 and 10) may have been less important due to their similarity with lower-ordinal end-members (like #3), which explain more variance in the sample set.

Conflicting conclusions can be drawn from the reordered, obliquely-rotated, varimax-rotated factor matrix. It was noted that while end-members #5 and 7 explained only one sample better than any other single end-member, end-member #10 explained fourteen samples better than any other single end-member. This suggested that an end-member with a high ordinal could be more important than one with a low ordinal. The higher-order theoretical factors permitted a broader range of phi sizes to be considered; it may have been that the higher-order factors acted as less discriminating collection bins for a wide variety of samples. Examination of the range of distribution curves for these factors indicates that in some cases this was true.

Two conclusions can be drawn from these experiments: first, as pointed out by Drapeau (1973), there is not always an advantage to permitting more factors to be chosen. Extraneous factors, while explaining more of the variance in a statistical sense, may have obscured geologically important relationships. Second, there were no clear guidelines for determining the optimal number of permitted factors, and no consistent way of recognizing that number from a range of permitted factors without careful examination of the original distributions.

3.1.2 R-mode Cluster Analyses

An R-mode cluster analysis was performed on the following six variables: depth, river mile, moment mean, standard deviation, skewness, and kurtosis. The data sets used were 200 samples from the 431 samples taken in June 1980 and 200 of the 435 samples obtained in February. The only variables that were closely related were moment mean and moment standard deviation which were correlated at 0.78. Otherwise, the variables were linked by correlations between 0.17 and -0.21. This demonstrated that the various statistical parameters were, in fact, largely independent variables and that, taken as a whole, they were poorly correlated with (1) each other, (2) water depth, and (3) distance from the river entrance. The high correlation between standard deviation (sorting) and mean grain size was even more apparent when these two parameters were plotted against each other (see discussion below). This relationship has been recognized by other workers (Inman 1949; Griffiths 1951, 1967) and is related to the mechanisms

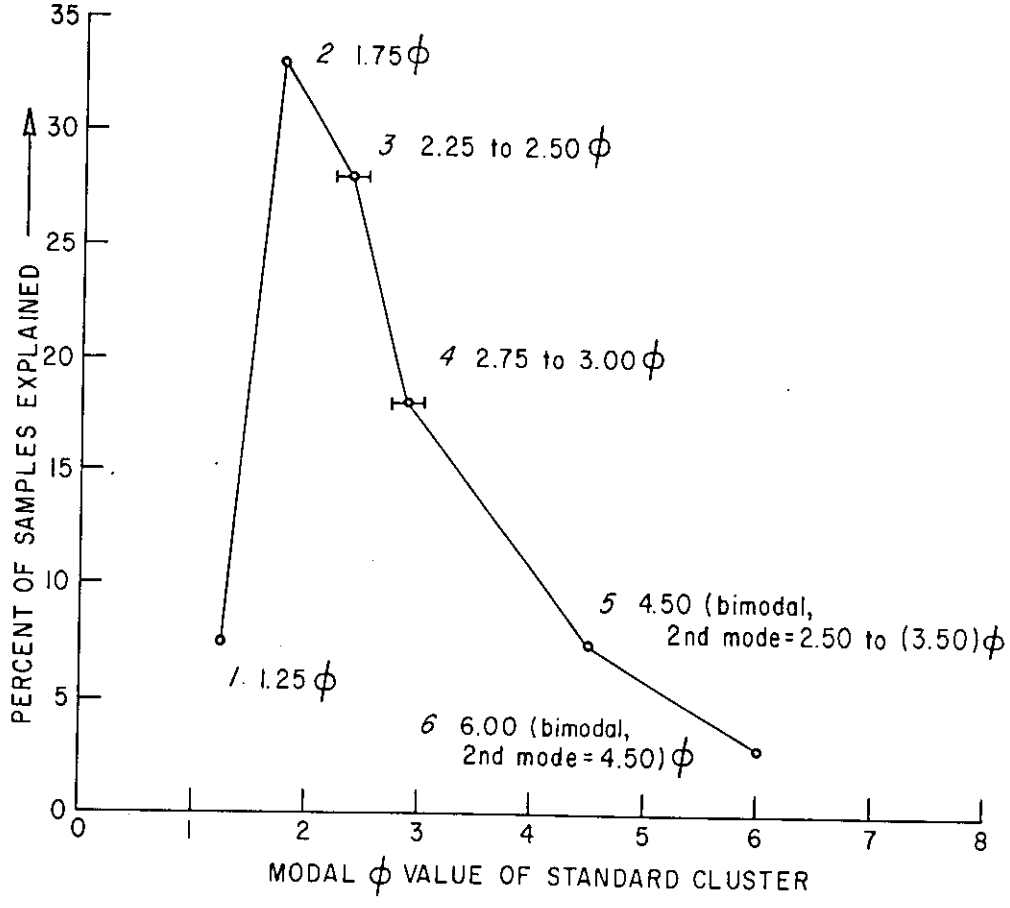

Figure 19. Relative importance of each of the standard clusters (from all three seasons).

of sediment transport. The implications are that, for most of the Columbia River Estuary sediments, consideration of both the mean and the standard deviation was redundant and that only one of the two needed to be considered.

3.1.3 Q-Mode Cluster Analysis

Dendrograms and Standard Clusters

The results of the cluster analysis of essentially all of the CREDDP samples are presented in several dendrograms (Figures 9-15). The 0.65 correlation level generally resulted in four to six large clusters and one to five small clusters representing only a few samples. The average fraction-weight histograms and cumulative curves for the clusters appear to the right of each dendrogram. In an attempt to compare grain size distributions within and among seasons, a subjective comparison of the 49 fraction-weight curves was made. On the basis of the means, modes, and general shapes of the grain size distribution curves, six "standard" clusters were chosen from the two June subsets. The modal grain size and respective contribution of each of these standard clusters is summarized in Figure 19 and in Table 5. In the following discussions, the

Table 5. Standard clusters chosen to represent 7 sets of 200 samples

Standard Type	Mode	Reference Curve	% of Samples
1	1.25	June 1980, Part II, Cluster 3/7	7.4
2	1.75	June 1980, Part II, Cluster 2/7	33.0
3	2.25-2.50	June 1980, Part II, Cluster 1/7	28.0
4	2.75-3.0	June 1980, Part I Cluster 6/6	18.0
5	4.5 (2nd=2.5-3.5)	June 1980, Part I, Cluster 5/6	7.4
6	6.0 (2nd=4.5)	June 1980, Part II Cluster 5/7	2.8

"reference curve" is the curve adopted as the standard for rating a curve similar to it as a "standard cluster type." The reference curves are included in Figures 14 and 15. The remaining 3.4% of the samples were included in clusters that could not be classified as any of the standard types. These clusters were assigned letters of the alphabet beginning

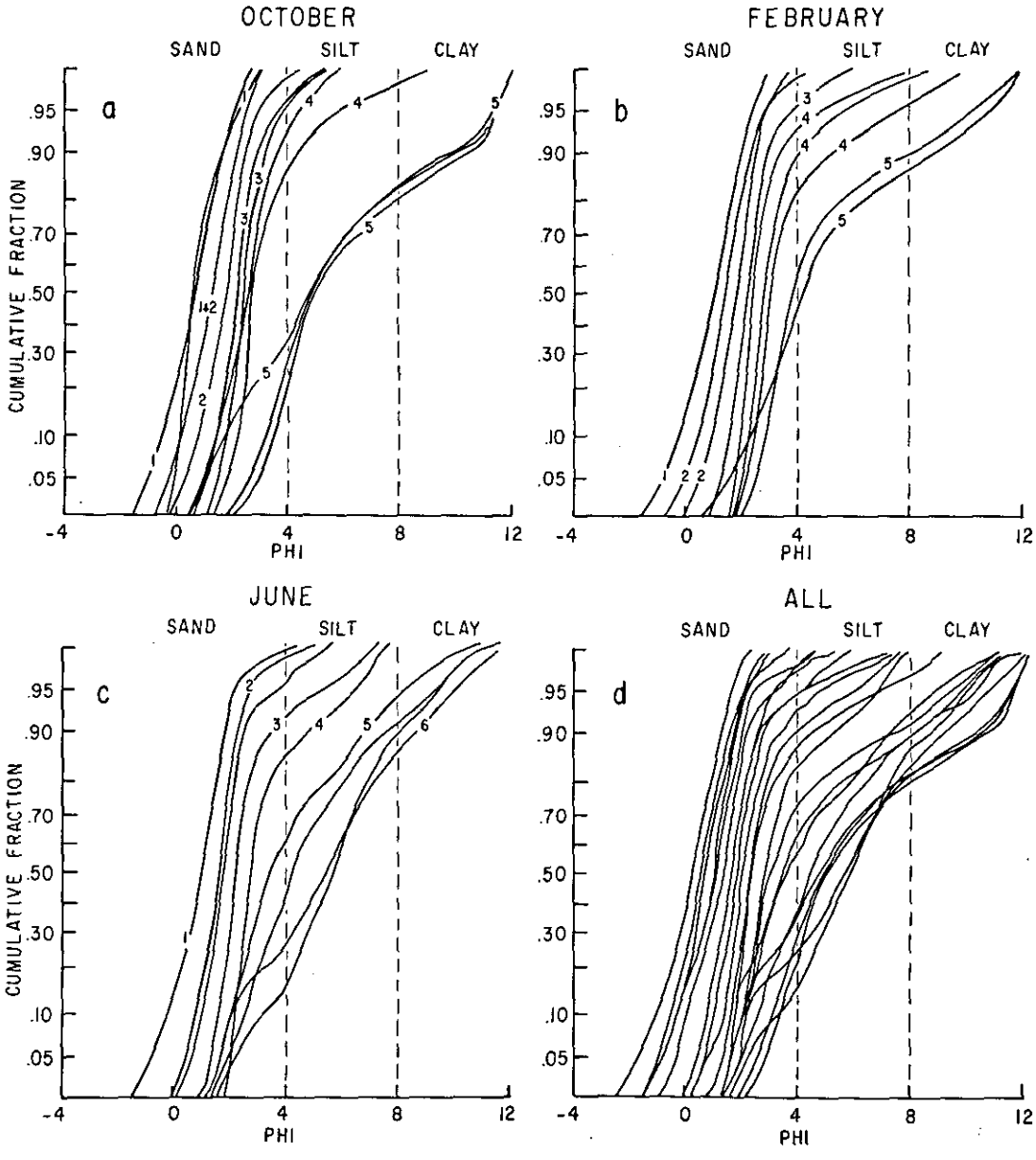

Figure 20. Cumulative sediment distribution curves of standard clusters (1 to 6) for the three seasons plotted separately (a, b, and c) and together (d).

with A, and ordered within each season by increasing mean phi size. Clusters with the same letter in different seasons were unrelated. Nearly one-third of all samples were similar to standard cluster 2, and another one-third resembled standard cluster 3. Approximately 90% of the samples tended to have sharply-defined peaks with distinct modes. As would be expected, kurtosis (peakedness) values were high and skewness (asymmetric departure from a normal distribution) values were near zero for many of the samples, especially those in the medium- to fine-sand range.

Ultimately, the success in a grouping scheme such as cluster analysis lies in its ability to repeatedly select groups of samples with consistent and distinct size distributions. Figure 20 demonstrates the superposition of the cumulative frequency curves of the major clusters from each run for all three seasons. In June 1980, the curves from each subset associated with each of the standard clusters were similar and distinct, implying that the cluster analysis made similar groupings in both runs. In October 1979, several of the clusters from the three runs were closely matched, but several were not. The most intraseason variablity occurred in February 1980. Figure 20 also includes cumulative frequency curves of the major clusters of all seven runs combined. Although the curves of some of the clusters with finer means demonstrate a tendency to group, the overall combination of clusters can only be described as a continuum. The implication is that either cluster analysis was not suitable for identification of grouping in the size-distribution data or that there was no intrinsic grouping in the data.

Areal Distribution of Clusters

The areal distribution of the clusters reflected the inability of the cluster analysis technique to consistently group the size data. The data represented a continuum which was somewhat arbitrarily subdivided by the clustering technique. The boundaries of these subdivisions varied with the chosen clusters, and the resultant distribution of clusters on the map shifted between seasons and subsets. An analogous effect might have been achieved by clustering bathymetry; if the resultant depth groupings (contours) had varied, they would have produced contour maps with different aspects. Among the clustered subsets from each season, the variation was minimal, and reasonable agreement among cluster distribution allowed the subsets to be combined into representative maps for each season. However, seasonal comparison was difficult because of the lack of one-to-one correspondence of clusters across seasons.

Figure 21 presents a generalized view of the distribution of the clusters in October 1979. Cluster 1, which grouped the coarsest sediments (1.00 phi mode), appeared

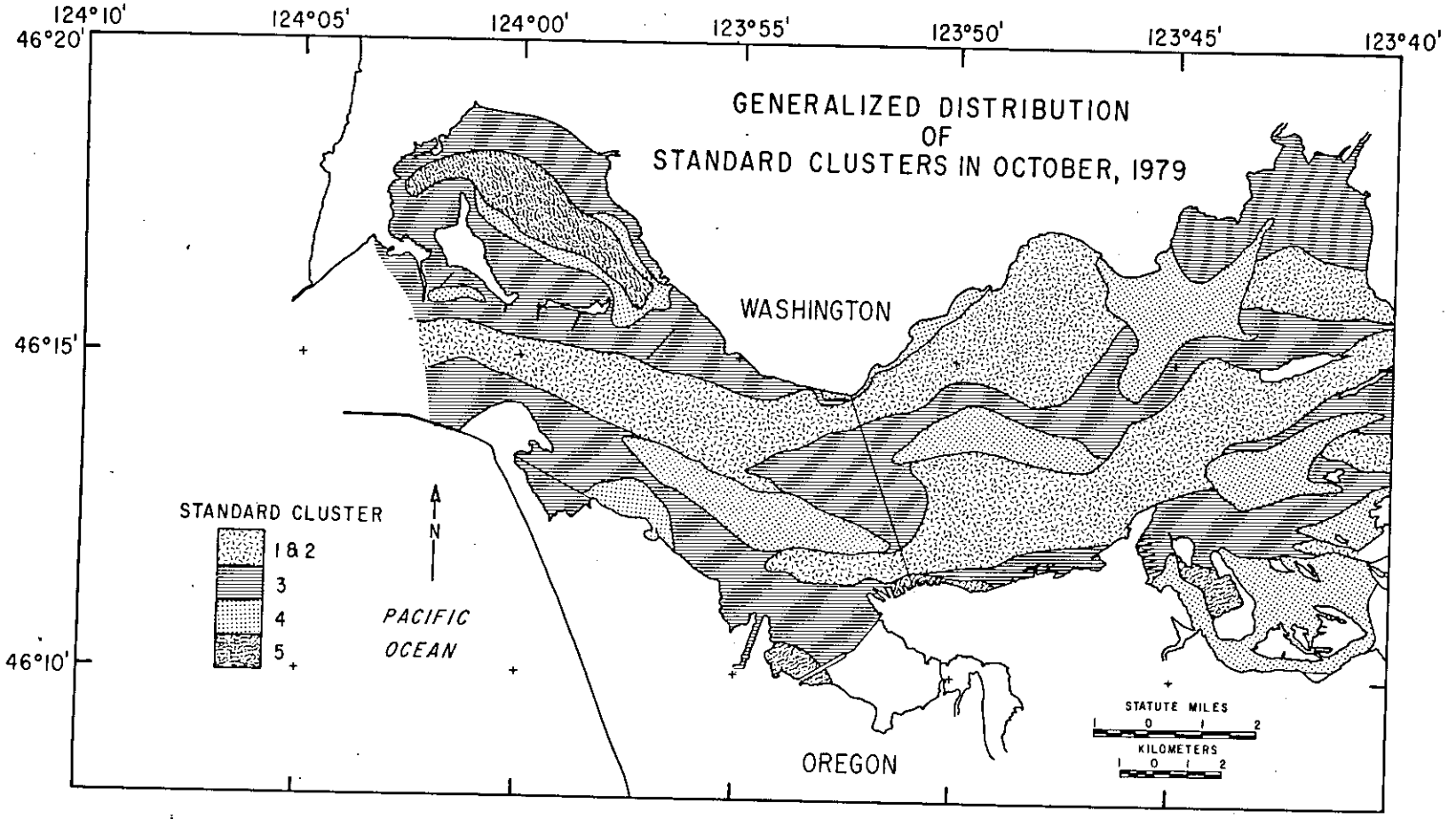

Figure 21. Generalized distribution of standard clusters in October 1979.

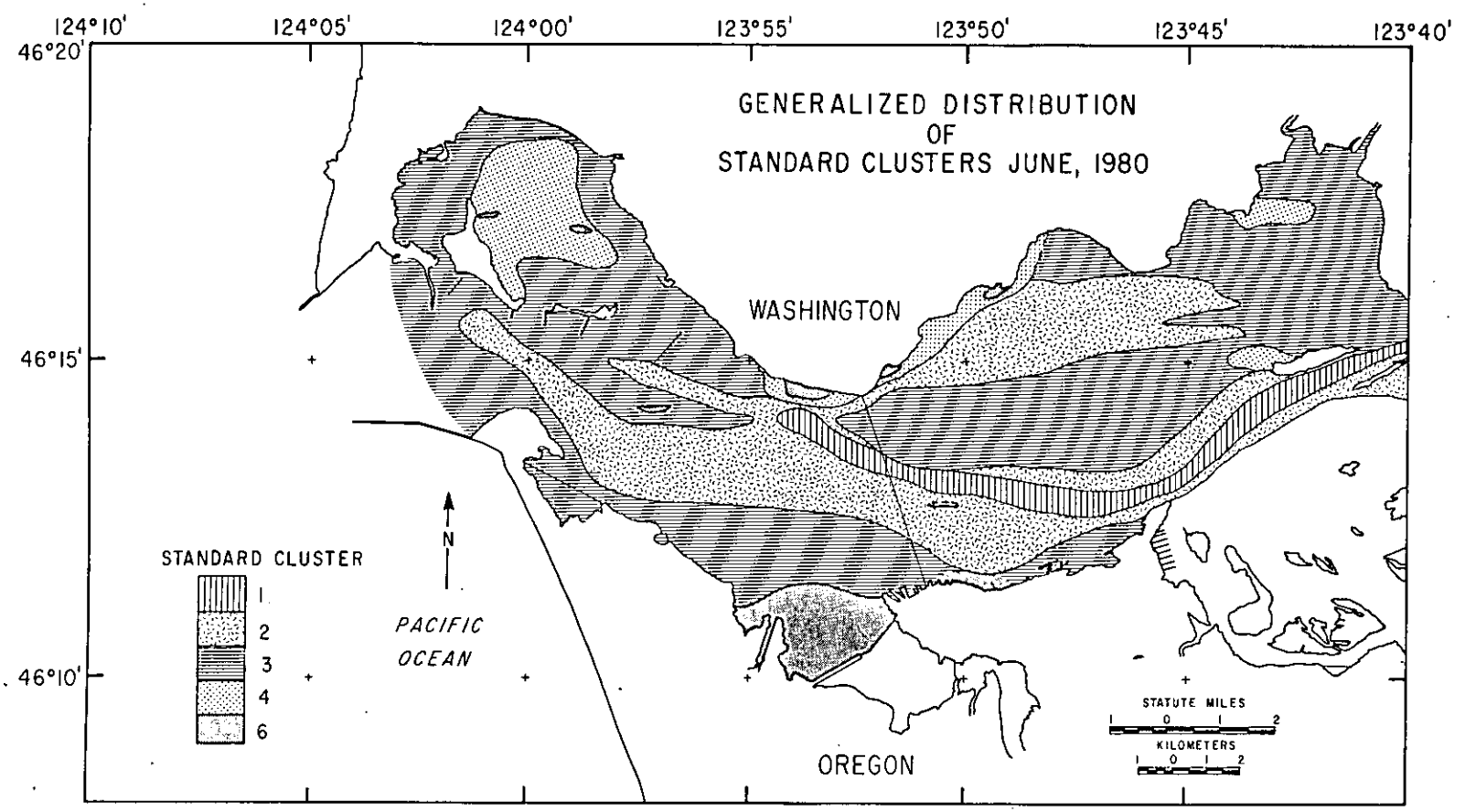

Figure 22. Generalized distribution of standard clusters in June 1980.

only in the main river channel near Rice Island, and is not shown separately on Figure 21. Sediments with modes between 1.50 and 2.75 phi (clusters 2 and 3) dominated most of the channel areas and extended across the shallow channel connecting the North Channel with the navigation channel near the Astoria-Megler Bridge. Cluster 4 (2.75 to 3.00 phi) appeared on both Desdemona Sands and Taylor Sands, as well as on the shoals of Cathlamet Bay. The broad channel system of Grays Bay was also characterized by cluster 4. Cluster 5 (4.50 to 6.00 phi) appeared almost exclusively in the dredged basin south and west of Mott and Lois Islands (Mott Basin). The upriver channels displayed a range of sediment in the medium-fine sand size classes (clusters 2, 3, and 4).

The distribution in June 1980 was markedly different, but it was difficult to determine how much of this difference was due to actual seasonal variation in the sediment size and how much was due to the variation in cluster grouping. Cluster 1 assumed a more important role in June (Figure 22) and occupied portions of the North Channel from Sand Island to the Astoria-Megler Bridge. The coarsest sediments (Cluster 1) extended across the connecting channel to the main channel near the bridge and were found in the main channel from Astoria to the upriver limits of the study area. Cluster 4 was present in much lower proportion during June, and was replaced on many of the mid-estuary shoals (Desdemona Sands and Taylor Sands) by either cluster 2 or 3. These clusters dominated most of the channels and shoals in the study area. Cluster 6, which contained samples with fine silt- and clay-size modes, was present only in June and was found in shallow embayments, notably Baker Bay, as well as in several small channels. Cluster 6 was found also in the larger channels, including the North Channel between Sand Island and Megler, and the South (main) Channel in the vicinity of Flavel Bar. The areal distribution of clusters in February demonstrated some of the characteristics of both October and June.

Q-mode Cluster Analysis With Six Variables

During the experiment in which six parameters (depth, river mile, mean, standard deviation, skewness and kurtosis) were used as variables in Q-mode cluster analysis, five clusters were produced at the 0.65 level of the cosine-theta similarity coefficient. The first and second largest clusters, which together accounted for 96% of the samples, matched standard cluster types 4 and 2, respectively, and corresponded to end-members #4 and 1 (from factor analysis), respectively. The fourth and fifth clusters both contained one sample, and both of these outliers were also identified as outliers in factor analysis and the other Q-mode cluster analysis. The third cluster (which had three samples) greatly resembled a cluster identified by the Q-mode cluster

analysis using all 47 size classes as variables in the same data set (and for two out of three parts of the complete October data set). The size-distribution curve of this cluster also resembled end-member #9 chosen during the factor analysis of the same data.

This Q-mode analysis determined characteristic groups of samples that corresponded well with the groups determined by factor analysis and the other Q-mode cluster analysis for the same data set. Considerably less input and less computation time was required to run the six-variable cluster analysis on the computer, yet the analysis yielded similar results. It did not discriminate as sharply as the methods using complete grain size distributions and, as a result, yielded fewer clusters at the 0.65 correlation level. The experiment emphasized the importance of two broad size-classes: those in the fine- to medium-sand range, and those in the fine-sand to silt range.

3.1.4 Relationships Among Sediment Parameters

Mean and Standard Deviation

As suggested by the results in the R-mode cluster analysis with six variables, there existed a well-defined relationship between the moment measures of mean and standard deviation in the CREDDP data. It is clear in Figure 23 that the best sorting (least standard deviation) occurred for samples with means near 2.25 phi. In general, well-sorted samples in this medium- to fine-sand range showed progressively worse sorting (higher standard deviations) both as the mean phi value increased (finer) and as the mean phi value decreased (coarser). Early workers have noted this phenomenon (Inman 1949; Griffiths 1951, 1967). Recently, Sly et al. (1983) presented figures very similar to Figure 23 and argued that the best sorting occurs in the 1.75 to 3.00 phi range because, as suggested by Hjulstrom (1939), it is in this range that sediment is most easily eroded. Sorting decreases beyond this range as the mobility of the sediment decreases. The plots of mean grain size and sorting support the results of the R-mode cluster analysis in suggesting that only one of these two parameters needed to be considered in evaluating the grain size distributions.

Mean, Skewness and Kurtosis

The variation of skewness and kurtosis with mean size is depicted in Figures 24, 25 and 26. These plots indicate that most of the negatively-skewed samples in the estuary had means of -0.5 to 3.00 phi, and that there was a well-defined tendency for skewness to increase with increasing mean phi value in the sand range. Samples in the silt range, however, tended to show a decrease in skewness with

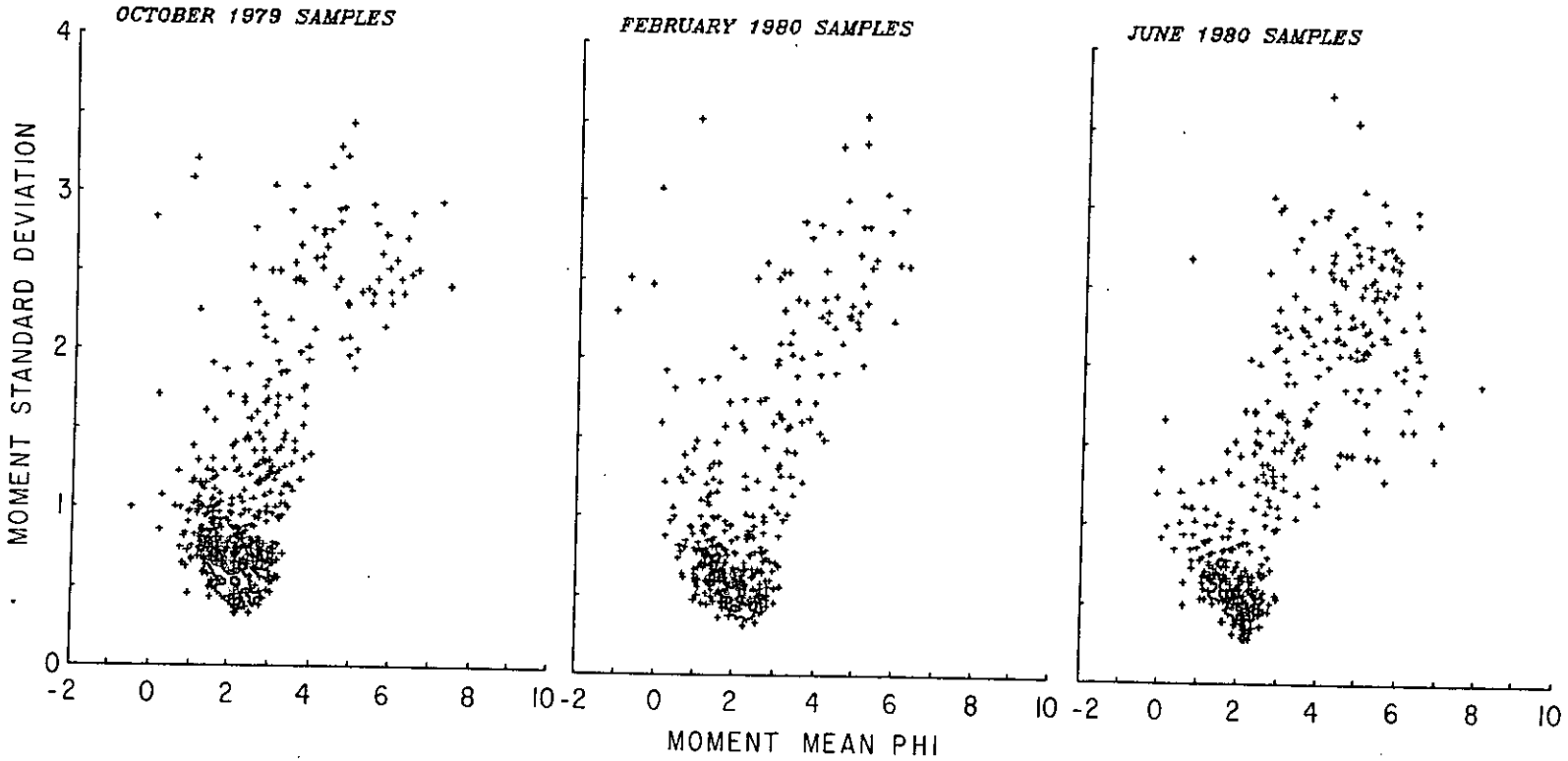

Figure 23. Relationship between standard deviation and mean grain size for three seasons.

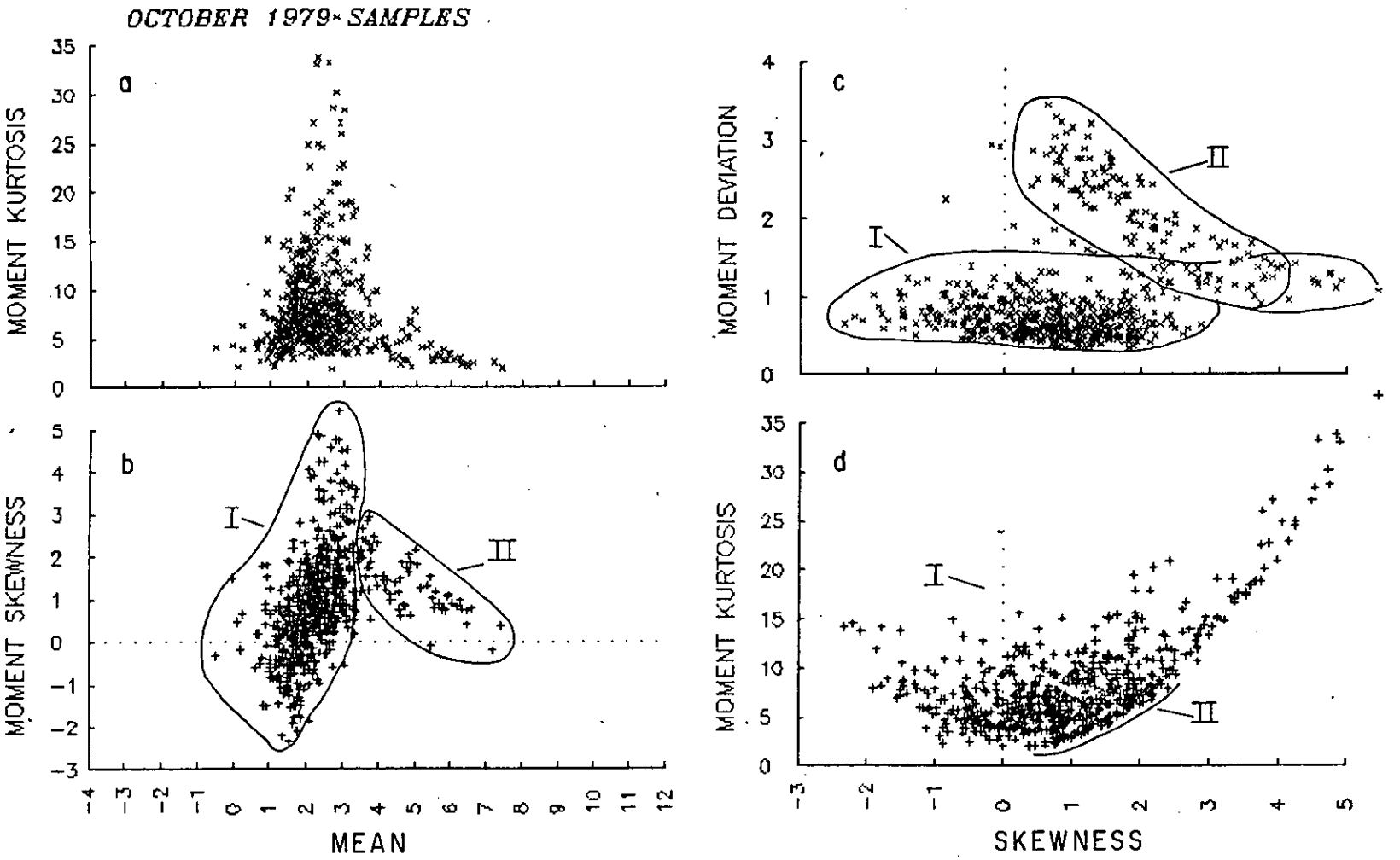

Figure 24. Plots of skewness and kurtosis versus mean (a and b), and standard deviation and kurtosis versus skewness (c and d) for all October 1979 samples.

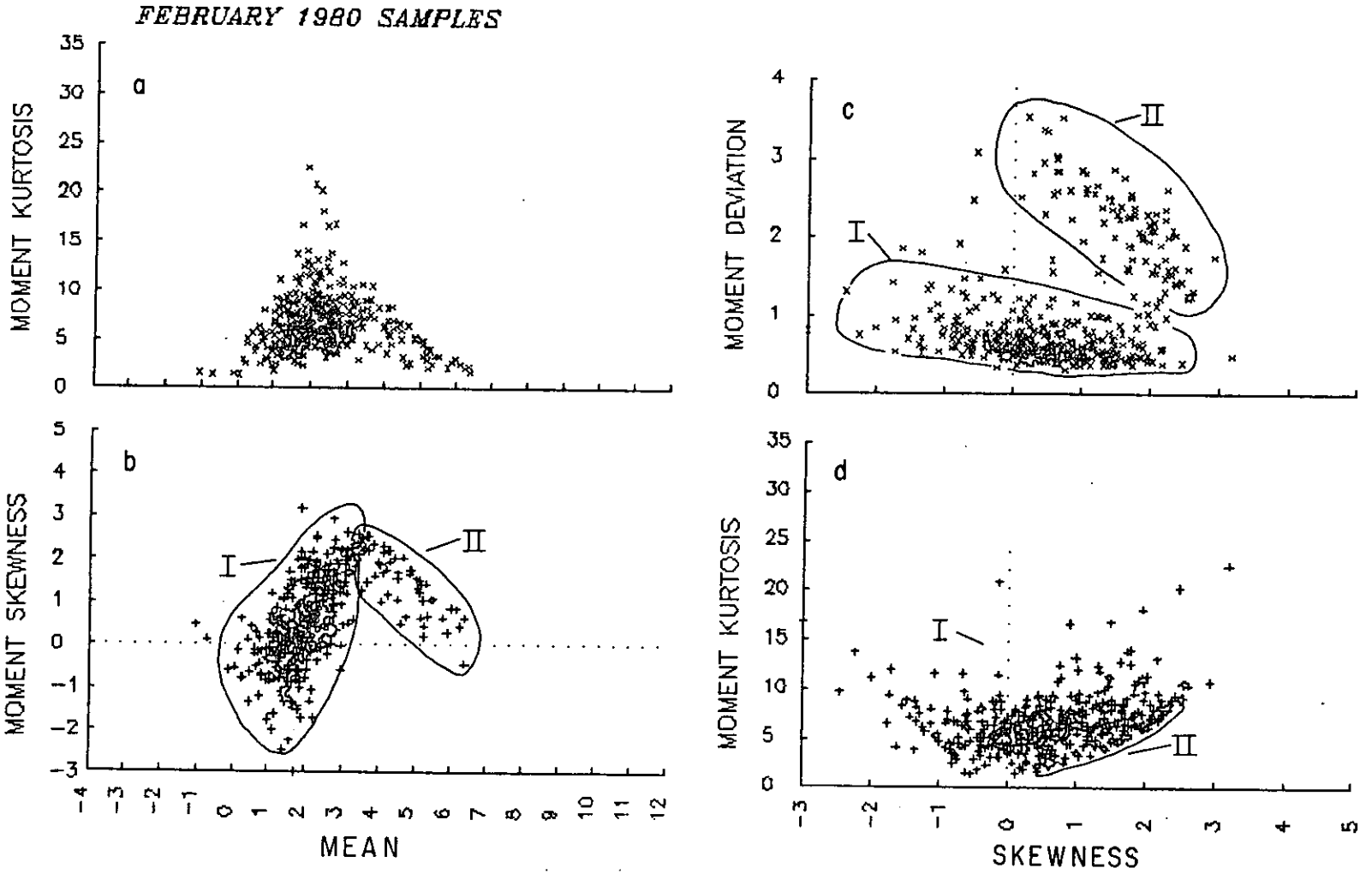

Figure 25. Plots of skewness and kurtosis versus mean (a and b), and standard deviation and kurtosis versus skewness (c and d) for all February 1980 samples.

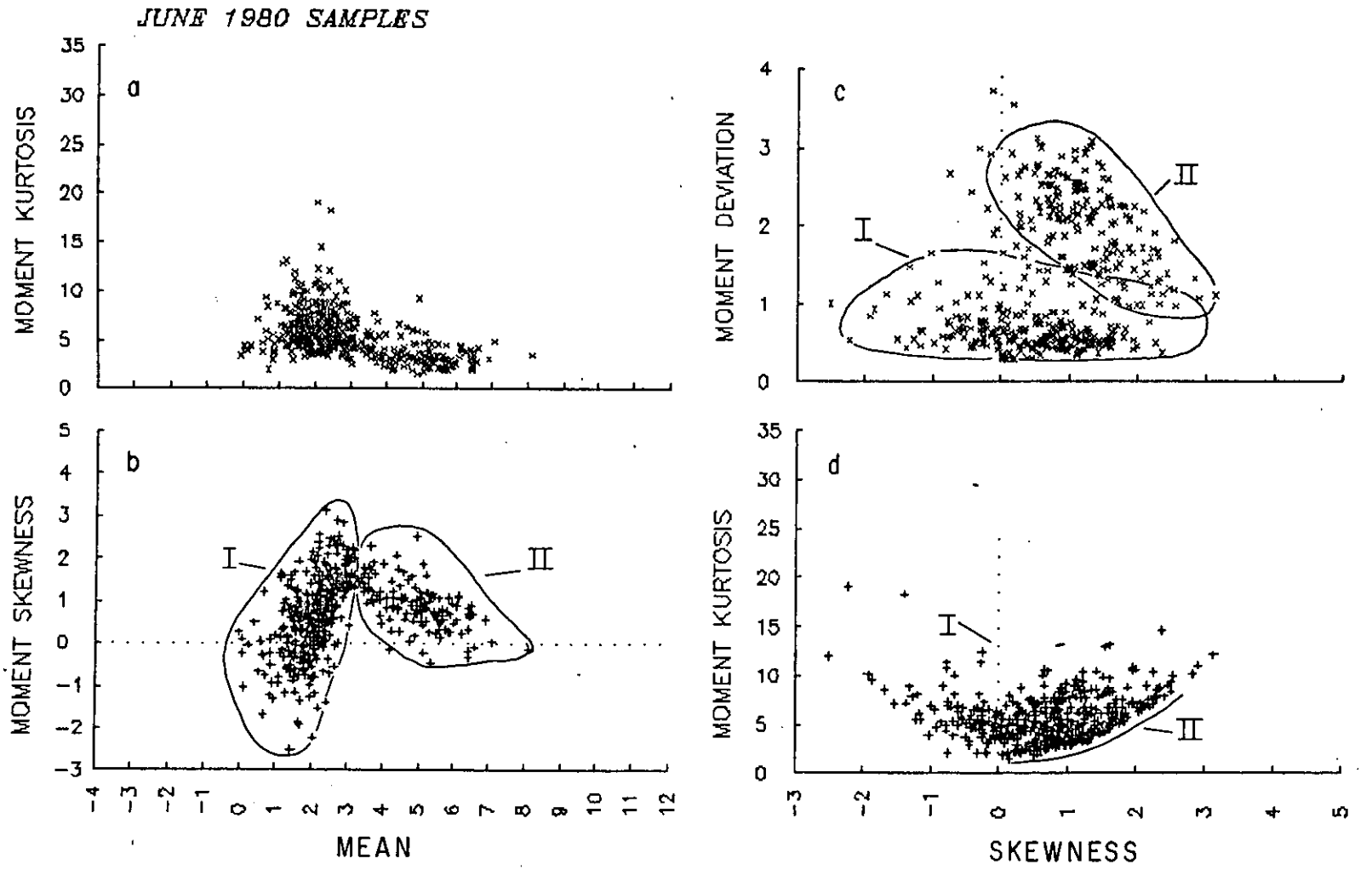

Figure 26. Plots of skewness and kurtosis versus mean (a and b), and standard deviation and kurtosis versus skewness (c and d) for all June 1980 samples.

increasing mean phi value, but only a few fine-grained samples (samples with means greater than 4.00 phi) actually had negatively-skewed distributions. The widest range of skewness values occurred in the fine sand sizes, those with means of 1.75 to 3.00 phi, while the narrowest range occured at 3.00 to 3.25 phi. This zone served to separate the two "fields" of samples that will also be encountered in other plots (Fields I and II, Figures 24, 25, and 26).

The plots of kurtosis against mean (Figures 24a, 25a, and 26a) show that kurtosis was the most variable and also achieved the highest values in the same medium- to fine-sand range. The highest values of kurtosis were found in the October data, and were associated with highly positively-skewed distributions.

Plots of Kurtosis and Deviation Against Skewness

Plots of the relationships between standard deviation and skewness and kurtosis and skewness for the three seasonal sampling efforts are presented as Figures 24c and d, 25c and d, and 26c and d. In all three seasons, two fairly discrete fields (labelled I and II) again occurred in the plots of standard deviation versus skewness: (1) for low values of standard deviation (sorting), skewness values occurred throughout a broad range from -2.5 to >5.0, but (2) in the skewness range of 0.0 to 3.0, a group of samples showed anomalously high standard deviations. This field of distributions began with high values of standard deviation (2.5 to 3.0) and skewness values of near zero and showed regular decrease in standard deviation with increasing skewness until it merged with the larger population with standard deviations near 2.0 and skewness values between 2.0 and 4.0 (Figures 24c, 25c, and 26c). Plots of the cluster numbers on the same axes indicated that nearly all of the cluster 5 samples from October and many (but not all) of the cluster 4 samples were to be found in this upper field of distributions (Field II). Although the field was dominated by these two clusters, it also contained several samples grouped with several other clusters, including clusters 2 and 3.

Plots of kurtosis against skewness are present in the lower portions of the same three figures (Figures 24d, 25d, and 26d). Sample distributions from all three seasons were delineated by a hyperbola-shaped boundary. In each case, the lowest kurtosis values and greatest ranges in kurtosis values occurred at zero skewness. As skewness values increased or decreased from zero, the lowest kurtosis values increased as a power function, and the ranges (but not maximum values) of kurtosis for a given skewness decreased. The field of samples (Field II) discussed above again appeared as a distinct grouping on the kurtosis/skewness plots. In this instance, the samples fell

along a narrow line, outlined on Figures 24d, 25d, and 26d. Over a skewness range of 0.3 to 2.0, this group of samples had the lowest kurtosis values in the estuary, ranging from approximately 2.0 to 7.0. The fields apparently merged at higher kurtosis values. Inspection of the actual samples involved in the fields (Field II) in these plots revealed that the same samples always formed the fine-fraction fields (Field II). In Figures 23b, 24b and 25b these samples appeared as a group with means greater than about 3.00 phi and large positive skewness values that decreased with increasing value of the mean.

The clear impression conveyed by the various plots was that two distinct groupings of sediment distribution occurred in the Columbia River Estuary. The numerically dominant group had means coarser than 3.00 phi, a variety of low to medium standard deviation values, and a wide range of skewness values. The skewness values for this group ranged from large negative to large positive values and generally increased with finer means. This group also contains the greatest range and highest values of kurtosis. Generally, the smaller group was finer grained, with higher mean phi values and poorer sorting (higher standard deviations). The skewness tended to decrease with increasing mean phi value for these samples, and the kurtosis values were low. This fine-grained group was commonly, but not exclusively, associated with clusters 4, 5 and 6. The implications of these relationships among the sediment parameters will be more fully explored in the Discussion section.

Passega Diagrams

Another graphic presentation of the sediment distributions is presented in Figures 27a-d. These plots relate the phi size at the coarsest one-percentile (C) with the median grain size of the distribution (M). Also known as C-M diagrams, these diagrams were introduced by Passega (1957, 1964) and were intended to group the distributions by their primary depositional agent. The fields and line segments superimposed on Figures 27a are after Passega (1957, 1977) and are meant to represent various relationships between the coarsest fraction of the sample and the median grain size of the sample. These diagrams may be valuable in identifying the depositional mechanism within one general environment (e.g., fluvial, pelagic-marine, beaches) or between environments. Within the fluvial environment, the distributions falling along line P-Q are associated with "tractive currents" (bedload transport), while those falling along line Q-R show the closest relationship and reflect the sorting capabilities of "bottom turbulence" (shear stress) in this easily-eroded size range. Distributions occurring along the R-S line have relatively fine-grained coarse fractions that are unrelated to the median grain size. Passega (1977) suggests that

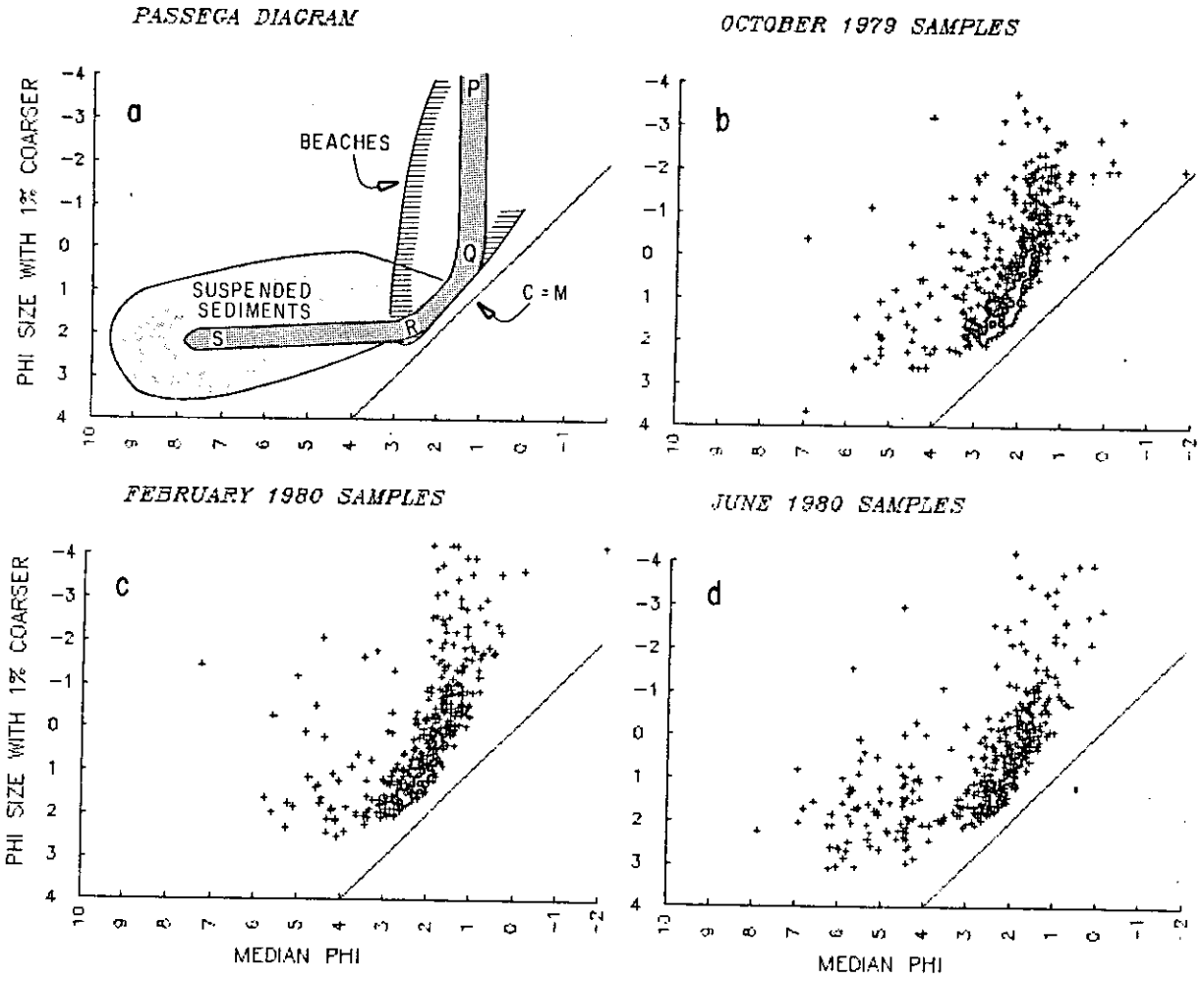

Figure 27. Passega diagrams.

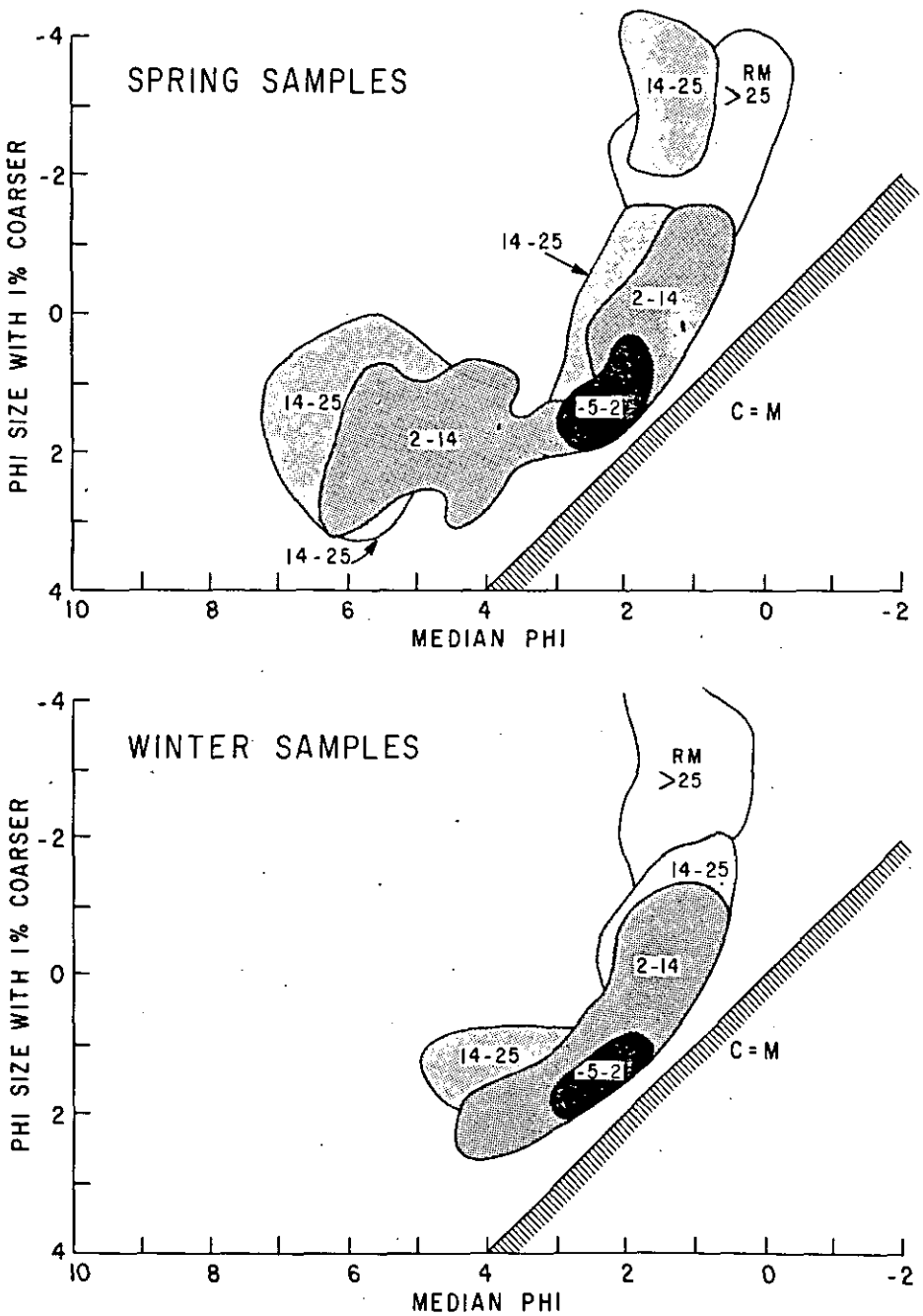

PASSEGA DIAGRAM
and
DISTANCE UPRIVER IN APPROXIMATE MILES (RM)

Figure 28. Passega diagrams and C-M fields associated with river mile location of samples.

these are the most poorly-sorted samples in the system, because the currents are insufficient to move the coarsest fraction, and fine-grained material from suspension can be admixed in any quantity. Application of the concept to the estuary sediments, however, is not straightforward. Figure 28 displays fields that represent the majority of the samples from each of four sections of the estuary in the winter season and in spring. The figure suggests that in the most seaward portions of the estuary (between RM--5 and RM-2) the sediments were tightly bunched and fell along the R-S portion of the Passega diagram. (RM refers to Columbia River Mile, measured in statute miles from the entrance to the estuary.) The samples from the more upriver portions of the estuary, RM-2 to RM-14, RM-14 to RM-25 and RM-25 were spread more widely across the plot. There was a tendency for the highest values of C to increase upriver, but a fine-grain contribution also appeared, especially in mid-estuary in winter. Although no full understanding of the sedimentation could be derived from the Passega diagrams alone, they did serve to emphasize that different processes may have been occurring throughout the estuary and that there were grain size variations along the estuary. The spatial distribution of grain size is reported in the following sections.

3.1.5 Spatial Variability of Grain Size

Variation of Grain Size With Depth

In several sedimentary environments the relation of grain size variation to flow depth is readily correlated with the processes active in that environment. For example, the classic model of fluvial sedimentation incorporates a fining-upward of grain size, whereas the model of beach and nearshore sedimentation includes a coarsening-upward of grain size (Reading 1978). The greater shear stress often found in the deeper portions of channel flows is associated with coarser sediments. In marine environments, where wave energy may be important only in shallow regions, the sediments are finer in deeper water. In the Columbia River Estuary the presence of similar trends would provide evidence for or against various sedimentary process models. The plots of moment mean grain size and sorting (standard deviation) as a function of depth are shown in Figure 29. In all three seasons, there was a weak tendency for mean grain size to increase with depth. Although least-squares linear fits to these trends yielded low correlation coefficients, the presence of the trend in all three seasons suggested that it was real, if not striking. Roy et al. (1982) presented a plot of factor extremal against depth and found the same weak correlation. They noted that the influence of several coarse samples from depths greater than 50 ft was important in defining the pattern and that if only the shallower-water data were considered, no discernible

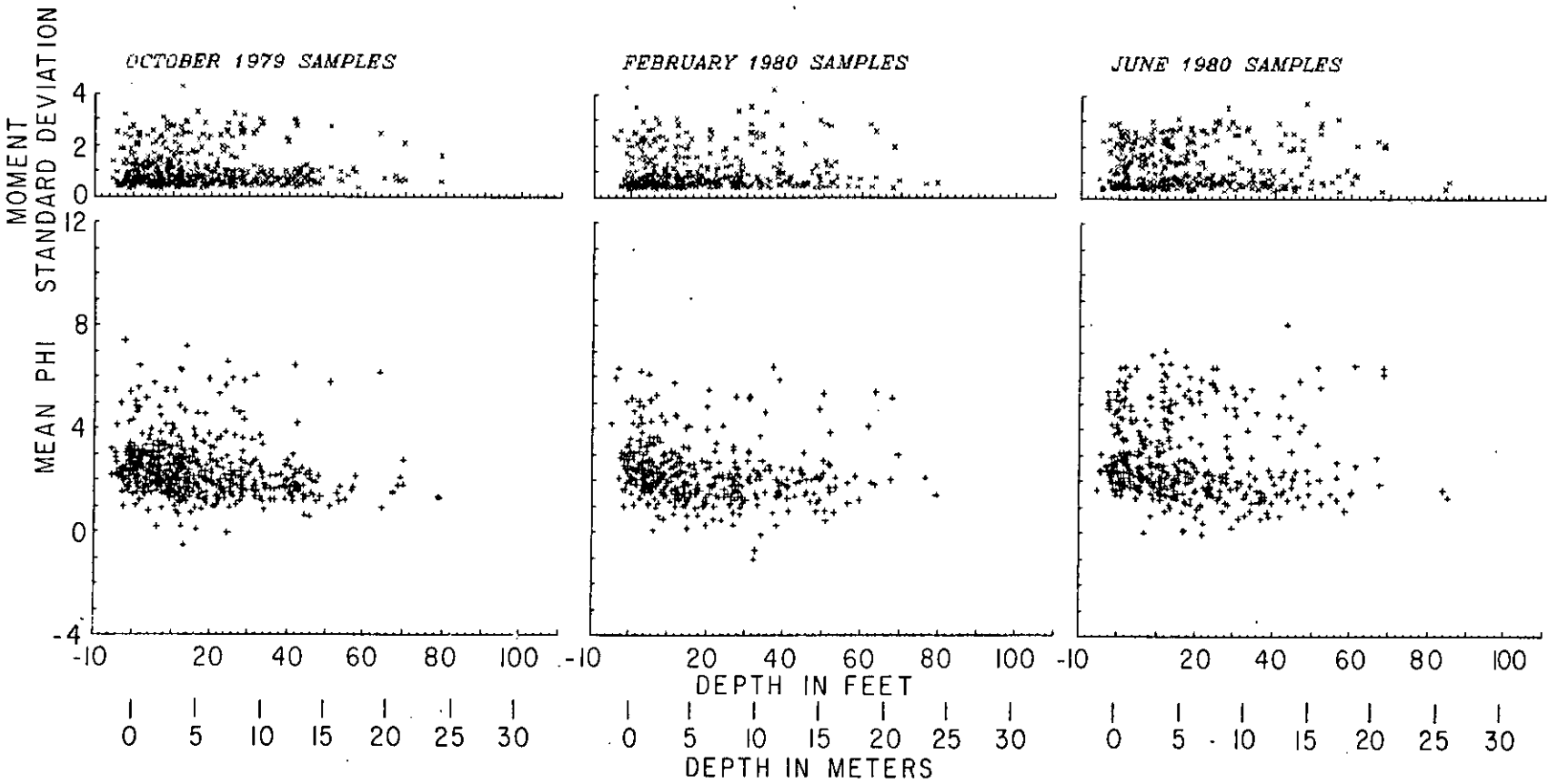

Figure 29. Mean and standard deviation (sorting) versus depth for all three seasons.

trend occurred. There was no apparent trend in sorting with depth.

In order to further resolve the data, the samples were partitioned by distance upriver (from the entrance) and by depth intervals. The distance sections chosen were actually based on the longitude of the sample location, but have been reported here with the corresponding approximate river mile. The most seaward section (RM--5 to RM-2) included all of the samples from beyond the jetties and the samples in the entrance channel to Jetty A. The section from RM-2 to RM-14 included the lower estuary to Astoria; the next section landward included the upper estuary to the usual upper limit of salinity intrusion, Harrington Point. The furthest upriver section included all those tidal-fluvial samples east of RM-25, i.e., from Harrington Point to the eastern tip of Puget Island.

The samples were divided into depth intervals that reflected processes and bathymetry. The shallowest interval (<3 ft, <1 m) incorporated all of the intertidal samples and probably most of those within the wavebase of the locally generated windwaves. The deepest interval (>30 ft, >10 m) was designed to exclude all samples except those from major channels of the estuary. The intervening depths were divided into two roughly equal intervals proscribed by the available bathymetric contours; the shallower included samples from between 3 to 18 ft (1 to 6 m) and the deeper included samples from depths 18 to 30 ft (1 to 6 m).

When the mean grain sizes were averaged for each of the depth intervals in each of the distance sections, trends in size variation with depth became more apparent. The hand-fit curves in Figure 30 depict the trends in the mean of 15 to 108 means from each distance-depth group. Data from all three CREDDP seasonal sampling efforts were combined with seasonal data from the Corps of Engineers cruises for these analyses. All but a few of the earlier samples were located in the two seaward sections (RM--5 to RM-2 and RM-2 to RM-14). Although high variances were associated with the means (Figure 30), the repetition of the curve-shapes for several seasons argues the case for accepting the trends as significant.

The variation among mean grain sizes with depth was most pronounced in the upriver (>RM-25) section. In all three seasons, a continuous fining-upward trend (i.e., finer with decreasing depth) was present. The greatest variation with depth in this upriver section occurred in winter, where the mean size of the deepest samples was 1.48 phi and the mean size of the shallow samples was 3.15 phi. The deep samples were only slightly finer in fall (1.68 phi) but fined less rapidly to 2.63 phi in water less than 3 ft deep. The spring samples were, in general, finer than those

of the other two seasons. The deep samples averaged 1.87 phi while the mean of the shallow samples was the finest average value obtained in all distance-depth groups (3.34 phi).

The curves from the upper estuary (RM-14 to RM-25, Figure 30) demonstrated less consistent trends. In fall and spring, the general trend was fining-upwards, but the finest sediments actually occurred in the intermediate depth intervals. The spring samples were generally finer than either of the other two seasons. The curve was reversed in the winter, when the deepest samples were slightly finer than those from fall, and where the intermediate-depth samples were slightly coarser than those of other seasons.

In the lower estuary, (RM-2 to RM-14), the curves from all three seasons were characterized by substantially finer sediments in the 3 to 18 ft depth intervals. The sediments generally fined upwards to this interval and then coarsened slightly in the intertidal depth interval (<3 ft). The spring samples were again dramatically finer, with a mean size of 3.28 phi in the 3 to 18 ft interval.

The only other occurrence of a coarsening-upward trend was noted in the seaward section (RM--5 to RM-2). The data in this section were supplemented with samples collected in the nearshore zone by Ballard (1964). The points plotted in Figure 30 represent the Inman (1952) means of Ballard's "trough" samples from Clatsop Spit (variable depths, generally less than 20 ft). Although no samples were obtained from the intertidal zone on either Clatsop Beach or Benson Beach (on Peacock Spit), it is likely that samples from these areas would have been as coarse or coarser than those from the nearshore troughs sampled by Ballard. Even without such samples, the coarsening-upward sequence was distinctive, when comparing the 18- to 30-ft and 3- to 18-ft depth intervals. The trend reversed at depth in most seasons. The mean size of the samples at >30 ft depths was coarser than the 18- to 30-ft samples in fall and winter but finer in spring. Although complex, the trends shown in these curves correlated well between seasons and are incorporated in the discussion of processes in the estuary.

Variation of Grain Size With Distance

All Samples: Three Seasons

A plot of mean grain size and sorting (standard deviation) for all of the CREDDP samples and all of the Corps of Engineers samples for each of the three seasons is shown in Figure 31. A wide scatter in both the mean size and the sorting is evident, but several prominent features may be observed. The envelope of the coarsest samples

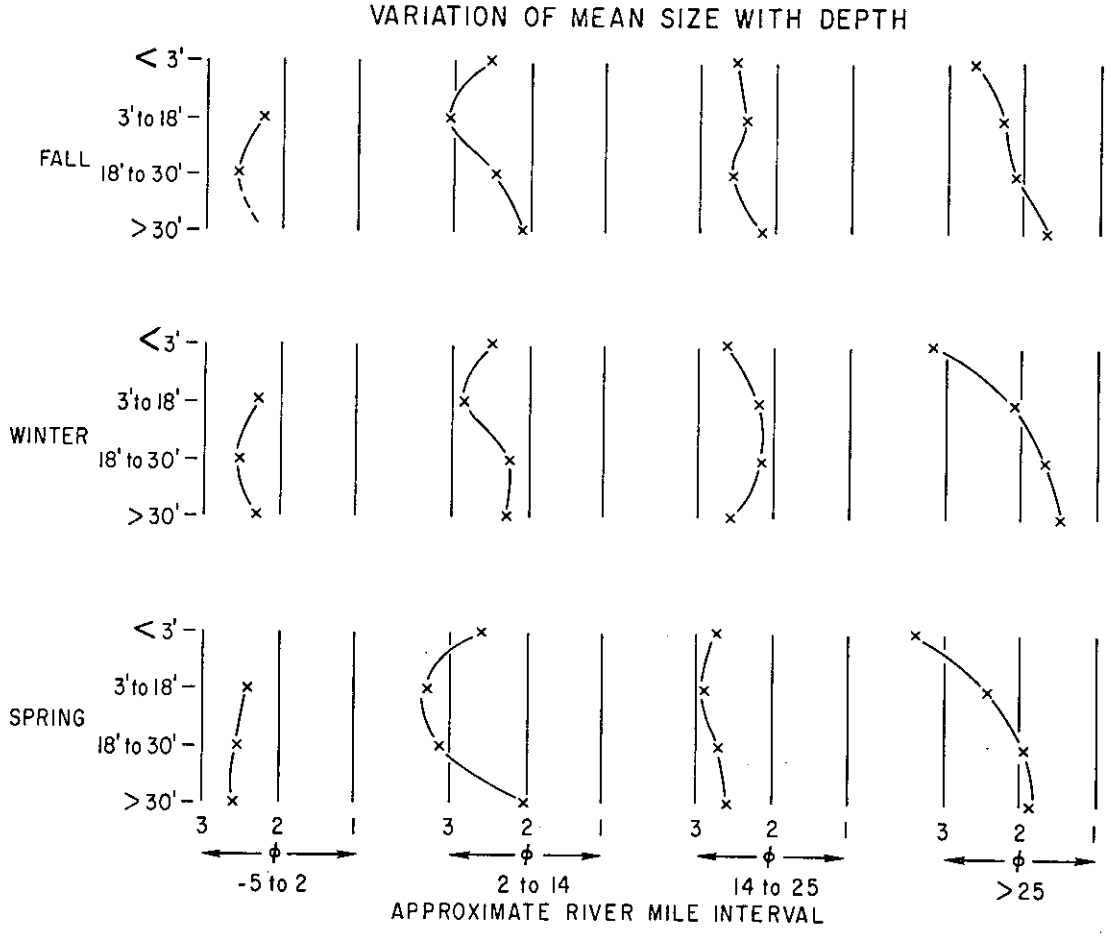

Figure 30. Variation of mean grain size with depth for four river mile intervals and three seasons.

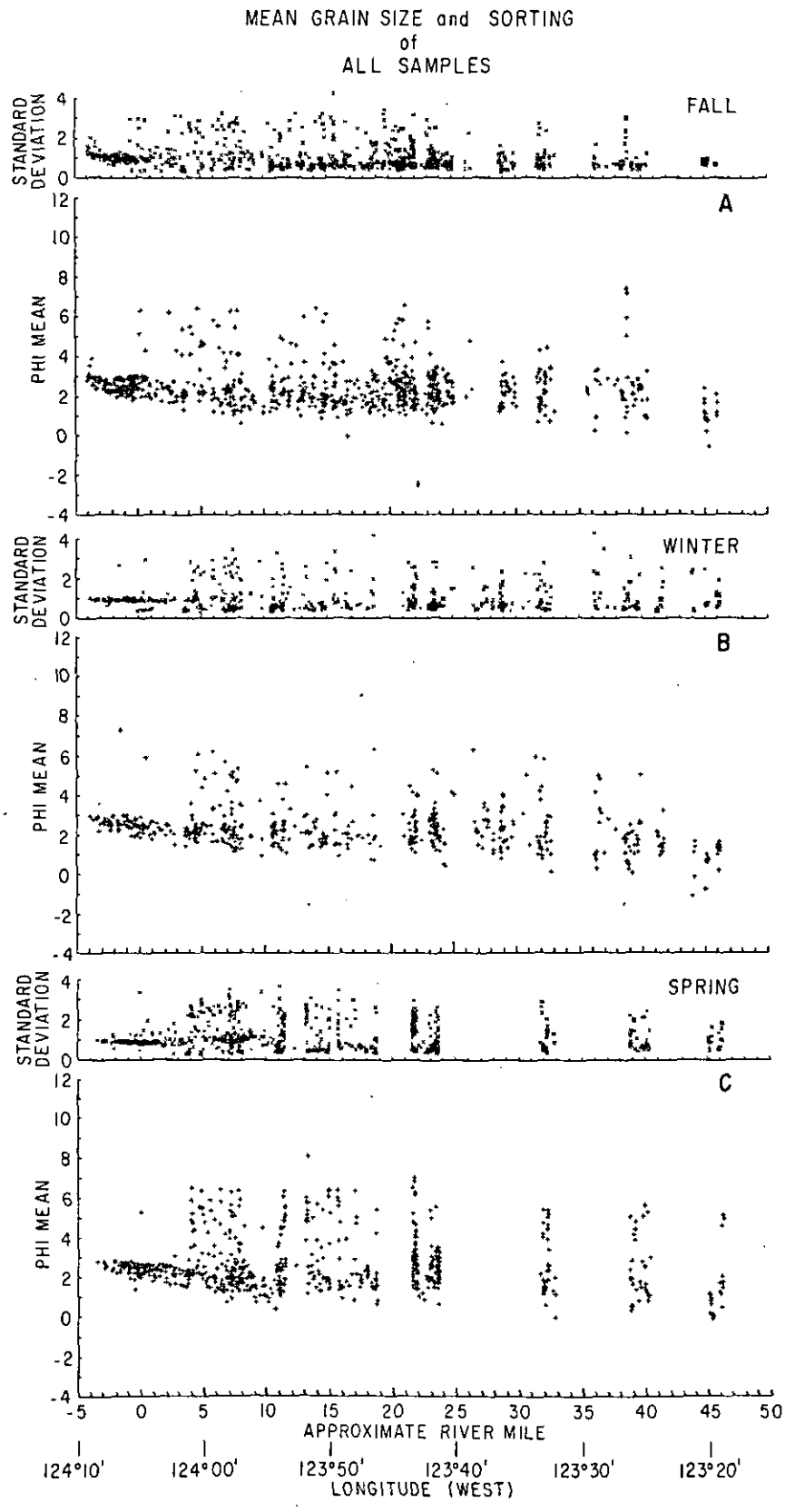

Figure 31. Mean and standard deviation (sorting) versus river mile for all samples from three seasons.

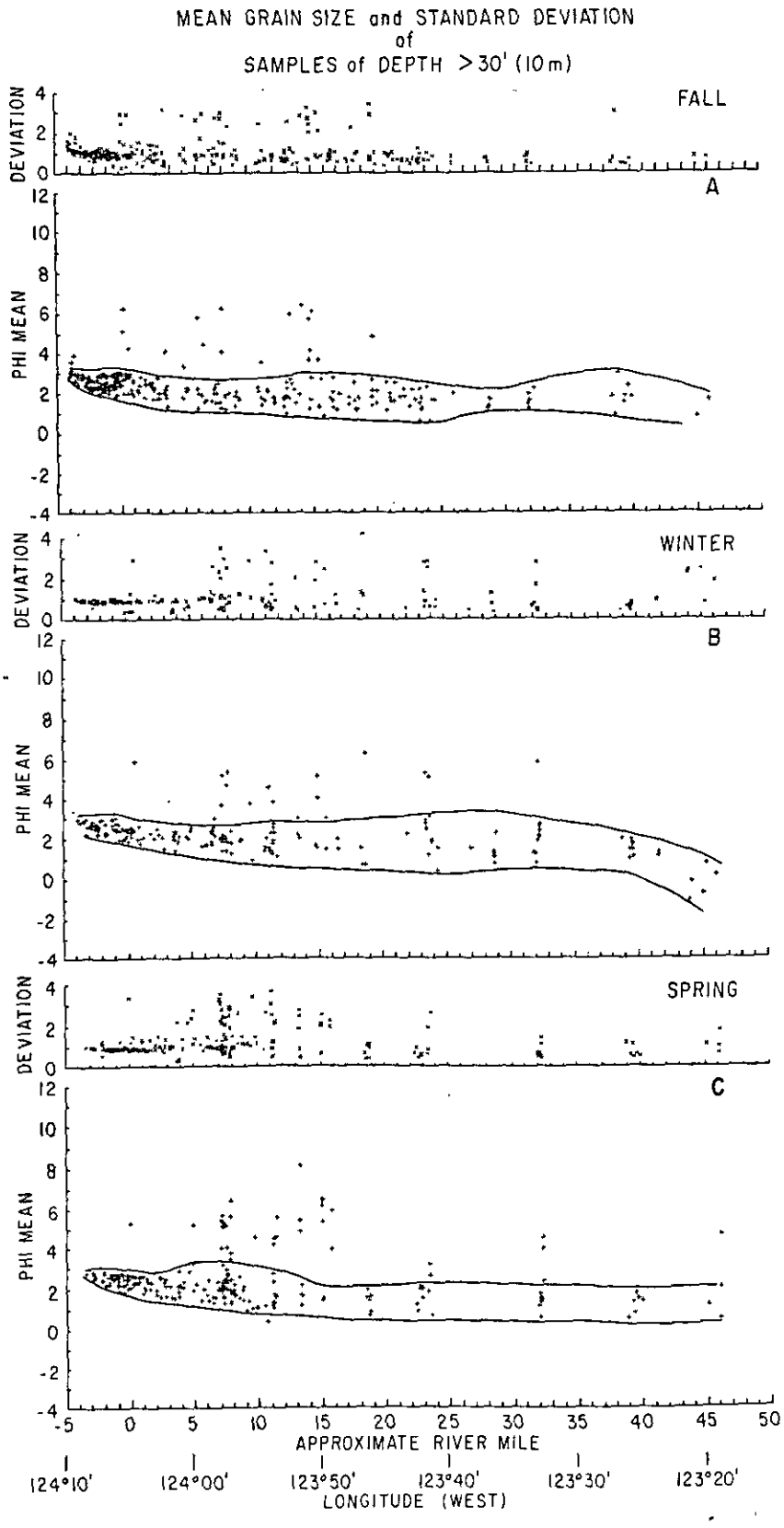

Figure 32. Mean grain size and standard deviation (sorting) versus river mile for channel samples (>30 ft) during three seasons.

appears to fine slightly downriver (seaward) in the eastern (upriver) sections (>RM-25). No trend with distance is noted in the upper or lower estuary until approximately RM-10. From RM-10 (approximately Hammond) seaward, the mean size of the coarsest samples increases steadily.

The envelope surrounding the finest samples is more variable than that surrounding the coarsest samples. Several groups of fine samples were present over sections of the estuary, and inspection shows that a large portion of these samples was collected from the several peripheral bays. Many of the fine samples located between RM-3 and RM-9 (Figure 31) were from Baker Bay; many of those in the fine group between RM-11 and RM-17 were from Youngs Bay; and many of the finer samples from RM-17 to RM-25 were from either Grays Bay or Cathlamet Bay.

In order to present various aspects of the grain size distribution with distance from the entrance, several plots are considered in the following discussion. Figure 32 is a plot of the mean size and sorting of the samples obtained from depths greater than 30 ft. Almost all of the samples from the peripheral bays have been excluded by this depth criterion, and the reduced variation in the mean grain size reflects that fact. Figure 33a presents the average grain sizes obtained by partitioning the data in Figure 32 into the same distance sections used above. On this plot, the vertical error bars represent one standard deviation around the average mean size, a measure of the sorting among the samples of each reach. The horizontal error bars indicate one standard deviation around the mean location (in RM) of the samples from each section. These were used as an estimate of locational bias in the sampling scheme; the overlap among seasons suggested that, with one exception, the samples were obtained from comparable reaches of the estuary. The somewhat anomalous location of the fall sample mean in the RM-2 to RM-14 section resulted from missing depth data in the older fall seasonal files. No data for the RM--5 to RM-2 section is presented for the same reason. The inclusion of estimated depths for the fall seasonal data from the Corps of Engineers samples would restore this point to the appropriate location further seaward.

Samples From >30 ft: Three Seasons

Considered together, Figures 32 and 33 define several trends among the samples from deeper than 30 feet. Most of the samples fall into a fairly narrow mean size range, which has been emphasized in Figure 32. Sample means near the entrance of the estuary and upriver to approximately RM-5 or RM-6 were very tightly grouped and exhibited a distinct tendency to fine seaward. The coarsest mean size found near RM-5 was about 1.25 phi and the coarsest mean size found

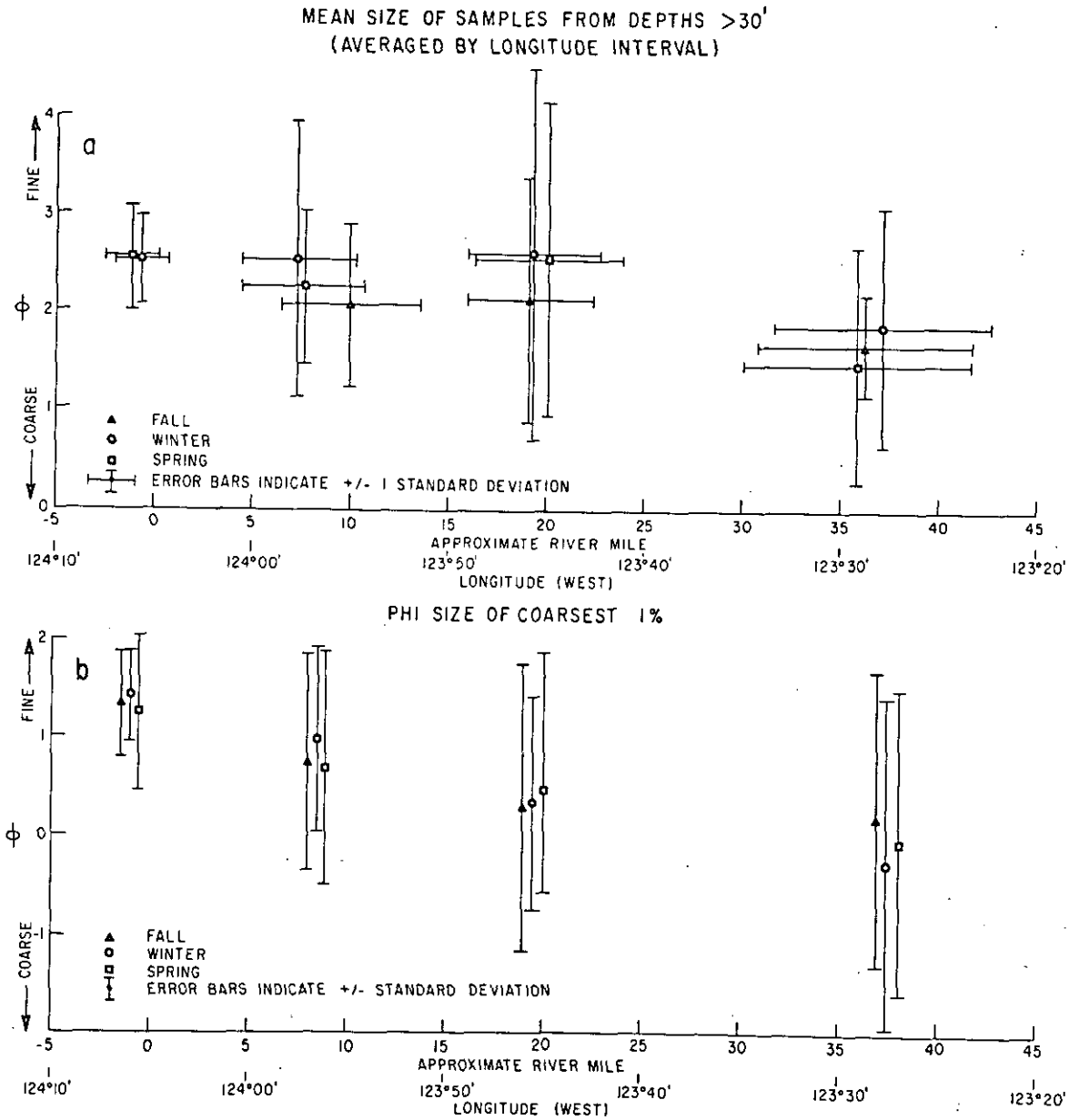

Figure 33. (a) Average mean grain size of samples from four river mile intervals and three seasons. (b) (b) Average phi size of the coarsest one-percentile from four river mile intervals and three seasons.

further seaward at RM--5 was finer than 2.00 phi. Samples from the entrance region also displayed the best sorting, as measured by both the standard deviation (within samples) and by the variance of the means (among samples). No difference among the seasons was evident in this area.

The samples from the upriver portions of the study area showed less variance about the average mean grain size than those from the two middle sections, but more than those near the entrance. The mean size in the upriver section (>RM-25) was coarser than the mean size in the more seaward sections in all three seasons. Figure 33a suggests that the mean grain size decreased from the upriver section to the upper estuary section (RM-14 to RM-25), showed no well-defined trend between the middle sections, and then continued to decrease seaward from the lower estuary to the entrance section (RM--5 to RM-2). The variation among sample means was higher in the middle sections than in either the upriver section or the entrance section. The source of this variation in middle sections (RM-2 to RM-14 and RM-14 to RM-25) is evident in Figure 32. Between approximately RM-5 and RM-20, a "bulge" in the graph consisting of finer samples extends above the majority of the samples. Unlike most of the fine samples included in Figure 31 (which also includes these samples), the samples were not associated with peripheral bays, but were located in the main channels of the estuary. This concentration of fine samples from the deeper portions of the estuary, and their localized distribution in distance from the entrance is an important result of these investigations and is addressed in the Discussion section.

Coarsest One-Percentile: Three Seasons

An important trend identified in Figure 33a is re-emphasized in Figure 33b. Figure 33b depicts the variation in the mean of the coarsest one-percentile (C of the Passega diagram) of each of the samples with distance, as well as the standard deviations about these means. The means were calculated for all of the samples in each of the four distance sections without regard to depth. A well-defined trend appeared in the means; the size of the coarsest one-percentile decreased continuously with distance downriver (seaward). The variance around these means also decreased, with the result that the estimated coarsest fraction in the river (i.e., one standard deviation coarser than the mean coarsest one-percentile) decreased from about -2.00 phi in the upriver section to 0.5 phi in the most seaward section. This trend has important implications to the sedimentology of the estuary and is discussed in more detail below.

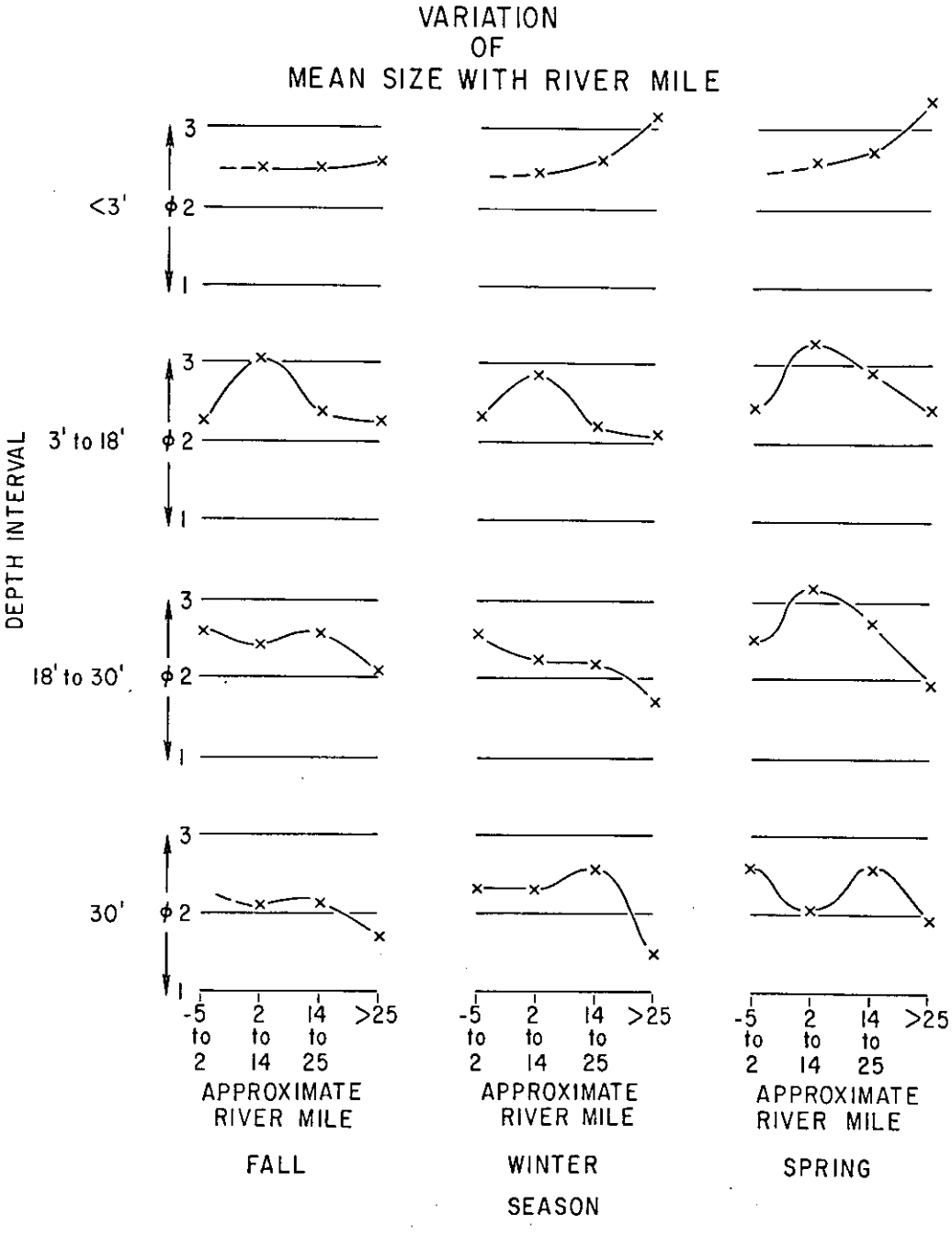

Figure 34. Variation of average mean grain size with river mile, for four depth intervals and three seasons.

Overall Trends

To present the results of the mean grain size data by depth interval and by distance section in a manner that emphasizes the variation with distance, the same data used in Figure 30 have been replotted in Figure 34. Figure 34 presents the hand-fit trends for the mean size in each of the four standard-depth intervals, but in this case each curve represents the grain size trend for the entire estuary for one season and one of the four depth intervals. The contribution from samples in each of the depth intervals was evaluated from these curves. One trend exhibited in these data was in contradiction to the fining-seaward trends already discussed. The intertidal sediments (depth <3 ft) became increasingly coarser seaward (downriver). This trend was more marked in spring and winter, but was also present in fall. Samples from the upriver section (>RM-25) were especially fine in spring (3.34 phi), but all three seasons displayed approximately the same mean grain size in the lower estuary (2.5 phi, RM-2 to RM-14). This tendency for the shallowest samples to become coarser with distance seaward was important evidence relating to the dominant processes in the estuary and is referred to again in the Discussion section.

Another important trend appeared consistently across seasons in the depth interval between 3 and 18 ft. The samples from these depths fined dramatically from the upriver section (<RM-25) to the lower estuary (RM-2 to RM-14). For example, in fall the mean grain size in the upriver section in this depth interval was 2.24 phi; it increased (became finer)in the upper estuary (RM-14 to RM-25) to 2.37 phi; and it jumped to 3.05 phi in the lower estuary. This trend appeared to a greater or lesser extent in fall and spring as well.

The data from the lower two depth intervals were less coherent. In the 18 to 30 ft interval, the samples exhibited an overall tendency to fine seaward, but the location of the finest sediments varied from season to season. In the lowest interval, the fining-seaward trend that is apparent in Figure 33 was aliased by the averaging scheme and the bulge containing fine sediments. The resultant curves that are flattened near the seaward section, also contained a fine mean that changed position with season.

The data plotted in Figure 34 contain two other significant results: 1) regardless of the variation in the other sections, the seaward section (RM--5 to RM-2) showed the least seasonal variation, and 2) the samples from spring (represented almost exclusively by June 1980, except in the two seaward sections) were generally finer than those from the other two seasons. These results are interpreted in the

Discussion section as well.

Areal Distribution of Sediments: Three Seasons

During the course of this study, maps were generated that depicted the areal distribution of mean grain size, sorting, coarsest one-percentile, skewness, and percent silt plus clay. For the purpose of presenting the results of these efforts, the parameters that provided the most information were compiled on two kinds of maps: 1) the generalized sediment distribution maps, one for each of the three seasons (Figures 35, 36, and 37), and 2) a generalized silt plus clay map which combines the data from all three seasons and summarizes the results of more than 2000 grain size analyses (Figure 38). The density of data in some areas of the estuary precludes adequate resolution of the distributions at the map scale used in this report, and the reader is encouraged to refer to the Atlas of Physical and Biological Characteristics (Fox 1984) for a more detailed graphical representation of the sediment distribution in the estuary. On the other hand, sample density in some areas was insufficient to allow confident extrapolations to be made. In the absence of other data, extrapolations in were made along bathymetric contours or on the basis of other morphologic considerations. Many of the biases and working hypothesis of the investigators are imbedded in the resultant mapped distributions.

For the generalized sediment distribution maps, the following parameters were mapped: 1) mean grain size, in three broad intervals: <2.25 phi, 2.25 phi to 3.00 phi, and >3.00 phi, 2) skewness, <0.0 and >0.0, 3) location of two-layered samples, shown as coarse sediments overlying fine or fine over coarse, 4) location of sandy-silt clasts ("mudballs" in Roy et al. 1982), and 5) location of acoustically reflective bottoms from side-scan sonar records that are interpreted as bedrock, talus or coarse gravel.

Overall Trends

The gross patterns of sediment distribution were similar in all three seasons. Most of the estuary was floored in either fine- or medium-grained sand. The offshore regions, including the outer tidal delta and most of the seaward portions of the estuary excluding the channel proper, were characterized by fine-sand sediments. Fine sand was also found on most of the large sandy shoals in the lower and upper estuary, especially the Sand Islands, Desdemona Sands, and Taylor Sands, and the unvegetated shoals of Cathlamet Bay. Medium sand predominated in most of the remaining channel areas. The sands with the coarsest mean grain size were generally found along the main (navigation) channel in the fluvial reaches and the upper estuary. These sands were usually negatively-skewed and

have one-percentiles coarser than 0.0 phi. The coarsest sands were obtained from the deep bathymetric depressions found near some of the Tertiary rock headlands and man-made dikes and jetties, or when the troughs of large bedforms in the fluvial reaches that were selectively sampled. Only a few samples containing any gravel-sized material were recovered, and these were located in the immediate vicinity of rock headlands or talus slopes. The sampling equipment was not ideal for recovering gravel-sized material; the talus and gravel distributions indicated on the maps were inferred from highly reflective bottom returns on the side-scan records. Some of these reflections may also have been bedrock outcrops.

The finest sediments were found in the peripheral bays, notably Baker Bay, Youngs Bay, Cathlamet Bay, and Mott Basin. Fine sediments (sandy-silt and silt-clay) were also found in both small and large channels in samples from some seasons. These channel silts were often found in thin (1- to 2-in, 2- to 5-cm) layers that were deposited over fine-medium, well-sorted sands. The locations of samples that contained any obvious stratigraphy are indicated on the three seasonal sediment distribution maps. Only a few of these layered samples displayed the inverse relationship of coarse material overlying finer sediments.

Seasonal Variation

The overall sediment distribution was remarkably similar to that described by Hubbell and Glenn (1973) on the basis of many fewer samples from only one season. They described the variation of grain size with location as follows:

> "For samples from the channels, [mean grain size] increases (samples become finer), [sorting] remains relatively unchanged, and [skewness] becomes positive or less negative (distributions become less skewed toward the coarse particles) from the head to mouth of the estuary"

(Hubbell and Glenn 1973, p. L-18). The present study, however, has been able to detect seasonal changes in the grain size distribution patterns. Comparison of Figures 35, 36, and 37 reveals that the distribution of negatively-skewed, coarse to medium sand varied considerably with season. In spring, a tongue of this coarse material extended downriver along the main channel to approximately Astoria, where it crossed to the North Channel along the trend of the broad diagonal channel between Taylor Sands and Desdemona Sands. In fall, this coarse material was observed in the main river channel to Tongue Point, but seaward of Tongue Point, the distribution became patchy along the diagonal channel. In winter, the upriver pattern was again

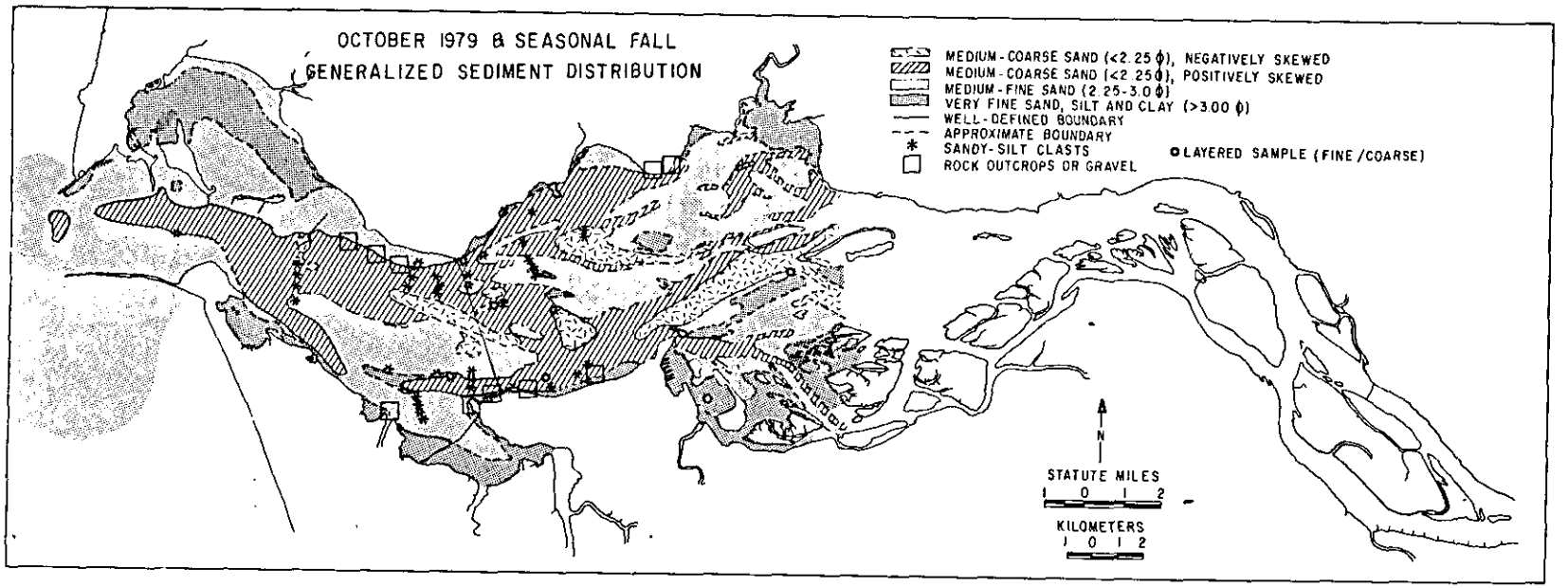

Figure 35. Generalized sediment distribution map for October 1979 and seasonal fall samples.

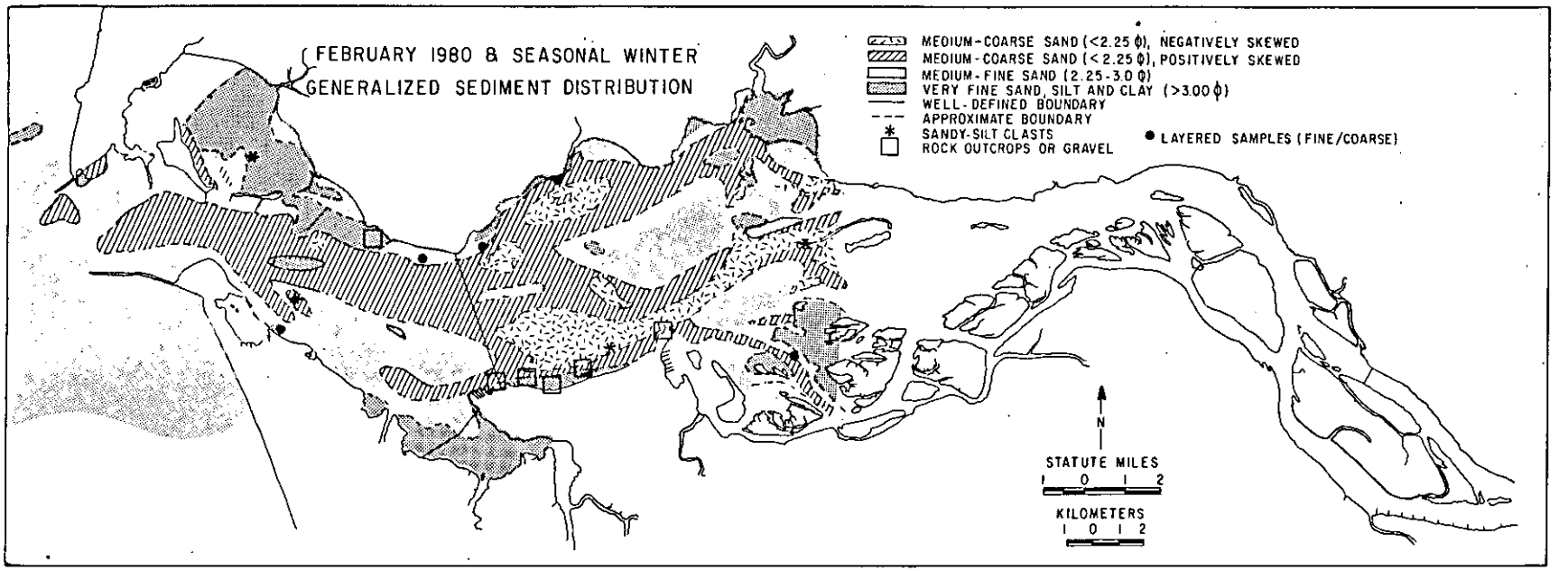

Figure 36. Generalized sediment distribution map for February 1980 and seasonal winter samples.

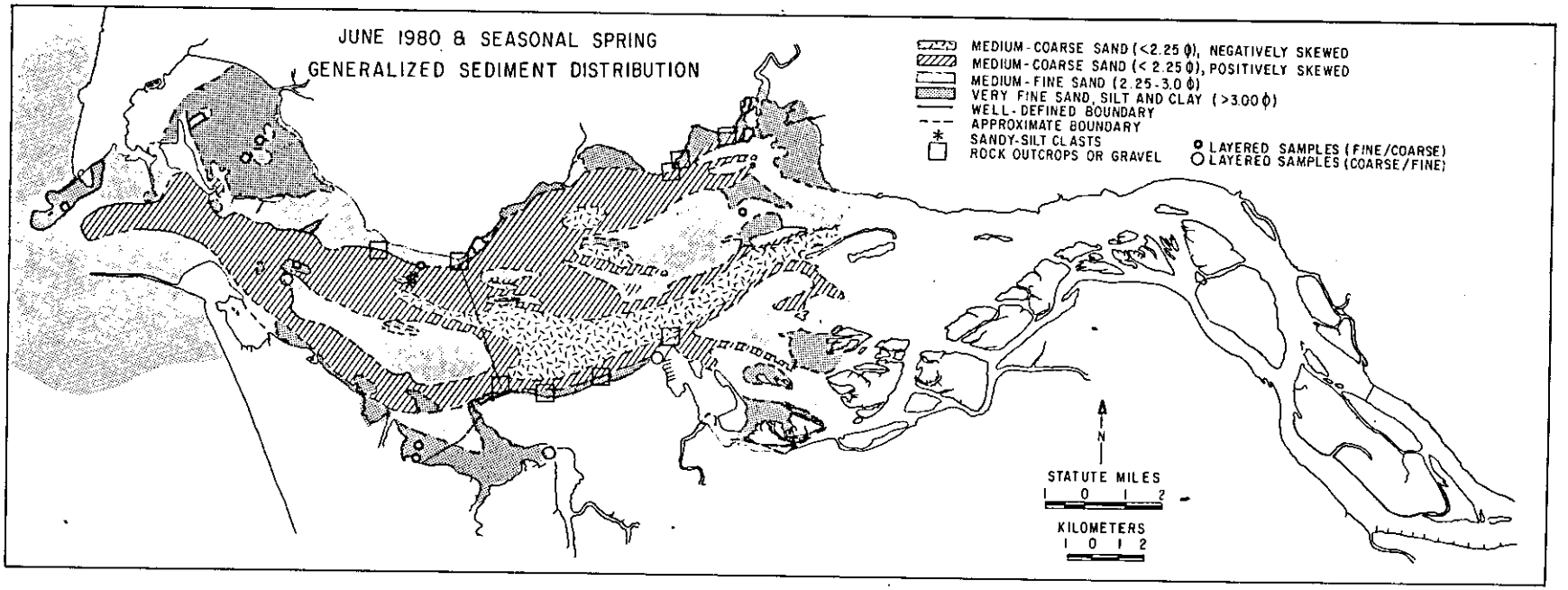

Figure 37. Generalized sediment distribution map for June 1980 and seasonal spring samples.

similar, and continuous to almost Astoria, where it terminates without crossing the diagonal channel. In all three seasons, areas with the coarse (<2.25 phi) negatively-skewed sand were found in the channels of Grays Bay. There was one small patch in the lower estuary, present only in fall and winter, and located in the bathymetric depression near the Chinook pile dike.

The distribution of the coarse- to medium-grained, negatively-skewed sand varied in response to the shifts in the positively-skewed material, and displayed further seasonal changes in the South Channel (main navigation) between Hammond and Astoria (RM-5 to RM-15). In spring, this portion of the South Channel, which crosses Flavel Bar, exhibited coarse material along entire reach. In fall, however, coarse sand extended seaward from Astoria only part of the way across Flavel Bar and extended upriver from the entrance only as far as Hammond (Figure 35). An even longer "gap" in the distribution of coarse material in the South Channel was found in winter (Figure 36). It is noteworthy that the distribution of coarse sand near the entrace did not appear to vary significantly among seasons.

Fine-grained sediments (>3.00 phi) occurred in various distributions in the three seasons. They were most common in spring, when they dominated the grain size distributions in Baker Bay, Youngs Bay and Cathlamet Bay. These areas were also predominantly fine-grained in winter, but in the fall, the proportion of samples with fine to medium sand (2.50 to 3.00 phi) increased in these areas. In addition to the shallow bays, very fine sand-, silt- and clay-sized sediments were found in both the large and small channels of the estuary. Small channels in Grays Bay and Cathlamet Bay and the sloughs in the upriver portions of the study area occasionally had finer sediments than their respective flanks (Roy et al. 1982). Fine-grained deposits in the large channels were localized, mostly in the lower estuary. In spring, patches of fine-grained sediment occurred in the vicinity of Flavel Bar in the South Channel and near Site D in the North Channel. In the fall and winter, the only sizable deposits of sediment >3.00 phi occurred in the North Channel at and slightly seaward of Site D.

Sandy-Silt Clasts and Layered Samples

The distribution of sandy-silt clasts recovered in numerous samples and the distribution of layered samples are also included in Figures 35-37. As noted by Roy et al. (1982) the sandy-silt clasts were usually slightly consolidated, rounded, disc-shaped clasts with a mean size in the coarse silt range. They are found predominantly in the lower estuary, often associated with otherwise fine to medium sands. Most of the few that were found upriver of

Tongue Point were more highly compacted clays, some of which have root traces, and appeared to be of a different origin. More mudballs were found during the fall cruises, even when the increased number of samples were taken into account.

Two-layered samples were obtained over a range of depths and in various parts of the estuary but, except for three samples found in spring, the finer material was always found over the coarse material. Typical two-layer samples exhibited a sandy-silt layer (mean size from 3.00 to 6.00 phi) over fine-medium sand (mean size between 2.00 and 2.75 phi). The composition of the sandy-silt layers was very similar to the composition of the sandy-silt clasts described above.

Ephemeral Deposition of Silt and Clay

Figure 38 indicates the distribution of percent silt and clay as either greater than 10% or less than 10%. An overlap existed where samples obtained from the same area in different seasons fell into different categories; in these areas, deposition of silt and clay was ephermeral. This map is based on all of the available samples in the estuary and has the best resolution and highest confidence level of all of the sediment distribution maps presented in this report. Throughout the discharge year silt and clay occur along the margins of the estuary, in the peripheral bays, and among the vegetated islands of the upriver portions of the study area. However, from time to time, fine-grained sediments appeared on some parts of the mid-estuary shoals (Desdemona Sands, Taylor Sands, and the shoals in Cathlamet Bay). Silt and clay also appeared on an intermittent basis in both the large channels (including the main navigation channel and the North Channel) and in the smaller channels dissecting the shoals. When present in the large channels, fine-grained deposits were confined to the lower estuary; in fact, they appeared mostly in the vicinity of Flavel Bar in the South Channel and in the North Channel between the Chinook pile dike and Cliff Point. The broad channel connecting the Astoria mooring basin with the North Channel was floored in fine-grained sediments on a seasonal basis, as were several of the smaller channels in Cathlamet Bay and Grays Bay. The other areas in which silt and clay were seasonally present in appreciable amount were the outer fringes of Youngs Bay and Baker Bay. The inner parts of these bays had fine-grained sediments in all three seasons.

The remainder of the estuary, that part in which silt and clay were never present in significant amounts, constituted the largest portion. Sand-sized material was found over this entire area, ranging from coarse sand (usually finer than 0.0 phi) to very fine sand (3.00 phi). Much of this material actually fell into the highly-mobile sand range between 1.75 phi and 3.00 phi.

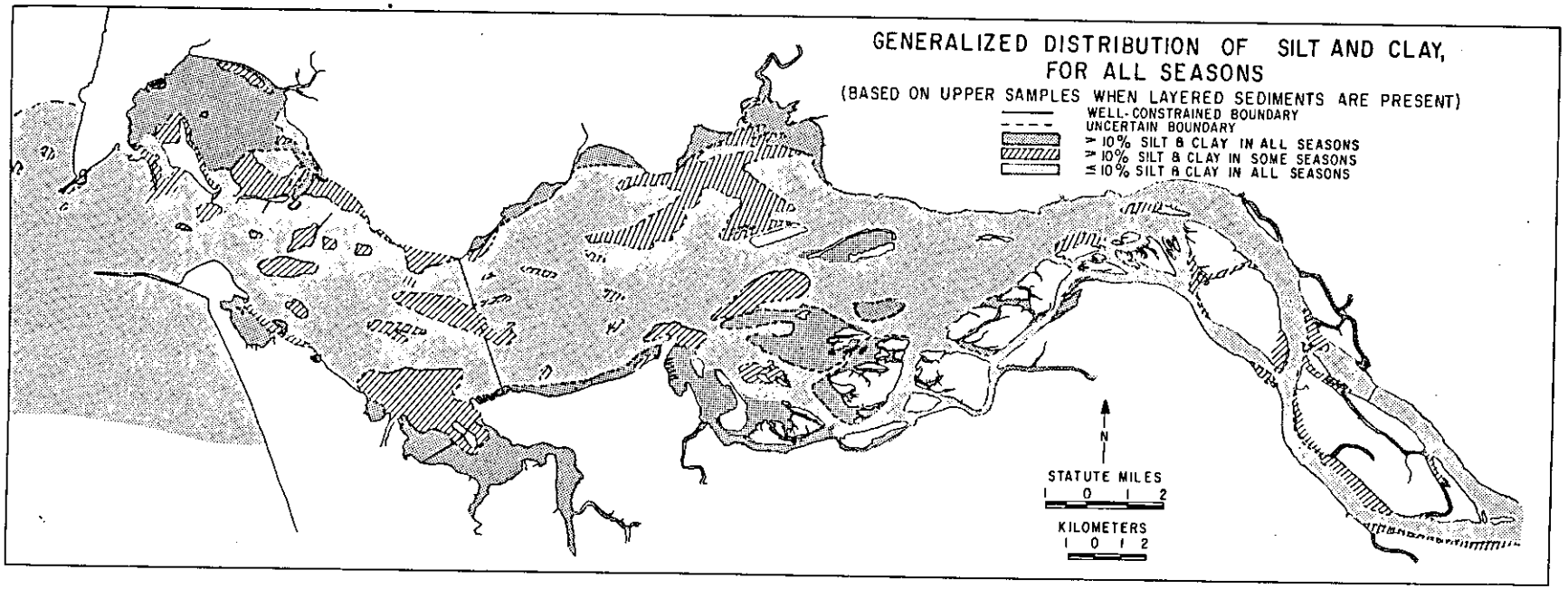

Figure 38. Generalized silt plus clay distribution including all samples.

3.2 SUSPENDED SEDIMENTS

3.2.1 Texture

Suspended sediment samples from station 11 upriver of the study area (Figure 17) near Port Westward were representative of the river input of material to the estuarine system. Conomos (1968) found that the river-borne suspended material was predominately lithogeneous, composed of discrete mineral grains and lithic fragments and, for low discharge conditions, had an average modal diameter of 6.5 phi. Results from this study showed a similar predominance of lithogeneous material as the percent organics (by weight) at this station were betweeen 1 and 4%. Figure 39 shows the size frequency distribution for two samples from this station. A sample (Figure 39b) taken approximately 30 ft (9 m) above the bottom had a fine silt mode and was characteristic of most of the samples obtained from this station. The increase in volume percent at 10 phi was probably artificial, resulting from electronic noise in the equipment during analysis. A second sample (Figure 39a) taken approximately 20 ft (6 m) above the bottom at approximately the same location, had a medium to coarse silt mode, and characterized those samples collected during the late ebb part of the tidal cycle. The mode at 7 1/3 phi in Figure 39b and the shoulders in the phi distributions in both Figures 39a and b are evidence that the washload of the Columbia River was coarse clay-fine silt and that local resuspension at this station, which occurred during late ebb, added a medium- to coarse-silt component to the suspended load.

Suspended sediment samples from station 2N (Figure 40) were representative of the oceanic input of material to the estuarine system. The oceanic source of suspended material to the estuary was predominately biogenous (Conomos et al. 1972). Samples obtained from stations near the mouth during this study had highly variable percentages of organic matter, which tended to be fibrous and clogged the Coulter counter aperture, so that size distributions of the oceanic source were not available.

3.2.2 Transmissivity

Evidence for the importance of fortnightly tidal variations on the suspended sediment field can be seen in the time-series in Figure 41. This time-series displays results from a transmissometer instrument array mounted approximately 3 ft (1 m) above the bottom on the Astoria-Megler Bridge during the summer of 1980. The record clearly shows the correlation among current speed, salinity and transmissivity during both the spring and neap tides. During the spring tides there was a good correlation among higher flow speeds, lower average salinities, and lower

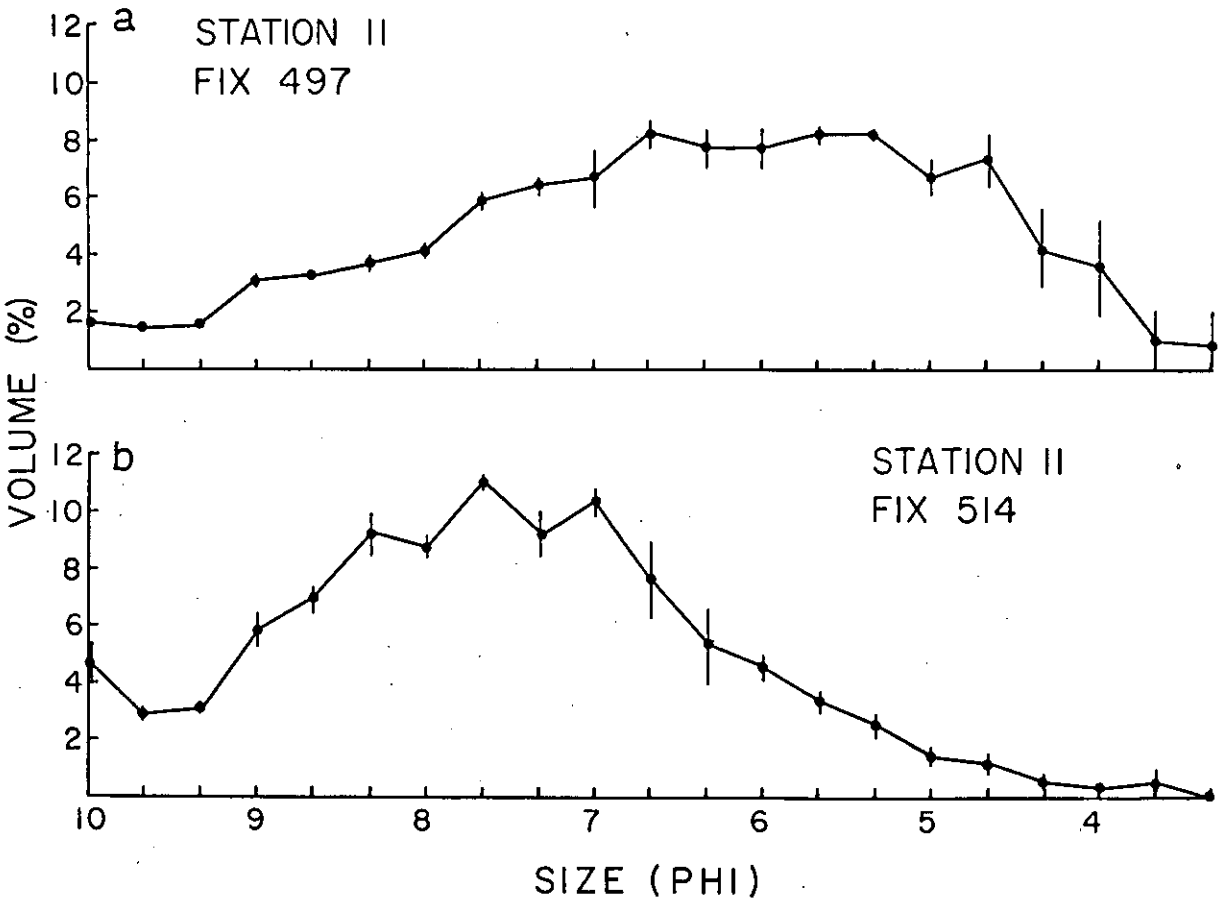

Figure 39. Size frequency of two suspended sediment samples from station 11.
(a) Sample from 20 ft (6 m) above the bed with coarse silt mode.
(b) Sample from 30 ft (9 m) above the bed with fine silt mode.

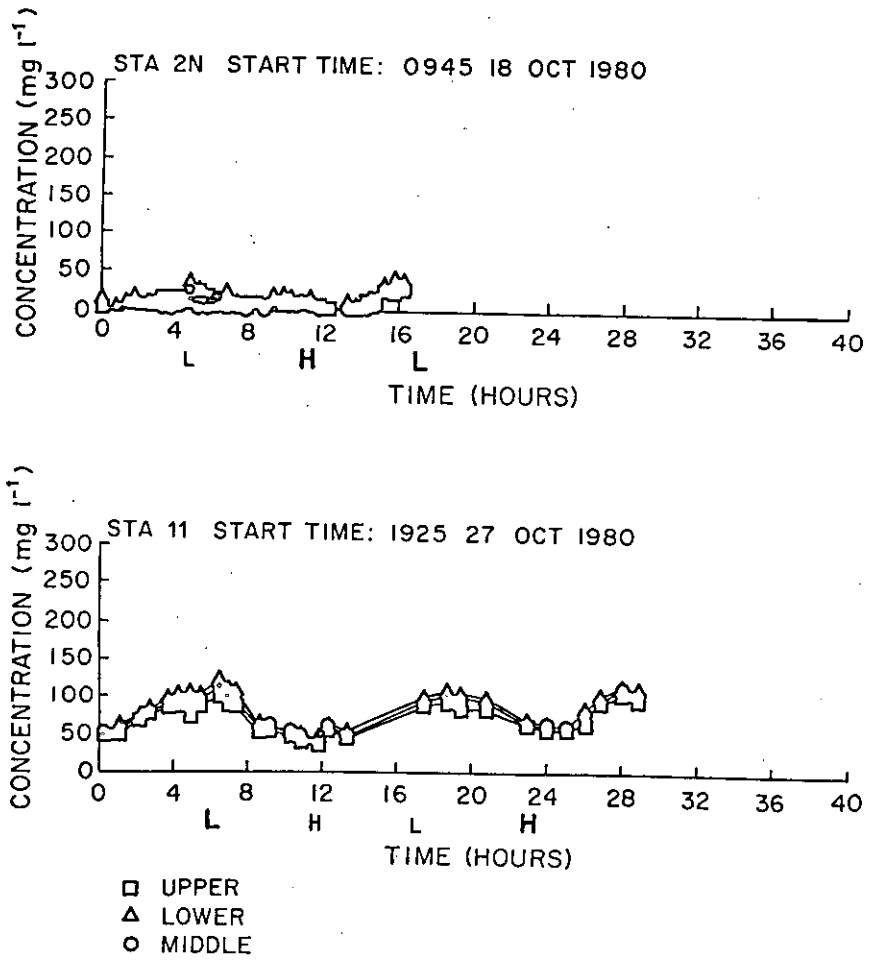

Figure 40. Time series of depth-averaged suspended sediment concentrations obtained from profiling nephelometer station 2N, the farthest seaward station, and for station 11, the farthest landward station.

transmissivity between 11 and 15 July and again between 27 to 31 July. Conversely, during neap tides, from 18 to 22 July and again from 3 to 7 August, there was a strong correlation among lower flow speeds, higher average salinities, and higher transmissivity. The close association among these quantities was substantiated by observing that the second neap tide (3 to 7 August) had higher speeds than the first neap tide and that the transmissivity was correspondingly lower than during the first neap cycle.

3.2.3 Nephelometry

Data representing the seaward and landward limits of the study area were obtained from station 2N near the entrance and from station 11 near Port Westward, respectively. A nephelometer time-series of suspended sediment concentrations for station 2N, the farthest seaward station, is shown in Figure 40. At this station there was no vertical structure in the suspended sediment field (as shown by the superposition of the three curves), and concentrations were low, varying between 5 and 40 milligrams per liter (mg l^{-1}). These concentrations were some of the lowest found anywhere in the estuary. Figure 40 also presents results for station 11, the farthest landward station, at approximately RM-50. These data show a similar lack of vertical stratification; however, the concentrations were higher than at the entrance, varying between approximately 40 and 100 mg l^{-1}.

A tidal periodicity was observed in the suspended sediment concentrations at station 11. The periodicity corresponded to the semidiurnal tide and, as discussed in the texture section above, was a result of local resuspension during the higher flow conditions of late ebb. The nephelometer records therefore indicated that at the boundaries of the estuary system, ocean waters contained low concentrations of suspended sediment and essentially no vertical stratification, while tidal-fluvial conditions were characterized by slightly higher concentrations, relatively little vertical stratification and a tidal periodicity in the suspended load.

The central part of the estuary, characterized by stations 4S near Hammond and 6S near Tongue Point, has high suspended sediment concentrations during spring tidal conditions, implying the presence of a turbidity maximum (Figure 42). Suspended sediment concentrations in the turbidity maximum were almost an order of magnitude greater than incoming river concentrations and 10 to 20 times greater than the ocean concentrations. At both stations there was a strong semi-diurnal dependence.

Examination of the two time-series in Figure 42 reveals

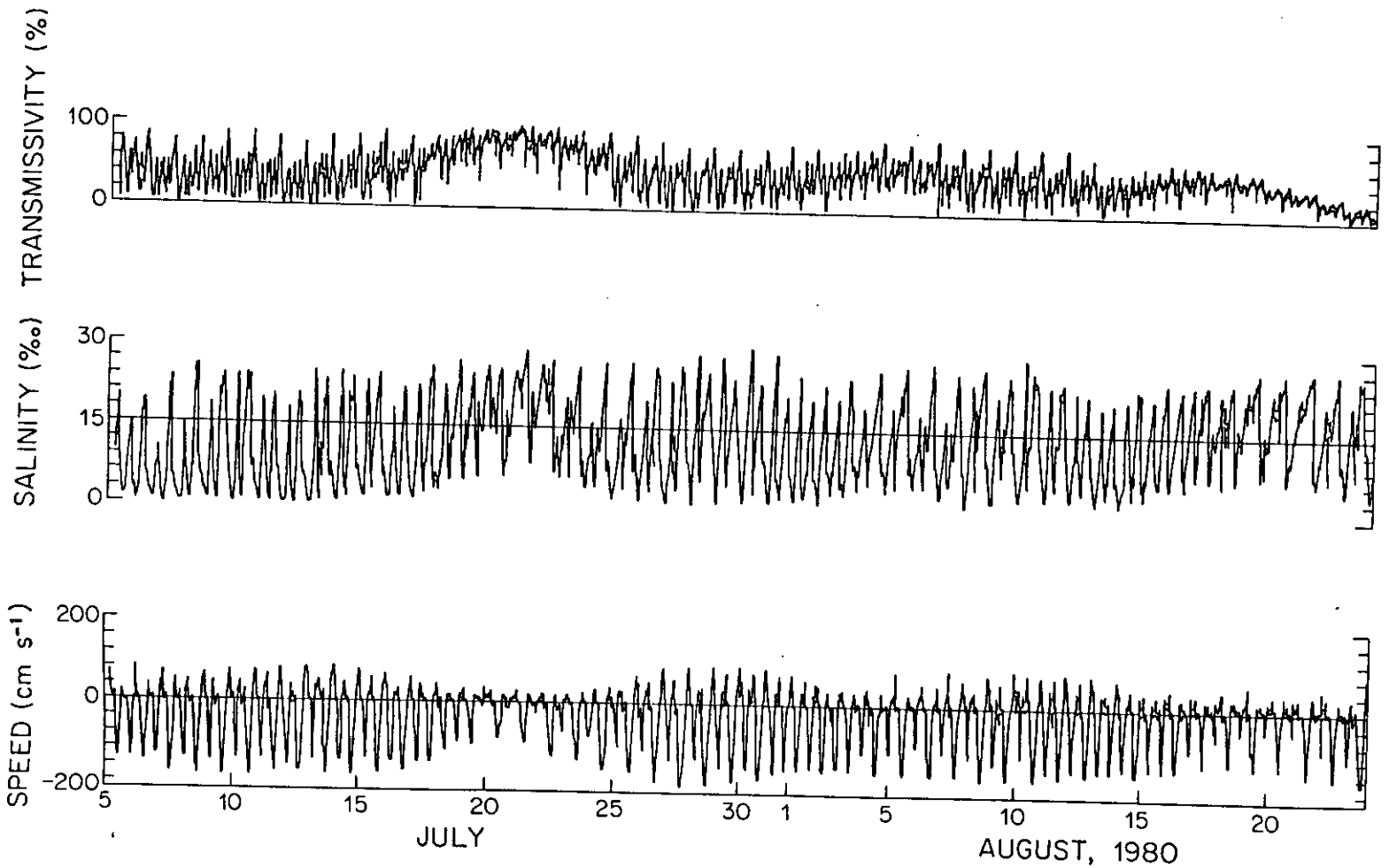

Figure 41. Time series of speed, salinity, and transmissivity obtained from the bridge-mounted instrument array between 4 July and 23 August 1980.

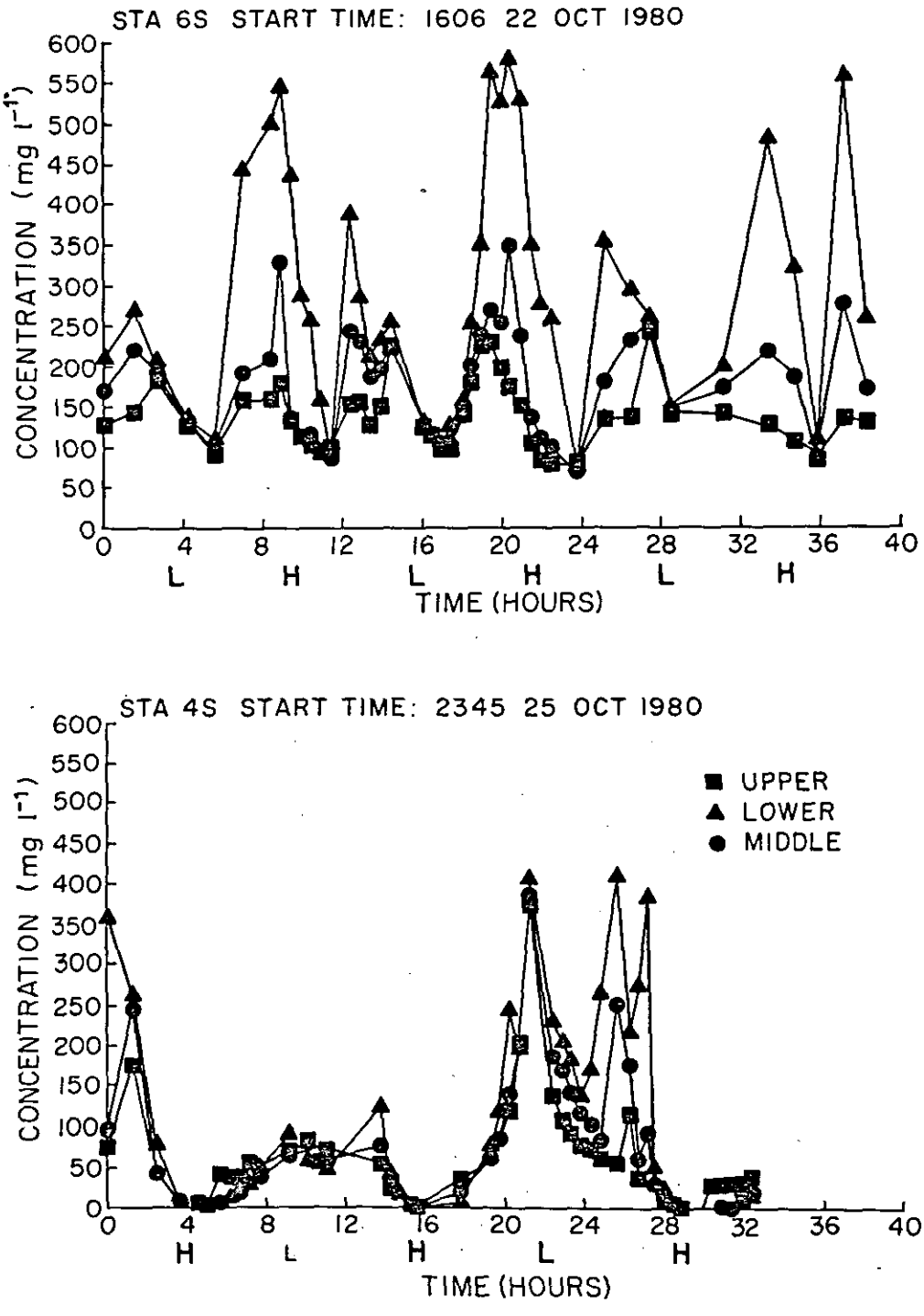

Figure 42. Time series of depth-averaged suspended sediment concentrations for stations 6S and 4S; the central part of the estuary.

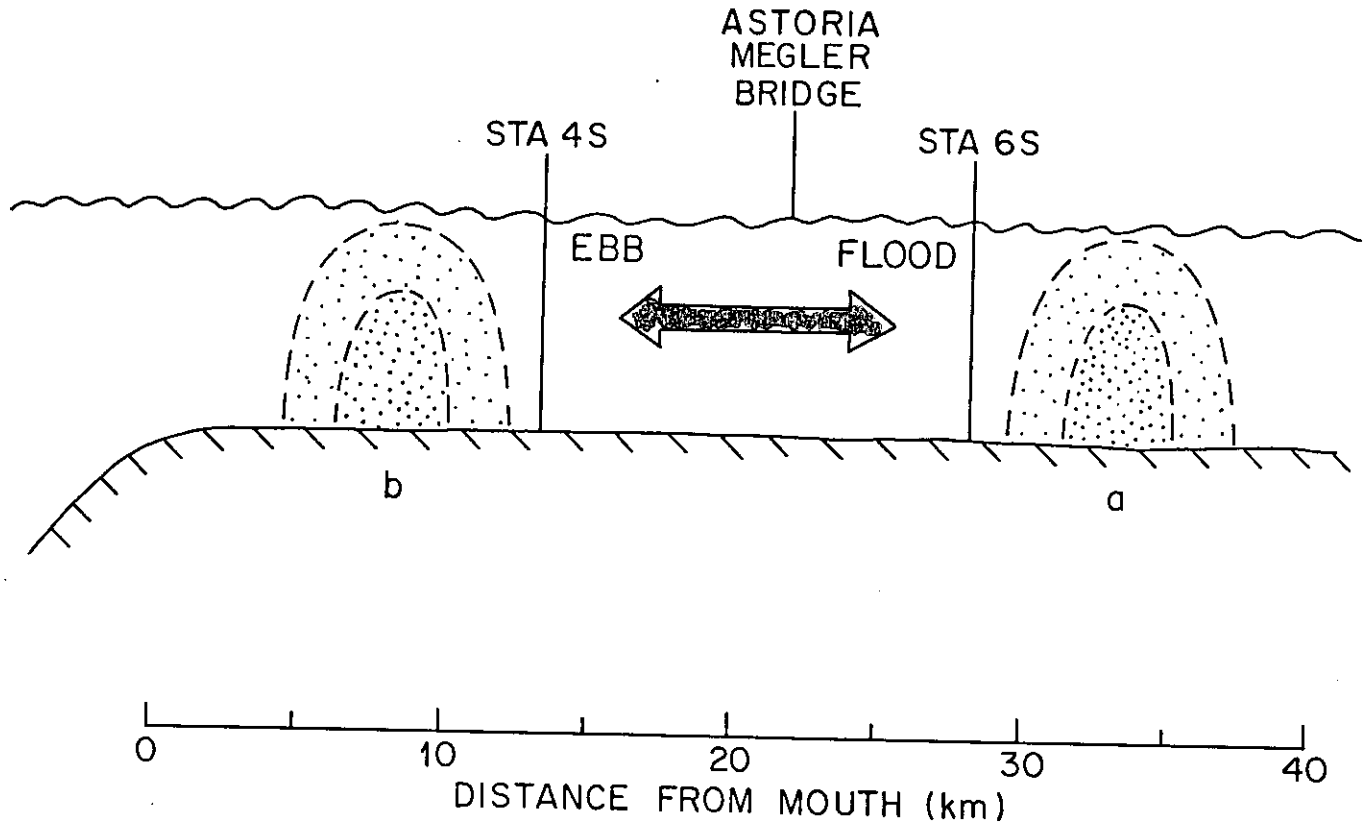

Figure 43. Schematic representation of semidiurnal tidal excursion of the turbidity maximum.

the occurrence of pairs of high suspended sediment concentration peaks. At station 4S the pairs of peaks were centered around a time which was approximately two hours after low water. Conversely, at station 6S, farther landward, the pairs of peaks were centered approximately two hours after high water. The occurrence of these pairs of peaks suggests that the turbidity maximum was being advected alternately landward with the flood and seaward with the ebb. Thus, the time period between peaks was related to the extent of landward or seaward excursion of the turbidity maximum beyond the sampling station. For example, from Station 6S the turbidity maximum was advected landward, just beyond the sampling location during late flood, and then was advected seaward past the station again during early ebb. Therefore, the pairs of peaks centered around high water for station 6S and around low water for station 4S suggest that, for these discharge and tidal conditions, station 6S was located just seaward of the maximum intrusion of the turbidity maximum and station 4S was located just landward of the maximum retreat of the turbidity maximum. As shown in the schematic representation of the excursion of the turbidity maximum (Figure 43), the approximate average longitudinal location of the turbidity maximum during this low river flow condition was RM-14 near Astoria. This location corresponds to the one reported by Hubbell et al. (1971) for similar discharge conditions.

A simple watermass excursion calculation, based on the assumption of a uniform channel, supports these results. For an average maximum velocity of 150 cm s^{-1} for the middle of the water column a tidal excursion for the turbidity maximum of 13 statute miles (21 km) was calculated. The distance between stations 4S and 6S was approximately 9 statute miles (15 km). Although errors are inherent in this type of calculation, the relative agreement between the excursion calculation and the nephelometer results indicated the plausibility of the turbidity maximum advecting approximately 13 miles (20 km) tidally.

Slightly more sopisticated calculations performed using the one-dimensional tidal model presented by Jay (1984) suggest that, in fact, there was not enough tidal excursion to allow the turbidity maximum to spend the observed amount of time below the downstream station and above the upstream station and still travel between the two. An alternate hypothesis to the simple advection scheme might be to attribute the changes to settling and resuspension, rather than advection. Calculations of the settling time (based on samples from the turbidity maximum), however, suggest that insufficient time existed for the relatively fine material to settle more than a few meters during the slack water interval. Although settling and resuspension are clearly important in other estuaries (Schubel et al. 1978) and are equally, if not more important in the Columbia River

Estuary, the turbidity peaks centered around high and low water are believed to be related to advection processes. Because it seems that the semidiurnal excursion is insufficient to account for the observed data, it is suggested here that the mean location of turbidity maximum is also advected on a neap-spring basis. This hypothesis accounts for the observed data (note that the data are not synoptic) and is in accordance with the change of the mean position of the salinity distribution in the models presented by Hamilton (1984).

Implicit in these interpretations is an assumption that the longitudinal distribution of the turbidity maximum is small, relative to the excursion distance. The synoptic data of Hubbell et al. (1971) support this assumption.

Together with the tidal advection of the turbidity maximum, the nephelometer profiles also demonstrated the importance of the fortnightly tidal variations on the suspended sediment concentration field. Nephelometer data comparing suspended sediment concentrations during a spring and neap tide at a single location, station 6S, are shown in Figures 44 and 45, respectively. Bottom salinity data obtained concurrently with the nephelometer data during the spring tide had a strong tidal dependence with variations between 0 and 15°/₀₀. Nephelometer data collected during the spring tide, as discussed above, showed a vertical stratification of suspended sediments with maximum semidiurnal variations of 75 to 575 mg l^{-1}. Data collected during the previous neap tide at the same location showed different results (Figure 45). Bottom salinities at this location during the neap tide were greater than during the spring tide, varying between 5 and 25°/₀₀. The nephelometer time-series obtained during this neap tide showed a lack of vertical stratification and relatively low suspended sediment concentrations. These neap tide suspended sediment concentrations, ranging between 25 and 75 mg l^{-1}, were comparable with the washload concentrations found at Station 11.

Both the nephelometer data and the transmissometer data suggested that the lower flow velocities during the neap tide caused a decrease in mixing such that the salt intruded farther upriver. This lower flow condition also allowed the turbidity maximum to degenerate, or decrease in concentration, as (1) resuspension of bottom sediment decreased due to lower boundary shear stresses, and (2) settling to the bottom of advected river material increased due to lower turbulent mixing. Conversely, during the spring tide the turbidity maximum was regenerated, or increased in concentration, as both boundary shear stresses and turbulent mixing were increased.

The behavior of suspended sediment in the estuary is

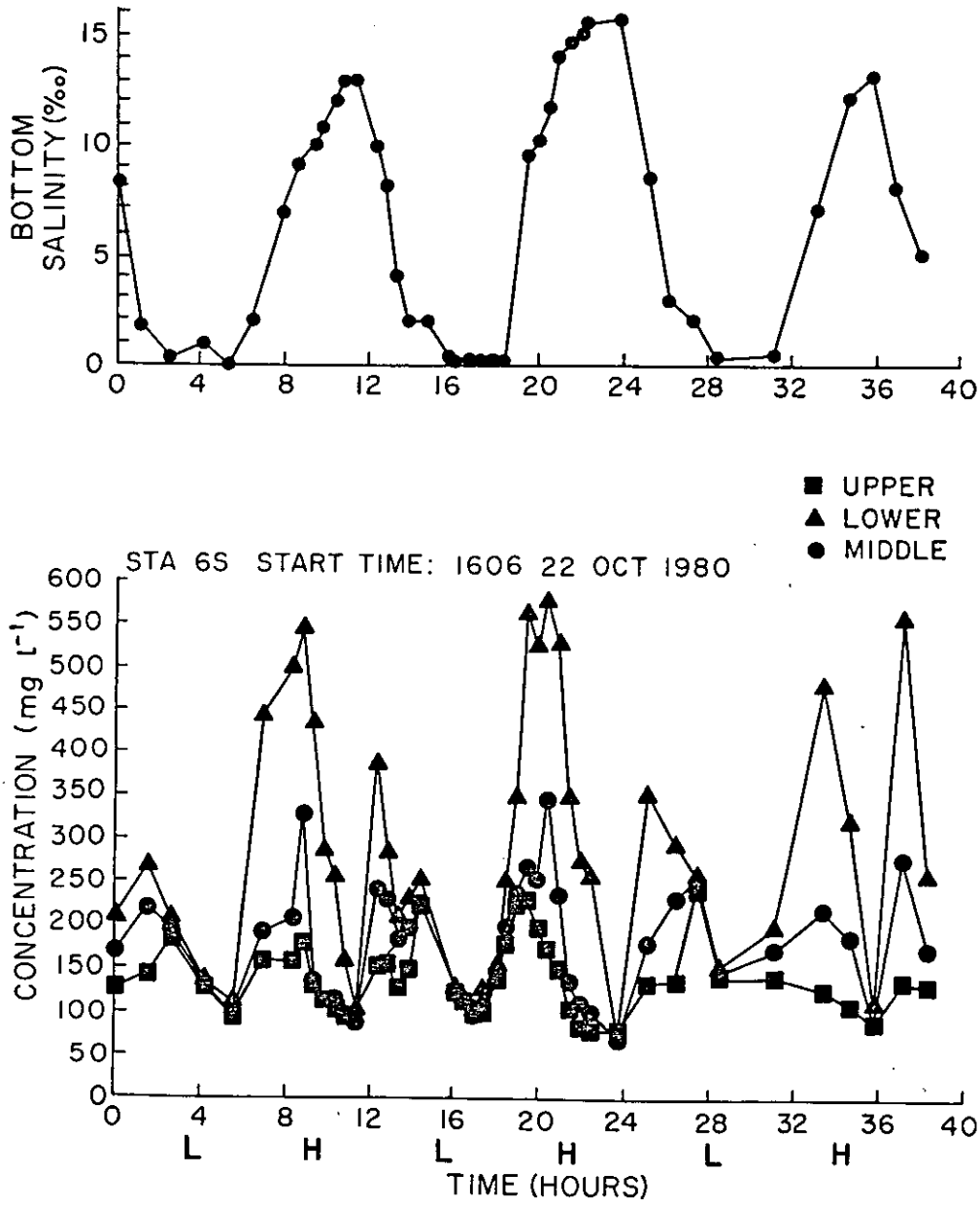

Figure 44. Time series of bottom salinity and depth-averaged suspended sediment concentrations for station 6S during a spring tide.

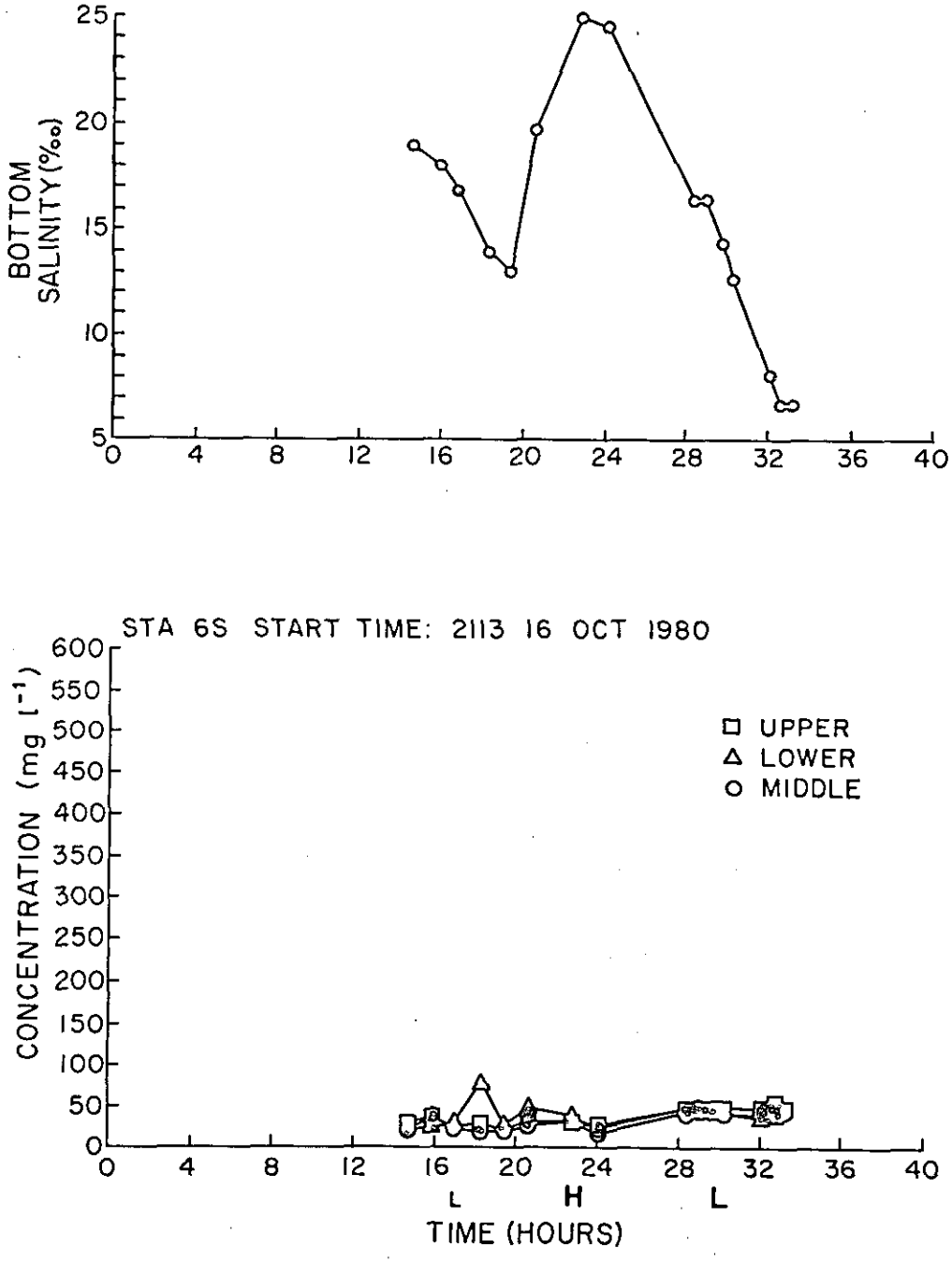

Figure 45. Time series of bottom salinity and depth-averaged suspended sediment concentrations for station 6S during a neap tide.

clearly complex. Concentrations in the tubidity maximum vary in response to neap and spring variations in flow conditions, the turbidity maximum is advected on a diurnal and fortnightly basis, and seasonal variations in discharge and ocean water salinity are expected to cause it to shift location seasonally. In addition, settling and resuspension are important phenomena, and lateral transport into and out of the many side channels and bays is likely to further complicate the situation. Thus, the conclusions reached in regard to the behavior of suspended sediment in the estuary are preliminary, and await further investigation.

3.3 BEDFORMS

3.3.1 Data Coverage

Side-scan sonar data collection was limited to the main channels and some minor channels west of Harrington Point. Operational constraints prevented side-scan investigation in water depths less than 20 ft (6 m) and, as a result, no information on bedforms in the shallow subtidal portions of the estuary was available. (Limited intertidal coverage was provided by the air photos taken during low tide in June 1980.) However, relatively complete coverage of the deeper portions of the lower estuary on both spatial and temporal sales was obtained. Tracklines for each of the three discharge seasons are shown in Figure 16a, b, and c. Spatial coverage of the channels west of Astoria-Megler Bridge was good for October 1980 and June 1980, but was limited by weather conditions in February 1980.

Overall, temporal coverage was sufficient to delineate seasonal changes in bedform distributions or other bottom characteristics over the entire estuary. Temporal coverage was adequate for identification of bedforms that reverse orientation with diurnal tides, but was insufficient for determining what percentage of the time each orientation prevaled. Temporal sampling density was reduced east of Tongue Point in the South (main) Channel and east of the Astoria-Megler Bridge in the North Channel after it was observed that tidal reversals in bedform orientation were uncommon in these landward portions of the estuary. At Site D, 25-hour coverage over consecutive neap-spring cycles provided the best temporal data for bedforms in the estuary.

3.3.2 General Bottom Characteristics

The extensive side-scan coverage for three discharge seasons and a variety of tidal stages permitted an acoustic characterization of most of the channel portions of the estuary. By combining side-scan, bottom sediment, and bathymetric information, a rather complete description of the bottom was developed. The estuary bed, especially in the channel portions west of Harrington Point, was composed

of medium- to mostly fine-sand (1.75 to 2.75 phi). Flume and field studies (reviewed in Harms et al. 1975, and Harms et al. 1982) demonstrated that a wide range of bed configurations may form in sediment of this size range under appropriate flow conditions. The side-scan data showed that currents in the estuary have produced a wide variety of bedforms which occupy most of the estuary bottom. Bedforms large enough to be resolved by the side-scan were absent only in a few of the areas studied. In the remainder of the estuary, bedforms were omnipresent. They ranged in height from 1 to 10 ft (0.3 to 3 m) and had wavelengths of from 4 to 300 ft (1 to 100 m). They displayed a variety of shapes: some were symmetrical, some clearly asymmetrical, some displayed steep slip-faces that were probably at the angle of repose for sand in water. In plan view, crests were relatively straight, sinuous, or were cuspate and continuous or discontinuous. Bedforms were superimposed on larger bedforms; in some areas as many as three orders of bedforms were present.

Some of the trends noted in bedform morphology in this study were apparently associated with depth; a weak correlation existed between longer wavelengths and increased depths, especially for larger bedforms. Previous workers have suggested that the height of fully developed bedforms is depth limited. Both experimental (Yalin 1964) and theoretical (Smith 1970) studies indicate that the height/depth ratio approaches a maximum of about 1/6. The large seaward-oriented fluvial bedforms in the landward portion of the estuary approached this depth-limited height. The landward-oriented bedforms produced by estuarine circulation did not approach this height. It is possible that the heights of the landward-oriented bedforms were not limited by total water depth but by the effective depth of the saline net-landward bottom flow. Many of the landward-oriented bedforms would have approached the 1/6 height/depth ratio if an interface 20 to 30 ft (6 to 10 m) below the surface was considered the effective water surface.

The various contributions to bedform formation resulted in a distribution that was complex and variable in both space and time. Bottom topography, sediment grain size, the average current velocity and the oscillatory flow all combined to produce the bedforms observed in this study. An attempt to classify bedforms on a morphological basis and to map the distributions of these bedforms over time and space has been made. Because bedform size and shape were controlled by flow conditions through the sediment transport process, bedform distributions provided insight into flow conditions and sediment transport patterns.

Figures 46, 47, and 48 are maps integrating the results of the side-scan studies and depicting general bottom

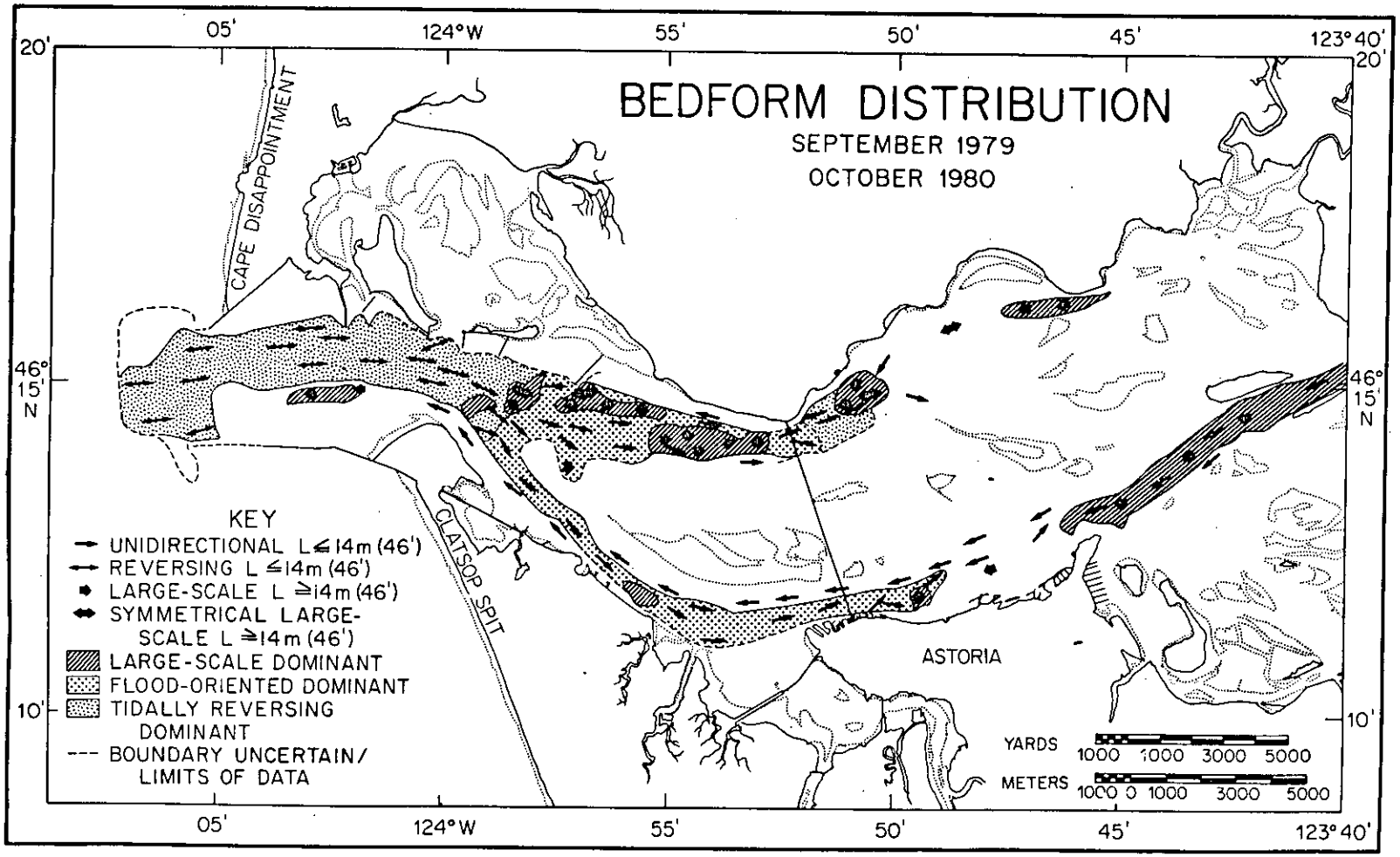

Figure 46. Bedform distribution based on side-scan sonar information obtained in September 1979 and October 1980.

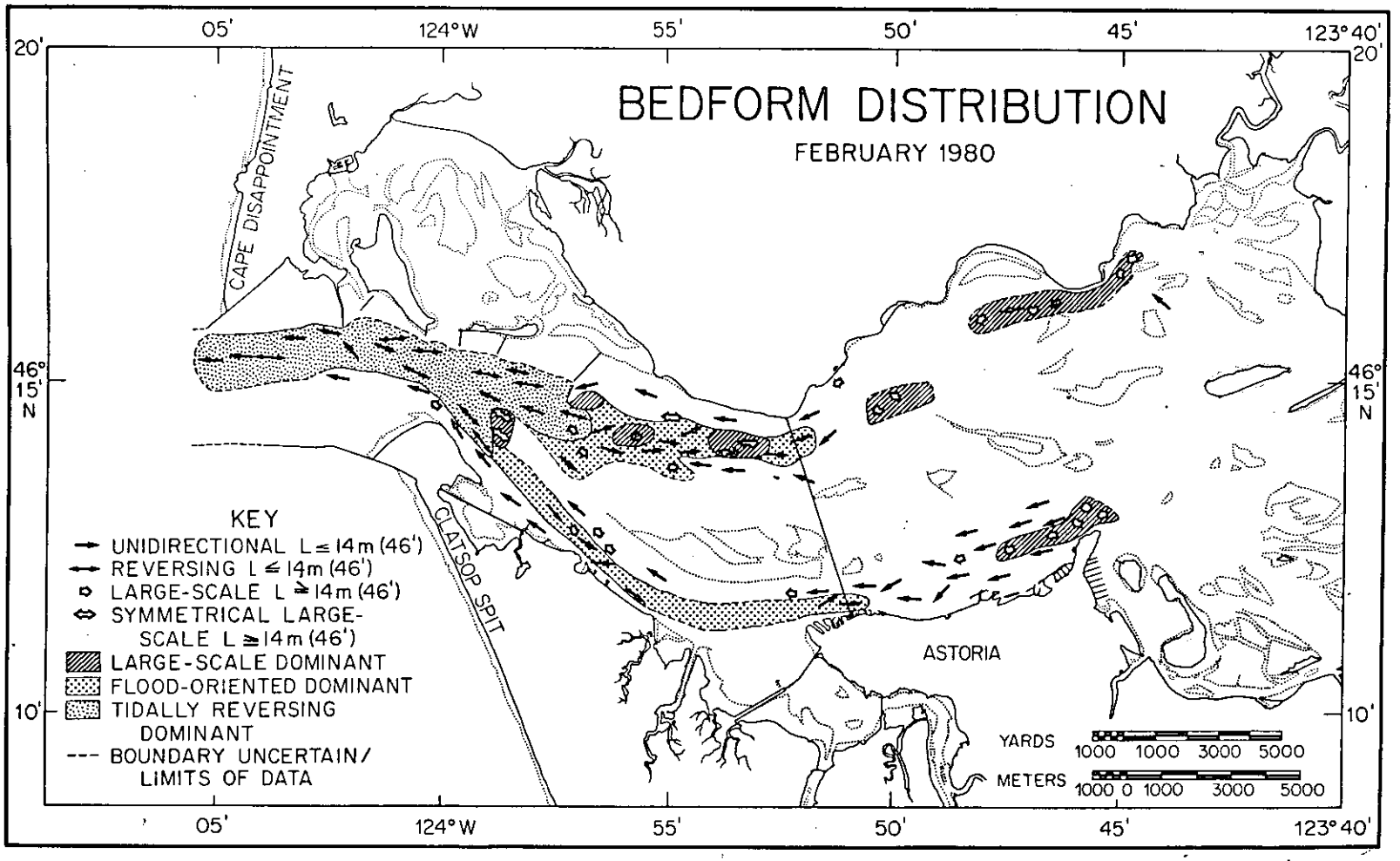

Figure 47. Bedform distribution based on side-scan sonar information obtained in February 1980.

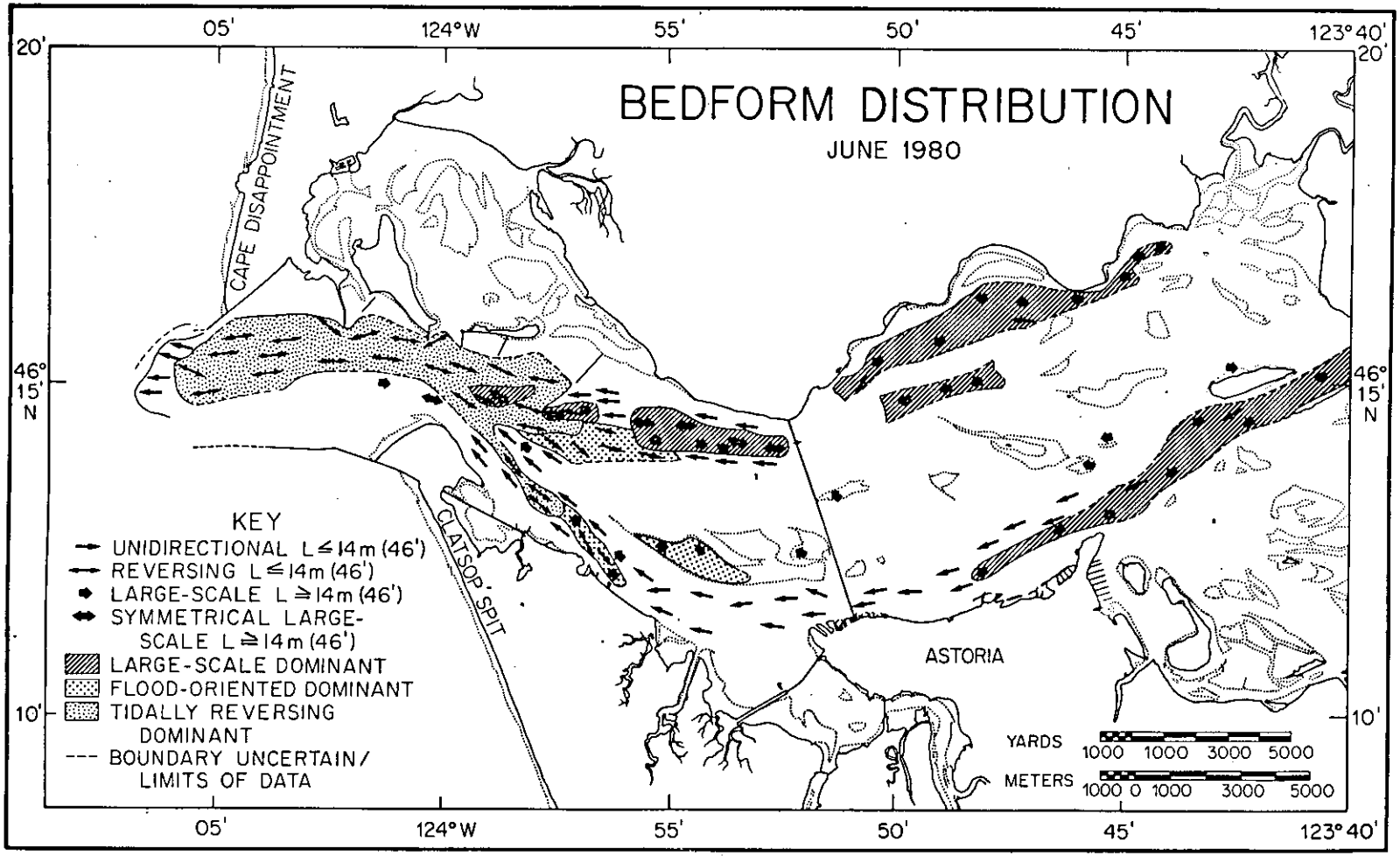

Figure 48. Bedform distribution based on side-scan sonar information obtained in June 1980.

characteristics of the estuary. Various fields of bedforms were recognized and mapped on the basis of similar size and shape characteristics. The boundaries of some of these fields shifted seasonally and are discussed below. Many features of the bedform distribution pattern, however, were observed to not vary significantly over the study period, and may be discussed in a general manner.

Unidirectional Seaward-Oriented Bedforms

Medium- and large-scale bedforms with downstream-oriented slip-faces were dominant in the landward portion of the estuary east of Tongue Point. In the deeper channels, these bedforms had heights of up to 10 ft (3 m) and wavelengths of more than 300 ft (100 m) (Figure 49). Smaller bedforms were commonly superimposed on the stoss (up-current) sides of larger bedforms. Troughs of some of the larger bedforms appeared as acoustically reflective, suggesting that coarse lag sediments occupied these troughs. Sediment samples confirmed that a substantial grain size difference exists between crest and trough sediments: near Puget Island, the crests of bedforms were formed of well-sorted coarse sand whereas the troughs contained poorly-sorted gravel (Table 6). Other troughs had

Table 6. Summary of results of sediment grain-size differences between crests and troughs of large-scale bedforms (Roy et al. 1982)

PARAMETER	CRESTS	TROUGHS
Average modal phi size	1.50	-0.13
Average percent gravel	0.0	49.66
Average percent mud	0.29	0.47
Average sorting	1.19	5.00
Average mean phi size	1.37	-0.58

a low reflectivity, possibly indicating finer-grained sedimentation. Most of the bedforms in this landward portion of the estuary were unidirectional. The steeper faces (generally well-developed slip-faces) of even the small bedforms retained seaward orientations over the entire tidal cycle.

Bedforms With Reversing Orientations

Generally smaller bedforms are present from the outer tidal delta east to Hammond in the South Channel and to the

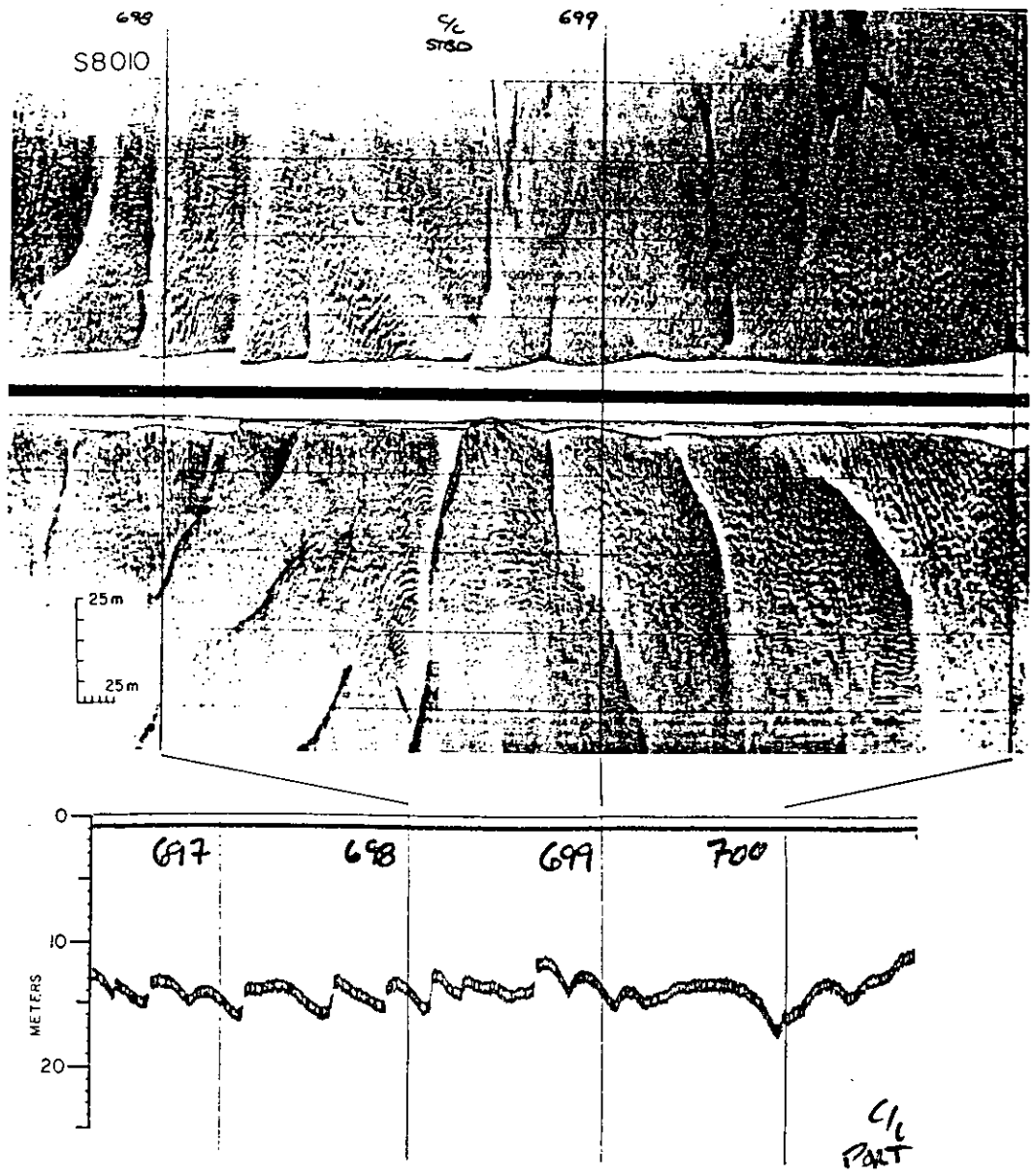

Figure 49. Side-scan sonar and echo-sounder records of large-scale, seaward-oriented bedforms in the fluvially-dominated upper estuary (vicinity of Rice Island).

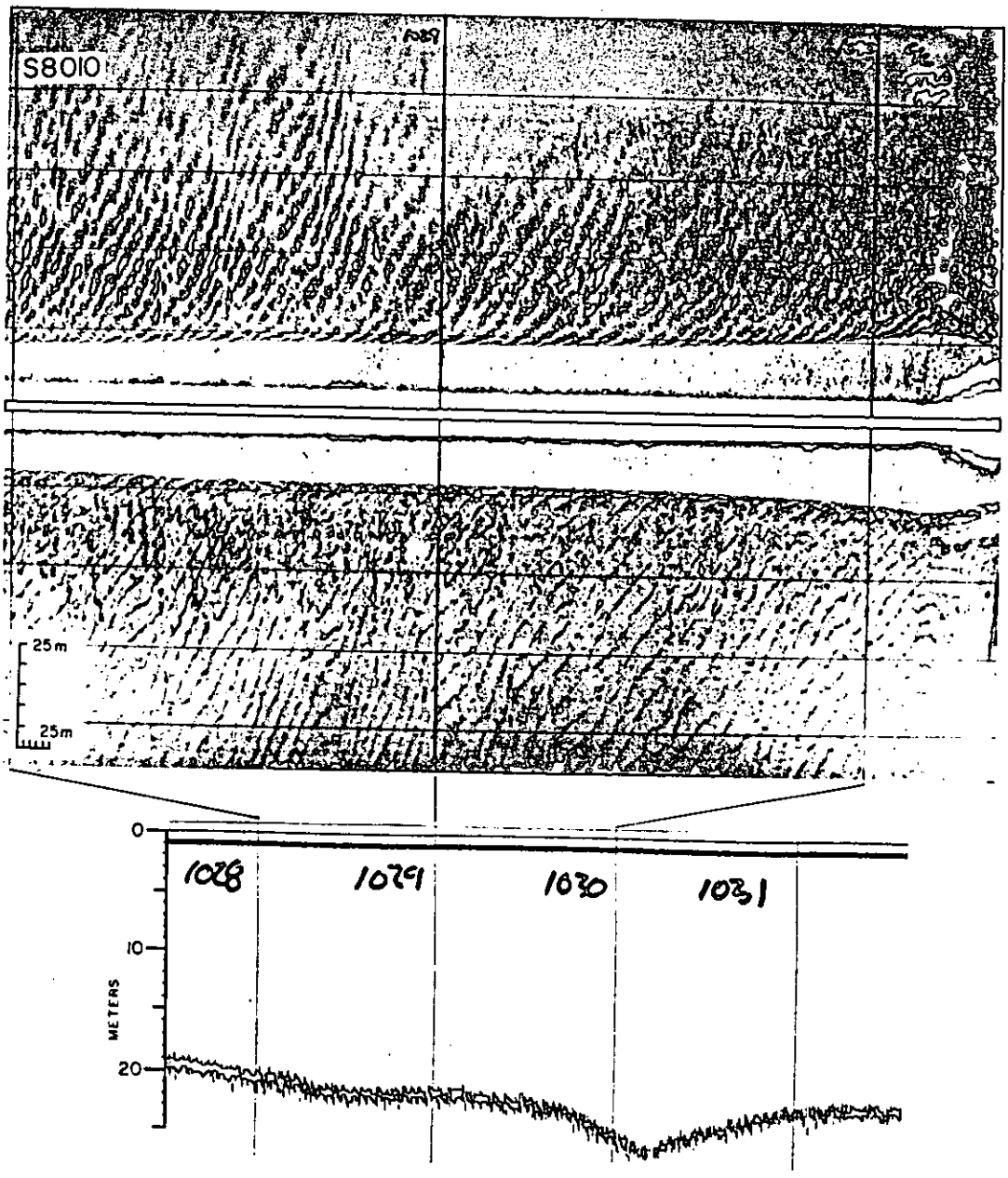

Figure 50. Side-scan sonar and echo-sounder records of small-scale, reversing bedforms in the tidally-dominated lower estuary (vicinity of Jetty A).

vicinity of the Chinook pile dike in the North Channel. These areas were occupied by bedforms with wavelengths of approximately 10 to 30 ft (3 to 10 m), heights of up to 3 ft (1 m), and linear to slightly sinuous crests (Figure 50). At different tidal stages, these bedforms displayed various geometries ranging from asymmetric with slip-faces oriented in either a landward or seaward direction to somewhat rounded and symmetric. Reversal of these bedforms over consecutive ebb and flood tides was documented in several instances, and orientation commensurate with the tidal current was the general rule for all of these bedforms. Bedforms with reversing orientations were commonly found in the channel portions of the estuary seaward of Chinook and Hammond and were found on some channel flanks and shoals in some seasons.

Landward-Oriented Bedforms

In the channels landward of the reversing bedforms described above, bedforms were found that did not reverse orientation; instead, they displayed landward-oriented steeper faces over the tidal cycle. The appearance of the bedforms varied with season and location. They ranged in height from less than a foot (0.3 m) to 6 ft (2 m) and in wavelength from 10 to 120 ft (3 to 40 m). The degree of asymmetry also varied; some of the larger bedforms were nearly symmetric and rounded, while others were highly asymmetric and had slip faces. The large, nearly symmetric bedforms frequently had smaller bedforms superimposed on them that reversed orientation in response to tidal currents. They occurred in small fields located on the northwestern extension of Desdemona Sands and on the shoal near Site D (Figures 46, 47, and 48).

The large asymmetric bedforms occurred in deeper portions of the North and South Channels, but their precise location varied seasonally. Figure 51 shows a particularly well-developed field of larger landward-oriented bedforms found in the North Channel. They had straight crests, landward-oriented steeper faces, and smaller superimposed bedforms. Their wavelength was approximately 140 ft (43 m) and their maximum height was 6 ft (2 m).

Smaller bedforms with landward-oriented steeper faces occupied large portions of both the North and South Channels between Hammond and the Astoria-Megler Bridge. In much of this area, the channel flanks and shoals were occupied by bedforms with seaward-oriented steeper faces. As a result, cross-channel side-scan transects show a reversal of bedform orientation with depth that remained unchanged over the tidal cycle. Figure 52 illustrates this situation schematically, and Figure 53 is a portion of side-scan record depicting a reversal with depth in the Flavel Bar region. In June, the depth of the depth-related reversals

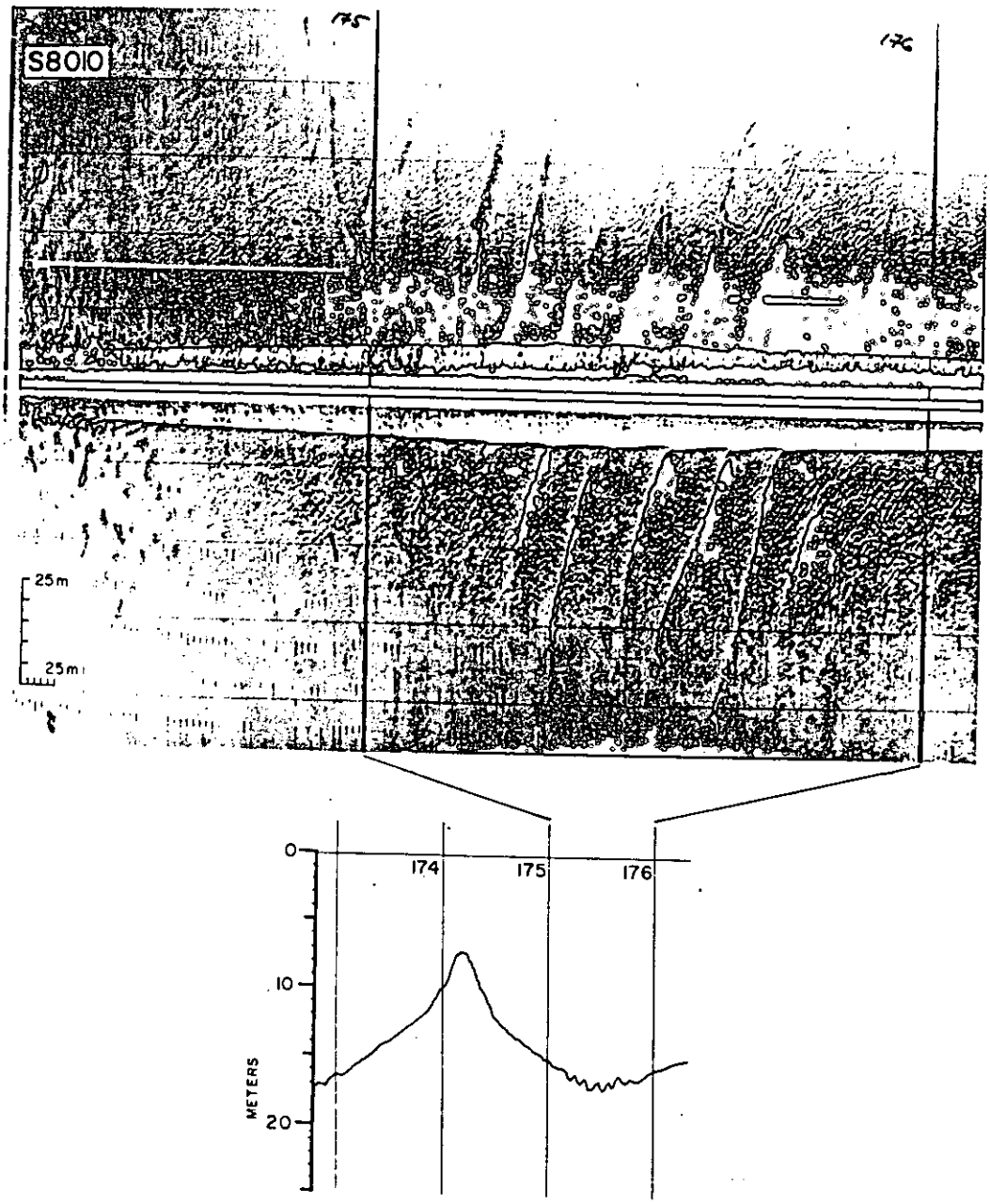

Figure 51. Side-scan sonar and echo-sounder records of landward-oriented bedforms generated by estuarine circulation in the North Channel (near Chinook).

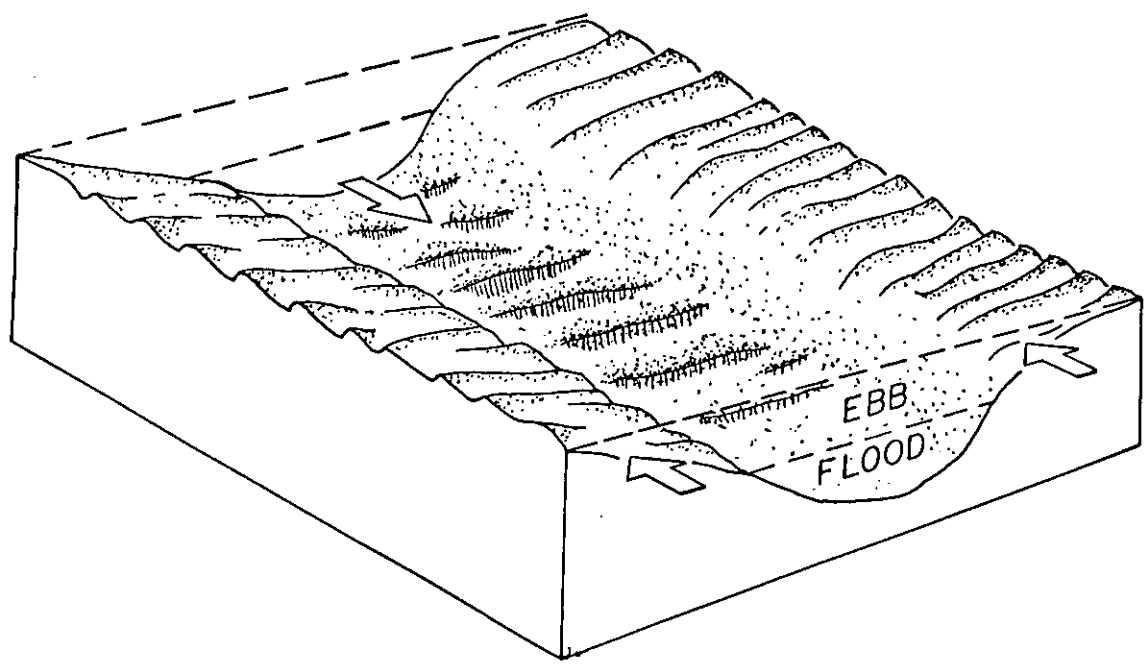

Figure 52. Schematic diagram of depth-related bedform orientation reversals.

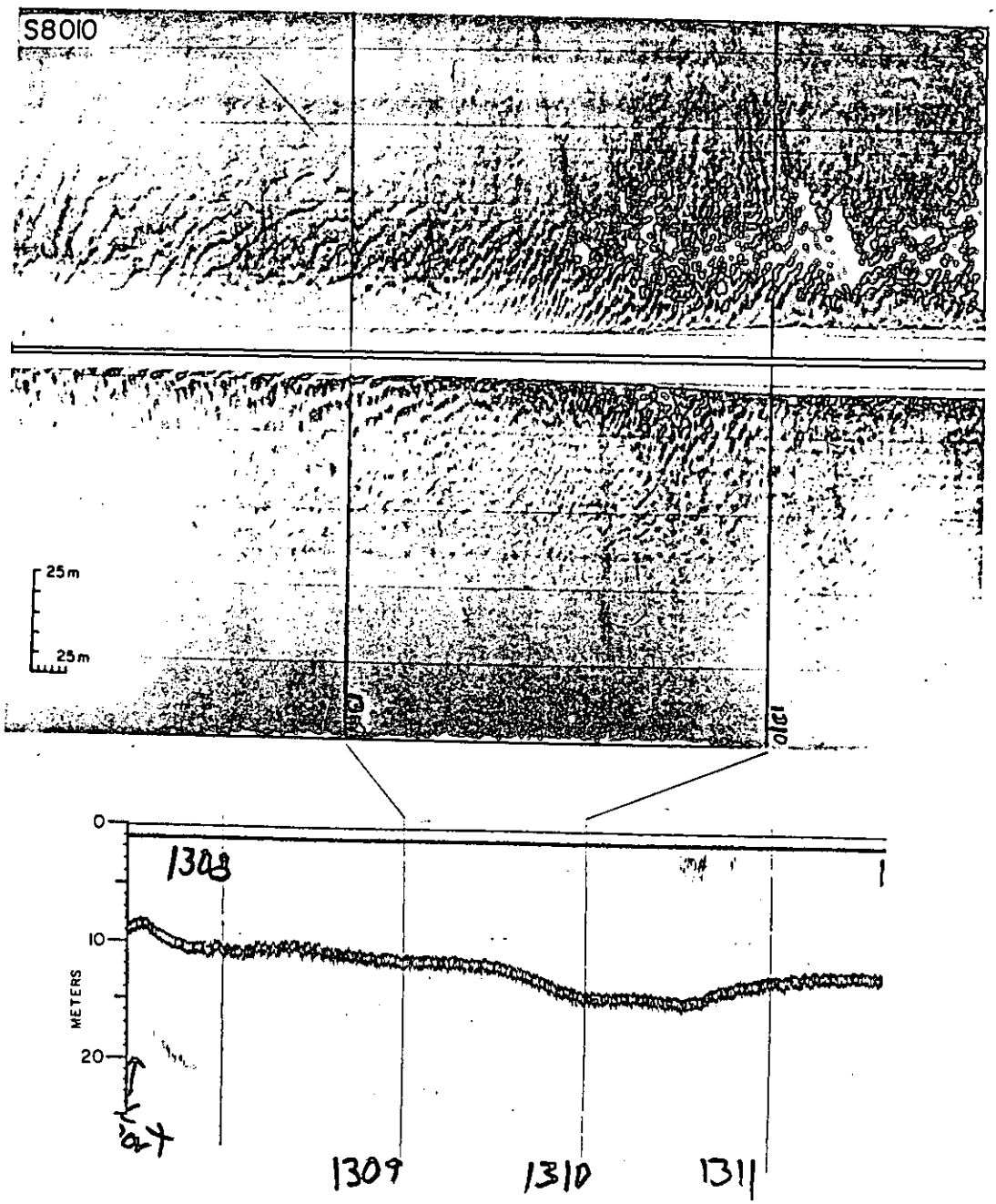

Figure 53. Side-scan sonar and echo-sounder records of bedforms whose orientation reverses with depth from the navigation channel (near Flavel Bar).

(Figure 54) tended to increase with distance upriver. This trend was not apparent in the October data, also shown in Figure 54. The seasonal changes in the distribution of landward-oriented bedforms and depth-related orientation reversals are dealt with in the Discussion section.

Other Bottom Features

In addition to the features mapped in Figures 46, 47, and 48, other characteristics of the estuary bottom were evident in the side-scan records. Some areas of the estuary were featureless at the resolution of the side-scan sonar. These areas were commonly found on channel flanks and rarely, and then only seasonally, found in channel bottoms. Occasionally, these smooth areas graded into areas with indistinct bedforms having no clear orientation. The outer portion of the outer tidal delta was typified by these indistinct bedforms. The bay south and west of Cape Disappointment is an example of an area which had no resolvable bedforms during any season. Seasonally, parts of the North Channel and the north flank of the South Channel were featureless.

The flanks of both channels occasionally displayed bedforms with non-linear crestline geometry ("three-dimensional" in Allen 1968). They were generally found in water depths of >45 ft (>14 m) and were not observed to reverse with daily tides, but may have changed to more linear-crested geometries with time.

The most common feature of the side-scan records not associated with bedforms were areas of very high reflectivity and uneven, often precipitous, topography. These were attributed to areas of rock outcrops, boulder talus, and gravel banks. These hard, erosion-resistant bottoms occurred on the outside of river bends (notably the Port of Astoria region) and near rock headlands such as Grays Point, Chinook Point, and Tongue Point. Reflective areas were also frequently associated with deep bathymetric depressions, as at Tongue Point, Grays Point, the Chinook Jetty, and Jetty A, where they were probably a result of coarser sediments.

Pilings, pile dikes, rip-rap, and sunken logs appeared in the side-scan images, as did fish, salinity fronts, and turbulence. Longitudinal furrows were located in the navigational channels (Figure 55) and are the result of Corps of Engineers dredging activities. Correlation with Corps of Engineers dredging records suggested that these scour marks remained identifiable for at least several days after the dredging activity, but they were not present in later seasons.

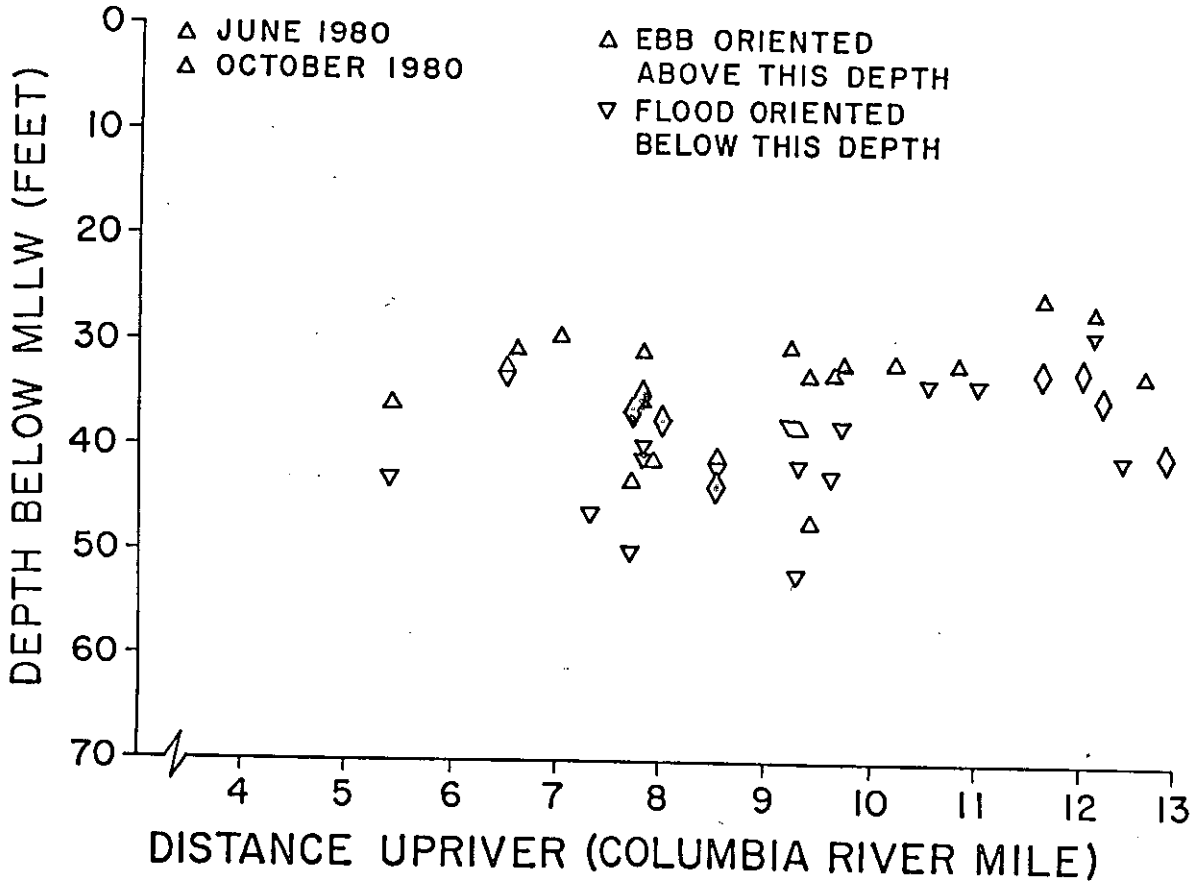

Figure 54. Plot of bedform orientation reversal depth against River Mile.

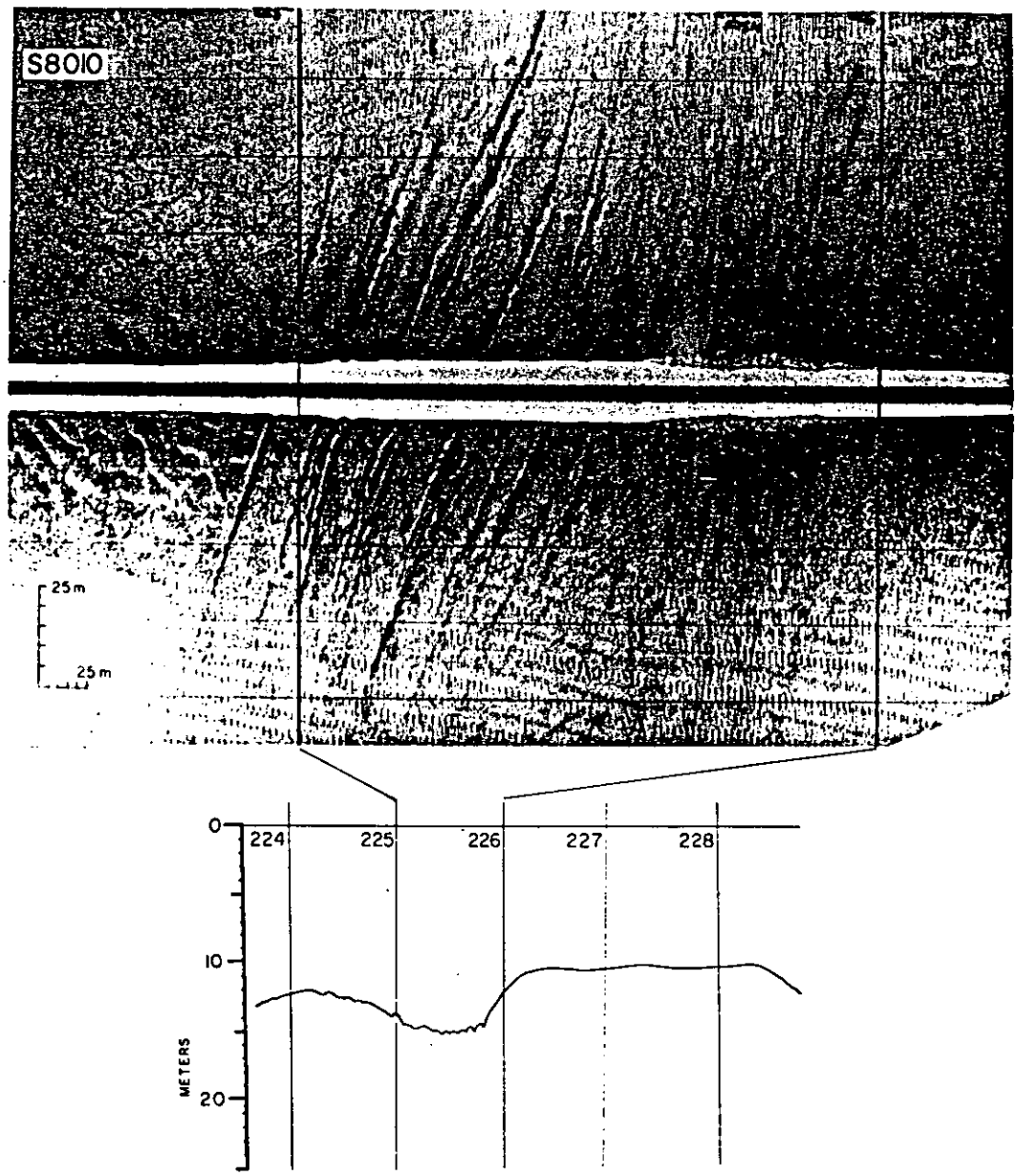

Figure 55. Side-scan sonar and echo-sounder records of dredge furrows in the navigation channel (Flavel Bar).

3.3.3 Seasonal Changes

The distribution and orientation of bedforms for each of the three discharge seasons are summarized in Figures 46, 47, and 48. Some of the similarities apparent in all three surveys have been discussed. Of particular interest are the seasonal variations in bedform distribution. The upriver extent of landward-oriented bedforms varied in response to discharge. During the low flow period of October 1980 (discharge = 140,000 cfs, 3,965 m^3s^{-1}) landward-oriented bedforms were observed nearly to Tongue Point in the South Channel and extended into both forks of North Channel south of Megler (Figure 56). Landward-oriented bedforms and partially reversed bedforms were also found farther east near Grays Point, but these were believed to be isolated cases caused by unique topography, and not associated with estuarine circulation. In February, during higher discharge (191,200 cfs, 5,415 m^3s^{-1}), the limit of landward oriented bedforms in the South Channel was pushed seaward to just east of the bridge. Similarly, in the North Channel the limit of landward-oriented bedforms lay just east of the Astoria-Megler Bridge. In June, with a high discharge (330,600 cfs, 9,363 m^3s^{-1}), no landward-oriented bedforms were found east of Tongue Point in the South Channel (Figure 56). The landward limit of landward oriented bedforms was pushed almost to Hammond in the South Channel. In the North Channel, while some symmetrical bedforms were observed east of the Astoria-Megler Bridge, the limit of landward-oriented bedforms was pushed seaward of the bridge.

The bedform distribution on the channel flanks also varied seasonally. During the low flow period of October 1980, the south flank of the South (main) Channel in the Flavel Bar region was dominated by landward-oriented bedforms. The data in this region were sparse in February, but in June the region was occupied by seaward-oriented bedforms. Similarly, in October the south flank of the North Channel was exclusively occupied by landward-oriented bedforms, but in June and February the eastern half of this area was occupied by either tidally reversing or dominantly seaward-oriented bedforms. On the north flank of the main (South) channel, tidal reversals of the bedform orientations were seen in October but not in February or June.

Coincident with the seasonal variations of bedform orientations in the channels and on the flanks were fluctuations in the depth of bedform reversals and transition zones. The limited number of well-defined reversals recorded with the side-scan is displayed in Figure 53. Some trends were suggested by the data. The depth of reversals for October and June fell roughly between 30 and 52 feet (9-16 m) and mostly occurred between 5 and 13 miles upriver from the entrance. In June, the reversal depth appeared to increase with distance upriver. This implied

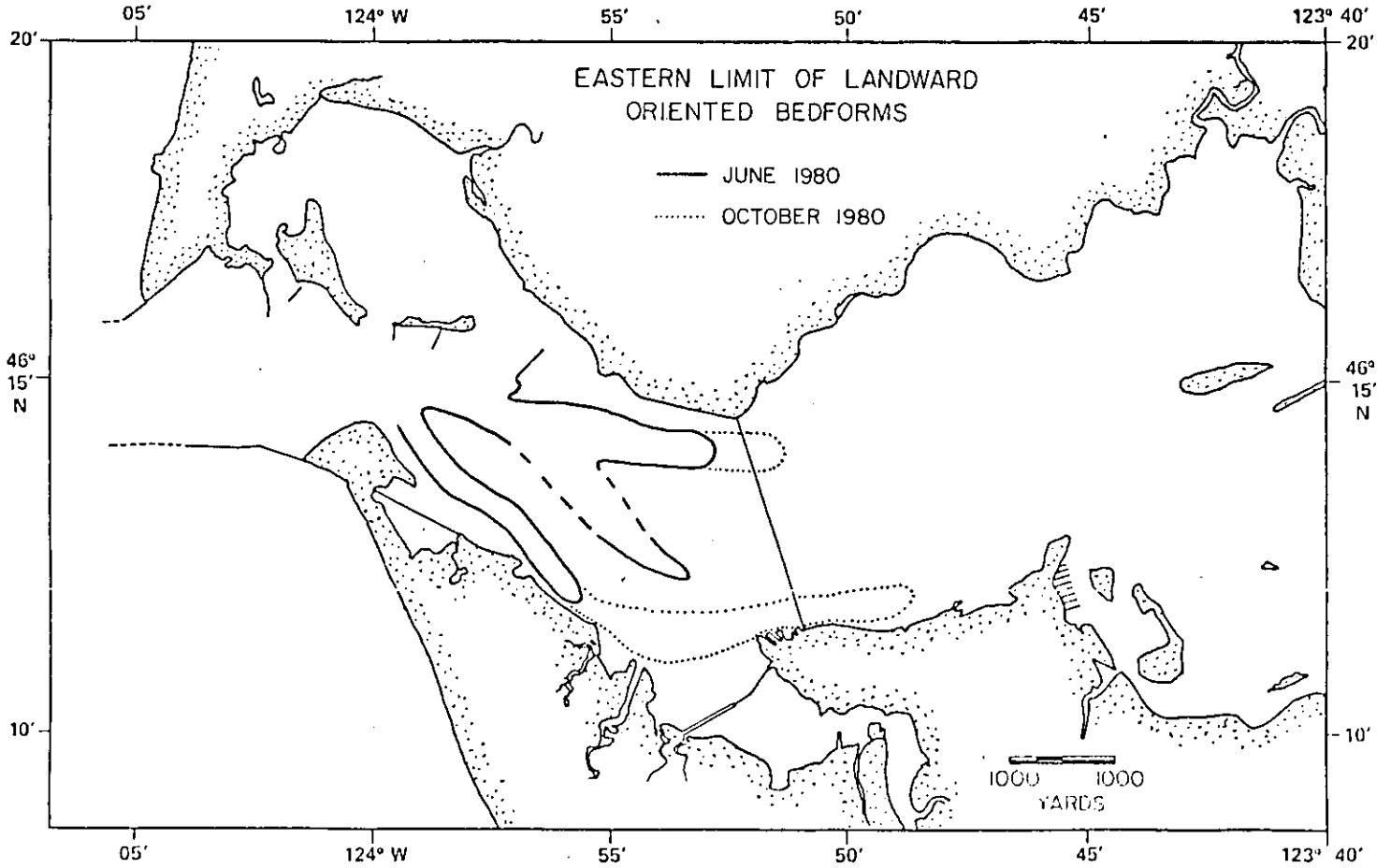

Figure 56. Schematic representation of the seasonal variation in the landward limit of landward-oriented bedforms for the high discharge season (June) and the low discharge season (October).

that the depths to which ebb currents influenced the bottom topography and created seaward-oriented bedforms decreased downriver. Correspondingly, the height above the bottom at which estuarine circulation was effective in generating landward-oriented bedforms in the channels decreased upriver. The bedform distribution and the bedform reversal depths reflected the net current regime and thus were indicative of the estuarine circulation pattern in the estuary. The depth-related orientation reversal plots (Figure 54) suggested that saline return flow occurred at a greater depth in June and did not extend as far landward as it did in October. In October there was more scatter in the reversal depths, but they were generally at more shallow depths than in June. It is plausible that the increased vertical mixing during lower discharge resulted in a more poorly defined boundary between flood and ebb dominated depths in October. Another interpretation is that the relative importance of spring-neap tidal differences was greater during low-discharge periods, causing bimonthly migration of the boundary between ebb- and flood-dominated portions of the channel-flanks system. Some of the scatter from both seasons may have been due to nondiscriminant sampling during spring and neap tides. No systematic variation in reversal depths was observed between the north and south flanks of the South Channel and data from both sides are plotted in Figure 54.

Finally, seasonal variations in the large landward-oriented bedforms in both channels were noted in the records. In the North Channel, during the low discharge season, large-scale bedforms with wavelengths of 120 to 210 ft (36 to 64 m) and heights of 4 to 6 ft (1.5 to 2 m) displayed steep, landward-oriented slip-faces. In February, the bedforms in the eastern, landward portion of the channel were rounded but still asymmetrical and oriented landward. In June, the asymmetrical bedforms were replaced by symmetrical bedforms with superimposed seaward-oriented bedforms of a smaller scale. The eastern extent of landward orientation of these large-scale bedforms varied with discharge in a manner similar to that of smaller landward-oriented bedforms (Figure 56). The same was true of large-scale bedforms in the South Channel, which were seen as far east as Tansy Point in October, and were pushed seaward to west of Hammond in February and were not found at all in the South Channel in June.

4. DISCUSSION

4.1 RELATION OF SEDIMENT TRANSPORT TO FLOW PROPERTIES

Erosion, transportation, and deposition of sediments are major factors in controlling the configuration and morphology of the Columbia River Estuary. Flows induced by river runoff, tides, density gradients, wind-driven set-up, and tidal residuals are all sheared and decelerated by drag imposed on them by the estuary bottom. The total boundary shear stress $[(\tau_b)_t]$ exerted on the boundary by the fluid is composed of a form drag component $[(\tau_b)_p]$ and a skin friction component $[(\tau_b)_s]$, so

$$(\tau_b)_t = (\tau_b)_p + (\tau_b)_s$$

The form drag component results from pressure differences as flow travels around large obstacles in an estuary; form drag arises from bends in the channel, constrictions in the channel, and large topographic features such as bars and bedforms. The skin friction component results from the small-scale roughness of the bed itself and depends primarily on the grain size of the sediment and the flow strength.

The skin friction component of the total shear stress is the most important variable in sediment transport. The size of sediment that can be moved by a particular flow, and the rate at which sediment will move as bedload are directly dependent on skin friction $(\tau_b)_s$. Shields (1936) developed an empirical relationship that can be used to predict the critical value of skin friction that will erode a particular size of non-cohesive sediment. Most of the empirical and quasi-deterministic sediment transport equations that have been developed can be written in terms that relate transport rate to some high power of $(\tau_b)_s$ (Smith 1977).

At sufficiently low values of $(\tau_b)_s$, no sediment will move. As the skin-friction increases, the threshold for sediment motion $[(\tau_b)_{crit}]$ will be exceeded and bedload transport will occur. Initially, individual grains move along the bottom in traction transport and saltation. The grains are dragged, rolled, and make short hops, but are confined to within a few grain diameters of the bottom. The various modes of movement are collectively termed as "bedload transport." As increasingly higher values of $(\tau_b)_s$ are achieved, sediment grains leave the bed for longer periods of time and are accelerated to the speed of the flow some distance above the bed. This mode of intermittent suspended transport grades into entirely suspended load transport at higher skin friction values. The rate of suspended sediment transport becomes a function of flow velocity, rather than the shear stress. As a result,

intermittent and suspended sediment transport occur at much higher rates than bedload transport.

When sediment is moving under moderate skin friction $(\tau_b)_s$ (relative to its grain size), minor instabilities in an otherwise steady, uniform flow cause ripples and larger bedforms to form and propagate along the bottom. These features exert a form drag on the flow, and because they extend to various heights into the shearing flow, skin friction varies along the surface of the bedform. The transport rates of sediment moving along the bedform vary accordingly, reaching a maximum near the crest (Smith and McLean 1977). At the crest, increased skin friction may be sufficient to cause sediment to go into suspension. If not, the sediment will fall down the steep lee face into a zone of low skin friction in the trough, to eventually be covered by later-deposited sediments. In this manner, the bedform advances (under continued quasi-steady flow) along the bottom. When no sediment is being thrown into suspension at the crests, the rate of bedload transport will equal the rate of bedform transport as determined by the geometry and rate at which the bedform is moving.

Erosion or deposition occurs when sediment transport diverges or converges in an area, or when sediment is suspended or deposited from the water column. The "erosion equation" relates the rate of change of bed elevation (η) to the divergence of sediment transport ($\nabla \cdot Q_s$) and to changes in the amount of sediment suspended in the water column above the bed with time $(\frac{\partial V_s}{\partial t})$:

$$\frac{\partial}{\partial t} = \frac{-1}{C_b} \left(\nabla \cdot Q_s + \frac{\partial V_s}{\partial t} \right)$$

where C_b is the fractional concentration of sediment (to water) in the bed, usually about 0.6. In the case of bedload transport, V_s and $\frac{\partial V_s}{\partial t}$ are relatively small; therefore, when the transport rate out of an area exceeds the transport rate into the area, erosion occurs. Conversely, when more sediment is carried into an area than is removed, accretion occurs. Rapid transport can occur without deposition or erosion, just as very steady accumulation can occur with continued, slow sediment input and no removal. The changes in bottom configuration that result from erosion or deposition affect the flow by changing the form drag $(\tau_b)_p$.

Because sediment transport is a function of skin friction ($Q_s = f[(\tau_b)_s]$) and skin friction is related to the form drag and the total boundary shear stress, a feedback loop exists that makes the

flow-field - sedimentation relationship non-linear. As a result of this non-linearity, it is difficult to attain even a dynamic equilibrium among the sediments, the morphology at the bottom, and the flow field. In order to achieve a dynamic balance over some time interval two conditions must be met: 1) the mean flow conditions for that period must remain constant, and 2) the input and output of material to the estuary must balance over the time interval. In the Columbia River Estuary, it is difficult to identify any time interval that meets these criteria. Average flow conditions at any point include turbulent fluctuations (period $1\text{-}10^2$s) and flow variation over the tidal period ($10^2\text{-}10^4$s). The semidiurnal tides result in mean flow strength changes over a tidal day, and on a fortnightly (neap-spring) time scale as well ($10^4\text{-}10^5$s). Examination of tidal records from the estuary confirms that mean current speeds vary over periods of days to months in response to freshwater discharge fluctuations and in response to meteorological forcing from both within the estuary and from the continental shelf (Jay 1984). Clearly, the shortest time interval over which a dynamic equilibrium might be established is an entire hydrologic year. Interannual climatic variability requires that some longer-term mean (ten years?) be used to establish criteria for a "typical" year. However, during every ten-year interval some significant external variable has affected the estuary. Freshwater discharge has been changed by dam construction, power needs, or resource needs at least once in any recent ten-year period. Construction of jetties and dikes and channel modifications have resulted in changed bed morphology on an irregular but continuing basis (Table 7). The changed morphology results in a new flow field and new local values for sediment-transporting skin friction. Over very long time scales, changing sea level has affected the relationship between the flow field and morphology. As discussed in the Introduction, relative sea level is presently falling at Astoria. In the recent geologic past, sea level was apparently rising, and it may have fluctuated several times since the channel that the estuary occupies was cut into Tertiary rocks. Sea level has probably never been constant relative to the Columbia River Estuary. It is apparent that in the truest sense the first criterion of an interval of invariant mean flow conditions is never met.

It is important to note that even if the mean flow in the Columbia River Estuary were constant on, for example, an annual basis, a dynamic equilibrium between the morphology and the flow conditions could still not exist. This is because in the natural estuarine system the second criterion would not be met. Results that are discussed below indicate that substantially more sediment is entering the estuary than is leaving the estuary. The estuary is depositional and cannot, by definition, attain an equilibrium until a mass balance is achieved between the sediment supplied to the estuary by the river and the output of sediment to the

Table 7. Man's major influences on the Columbia River Estuary (Lockett 1963; Lockett 1967; Pacific N.W. River Basin Commission 1972)

DATE	ACTIVITY
Before 1885	Sporadic dredging - minimal amounts
1885	30-foot Entrance Project initiated
1885-1893	Construction of South Jetty at entrance
1903-1904	Extension of South Jetty
1905	40-foot Entrance Project initiated
1913-1917	Construction of North Jetty
1932	Chinook Pile Dike
1933	Rock Island Dam
1938	Bonneville Dam
1939	Jetty A
1941	Grand Coulee Dam
1945	Regular annual dredging initiated
1953	McNary Dam
1954	48-foot Entrance Project initiated
1955	Chief Joseph Dam
1957	The Dalles Dam
1959	Priest Rapids Dam
1961	Rocky Reach Dam
1963	Wanapum Dam
1967	Wells Dam
1968	John Day Dam
1972	Mica Lake, Arrow Lake Dams
1977	52-foot Entrance Project initiated

From Roy et al. (1982). (Also refer to Table 17 in Appendix C.)

continental shelf or beaches. An artificial equilibrium might be established by removal of sufficient amounts of sediment from the system through dredging. However, this discussion concentrates on the natural processes occurring in the estuary.

The conclusion that must be drawn from the discussion thus far is that neither a "steady state" approach nor a "dynamic equilibrium" concept is applicable to the physical processes in the estuary. Instead, it is better to consider trends, both spatial and temporal, in the physical processes that control sedimentation in the estuary. Although there is some limited value in discussing time-averaged values of salinity structure, flow conditions, bottom morphology, or sediment distribution, it is important to remember that these are transient characteristics best used to estimate trends. The selection of appropriate time and space scales is crucial to the interpretation of any phenomenon measured in the estuary. In the case of sediment transport, the controlling factors (flow conditions and the resultant skin-friction component of the boundary shear stress) occur locally and instantaneously. Dense temporal and spatial sampling must be averaged to obtain long-term trends. For this reason, only a few of the physical processes lend themselves to long-term measurement. In this study, the only parameters measured continuously (relative to their important frequencies) were tidal heights and freshwater discharge. Continuous measurements of currents, temperature, salinity, and turbidity were made in some areas for relatively brief intervals, but not at a spatial density sufficient to adequately characterize their fields.

Fortunately, the processes of sediment transport and deposition tend to integrate the effects of time-variant processes. It is possible, by observing bedforms for example, to determine the dominant trends in bedload transport for some time interval. Similarly, the distribution of sediments reflects the divergence or convergence of the sediment transport field over a finite time period. The large-scale morphology of the estuary is clearly the cumulative result of processes acting over a longer time scale. This study utilizes the integrating effect of the distribution of bedforms, bottom morphology and sediment distribution to approach an understanding of the trends in sedimentation over various time scales in the estuary.

The remainder of this discussion focuses on the relationships between the physical processes of sedimentation and the resulting distributions of sediments, bedforms and bottom morphology. The direct measurements of the suspended sediment processes will be included as a separate section to be integrated into the overall

description of sedimentary environments and patterns of shoaling and erosion in the estuary.

4.2 SEDIMENT DISTRIBUTION

4.2.1 Grain Size Distributions

Early sedimentologists realized that when plots of fraction weight by size-class interval were plotted against a logarithmic size scale, the resulting distribution was nearly normal (Krumbien and Pettijohn 1938). As a result, the phi notation was introduced to describe the size of sediment grains:

$$\phi = -\log_2 D$$

where ϕ is phi and D is the nominal particle diameter (in millimeters) (cf. Table 2). Although some controversy continues regarding the correct use or value of the phi notation (Pierce and Graus 1981; McManus 1982), it is generally agreed that the phi notation allows more sensitive statistical description of the size-distribution curve (McLaren and Bowles 1983). For that reason, this study utilizes moment measures calculated on the phi distribution. It is important to remember that these are statistics based on distributions that have undergone a log-transformation.

The method of determining grain size affects the interpretation of the results. Ideally, a direct measure of the hydraulic characteristics of the grains should be obtained in order to compare grain size distributions with sediment transport processes. Settling velocity of the grains conveniently provides such a measure while accounting for the variables such as grain shape and density. During the initial phases of these studies, techniques for measuring settling velocity and relating it to sieve-size analyses were developed (Creager et al. 1980). These efforts affirmed that, although a generally close relationship existed between settling velocity and grain size in the Columbia River Estuary sediments, enough variation existed between the measures to produce different results when factor analysis was performed on the data (Roy et al. 1982). In order to allow comparison of new results with the results of hundreds of samples previouly analyzed using the sieve-size technique, that technique was continued. The grain size data therefore represent the sieve-size distributions in the sand-size ranges of the sediment. The hydraulic behavior of these grains is loosely approximated by this measure, but deviations will occur if density, shape, or roundness vary systematically with size. However, the curves are considered only in relation to one another and therefore somewhat less error is likely to be involved with attributing hydraulic characteristics on

the basis of sieve-size. For the purposes of facilitating this discussion, the sieve-size distributions will be considered as relative measures of settling velocity.

McManus (1982) provides a succinct summary of the long history of interpretation of grain size distributions. He suggests that the development of the phi notation and the subsequent abundance of statistical descriptions of sediment distributions motivated an hypothesis that sedimentary environments could be identified by the grain size of the sediments. A wide variety of statistical parameters were combined in attempts to produce bivariate plots that effectively separated environments (i.e., Friedman 1961, 1967; Passega 1964, 1977; a long list of examples is presented by the Sedimentation Seminar 1981). As McManus (1982) points out, a substantial research effort was expended by sedimentologists in refuting this hypothesis (Middleton 1962; Tucker and Vacher 1980; Sedimentation Seminar 1981). The inability to characterize environments with one or two size parameters led to the application of multivariate techniques and factor analysis techniques (Klovan 1966; Allen et al. 1971; Drapeau 1973; Chambers and Upchurch 1979). Although these techniques are apparently more successful at discriminating between environments on the basis of grain size alone, they were developed during a growing realization among sedimentologists that grain size distributions are related to the sedimentary processes rather than the sedimentary environment (McManus 1982). More specifically, the grain size distributions are related to the mode of transport, i.e. rolling, sliding, and saltation (bedload transport), intermittent suspension, and suspension. The literature contains much discussion on how to dissect a sediment size distribution and identify the size contributions of various processes (Tanner 1959; Visher 1969; Middleton 1976). Although the arguments as to whether cumulative curves contain overlapping or truncated normal subdistributions are probably moot, the recognition that grain size is closely related to the mode of transport is crucial. This approach incorporates much of the knowledge gained by studies of fluid mechanics and sediment transport by workers such as Shields (1936), White (1940), Inman (1949), Hjulström (1953), and Sundborg (1956). However, the traditional approach has been to associate particular sizes with particular modes of transport and to describe the sediment distribution in terms of the relative importance of each mode of transport. The assignment of a transport mode on the basis of size (or settling velocity) ignores the continuous nature of the transition from one transport mode to another. More importantly, such an approach contributes very little to the interpretation of the higher order statistical parameters commonly calculated to describe the sediment distributions.

Recently, McLaren (1981, 1982) and McLaren and Bowles

(1983) have made a significant contribution to the intepretation of grain size distributions and their relationship with source sediments. In addition to stressing the continuous change of the statistical parameters describing the grain size distribution (earlier recognized by Krumbein 1938), McLaren emphasizes the need to consider the parameters relative to the way in which they change during erosion, transport, and deposition. Most importantly, he provides an intuitive model for envisioning the changes in mean size, sorting, and skewness for several cases involving partial erosion of samples with given size distributions and subsequent partial or complete deposition of the fraction eroded (McLaren 1981). In each case, the lag deposit remaining after the finer sediment has been eroded is coarser and more positively skewed than the transported fraction. Complete deposition of the transported fraction will produce a deposit finer and more negatively skewed than either the original source or the lag. Partial deposition of the transported fraction can produce a deposit either finer or coarser than the source, depending on the amount of the original deposit eroded. When a given skin friction results in transport of the erodable fraction of a bottom sediment, the amount of material removed from each size class in the original distribution should increase as a monotonic function of the excess shear stress. In a recent manuscript, McLaren and Bowles (1983) coin the term "transport function" for the curve describing the percentage of each original size class transported by a flow of a certain strength. They present experimental evidence indicating that this function does not increase with decreasing sediment size, but rather decreases after some point. The transport function can be described using the same statistical parameters used for the sediment distribution; McLaren and Bowles (1983) suggest that the "low energy" transport function is negatively skewed and becomes more symmetric with increasing energy. Comparison of source sediments with sediments derived from the source sediments is facilitated by simply differencing the transport functions. When McLaren and Bowles do this for their empirically-derived transport functions, they find a constant set of relationships among sediments and their source deposits. They argue that for sediments that display a decrease in grain size in the direction of transport, the size distributions will become more positively skewed (fine-skewed) in the direction of transport. Alternatively, sediments which exhibit coarser means in the direction of transport will have grain size distributions negatively skewed (coarse-skewed) with distance. In both cases the sorting may be at first reduced (higher standard deviations) but will eventually improve.

In general, the channel sediments in the Columbia River Estuary display a tendency to fine seaward and become more positively skewed, which could indicate either seaward

transport from the estuary or landward transport into the estuary. Sediments from the entrance region and the neighboring continental shelf also tend to become finer in a seaward direction, but do not display marked skewness trends. Application of the relationships developed by McLaren and Bowles do not provide unambiguous source/transport direction information. This is not surprising in light of the likely prospect of multiple sediment sources (river and shelf) and the complex transport pathways and erosion/deposition patterns that apparently exist. Apparently, a more complex set of processes is acting to obscure the relationship expected by transport of sediment from a single source. Various techniques were used to approach this problem and the ensuing discussion on statistics and the interpretation of the observed grain size distributions attempt to sort out these complex processes.

4.2.2 Exploratory Statistics

A substantial effort was devoted to the development and application of exploratory statistics (factor analysis and cluster analysis) statistics in this study. Despite the apparent success of these techniques in other environments (Imbrie and Van Andel 1964; Klovan 1966; Borgeld et al. 1979), factor analysis did not prove as useful in this study. Cluster analysis and the evaluation of the distribution of more "traditional" grain size statistics (mean size, sorting, skewness) eventually proved more useful for reasons that are discussed here.

One of the main limitations to the techniques used in this study was the criterion applied to determine the degree of similarity between samples. The use of the cosine-theta coefficient to compare samples based on the fraction weight of each size class made both the factor analysis and cluster analysis techniques very sensitive to the modal values of the sediment size distribution. The samples that were grouped by either technique tended to have similar modal values. When several modes were present, those samples with the same multiple modes were grouped; the dominant mode of those samples was less important than the combination of several modes. Although the modal phi-size of a sediment sample is clearly an important characteristic, and although the identification and grouping of polymodal samples is a valuable tool in size-distribution interpretation, the emphasis on modal measures meant that other, equally important, size parameters were being ignored. Specifically, the shape of the distribution curve and the nature of the tails of the curve were left unaccounted for by the cosine-theta measure of similarity. As has been implied in this report, the sorting, skewness, kurtosis, and the size of the coarsest first percentile are all important aspects of the grain size distribution. The conclusion reached during this study is that the factor and cluster analysis

techniques rely on only a subset of the total information available in a suite of size distribution curves, and that only under special circumstances are the techniques more useful than direct analysis of the distribution curves.

The true value of the factor and cluster analysis techniques becomes apparent when the data conform to one of the following criteria: 1) The data represent a combination of end-members mixed in various proportions, or 2) the data consist of fairly discrete groups defined by some combination of the measured variables. In fact, both techniques will provide useful data when either assumption is true, but factor analysis is conceptually better suited for the interpretation of the first case and cluster analysis for the second. In grain size analysis, where the n-dimensional space consists of vectors related to size classes and the associated amplitudes represent fraction-percent in those size casses, application of either of the two interpretations has distinct geological significance. The selection of several end-members and the subsequent description of the remaining samples as some combination of the end-member samples suggests a mixing process and imparts special source or sink characteristics to the end-members. Alternatively, the grouping assumption suggests the presence of discrete sediment types at various locations. Either of these constructs may be useful in certain sedimentary settings. The value of the exploratory statistics is in suggesting which (if any) of these scenarios is useful, and in identifying the samples associated with each end-member or group. If the distribution is largely homogenous or represents one or more continua, neither technique is adequate. The selection of end-members or groups is largely artificial and somewhat arbitrary, and a subsequent interpretation would be built on false assumptions. The inability of the factor analysis to reproduce similar factors in each run and the inability of cluster analysis to identify a stable set of groups in the various runs is evidence that in the Columbia River Estuary the grain size distribution is not controlled by either an admixture of end-members or by several discrete grain size groups. It may also reflect the rather narrow range of sediment sizes present in the estuary. This is not to imply that mixtures of various size classes do not occur or that discrete size types do not exist, but rather that the overall nature of the grain size distribution in the estuary is continuous and gradational. Examination of most of the bivariate plots of sediment size parameters bears this out (Figures 24, 25, and 26).

Another drawback to the exploratory statistical techniques should be mentioned here. Neither technique is designed to provide the interpreter with much information on why samples are grouped. In factor analysis in particular, the selection of an end-member in the final oblique rotation

may mislead an interpreter who indiscriminately assigns all the attributes of that sample to the other samples that load highly on that end-member. Cluster analysis does not provide potentially misleading representatives for each of the groupings, but the interpreter is forced to examine the distribution curves of the clusters to arrive at a geologically meaningful characterization of the cluster. Because the use of the cosine-theta coefficient on the size-class fractions emphasizes the modal values of the samples, the clustering technique turns out to be unnecessary.

4.2.3 Characterstics of the Overall Grain size Distributions

Figures 24, 25, and 26 suggest that the continuous distribution of mean size and skewness may be subdivided into two groups with distinct trends. The finer sediments (mean finer than 3.00 phi) represent the fraction transported exclusively as suspended load. For sediments finer than about 3.00 phi, when the critical shear stress needed to erode the sediment is reached, the ratio of settling velocity to the friction velocity is such that the sediment travels almost entirely as suspended load. Therefore, for the finer sediments (finer than about 3.00 phi), transport will occur as suspended load. These fine sediments display a tendency towards less positive skewness with increasingly finer mean size. In contrast, the samples with means of 1.5 to 3.00 phi show a trend of increasingly positive skewness with increasingly finer mean size. These sediments move as intermittently suspended sediments. The coarser sizes in this range are moved as suspended load only under the highest values of $(\tau_b)_s$ encountered in the estuary and are generally transported as bedload.

Because of the narrow overall range in sediment size in the estuary and the high local variability, only generalized patterns of sediment distribution can be mapped. Figures 35, 36, 37, and 38 depict the areal distribution of sediments in the estuary; Figures 30, 31, 32, 33, and 34 depict the changes in sediment size with distance downriver.

There is an overall tendency for grain size to decrease from the upriver reaches into the upper estuary. The channel sediments in the upriver reaches are coarse (0.0 to 2.5 phi) and negatively skewed. These sediments apparently are representative of the material transported to the estuary system from the river as bedload. Moving seaward, mean grain size of the channel sediments decreases near the upriver limit of salinity intrusion (RM-25) and the variablility in the mean sediment size increases substantially. The increased variability is attributed to the wide variety of channel environments that occur in the estuary. The decrease in grain size suggests that the mean boundary shear stress is lower in the estuary than in the river and that some of the material that was transported as suspended

load is deposited in the estuary channels. Throughout the length of the estuary, mean grain size varies between 0.75 and 2.5 in the main channels and 1.5 to 3.00 phi on the mid-estuary shoals. Near the entrance, the mean size begins to fine seaward again and the sediments become much better sorted. Jay (1984) notes that the highest tidal energy in the estuary is found in this narrow entrance region. The tidal currents act to winnow out fine sediment and there is apparently no source of coarse material; as a result, the sediments in the entrance channel are confined to a very narrow grain size range of 1.75 to 2.75 phi.

Several lines of evidence suggest that sediment is not moving out of the estuary as bedload. The well-sorted, fine sediments found in the entrance channel are finer than the upriver channel sediments despite evidence that they are subjected to the highest shear stresses in the estuary. The general decrease in grain size toward the mouth of the estuary suggests that the coarsest material is not transported from the upriver reaches to the entrance. The patterns of coarse, negatively-skewed sediment that extend from these upriver reaches end near the Astoria-Megler bridge or the Chinook pile dike, depending on the season. Beginning near RM-25 the grain size of the coarsest first-percentile decreases continuously in the seaward direction. All of this evidence suggest that bedload sediment is not transported out of the estuary and that, in fact, the fine, well-sorted sediment found near the entrance is being transported into the estuary from the offshore regions adjacent to the estuary. An offshore source for these sediments would account for the lack of coarse material, for the high sorting values they display, and for the distribution patterns observed in the estuary.

It should be noted that a tongue of coarser sediments (2.5 phi as opposed to 2.75 phi) exists in the offshore extension at the entrance channel (Borgeld et al. 1978). The channel dissects the outer tidal delta, which has been displaced a significant distance seaward since the construction of the north and south entrance jetties. Two interpretations of this distribution are possible: 1) these coarser sediments are transported seaward from the estuary, in contrast to the model discussed above, or 2) they represent winnowed offshore sediments, from which the finer fraction has been removed by strong tidal action. Arguments in favor of the first interpretation are based on the assumption that the sediments comprising the outer tidal delta are fine (2.75 phi) and that the only source of coarse (2.5 phi) sediment is the estuary. However, the second interpretation seems more reasonable in light of the presumed flood dominance of the deeper entrance-channel currents during all but the most extreme high-flow conditions, and the high tidal currents available to winnow away the fine fraction from the channel.

Another aspect of the areal distribution of sediments is the presence of round and disc-shaped, sandy-silt clasts in many of the sediment samples from the lower estuary (Roy et al. 1982). These clasts were generally found in water deeper than 30 ft (10 m) and were usually found in the portion of the estuary seaward of Tongue Point (Figures 35, 36, and 37). The same areas often yielded two-layer samples which usually exhibited a thin (1- to 2-in, 2- to 6-cm) layer of silty sand (mean 3.5 to 5.00 phi) overlying moderately-sorted medium-fine sand. The inverse relationship (coarser sediment overlying fine sediment) was rarely observed. Gelfenbaum (1983) suggests that the degeneration of the turbidity maximum that occurs during neap tides results in the redeposition of the fine sand and silt suspended by the higher currents of spring tide. The locations of the two-layer samples and the samples containing silty-sand clasts correspond to the region over which the turbidity maximum is advected. It seems likely that the silty-sand clasts are in fact rip-up clasts originally deposited as a thin silty layer along the channel floors during the degeneration of a turbidity maximum, and subsequently eroded and transported by later currents. The fact that most are rounded suggests that they have undergone some transport; the fact that they are only semi-consolidated and somewhat fragile suggests that they have not been transported long distances.

An alternative hypothesis suggests that the silty-sand clasts are the result of erosion of older fluvial or estuarine deposits. Evidence for erosion of older channel deposits exists in several areas (c.f. Figure 57) and the historical bathymetry (CREDDP, 1983) clearly documents channel erosion. In fact, several samples contained more indurated clay clasts that resembled the material found along subaqueous cut banks upriver. However, these clasts were only found at sampling locations in the upper estuary and accounted for only a small fraction of the clasts recovered. The additional fact that most of the presumed rip-up clasts were found during the fall cruises, rather than during the higher discharge spring and winter cruises argues against a mechanism linked to discharge. Nonetheless, both processes may be producing rip-up clasts in the estuary.

Figure 38 depicts the areas which exhibit silt plus clay percentages of more than 10% during some season. Most of the fine sediments found seasonally in the channel bottoms are associated with the two-layer sample and the mudball distributions. Fine sediments are also found in the shallow and protected peripheral bays, including Cathlamet, Grays Bay, Youngs Bay, and Baker Bay. These areas are subjected to only moderate wave action and relatively low currents; as a result they are largely depositional areas and serve as accumulation sites for fine-grained

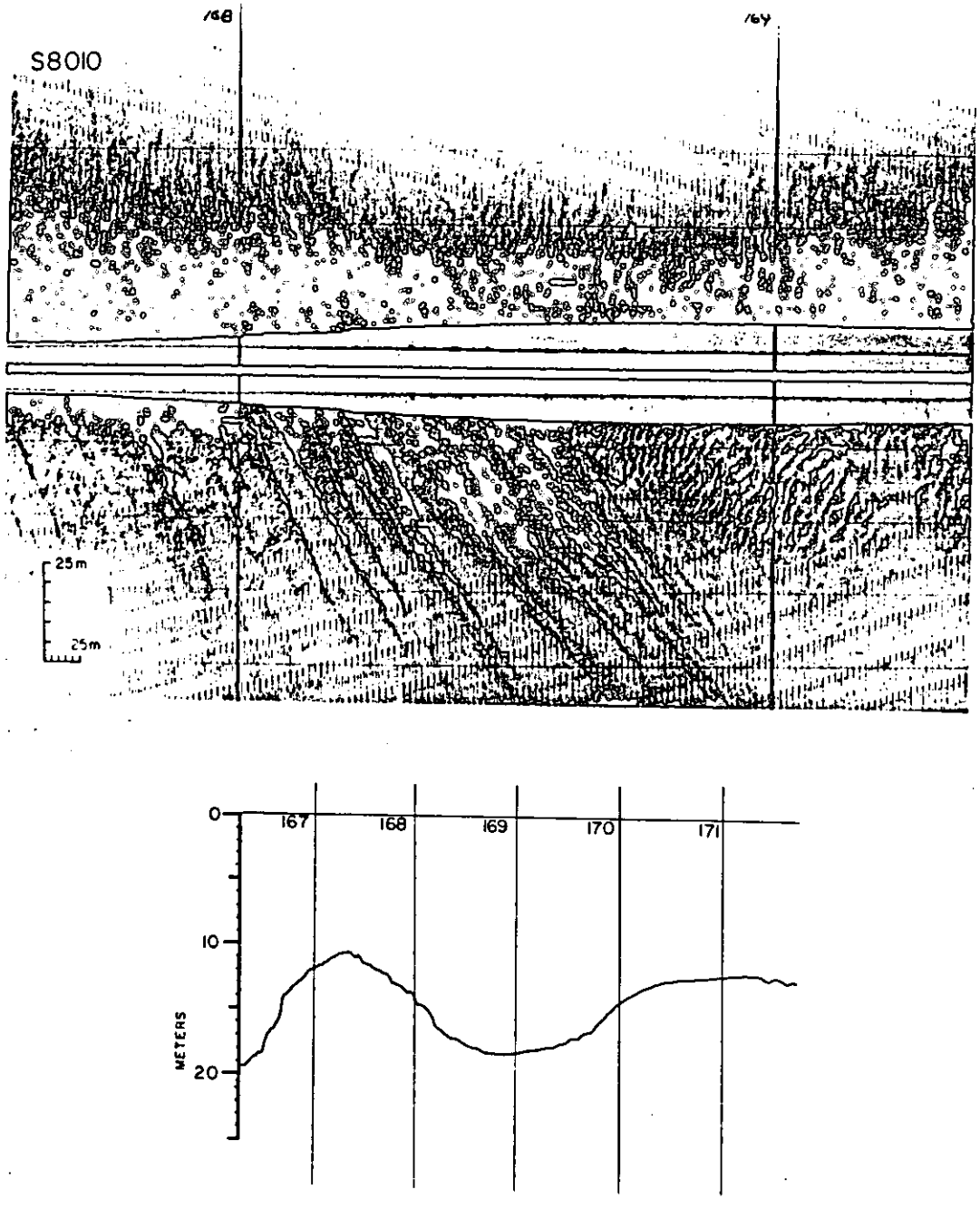

Figure 57. Side-scan sonar and echo-sounder records of differential erosion of exposed strata along the south flank of the North Channel.

sediments. Creager et al. (1980) have shown that, in some instances, the effects of wind-waves serve to differentiate the fine samples between protected and unprotected peripheral bays.

In order to examine the products of fine-grain sedimentation in the estuary, several samples from Mott Basin were chosen for grain size analysis. This shallow basin (24 ft, 7 m) was created by dredging during World War II and is well-protected by Mott and Lois Islands. A continuation of Prairie Channel runs through the western edge of the basin, but very little current or wave action affects most of the basin. Bathymetric differencing maps (CREDDP, 1983) indicate that an average of five feet of accumulation has occurred over most of the basin since 1958. In the undisturbed center of the basin, the mean size of the depositional sediments is between 3.5 and 6.60 phi. If these sediments are characteristic of the deposition from suspension in the estuary, it appears that silt is quantitatively more important than clay in fine-grain deposition in the estuary. Neal (1972) and Gelfenaum (1983) provide corroborative evidence with their suspended sediment grain size distributions. They find that the modal size of the sediments is in the coarse clay-fine silt range. Thus, it appears that two processes are involved in the deposition of fine-grain sediments in the estuary. Deposition during the degeneration of the turbidity maximum produces deposits in the channels, while deposition from suspension of material in quiet water produces deposits in the peripheral bays. The processes that produce these deposits are discussed in detail below.

4.3 SUSPENDED SEDIMENT TRANSPORT

Existing models of estuarine suspended sediment transport are based predominantly on observations from estuaries of the Atlantic seaboard of the United States (e.g., Simmons 1966; Meade 1967; Festa and Hansen 1978; Officer 1980). There are a few significant differences, however, between the Columbia River Estuary and the other well-studied estuaries, including a larger tidal range to depth ratio, significant fortnightly tidal range variations and larger freshwater discharge. These differences make the turbidity maximum in the Columbia River Estuary an unsteady feature that undergoes significant variations in location and concentration of suspended sediment. In the Columbia River the turbidity maximum is advected on a semidiurnal time scale and degenerates and regenerates on a fortnightly time scale.

In addition to the semidiurnal tidal excursions and the fortnightly concentration variations of the turbidity maximum, data from Hubbell et al. (1971) indicate variations in the magnitude and location of the turbidity maximum on a

seasonal basis. The magnitude of the turbidity maximum varied between 260 mg l^{-1} during the low discharge season (September 1969) and 750 mg l^{-1} during high discharge (May 1970). Although the general shape of the turbidity maximum remained nearly the same, the entire feature was shifted longitudinally from one discharge season to the next. In May, the turbidity maximum was centered around Hammond (RM-10) while in September it was centered at RM-16, farther upriver between Astoria and Tongue Point. A question arises as to whether Hubbell et al. (1971) were measuring fortnightly variations instead of seasonal variations. Tide table predictions for the two seasonal sampling periods indicate that the differences in tidal ranges from those times were small. Therefore, Hubbell et al. were actually measuring seasonal and not fortnightly variations in suspended sediment concentrations. Prior to the present study, these seasonal variations in suspended sediment concentrations were thought to be the most important variations that occurred in the estuary.

Table 8 summarizes the variations in the suspended sediment concentration that could be observed at a single location within the estuary. The values in Table 8 represent the maximum values observed approximately 5 ft (1.5 m) above the bed over the indicated time scales. Horizontal excursions of the turbidity maximum are predominately responsible for the semidiurnal concentration variations and do not indicate changes in the turbidity maximum itself. Both the fortnightly and the seasonal

Table 8. Comparison of suspended sediment concentration range over several time scales (Hubbell et al. 1971).

Time scale	Suspended sediment concentration
semidiurnal	90 - 640 mg l^{-1}
fortnightly	95 - 640 mg l^{-1}
seasonal	260 - 750 mg l^{-1}

variations, however, are actual changes in the suspended sediment concentrations of the turbidity maximum. Because the magnitudes of these variations are similar, any consideration of suspended sediment dynamics should include the semidiurnal and fortnightly as well as the seasonal variations.

With regard to sedimentation predictions, large tidal excursion of the turbidity maximum makes much of the estuary a potential sink of fine-grained material. During a single neap tide, however, calculations indicate that deposition of

suspended sediment from the turbidity maximum will probably be negligible. Within the fortnightly time frame, concentrations of suspended particles in the turbidity maximum may vary between washload levels as low as 50 mg l^{-1} during the neap tide and as high as 600 mg l^{-1} during the spring tide. If all of the material in the turbidity maximum present during a spring tide was deposited during the following neap tide by settling directly to the bottom, the thickness of the layer would be approximately 4 mm. Considering, however, the large excursion range of the turbidity maximum, deposition of suspended material during a neap tide will be spread over the entire range more thinly than if the turbidity maximum were not being tidally advected. Based on the Hubbel et al. (1971) longitudinal distribution of the turbidity maximum during low discharge conditions, a maximum concentration of 600 mg l^{-1} from this study, an average water depth of 30 ft (10 m) and a porosity of 50%, a layer 1.4 mm thick, on average, may be deposited over the entire 12 mile (20 km) excursion range. A layer this thick might comprise only 2 to 3% of a bottom grab sample and would go unnoticed in the bottom sediment size analysis. The actual deposit during a neap tide will probably not be evenly distributed over the entire range, however, but will tend to be greater in some areas and less in others. Deposits related to the turbidity maximum have been tentatively identified in some samples, and the role of the suspended sediment field in estuarine deposition is discussed below.

4.4 BEDLOAD SEDIMENT TRANSPORT

The side-scan sonar studies provided valuable information on the temporal and spatial distributions of bedforms in the estuary. In order to interpret these distributions in terms of rates and directions of bedload sediment transport, several assumptions must be made. The assumptions are based on research performed on bedforms by sedimentologists over the last twenty years. Numerous flume studies are available which provide empirical relationships between some measure of flow strength, grain size, sediment transport rates and bedform morphology for shallow, steady flow (Simons et al. 1965; Allen 1968; Costello 1974; Costello and Southard 1981; Harms et al. 1975; Harms et al. 1982). The problem of relating transport rates to bedform morphology in unsteady oscillatory flow of varying depth is much more complex and has motivated field investigations in intertidal and subtidal coastal environments. In these environments, it is more difficult to measure the parameters that affect bedform morphology and to know how important flow oscillations and depth variations are on the ultimate geometry of the bedforms. Nonetheless, several workers have extended the depth-velocity-flow concept from the flume to natural environments and discussed the relationships between sediment transport rates and bedform shape (e.g., Boothroyd

and Hubbard 1975; Dalrymple et al. 1978; Rubin and McCulloch 1980). These studies permit the following assumptions to be made regarding the relationship of sediment transport rates to the morphology of bedforms in the estuary:

1) Bedform sediment transport occurs in a direction approximately normal to the strike of the crest axis and in the direction of the steeper side of the bedform.

2) Transport is more rapid and/or has occurred more recently when the steeper face is at the angle of repose (a "slip-face").

3) Conversely, the absence of a slip-face indicates that transport has occurred in both directions. In these instances, it is assumed that net transport has been in the direction of the steeper face, but it is recognized that both instantaneous and recent net transport directions may differ from the assumed longer-term net transport direction.

4) Because large bedforms contain more sediment, more sediment transport is necessary to significantly alter their characteristic geometry. Therefore, their morphology responds more slowly to changes in flow conditions than that of smaller features. Larger bedforms tend to integrate the effects of flow conditions over a longer period of time.

5) As a corollary to (4) it is assumed that smaller bedforms reflect instantaneous flow conditions more closely than larger bedforms.

6) In areas where both large- and small-scale bedforms are present, and where the small bedforms change orientation in response to tidal flow oscillations, the rate and direction of net sediment transport is best estimated from the larger bedforms.

7) Among bedforms with slip-faces, the rate of bedform migration, and, therefore, the rate of bedform sediment transport, can be estimated by the crest geometry; when the crestlines become less linear and more sinuous or even cuspate, they are reflecting stronger flow conditions and increased sediment transport rates.

8) Although intepretation of sediment transport rates is mostly based on the relation of bedform geometry and inferred rates and direction of bedform migration (i.e., bedform transport), bedform morphology may sometimes indicate that high flow conditions are placing bed material into suspension and high rates of suspended sediment tranport are occurring. In particular, bedforms with irregular crest geometry or "planed-off" crests were used as indications that significant suspended sediment transport might be occurring.

Most of these assumptions are supported by evidence from the Columbia River Estuary, and the data provide much new material with which to test and refine many of the current hypotheses regarding bedform morphology. However, the intent of this study was to utilize the bedform information to gain insight into the patterns of sediment transport in the estuary. To this end, the assumptions and the data have been used to qualitatively identify bedform sediment transport vectors and their convergence and divergence in the estuary. In the manner discussed above, areas of convergence indicate net accumulation of sediment, and areas of divergence indicate erosion. It is important to remember that, in this situation, only the bedform transport is being considered; the total convergence of all transport (bedload and suspended load) must be included to predict erosion or deposition correctly. However, because convergence of bedload transport is apparently responsible for most of the shoaling in the estuary and because much of the deposition of finer sediments from suspension occurs on an ephemeral basis, the predictions of erosion and deposition based on the bedform transport field alone are of considerable value. The following sections first discuss bedform sediment transport at specific locations in the estuary, and then attempt to present an overview of sediment transport patterns in the estuary.

4.4.1 Site-Specific Discussions

Side-scan sonar record quality is notoriously poor for all seasons over the subaqueous extension of Clatsop Spit (opposite Cape Disappointment). Much of the problem is attributable to strong wave activity, the presence of salinity fronts in the water column, and turbulence. The few satisfactory records show a patchy distribution of small-scale bedforms and some large-scale, vaguely undulatory topography. The bottom is more often obscured by turbulence and, presumably, high concentrations of suspended sediments. Along the south shore of the estuary east of Clatsop Spit, bedforms are oriented seaward, regardless of tidal stage, for all three seasons. Seaward of Clatsop Spit, bedforms in the deeper waters of the entrance reverse tidally. It is suspected, on the basis of the high energy nature of this area and the observed turbulence in side-scan records, that the smooth topography of subaqueous Clatsop Spit is upper-flow regime plane bed (Simons et al. 1965) and represents a rapid flux of sediment. The predominately unidirectional seaward transport along the south flank of the South Channel ends at Clatsop Spit. Seaward of Clatsop Spit transport directions reverse tidally and the resultant net transport is ambiguous, but probably occurs at low rates.

Tracer studies conducted in this area suggest that net transport is seaward at a low rate (Creager et al. 1980). High unidirectional flux rates into the Clatsop Spit area

and low net transport away from this area results in a convergence of sediment transport, and suggest that the region is depositional (Figure 57). Historically, the subaqueous extension of Clatsop Spit has grown northward and infringed on the navigation channel, requiring maintenance dredging.

The Flavel Bar region of the South Channel also requires frequent dredging. Examination of the seasonal locations of the nodes of bedform transport reveals that Flavel Bar is midway between the seasonal extremes in upstream bedform transport (Figure 56). Seaward transport along the north side of the South Channel converges with tidally reversing transport to the west at various locations dependent on season. In October, reversing bedforms on the channel flank extend past Tansy Point, but in June, transport is seaward nearly to the tip of Desdemona Sands. West of Tansy Point, strong seaward transport occurs on the south side of the South Channel in all seasons, establishing a mechanism for removing sediment from this reach. However, east of Tansy Point on the south side, October data show landward transport. Hence, the south side of the South Channel adjacent to Tansy Point is a zone of divergence and net erosion. A convergence of transport in the Flavel Bar region is suggested by both its location beneath the end of bedform transport in the channel (Figure 56 and 58), and by a confluence of transport, at least during low flow periods, along the bordering shoals (Figure 58).

In the North Channel, landward transport apparently occurs in the western portion of the channel during all seasons and extends landward to the Astoria-Megler bridge and beyond during low flow periods (Figure 56). Seaward transport is rapid along the north flank in June, as evidenced by scour marks and cuspate bedforms in this area. The shallow channel east of the Chinook pile dike exhibits seaward transport during most seasons, but the 35-ft shoal near Site D displays seasonal variation in various transport directions and is occasionally the site of large, rounded, somewhat symmetrical bedforms (Figures 46, 47, and 48). Historically, this shoal has grown since the completion of the Chinook pile dike in 1935. Transport along the seaward portion of the south side of the North Channel and western tip of Desdemona Sands is dominantly landward for all seasons. Seaward transport along the landward portion of the south side of the North Channel occurs only during Feburary and June. These transport directions indicate convergence of sediment on the south flank of the North Channel, which would suggest deposition. However, records from this area often display a highly reflective character, and step-like features along the south side of the channel resemble erosional features associated with differential erosion of sedimentary strata (Figure 58). Investigation of the historical bathymetry

SCHEMATIC SUMMARY OF SEDIMENT TRANSPORT AND DEPOSITION PATTERNS

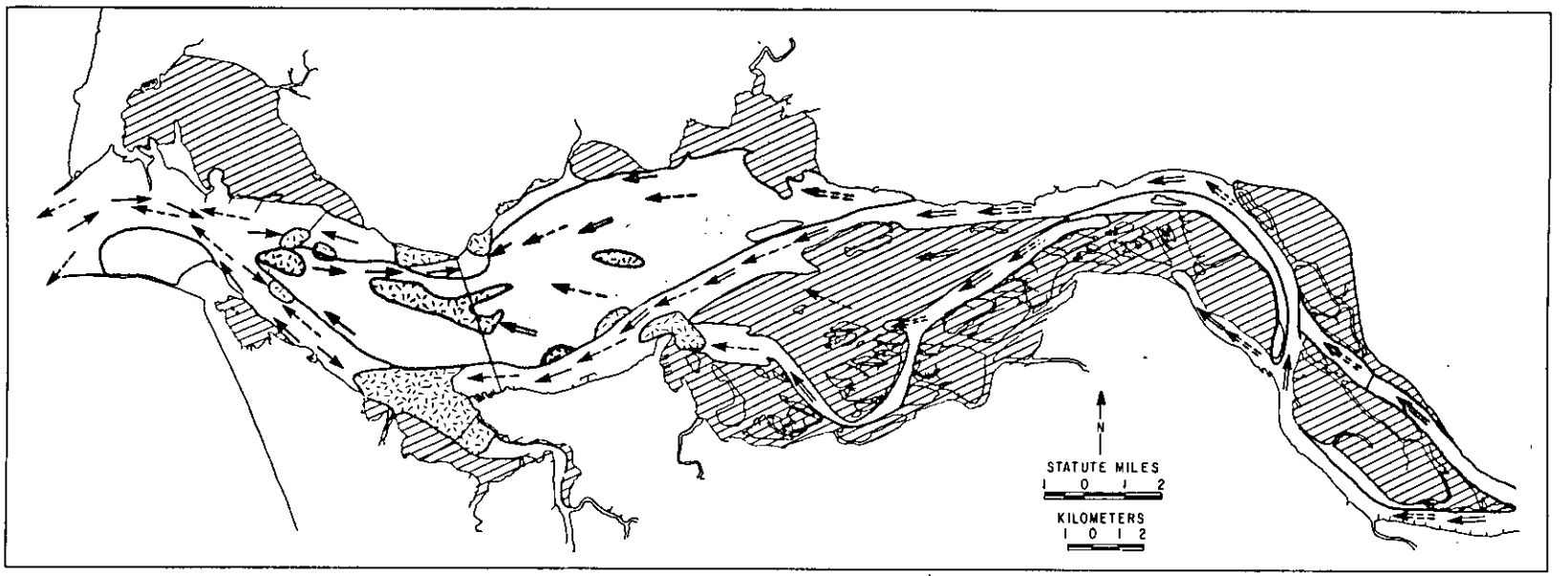

Long-term deposition of coarser sediments in association with channel migration and/or split growth

Ephemeral deposition of fine sediments in association with turbidity maximum processes

Long-term deposition of fine sediments

Non-deposition or erosion

BEDLOAD TRANPORT

→ Net of reversing transport

⟹ Unidirectional transport

SUSPENDED LOAD TRANSPORT

--→ Net of reversing transport

==⇒ Unidirectional transport

Figure 58. Sedimentation patterns in the Columbia River Estuary based on convergences and divergences of bedform sediment transport. Unidirectional transport arrows reflect dominant transport directions for all seasons. Net transport direction arrows reflect resultant direction of reversing transport indications, integrated over tidal and seasonal time frames.

reveals that the North Channel has recently migrated south, probably in response to the construction of the Chinook pile dike. Consequently, this area has been mapped as erosional in Figure 58.

The net landward transport at depth in the North Channel converges with seaward transport east of the Astoria-Megler bridge. On the basis of this evidence and the presence of large, symmetrical bedforms in the North Channel during June (Figure 48), the eastern portion of the North Channel has been mapped as depositional in Figure 58.

4.4.2 General Patterns of Bedform Sediment Transport

On the basis of the bedform distribution and inferred transport directions in the estuary seaward of Harrington Point, three roughly defined zones characterize flow and transport conditions. In the eastern, landward portion of the estuary, between Tongue Point and Harrington Point, large-scale, seaward-oriented bedforms develop and reversals of bedform orientation with tidal flow are uncommon. In this zone, fluvial processes dominate and bedform morphology is similar to that of a comparable river system.

Near the mouth, bedforms tend to be small with linear crests and to reverse direction in response to tidal currents. Often they are symmetric. Large-scale bedforms may form, especially on shoals (notably Clatsop Spit and the west tip of Desdemona Sands) but these rarely develop slip-faces. Tidal forces dominate in this zone. Although instantaneous transport rates may be high, net transport rates are low and not easily determined. These rates vary in response to fortnightly tidal flow variations.

Between these zones, flow conditions are more complex. Tidal reversals in bedform orientation are seen on some shoals, and landward-orientations frequently exist in channels. Bedform orientation reversals with depth are common, and transport pathways vary with depth. The effects of density-induced circulation dominate in this zone. Saline return flow at depth results in the growth of large, landward-oriented bedforms in the deep channels, while river outflow results in seaward-oriented bedforms on many shoals. Predictably, the morphology of this zone varies greatly with season. During low-discharge (October), landward-oriented bedforms extend further upriver in the channels, but during high-flow months (June) the landward oriented bedforms are forced west by as much as 12 to 13 statute miles. The erosion is less in the North Channel, consistent with evidence presented in Jay (1984) that shows less seasonal variation in North Channel circulation. Tidal monthly flow variations are expected to affect bedform morphology. The lagtime of bedform response, the sampling interval, and side-scan resolution are inadequate to address

this question except at Site D. The data from Site D do, however, show a variation in bedform character between spring and neap tides (Roy et al. 1982).

Examination of the bedform distribution patterns in the estuary provides some useful information on sedimentation patterns. Pathways of sediment movement in the estuary are summarized in Figure 58, and zones of likely transport convergence and deposition noted; areas of sediment transport divergence are mapped as erosional. Additional evidence from grain size studies and bathymetric studies is used to supplement side-scan data in the construction of this map. Two areas mapped as depositional, the subaqueous extension of Clatsop Spit and the Flavel Bar region are areas where routine dredging is required for channel maintenance. Both exhibit somewhat finer-grain sediment than surrounding areas. Flavel Bar is also located in a node for suspended sediment transport. The depositional area in the North Channel is predicted on the basis of bedform transport directions, and evidence obtained at Site D supports the conclusion that sedimentation is occurring in the North Channel (Roy et al. 1982). The erosional areas all display reflective bottoms. Sediment samples from the nearshore portion of the north side of the North Channel are fine-grained, suggesting that the generalized erosional nature of this area may not extend to the shoreline. Additional areas of erosion and deposition are expected to occur in conjunction with the migration of channels and point bars, as discussed below.

4.5 SYNTHESIS OF OBSERVATIONS

The following section makes use of inferences drawn from the data obtained during this study in an attempt to provide a synthesis of the observations on both physical processes and sedimentation in the estuary.

4.5.1 Friction Effects

Tides are the dominant source of energy in the estuary. Of the four modes contributing to circulation in the estuary, only the tidal flow is a first-order effect. The higher-order effects, including the tidal higher harmonics, the density-driven circulation, and the residual circulation (resulting from the combined effects of steady density-driven circulation, low frequency tidal flow, and atmospherically driven circulation) all represent relatively minor modifications to the basic tidal flow (Jay 1984). As a result, sediment transport is closely linked to the semidiurnal tides, and transport rates throughout the estuary vary in phase with the M2 tide.

Discharge variations have a pronounced effect on the tidal circulation. During periods of high runoff, the tidal

wave is damped significantly and tidal flows are reduced. Reduction in the tidal wave amplitude and increases in stratification combine to reduce vertical mixing during neap tides and high discharge periods. Entrainment of both salt and suspended sediment becomes less important under periods of increased stratification and advective transport more important. In addition, the effect of reduced mixing and increased stratification is to enhance the density-driven circulation (Jay 1984). The effect of these changes in the circulation patterns on sediment transport is to change the location of the suspended sediment field, to change the rate of advection of suspended sediment, and to alter the bottom shear stress.

Attempts to model the tidal wave in the Columbia River have led to the conclusion that the effective overall friction of the estuary is lowest from the entrance region (in this case, to approximately RM-17) and higher in the central estuary (RM-17 to RM-30). In the upriver reaches (>RM-30) the friction factor depends on river discharge; high discharge acts to reduce the friction to less than that in the central estuary, but during average and low discharge, the friction is highest in these upriver reaches (Benjamin Giese, pers. communication; Hamilton 1981). The friction factor in these models includes the effects of the Reynolds stress (momentum transfer through mixing) and the boundary shear stress. The boundary shear stress may be subdivided into two components: the skin friction and the form drag. Although data are not available that would permit the separation of the three contributions to the friction factor, some qualitative observations may be made concerning the relative importance of each in various parts of the estuary. In the entrance region, very little friction is exerted on the tidal wave because form drag from the wide, deep channel is low and mixing rates are generally low. The generally shallower upper estuary contains a more complex series of channels and shoals which exert more form drag on the flow than the simple pair of deep channels in the lower estuary. Because the total shear stress exerted on the bottom is composed of both the form drag and the skin fiction, by increasing the form drag and maintaining the total shear stress, the skin friction $(\tau_b)_s$ will be reduced. An additional reduction in the skin friction contribution to the shear stress occurs in the central and lower estuary as a result of decoupling of the flow from the bottom. Although the total stress may vary with distance from the entrance, the effective skin friction component of boundary shear stress is likely to be highest at the entrance, where form drag is lowest, lowest in the central estuary where form drag and mixing contribute the most to the total friction, and higher again upriver where mixing becomes unimportant and the flow is well coupled to the bottom.

4.5.2 Deposition of Fine Sediment

Deposits of fine-grained sediments occur in two different areas of the estuary: protected peripheral bays and channel bottoms of the mid- to upper-estuary. In both types of deposits, the grain size distribution seldom contains a mode finer than 8 to 9 phi. The absence of finer (clay-size) material is consistent with the size of material transported to the estuary by the Columbia River; samples of suspended sediment taken in the upper portions of the fluvial water column indicate that the river washload has a modal phi size of 8 to 9 phi. Samples from the peripheral bays apparently represent deposition of sediment suspended in the mid- to upper-water column. The bays are generally shallow, which would preclude the development of a turbidity maximum associated with salinity gradients and density-driven circulation. Sedimentation in these bays appears to be straight-forward: during the quiescent parts of the diurnal tidal cycle, and possibly also the neap-spring cycle, deposition occurs by settling. The settling-lag hypothesis developed by workers who have studied mudflat deposition (Van Straaten and Kuenen 1958; Postma 1967) may be applicable to the process in the estuary. The supply of fine suspended load from the river is the other factor in determining rates of deposition in these shallow areas. The accumulation of relatively well sorted 6 to 7 phi sediments in the peripheral bays subsequent to the May 1980 eruption of Mt. St. Helens supports this contention. Thus, the most favorable conditions for fine-grain deposition occur during periods of high sediment supply (often correlated with high river discharge), neap tides (decreased vertical mixing, increased advective transport of salt and suspended sediment), slack water, and calm weather.

Deposition of fine material in channels is more closely related to the behavior of the turbidity maximum. During spring tides, increased tidal amplitudes and increased vertical mixing both act to increase the boundary shear stress along the bottom of the estuary. Coarse to fine silt is suspended by these strong shear stresses and concentrated by density-driven circulation. The resuspension and subsequent tidal advection of the turbidity maximum is best developed during low discharges (less stratification) and large tidal ranges (increased vertical mixing). Under these conditions, transport of salt and suspended sediment occurs largely through mixing and entrainment, in contrast to tidal advection. Very high concentrations of suspended sediments in the lower portions of the water column have been measured under these conditions, but deposition is not likely to occur in the high energy, better-mixed spring tide conditions. Instead, deposition of these sediments is thought to occur as tidal range decreases. Deposition of sediments from the turbidity maximum is likely to contain coarser (fine to coarse silt) material and to be confined to

the excursion range of the turbidity maximum. In addition, sedimentation from the turbidity maximum is expected to be restricted to deeper portions of the estuary.

The paucity of fine sediments in the estuary channels suggests that the process of channel deposition beneath the turbidity maximum is ineffective in accumulating fine-grain material in the long term. The rip-up clasts and two-layer samples suggest that the layers of silty-sand deposited, presumably by the degeneration of the turbidity maximum, are eroded at subsequent intervals of high boundary shear stresses. The clasts are transported as bedload and abraded or buried within bedload deposits. Thus, it seems that fine-grain sediment accumulation occurs mostly in the peripheral bays and comparable environments, at a rate that is probably largely a function of the fluvial supply of fine silts and coarse clays.

Several mechanisms are available for the transport of fine material from the estuary: sediment can by-pass the estuary immediately in the fresh-water plume, it can be temporarily trapped in the turbidity maximum and subsequently entrained in water that leaves the estuary, or it can be stored for some period of time as an ephemeral deposit, to be eroded and transported out of the estuary at a later date. Evidence presented in Appendix C suggest that in the long-term only 20% of the silt and clay supplied to the estuary is left to accumulate in the estuary.

4.5.3 Deposition of Coarse Sediments

Most of the sediment retained in the estuary is fine to medium sand. In part, this is due to a limited range in the size of sediments available to the system, and especially to the lack of a supply of coarser material to the estuary. Fine material is maintained in suspension or resuspended often enough to be flushed eventually from the estuary. The remaining narrow range of sediments found in the estuary is transported easily as either bedload or intermittent suspension; it is, therefore, an understanding of the processes of bedload and intermittent suspension that will provide the most insight to the patterns of sediment transportation, shoaling, and erosion in the estuary. The complexity of the bedform distribution pattern reflects the bedload transport field and indicates that bedload transport is affected by diurnal and seasonal fluctuations in the flow characteristics. Evidence from the Site D experiments and knowledge of the flow behavior during spring and neap tides suggests that fortnightly changes are also important.

In the fluvial portions of the estuary, bedload and intermittently suspended sediment transport are driven by shear stress distributions similar to those found in fluvial systems. Channel morphology controls the large-scale

distribution of shear stress, while bedforms modify the stress distribution on a local scale. The sediment distribution reflects these processes, showing normal variations between the crests and troughs of the bedforms and with depth in the channel. Sediments generally become coarse with increasing depth in the channels, and the sediments on the crests of bedforms are finer and better sorted than the lag deposits found in the bedform troughs. However, near the entrance and in portions of the lower estuary, large tidal amplitudes and low channel form drag combine to produce a tidally-dominated sediment transport regime. The ebb-flood asymmetry imposed by the density-driven circulation results in net landward transport of marine sediments, at least in the northern portions of the entrance channel. The tidal currents, however, dominate and produce relatively small reversing bedforms. Sediment size is not greatly affected by local shear stress conditions over these bedforms, and is less dependent on depth. As a result, textural changes in the lower estuary reflect the contribution of a finer marine source, and large scale circulation patterns, but these conditions are subtle and complex.

In the central portion of the estuary, the effects of stratification and gravitational circulation are most evident. Stratification tends to reduce vertical mixing and shield the bottom from strong ebb currents, while density-driven circulation causes net landward transport along the bottom. Instantaneous transport rates are probably lower in the portion of the estuary where secondary density-driven circulation is important, but net rates of transport are comparable to those found elsewhere in the estuary. Large-scale circulation patterns exist in this central portion of the estuary which are important to long-term sedimentation patterns. Flood dominance of the North Channel (Lutz et al., 1975) is the most notable of these, and ebb- or flood-dominant transport on and around many of the shoals probably contributes much to the net direction of the bedload sediment transport. The sediment textures display a greater temporal variability in this portion of the estuary. Complex vertical and horizontal distribution patterns are caused by the wide variety of small and large, active and inactive channels, shoals (both sub- and intertidal) and broad, protected embayments. The central reaches of the estuary thus contain the widest variety of sediment textures and depositional settings.

Energy input from waves increases the effective shear stress in exposed shallow areas of the estuary. The increased boundary shear stress tends to increase the amount of intermittent suspension and enhance sediment transport rates, effectively winnowing away the finer fractions of sediment on the beaches and nearshore environments of the estuary. Near the entrance and along the ocean beaches,

ocean waves are particularly effective at producing well-sorted sediments, and some intertidal areas within the estuary that are exposed to wind-waves exhibit sorting and grain size effects which suggest that wave activity is important. These sediments are believed to cause the coarsening-seaward trend observed in Figure 34 and the coarsening-upward trends observed in the seaward regions, shown in Figure 30.

4.5.4 Shoaling Patterns

The gross morphology of the estuary (Figure 2) reflects the influence of tidal transport in the lower reaches, fluvial transport in the upper reaches, and a complex interaction between the two in the central portion of the estuary. The channel morphology in the reaches upriver of Tenasillahe Island are distinctly fluvial in nature. The channel has meandered across a narrow flood plain incised into Tertiary rock and, in most cases, the outside of river bends are confined by bedrock. The river channel exhibits bar-pool topography, with deep pools located on the outside of bends (especially adjacent to bedrock) and point-bar deposits on the inside of the bends. Much modification of the natural channel has occurred due to the construction of pile dikes. The channel modifications tend to confine the channel within a narrow cross-section, especially along the straight reaches, where the natural tendency would be to produce a relatively wide, flat-bottomed channel. Seaward of Tenasillahe Island, the bedrock channel broadens, and interaction of tidal flow and river discharge act to produce a complex series of anastomosing channels. These channels migrate and shift naturally where not confined by dikes or dredging. Examination of the historical bathymetry (CREDDP 1983) suggests that the locations of small channels shift more frequently with distance down-river, probably reflecting the stabilizing influence of vegetation on the more landward islands. The channel morphology in the lower estuary is much simpler: a single entrance channel bifurcates to form two smaller channels. The location of the South (navigation) Channel is controlled by regular channel maintenance activities. The North Channel is a more natural system that has shifted its axis north and south during historical time.

Island and shoal morphologies also reflect the dominant processes in the various parts of the estuary. The Sand Islands and Clatsop Spit (Figure 2) are located in the seaward portion of the estuary and are exposed to Pacific Ocean waves. These areas display recurved spits that reflect the influence of wave-induced littoral drift. Desdemona Sands, located in the tidally-dominated lower estuary, displays many of the characteristics of the classic flood-tidal delta model of Hayes (1975) (Figure 59a,b). The shoals in the more landward portions of the estuary (for

example, Taylor Sands, Figure 59c) reflect increasing shape modifications that appear to be related to increased influence of ebb flow and the action of wind waves. These shoals, located in the reaches betweeen the Astoria-Megler bridge and Harrington Point, have an extremely complex morphology, and no close analogues have been encountered in estuarine literature. They appear to be a product of the time-variant influences of tidal currents during most of the year and nearly fluvial flow during high discharge periods.

In the southern parts of Cathlamet Bay and upriver of Harrington Point, the intertidal shoals grade into vegetated islands. The islands display a characteristic morphology that is related to the ebb-dominant flow of the upper estuary (Figure 59d). The upriver edge of the island is generally steep and erosional, while slopes on the downstream edge are gentle and reflect depositional processes. The centers of these islands are vegetated and dissected by tidal drainage channels.

In the upper estuary, it appears that much of the deposition of sand-sized sediments occurs in conjunction with the lateral migration of the small channels between islands and shoals. Channel migration in the upper reaches of the estuary results in a net downriver displacement of the channel. Evidence for downriver offset can be found by comparing the relative locations of cut-banks and point-bars among the small islands. In general, steep-sided channel margins are located on the upriver edge of the islands, while depositional bars tend to be found on the seaward side of the islands. Although relatively little data were obtained among the complex series of small channels and islands that occupy this region, it appears that horizontal accretion of fluvially associated point-bar deposits represents an important part of the natural depositional system of the Columbia River Estuary. The point-bars represent deposition of bedload material and are associated with the fluvial bedforms that have been observed in the channels of the upper estuary. The importance of is contrasted against the vertical accretion models that are invoked in many estuaries and which are also suggested for the peripheral bays in the Columbia River Estuary. Horizontal accretion explains many of the characteristics of the sediment distribution and morphology of the estuary, including the spatial variability of the sediment distribution, the discontinuous but linear trends in sediment distribution, the fining-upward trends in the sediments of the upper estuary, the shape of the islands, and the general channel morphology of the estuary. Further, on the basis of a channel migration model, one would predict localized shoaling and erosion rather than widespread deposition. This, in fact, is what is observed in the estuary. The Corps of Engineers concentrates its dredging efforts in a few locations where shoaling of a fluvial

a. CLASSICAL FLOOD-TIDAL DELTA
(Hayes, 1975)

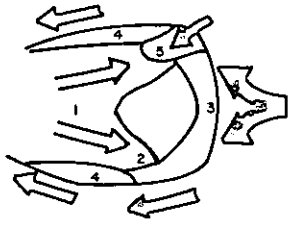

FLOOD
EBB
1 FLOOD RAMP
2 FLOOD CHANNEL
3 EBB SHEILD
4 EBB SPIT
5 SPILLOVER LOBE

b. DESDEMONA SANDS

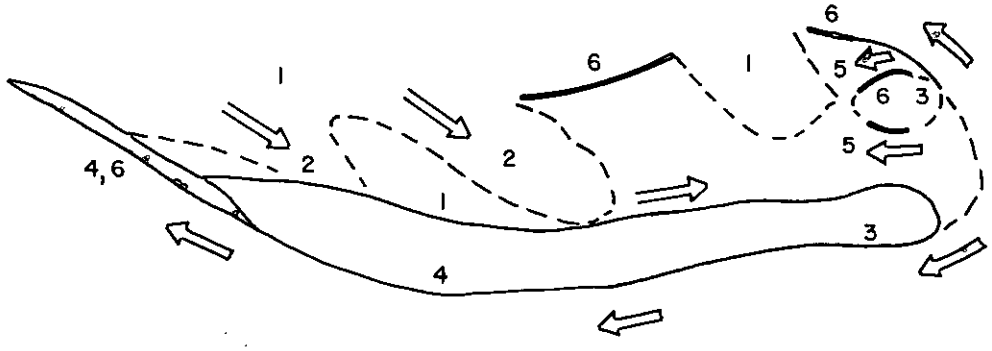

FLOOD
EBB
1-5 AS ABOVE
6 BEACH

Figure 59. Comparative morphology of shoals and islands. (a) Components of the Hayes (1975) model of a mesotidal flood-tidal delta. (b) Schematic of Desdemona Sands and components of flood tidal delta.

c. TAYLOR SANDS

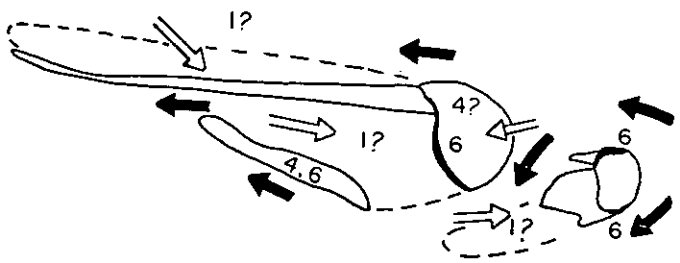

d. VEGETATED FLUVIAL ISLAND

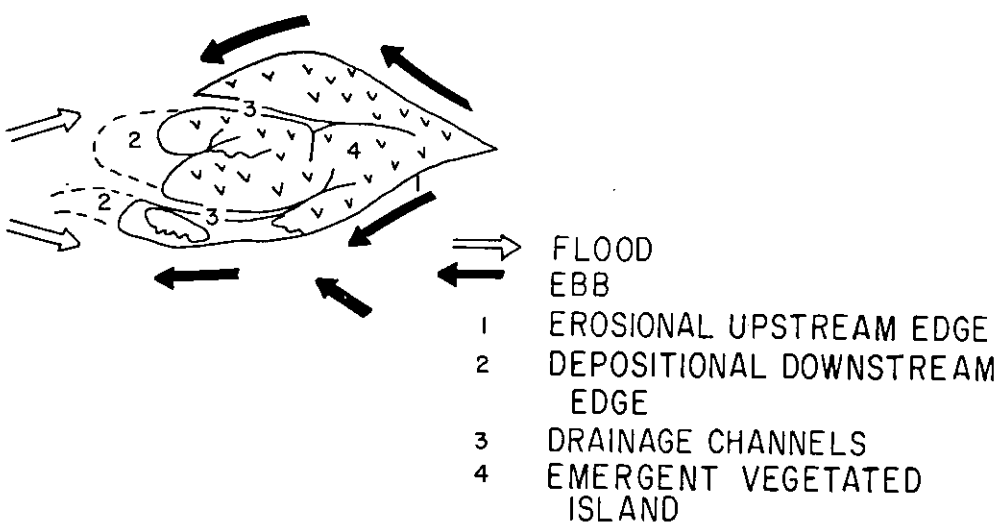

Figure 59. (c) Schematic of Taylor Sands and components of a flood-tidal delta with fluvial influence. (d) Schematic of a vegetated fluvial island and components.

nature occurs, including all of the bars upriver of Tongue Point. Only a few frequently dredged reaches in the lower estuary, notably in the area of Clatsop Spit and Flavel Bar, appear to reflect deposition that is dominated by reversing transport or effects of estuarine circulation. In short, the estuary resembles a fluvial system in many aspects of shoaling patterns and bottom morphology, and it is suggested here that the long-term accumulation of sediments occurring in the upper reaches of the estuary reflect mostly fluvial processes.

4.5.5 Sedimentary Environments

In order to summarize the preceding discussion of sedimentary processes and shoaling patterns, a map of the generalized sedimentary environments is presented as Figure 60a. This map represents a simplification of the sedimentary environments compiled at a scale of 1:40000. A more detailed version of the map is presented in the Atlas (Fox et al. 1984).

The sedimentary environments are delineated according to the dominant processes operating in that environment and not by any particular physical characteristic, such as grain size. The processes operating in some of the environments produce predictable sedimentary parameters, but in others, the variable nature of the processes results in deposits with a wide range of characteristics. The most important processes within each portion of the estuary are illustrated schematically in Figure 60b.

The sedimentary environments were identified using a variety of sources. The sediment distribution maps developed in this study and the bathymetry prepared by Northwest Cartography, Inc. (CREDDP 1983) were used in conjunction with aerial photos, side-scan sonar records, NOAA charts, USGS maps, and habitat maps (Thomas 1983). The processes that are designated as indicators of sedimentary environments are those that this study and previous studies have identified as important in the estuary. Numerous extrapolations and judgments were involved in the preparation of Figure 60 and the more detailed Atlas version (Fox et al. 1984) and these reflect the biases of the authors.

The following listing enumerates the sedimentary environments found in the estuary system and discusses some of their important characteristics. The environments are organized by processes, but several environments have been grouped for presentation in Figure 60a. The most striking feature of the sedimentary environments is their complexity. They serve to emphasize the dynamic nature of the Columbia River Estuary and the variability in the distribution of its physical properties.

Sedimentary environments:

I. Wave transport dominant

Ocean beaches and nearshore

Generally restricted to depths less than 12 ft (4 m) and includes the nearshore zone, beachface and berm top. Sediment is usually coarse, well-sorted sand. Active sediment transport occurs frequently in conjunction with wave activity. Many of the areas classified as beaches and shoreface have been sites of significant accumulation in historical time, because the jetty construction has trapped littoral transport.

II. Wave and current combined

A. Exposed intertidal flats

1) Marine (exposed to ocean waves)

Depths are less than 3 ft (1 m) below MLLW. The beaches bordering the lower estuary are included in this environment. Sediment is generally well sorted and relatively coarse and the inter-tidal regions are unvegetated and highly mobile under some conditions. Sediment is reworked largely by wave action, and most of these areas have shifted significantly in historical time.

2) Brackish or fresh

Depths less than 3 ft (1 m). These intertidal flats are exposed to smaller waves generated within the estuary, and in the upper reaches of the estuary may represent the tops of point bars. Grain size decreases seaward in this environment, and sediments are relatively well-sorted. Most of these environments have shifted position considerably in historic times.

B. Open marine (exposed to ocean waves and continental shelf currents)

Depths greater than 3 to 12 ft (1 to 4 m). This environment encompasses the outer tidal delta, the offshore extension of the entrance channel, and the adjacent continental shelf. Here, wave-current interaction is important in placing sediments in transport. Both Columbia River and continental shelf circulation are important in determining transport directions. The outer tidal delta has been built seaward since the construction of the jetties. Sediment is generally well-sorted fine sand.

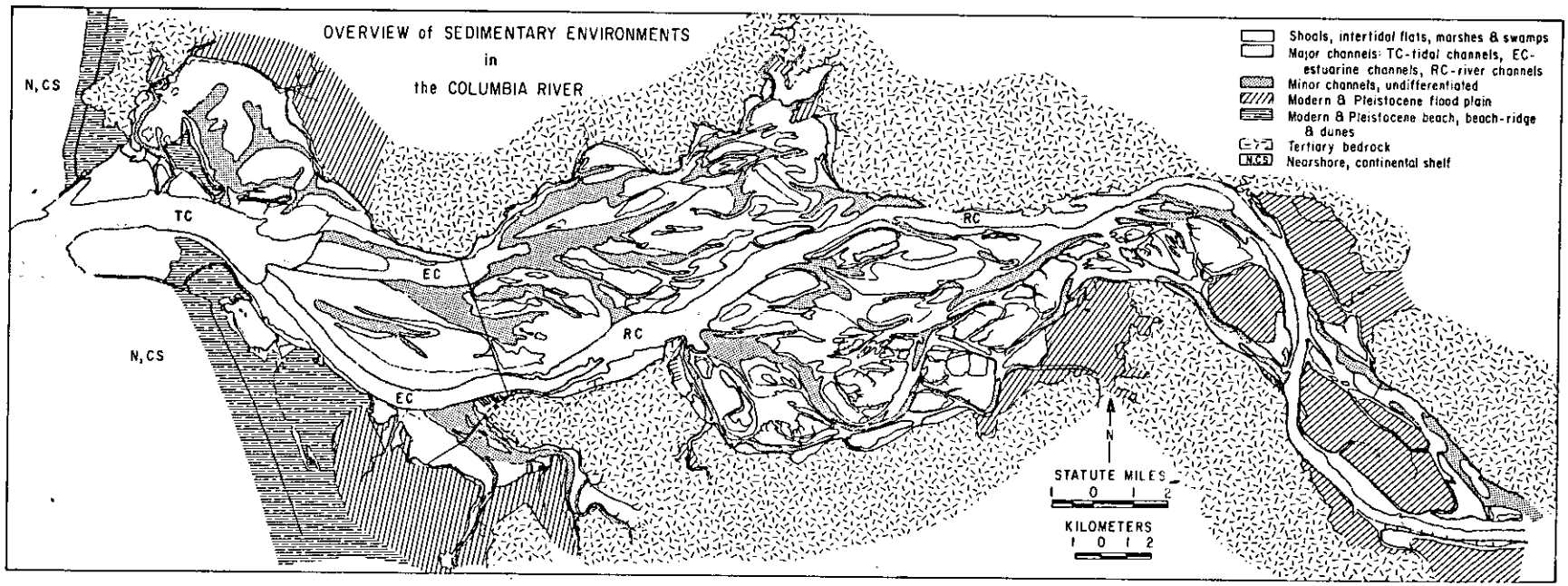

Figure 60a. Overview of sedimentary environments in the Columbia River Estuary.

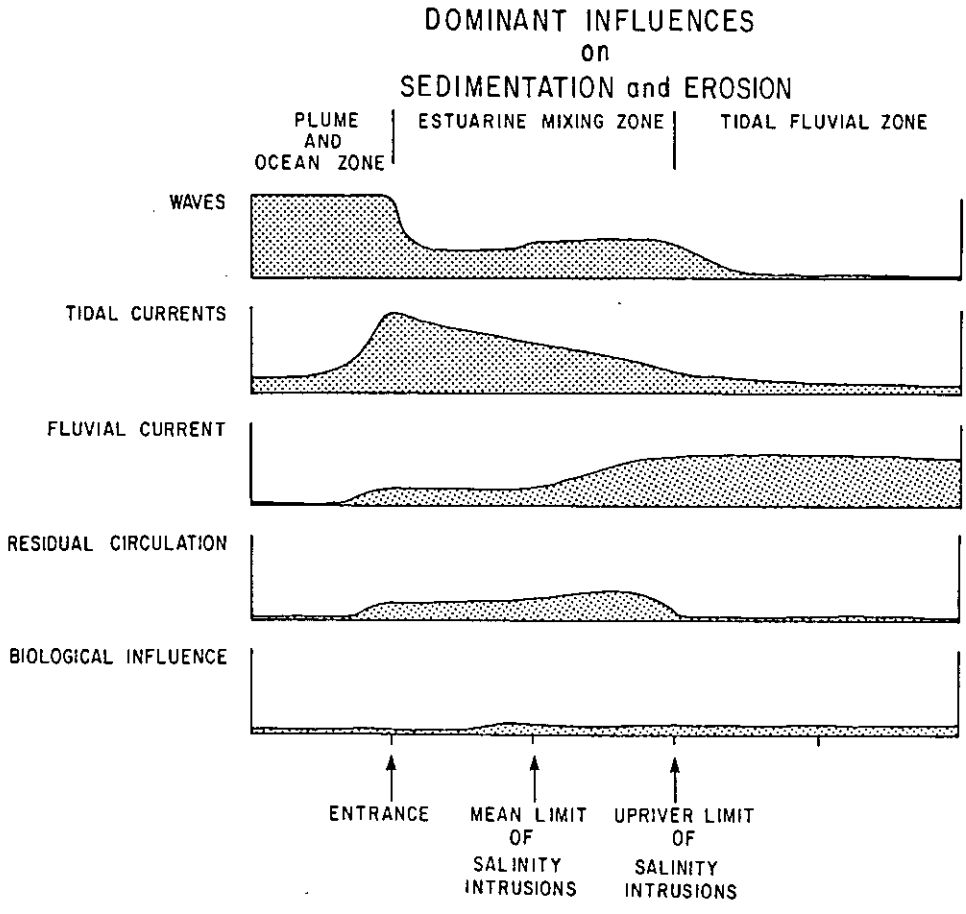

Figure 60b. Dominant influences on sedimentation and erosion.

III. Wave and current combined (low energy)

A. Protected intertidal flats (currents > waves)

1) Non-vegetated

a. marine

Depths less than 3 ft (1 m), with low wave activity. Sediment size is highly variable, but generally finer than that found in the brackish or fresh water equivalents upriver.

b. brackish or fresh

Depths less than 3 ft (1 m), with low wave activity. Morphology and grain size controlled by fluvial processes, especially during high discharge. Some deposits found in this environment reflect accumulation behind dikes and jetties in the upper reaches of the estuary. Many of these areas may become vegetated in the near future.

2) Vegetated (including high and low marsh)

a. marine

High and low salt marsh (actual elevations depend on local tide-heights). Restricted to areas bordering the ocean. Generally fine-grained and poorly-sorted sediments; transport rates low.

b. brackish or fresh

High and low marsh, swamp and low-lying woods (elevations vary). Sediments are variable and poorly sorted.

IV. Current transport dominant

A. Tidal oscillatory flow important (high energy)

1) Tidal shoals and bars

Depths below wave base (3 ft; 1 m), but generally less than 18 to 30 ft (6 to 10 m). Highly variable morphology and sediment character, but generally depositional, subtidal features. Transport rates are high. One of the criteria for this environment is the presence of reversing or upriver-oriented bedforms.

2) Small tidal channels

Depths greater than 3 to 30 ft (1 to 10 m). These

channels act as conduits for reversing tidal flow, and drain peripheral bays or mid-estuary shoals. They are floored in generally medium sands, but are sites of fine-sediment deposition when isolated by sills.

3) Tidal channel

Depths greater than 18 ft (6 m). Major conduits for tidal flow. They often contain reversing bedforms and demonstrate active bedload transport. Channel migration has occurred in the natural tidal channels, and extensive modifications have been made to navigation channels.

B. Density-driven estuarine circulation evident

1) Estuarine channel

Depths greater than 10 ft (6 m) and presence of land-oriented bedforms. Grain size varies and is highly influenced by seasonal variations and the turbidity maximum. Site of ephemeral fine-sediment deposition.

C. Fluvial processes dominate (high energy)

1) River shoals and bars

Depths from 3 to 30 ft (1 to 10 m). Variable sediment size and morphology, but ebb-dominant. Generally high transport rates, point-bar or lingoid bar morphology.

2) Shallow river channels

Depths from 3 to 18 ft (1 to 6 m). These are often side channels or "sloughs." They may or may not be active conduits; grain size will vary accordingly.

3) Deep river channels

Depths greater than 30 ft (10 m). Fluvial processes dominant. Large-scale, ebb-oriented bedforms; coarse sediments, active erosion, and point-bar deposition.

D. Low energy - depositional

1) Protected embayment

Depths between 3 and 30 ft (1 to 10 m). Peripheral bays with minimal energy input. Net depositional, site of fine-sediment accumulation.

V. Terrestrial environments (processes include eolian, overbank deposition, artificial fill, landsliding, etc.)

A. Beach-ridge/dune complexes that have accreted in historical times. These dune-ridges have been stabilized by dune-grass cultivation. The ridges represent a substantial accumulation of sediments caused by the construction of the entrance jetties.

B. Beach-ridge/dunes that accreted pre-1800's (older)

These Holocene and Pleistocene deposits represent natural accumulation of Columbia River and coastally-derived sediments before jetty construction.

C. Bedrock and talus (often Tertiary sediments)

Includes all pre-Holocene terranes and uplands. Mostly Eocene and Miocene volcanic and volcaniclastic sedimentary rocks, relatively resistant to erosion.

D. Holocene lowlands undifferentiated

Lagoon-fill and fluvial sediments above MLLW. Older Columbia River flood plain and flood plains of small tributaries are included.

E. Historical (emergent) fill when easily identified

Dredge fill or other artificial fill.

F. Rip-rap, coarse fill, including submerged fill

The construction of protective jetties, armoured embankments, causeways, levees, and dikes has had a significant effect on the sedimentary processes in the estuary.

G. Lakes, ponds, stagnant sloughs and tributaries

Fresh-water, low-energy environments.

5. CONCLUSION

This chapter presents a summary of the conclusions reached during this study and proposes avenues of research for future work.

5.1 SUMMARY OF CONCLUSIONS

Several conclusions have been drawn regarding the sedimentology of the Columbia River Estuary. They are enumerated here:

1) The energy levels available for transporting sediment in the Columbia River Estuary are high relative to many of the estuaries of the world. The combined effects of large tidal range, large fluvial discharge, high ocean wave regime and the various residual circulations produced by the interaction of these three energy inputs with the density distribution and the morphology of the estuary results in currents that are frequently more than sufficient to move most of the sediment sizes found in the estuary.

2) The energy sources are highly time dependent, resulting in a continuously changing current regime in the estuary. Although the circulation in the estuary is dominated by the semidiurnal tides, large diurnal and fortnightly effects are apparent in tide heights and circulation. Seasonal variations in the discharge and oceanic regimes are less energetic but still important in modifyng the circulatory processes that effect sediment tranpsort. Long-term changes in sea-level and river discharge introduce an even longer time scale that must be considered in evaluating the sedimentology of the estuary.

3) The relative importance of each of the energy inputs varies not only in time, but with position in the estuary. Fluvial influence decreases downriver, tidal energy decreases upriver, wave energy is related to ocean exposure and local fetch, and residual circulation, especially the net landward bottom flow, depends highly on local topography.

4) The ultimate source of sediment for the estuary is the Columbia River which contributes a somewhat restricted range of sizes generally finer than 1.00 phi. Local sources and allocthonous marine sources contribute only minor amounts of sediment to the estuary. Evidence suggests that some marine sediment consisting of older and/or relatively recent Columbia River sediment and minor amounts of sediment from headland erosion along the Oregon coast is being transported into the estuary.

5) The patterns of sediment distribution within the estuary are complex and reflect the variety of processes

acting over various time scales. Most of the estuary reflects an even more restricted range of sediment size than is supplied by the river; the mean size of the estuary sediment is 2.50 phi. Sediment is moved as bedload, intermittently suspended load, and suspended load. The intermittently suspended sediment is highly mobile and is an especially important fraction in determining the grain-size distributions. Finer sediment, because it is more easily transported, is quantitatively less important in the Columbia River Estuary. Sediment in the adjacent fluvial reaches is generally coarser than that of the estuary, while sediment in the adjacent marine environment is generally finer.

6) Examination of two "exploratory" statistical approaches to grain-size distributions (factor and cluster analyses) suggest that these techniques are best suited to geological situations that closely meet one of the following criteria: 1) sources with unique grain-size distributions exist and the sediment distributions are the result of admixtures of these sources, or 2) a single source provides sediment which is transported in one net direction, resulting in distributions closely related to sedimentological processes. Neither of these cases are met in the Columbia River Estuary. Two sources of sediment may be identified, the river system and the adjacent continental shelf. However, the sediment on the continental shelf is largely derived from the Columbia River. It, therefore, does not have a unique mineral assemblage and its grain-size distribution reflects only the reworking of river sediment by waves and current action. Because the sediment distribution in the Columbia River Estuary reflects a variety of transport processes acting over a range of time scales on a variable, single sediment source, the exploratory statistical approaches and the well-posed analytical approaches of McLaren and Bowles (1983) were found less useful than interpretation of graphical and mapped distributions of the fundamental parameters of grain-size (mean, mode, sorting, skewness, and coarsest one-percentile). These relatinships, along with knowledge of the relationship between these parameters and sedimentary processes, have allowed some insight into the sedimentary processes in the Columbia River ##he exploratory statistical approaches and the well-posed analytical approaches of McLaren and Bowles (1983) were found less useful than interpretation of graphical and mapped distributions of the fundamental parameters of grain-size (mean, mode, sorting, skewness, and coarsest one-percentile). These relatinships, along with knowledge of the relationship between these parameters and sedimentary processes, have allowed some insight into the sedimentary processes in the Columbia River Estuary to be gained.

7) Details of the sediment distribution suggest that

bedload sediment is not being transported out of the estuary. Finer sediment that may be intermittently suspended may be both entering and leaving the estuary through the tidally dominated entrance, but the net transport direction appears to be inward at depth.

8) Fine sediment that is normally transported in suspension comprises only a small percentage of the sediment found in the estuary. Fine sediment is found in the peripheral bays, and minor, inactive channels, especially in Cathlamet Bay. Fine sediments also occur in the channels of the central estuary, but these are ephemeral and do not contribute to long-term accumulation in the estuary.

9) Studies of bedform transport with side-scan sonar indicate that bedload transport is tidally dominated near the entrance, where bedform reversals occur, and fluvially dominated in the upper estuary. In the central estuary, bedforms indicate that upriver sediment transport occurs at depth in response to the net landward bottom flow, causing a bedload transport node in the main channels. The location of this node moves seasonally in response to discharge changes.

10) Studies of suspended sediment indicate the presence of a turbidity maximum that is related to both a trapping effect of the net circulation and a resuspension effect by the tidal currents. The turbidity maximum advects with the semidiurnal tide over much of the lower estuary. Concentrations in the turbidity maximum change in response to tidal energy on both a diurnal and neap-spring time scale. The location of the turbidity maximum is expected to shift with discharge changes.

11) Inspection of the distribution of rip-up clasts, fine sediment deposition, and the excursion of the turbidity maximum suggest that suspended sediments concentrated in the turbidity maximum may be mixed into upper layers of the water column and advected either out of the estuary or into one of the peripheral bays. In the latter instance, currents will be insufficient to resuspend the sediment if it settles to the bottom, and a mechanism for an advection and settling lag deposition in the fine bays is established. Deposition of fine sediments in the main channels occurs on an ephemeral basis beneath the turbidity maximum, but does not result in significant long term accumulation of fine material in the estuary.

12) The net effect of the behavior of the turbidity maximum is to increase the residence time of fine material in the estuary and to provide some fine material to the peripheral bays. However, in the long run, most (80%) of the fine material that enters the estuary is eventually discharged into the marine environment in the river plume.

13) Examination of the historical changes in bathymetry of the estuary suggest that it is shoaling rapidly, at an average annual rate of 0.5 cm yr^{-1}. Construction of the entrance jetties has caused tidal currents to transport subtantial amount of sediment both seaward and landward. The sediment transported into the estuary has accumulated in Trestle Bay and on Clatsop Spit, in Baker Bay and on the Sand Islands, and on Desdemona Sands. These accumulations, amounting to 157 million m^3, represent only half of the 315 million m^3 that has been deposited in the estuary since 1868. The remainder has been supplied by the Columbia River.

Sediment which had previously formed the shoals (inner and outer tidal deltas) near the natural river entrance was also forced seaward after jetty construction. Some of this sediment still resides in the outer tidal delta, but the losses of sediment from this region indicate that much of this sediment has been transported away by continental shelf processes. It is proposed here that normal, northward transport of this material has provided an unusually high sediment supply to the continental shelf, nearshore regions, and beaches north of the Columbia River during historical time. The reduction in the rate of loss from the outer tidal delta in more recent time suggests that this "pulse" of sediment has dwindled, and in the absence of increased supply from the river system, the sediment transport pathways north of the estuary, including the beaches, will experience a decreased supply of sediment.

14) Estimates of the shoaling rates, studies of the processes, and examination of the grain-size distributions all suggest that the estuary is trapping bedload sediment more effectively than before the jetties were constructed. Natural supply of bedload sediment to the estuary has also been reduced by flood regulation and partial control of catastrophic events, such as the eruption of Mt. St. Helens. This study has not addressed the effect of transport of material from the estuary during dredging operations, but neglecting dredging, the estuary is apparently trapping bedload sediments. In contrast, sediment moving in suspension is retained only briefly in most of the estuary, and accumulates permanently only in the peripheral bays. The suspended sediment budget has been less affected by changes within the estuary; significant changes in the river supply of suspended may or may not have occurred.

15) The morphology of the estuary reflects the processes that dominate the eventual deposition of sediment. Most of the upper estuary and above is characterized by a distinctly fluvial morphology, indicating the importance of fluvial processes such as point bar deposition and channel migration. In conjunction with other data, this suggests that the long term accumulation in the

estuary is associated with gradual horizontal accretion of bedload sediment via channel migration, rather than vertical accretion of fine material being deposited from suspension. This style of horizontal accretion of sandy sediments is in contrast to the vertical accretion that is often associated with estuarine sedimentation.

16) Finally, a complex set of depositional environments is created by the myriad of processes acting in an estuary of varied topography and over a complete spectrum of time scales.

5.2 RECOMMENDATIONS FOR FUTURE WORK

This program has provided a substantial data base on which future studies may rely, and has generated questions which may be answered by future research. The following paragraphs discuss proposed avenues of future research.

The importance of modelling efforts in predicting the effects of perturbations on the estuarine system can not be overstated. The complex, inter-related, and time-dependent aspects of circulation and sedimentation in the estuary is best approached through models. However, the present understanding of the frictional contribution of bedforms and density structure is limited: these terms are presently lumped together and parameterized as a single friction coefficient. This study and the circulation work conducted by David Jay (1984) clearly demonstrate the importance of bedforms and salinity structure in altering flow and sediment transport characteristics in the estuary; it is obviously important to include these effects in future models of the estuary. The detailed reconnaissance of the bottom and the NOS current and salinity measurements provide a fairly complete data set that will provide the information needed to incorporate the friction effects into future models. However, the mechanics of the friction effect that arises as form drag over bedforms is poorly understood. Basic research must be conducted on the interaction between bedforms and flow characteristics in order to develop techniques for the parameterization of form drag effects. This work is important from the standpoint of both circulation studies and sediment transport studies. When the friction effects are better understood, it will be appropriate to develop more detailed numerical flow models and, eventually, predictive sediment transport and shoaling models for the estuary. These modelling efforts were incorporated into the original CREDDP plan of study but were not funded. They remain valid and important goals for both scientific and applied research.

More immediate information on the sedimentology of the estuary could be obtained by determining the migration rates of the bedforms that are found in the estuary. Although

CREDDP work has provided a good description of the temporal and spatial distribution of bedforms in the estuary, bedform sediment transport rates were not obtained due to the difficulty in obtaining bedform migration rates. Because much of the bedload transport in the estuary occurs as bedform transport, application of reliable migration rates to the known bedform distributions would provide a method for mapping sediment transport vectors. Research into the relationship between bedform migration rates, bedform geometry, flow conditions, and sediment transport must be continued in order to provide the ability to map bedforms and thus obtain sediment transport data. Although the Columbia River Estuary is a difficult environment to work in, research accomplished in other areas can be combined with studies in the estuary to provide estimates of bedform behavior.

Broader approaches on the sedimentology of the estuary are needed as well. Avenues of research need to be followed in order to provide a comprehensive overview of the net effects of the physical and sedimentary proceses that have been observed in the estuary. One of these is to determine, on the basis of shallow marine seismic data and cores, the stratigraphy and deposition rates of the major sedimentary environments wihin the estuary. The work presented here predicts that shoaling rates have accelerated in historic time and that the bulk of the sediment that is accumulating in the estuary is coarser (fine sand) material associated with channel migration. Comparison of the stratigraphy in peripheral bays and channels is needed to confirm the hypothesis that sedimentation in the channel regions is volumetrically more important. Several events should aid in dating the cores: major floods and the eruption of Mt. St. Helens should provide historical markers in the deposits, while the effects of previous eruptions, including the eruption of Mt. Mazama and the effects of the catastrophic floods that drained glacial Lake Missoula may have left distinctive deposits in the older estuarine sediments. Because some of these early events occurred during a lower stand of sea level, the Pleistocene stratigraphy of the continental shelf, as inferred from seismic data, may prove extremely useful in unravelling the depositional history of the Columbia River valley and estuary system.

Finally, and most importantly, a sediment budget for the estuary and lower river valley (below the Bonneville Dam) is needed. The work included in Appendix C and based on the historical bathymetry provided by Northwest Cartography, Inc. (CREDDP 1983) is a crucial first step toward this budget. More work needs to be done to incorporate the significant contributions of change in shoreline topography and dredging activities of the Corps of Engineers into the budget. The budget must quantify the changes in fluvial sediment supply to the estuary due to dam

construction, agricultural and logging activities, and changes in the sediment storage along the lower reaches of the river. Such a budget will allow the question of sediment supply to the continental shelf and Washington beaches to be addressed and allow the effects of jetty construction on shoaling rates within the estuary to be set in context with historical changes upriver.

LITERATURE CITED

Ando, M.; Balazas, E.I. 1979. Geodetic evidence for a seismic subduction of the Juan de Fuca plate. J. Geophys. Res. 84: 3023-3028.

Allen, G.P.; Castaing, P.; Klingebiel, A. 1971. Distinction of elementary sand populations in the Gironde Estuary (France) by R-mode factor analysis of grain-size data. Sedimentology 19: 21-35.

Allen, J.R.L. 1968. Current ripples: their relation to patterns of water and sediment motion. Amsterdam: North Holland.

Atwater, T. 1970. Implications of plate tectonics for the Cenozoic tectonic evolution of western North America. Geol. Soc. Am. Bull. 81: 3513-3536.

Bagnall, M.G. 1916. Improvement of the mouth of the Columbia River. U. S. Corps of Engineers, Professional Memoirs 8: 687-720.

Ballard, R.L. 1964. Distribution of beach sediment near the Columbia River. Technical Report No. 98. Seattle: University of Washington, Department of Oceanography.

Barnes, C.A.; Duxbury, A.C.; Morse, B.A. 1972. Circulation and selected properties of the Columbia River effluent at sea. Pruter, A.T.; Alverson, P.L. eds. The Columbia River Estuary and adjacent ocean waters. Seattle: University of Washington Press.

Bartz, R.; Zanefeld, J.R.V.; Pak, H. 1978. A transmissometer for profiling and moored observations in water. S.P.I.E. 160, Ocean Optics 5: 102-108.

Blatt, H.; Middleton, G.; Murray, R. 1972. Origin of sedimentary rocks. New York: Prentice-Hall, Inc.

Boggs, S.; Jones, C.A. 1976. Seasonal reversal of flood-tide dominant sediment transport in a small Oregon estuary. Geol. Soc. Am. Bull. 37: 419-426.

Boothroyd, J.C.; Hubbard, D.K. 1975. Genesis of bedforms in mesotidal estuaries. Cronin, L.E. ed. Estuarine Research, II. New York: Academic Press.

Borgeld, J.C.; Creager, J.S.; Walter, S.R.; Roy, E.H. 1978. A geological investigation of the sedimentary environment at sites E, G, and H near the mouth of the Columbia River. Portland: Department of the Army, Corps of Engineers, Portland District.

Callaway, R.J. 1971. Applications of some numerical models to Pacific Northwest estuaries. Proceedings 1971 Technical Conference on Estuaries of the Pacific Northwest. Proc. Circ. 42, Eng. Experiment Station. Corvallis: Oregon State University.

Chambers, R.L.; Upchurch, S.B. 1979. Multivariate analysis of sedimentary environments using grain size frequency distributions. Math. Geology 11: 27-43.

Chelton, D.B.; Davis, R.E. 1982. Monthly mean sea-level variability along the west coast of North America. J. Phys. Ocean. 12: 757-784.

Clarke, T.L. 1978. An oblique factor analysis solution for the analysis of mixtures. Math. Geology 10: 225-241.

Clifton, H.E. 1983. Discrimination between subtidal and intertidal facies in Pleistocene deposits, Willapa Bay, Washington. J. Sed. Pet. 53: 353-370.

Clifton, H.E.; Phillips, R.L. 1980. Lateral trends and vertical sequences in estuarine sediments, Willapa Bay, Washington. Field, M.E.; Bouma, A.; Colburn, I.; Douglas, R; Ingle, J. eds. Pac. Coast Quat. Depositional Env. of the Pac. Coast. 4th Pac. Coast Paleogeography Sym. A.A.P.G., S.E.P.M. Pacific Section, California.

Columbia River Estuary Data Development Program (CREDDP) 1983. Bathymetric Atlas of the Columbia River Estuary. Astoria: Columbia River Estuary Data Development Program.

Conomos, T.J. 1968. Processes affecting suspended particulate matter in the Columbia River effluent system, summer, 1965, 1966. Ph.D. dissertation. Seattle: University of Washington.

Conomos, T.J.; Gross, M.G.; Barnes, C.A.; Richards, F.A. 1972. River-ocean nutrient relations in summer. Pruter, A.T.; Alverson, P.L. eds. The Columbia River Estuary and adjacent ocean waters. Seattle: University of Washington Press.

Cooper, W.S. 1958. Coastal sand dunes of Oregon and Washington. Geol. Soc. Am. Memoir 72, 169 pp.

Cooper, W.S. 1959. Sand-dune development and sea-level changes on the coast of North Oregon (abstract). Geol. Soc. Am. Bull. 65: 1373.

Costello, W.R. 1974. Development of bed configurations in coarse sands. Report No. 74-1. Cambridge: M.I.T., Dept. of Earth and Planet. Sci.

Costello, W.R.; Southard, J.B. 1981. Flume experiments on lower-flow-regime bedforms in coarse sand. J. Sed. Pet. 51: 849-864.

Creager, J.S.; McManus, D.A.; Collias, E.E. 1962. Electronic data processing in sedimentary size analysis. J. Sed. Pet. 32: 833-839.

Creager, J.S.; Sims, L.; Sherwood, C.; Roy, E.; Stewart, R.; Barnett, J.; Gelfenbaum, G. 1980. A sedimentological study of the Columbia River Estuary. Annual Report. Vancouver, WA: Pacific Northwest River Basins Commission.

Dalrymple, R.W.; Knight, R.J.; Lambiase, J.J. 1978. Bedforms and their hydraulic stability relationships in a tidal environment, Bay of Fundy, Canada. Nature 275: 100-104.

Davis, J.C. 1973. Statistics and data analysis in geology. New York: John Wiley and Sons.

Dearborn Associates 1980. Black Sand Mining Project: draft environmental impact statement. Prepared for the State of Washington and Pacific County Department of Natural Resources. Olympia.

Drapeau, G. 1973. Factor analysis: how it copes with complex geological problems. Math. Geology 5: 351-363.

Festa, J.F.; Hansen, D.V. 1978. Turbidity maxima in partially mixed estuaries: a two-dimensional numerical model. Est. and Coastal Mar. Sci. 7: 347-359.

Folk, R.L. 1974. Petrology of sedimentary rocks. Austin: Hemphill.

Folk, R.L.; Ward, W.C. 1957. Brazos River Bar: a study in the significance of grain-size parameters. J. Sed. Pet. 27: 3-26.

Fox, D.S.; Bell, S.; Nehlsen, W.; Damron, J. 1984. The Columbia River Estuary: atlas of physical and biological characteristics. Astoria, OR: Columbia River Estuary Data Development Program.

Friedman, G.M. 1961. Distinction between dune, beach and river sands from their textural characteristics. J. Sed. Pet. 31: 514-529.

Friedman, G.M. 1967. Dynamic processes and statistical parameters compared for size frequency distribution of beach and river sands. J. Sed. Pet. 37: 327-354.

Fullam, T.J. 1969. Measurement of bedload from sand wave migration in Bonneville Reservoir on the Columbia River. Ph.D. thesis, University of Washington, Seattle, WA.

Gelfenbaum, G. 1983. Suspended-sediment response to semidiurnal and fortnightly tidal variations in a mesotidal estuary: Columbia River, U.S.A. Mar. Geology 52: 39-57.

Glenn, J.L. 1973. Relations among radionuclide content and physical, chemical, and mineral characteristics of Columbia River sediments. Professional Paper 433M. Washington, D.C.: U.S. Geological Survey.

Glenn, J.L. 1978. Sediment sources and Holocene sedimentation history in Tillamook Bay, Oregon: data and preliminary interpretations. Open-file report 78-680. Denver: U.S. Geological Survey.

Griffiths, J.C. 1951. Size versus sorting in some Caribbean sediments. J. Geology 59: 211-243

Griffiths, J.C. 1967. Scientific method in analysis of sediments. New York: McGraw-Hill.

Hamilton, P. 1981. Columbia River Estuary hydrodynamic modeling. Unpublished report. Vancouver, WA: Columbia River Estuary Data Development Program.

Hamilton, P. 1983. Numerical modeling of the depth dependent salinity intrusion for the Coal Point Deepening Project in the Columbia River Estuary. Final report. Portland: U.S. Army Engineer District.

Hamilton, P. 1984. Hydrodynamic modeling of the Columbia River Estuary. Astoria, OR: Columbia River Estuary Data Development Program.

Harms, J.C.; Southard, J.B.; Spearing, D.R.; Walker, R.G. 1975. Depositional environments as interpreted from primary sedimentary structures and stratification sequences. Short Course No. 2. Tulsa: Society of Economic Paleontologists and Mineralogists.

Harms, J.C.; Southard, J.B.; Walker, R.G. 1982. Structures and sequences in clastic rocks. Short Course No. 9. Tulsa: Society of Economic Paleontologists and Mineralogists.

Haushild, W.L.; Perkins, R.W.; Stevens, H.H.; Dempster, G.R.; Glenn, J.L. 1966. Radionuclide transport in the Pasco to Vancouver, Washington reach of the Columbia River July 1962 to September 1963. Open File Report. Portland: U.S. Geological Survey.

Hayes, M.O. 1975. Morphology of sand accumulations in estuaries: an introduction to the symposium. Cronin, L.E. ed. Estuarine research, vol. 2. New York: Academic Press, Inc.

Herrmann, F.A. 1968. Model studies of navigation improvements, Columbia River Estuary Report. I. Hydraulic and salinity verification. Tech. Report 2-735. Vicksburg, MS: U.S. Army Engineers, Waterways Experiment Station.

Herrmann, F.A. 1970. Tidal prism measurements at the mouth of the Columbia River. Misc. Paper H-70-3. Vicksburg, MS: U.S. Army Engineers, Waterways Experiment Station.

Hicks, S.D. 1972. On the classification and trends of long period sea-level series. Shore Beach: 20-23.

Hicks, S.D. 1978. An average geopotential sea level series for the United States. J. Geophys. Res. 83: 1377-1379.

Hickson, R.E. 1922. Changes at the mouth of the Columbia River 1903 to 1921. Military Engineer 14: 2111-2114, 257-258.

Hickson, R.E. 1930. Shoaling on the lower Columbia River. Military Engineer 22: 217-219.

Hjulström, F. 1939. Transportation of detritus by moving water. Trask, P.D. ed. Recent marine sediments. Tulsa: Symposium American Association of Petroleum Geologists.

Hodge, E.T. 1934. Geology of beaches adjacent to mouth of Columbia River and petrography of their sands. Final report to Corps of Engineers, Pacific Division, Beach Erosion Investigation.

Hopkins, T.S. 1971. Velocity, temperature, and pressure observation from moored meters on the shelf near the Columbia River mouth, 1967-1969. Special Report No. 45. Seattle: University of Washington, Department of Oceanography.

House of Representatives Document 94. 1899. 56th Congress, 1st Session. 10 pp.

House of Representatives Document 195. 1928. 70th Congress, 1st Session. 50 pp.

House of Representatives Document 673. 1900. 56th Congress, 1st Session. 16 pp.

House of Representatives Document 692. 1946. 79th Congress, 2nd Session. 23 pp.

House of Representatives Document 1009. 1921. 66th Congress, 3rd Session. 35 pp.

House of Representatives Document 1222. 1919. 65th Congress, 2nd Session. 15 pp.

House of Representatives Document 2096. 1917. 64th Congress, 2nd Session. 11 pp.

House of Representatives, Report 3213. 1906. 59th Congress, 1st Session. 12 pp.

Hubbell, D.W.; Glenn, J.L. 1973. Distribution of radionuclides in bottom sediments of the Columbia River Estuary. Geol. Soc. Am. Professional Paper 433-L. Washington, D.C.: U.S. Government Printing Office.

Hubbell, D.W.; Glenn, J.L.; Stevens, H.H. Jr. 1971. Studies of sediment transport in the Columbia River Estuary. Proceedings 1971 Technical Conference on Estuaries of the Pacific Northwest. Proc. Circ. 42, Eng. Experiment Station. Corvallis: Oregon State University.

Hutton, C.O. 1950. Studies of heavy detrital minerals. Geol. Soc. Am. Bull 61: 655-716.

Imbrie, J.; Purdy, E.G. 1962. Classification of modern Bahamian carbonate sediments. Ham, W.E. ed. Classification of carbonate rocks: a symposium. Memoir 1. Tulsa: American Association of Petroleum Geologists.

Imbrie, J.; Van Andel, T.H. 1964. Vector analysis of heavy mineral data. Geol. Soc. Am. Bull. 75: 1131-1156.

Inman, D.L. 1949. Sorting of sediments in light of fluid mechanics. J. Sed. Pet. 19: 51-70.

Inman, D.L. 1952. Measures for describing the size distribution of sediments. J. Sed. Pet. 22: 125-145.

Jay, D.A. 1982. Columbia River Estuary salinity distribution. Report. U. S. Army Corps of Engineers, Portland District.

Jay, D.A. 1984. Circulatory processes in the Columbia River Estuary. Astoria, OR: Columbia River Estuary Data Development Program.

Johnson, V.G.; Cutshall, N.H. 1975. Geochemical baseline data, Youngs Bay, Oregon, 1974. Final report. Corvallis: Oregon State Univ., School of Oceanography.

Judson, S.; Ritter, D.F. 1964. Rates of regional denudation in the United States. J. Geophys. Res. 69: 3395-3401.

Kelley, J.C.; Whetten, J.T. 1969. Quantitative statistical analysis of Columbia River sediment samples. J. Sed. Pet. 39: 1167-1173.

Kidby, H.A.; Oliver, J.G. 1965. Erosion and accretion along Clatsop Spit. Chapter 26 in Coastal Engineering Santa Barbara Specialty Conference, October 1965. A.S.C.E.

Klovan, J.E. 1966. The use of factor analysis in determining depositional environments from grain-size distributions. J. Sed. Pet. 36: 115-125.

Knebel H.J.; Kelley, J.C.; Whetten, J.T. 1968. Clay minerals of the Columbia River: a qualitative, quantitative, and statistical evaluation. J. Sed. Pet. 38: 600-611.

Kraft, J.C. 1971. Sedimentary environment facies patterns and geologic history of a Holocene marine transgression. Geol. Soc. Am. Bull. 82: 2131-2158.

Krinsky, D.H.; Donahue, J. 1968. Environmental interpretation of sand grain surface texture by electron microscopy. Geol. Soc. Am. Bull. 79: 743-748.

Krumbein, W.C.; Pettijohn, F.J. 1938. Manual of sedimentary petrography. New York: Appleton-Century-Crafts Inc.

Kulm, L.D.; Scheidegger, K.F.; Byrne, J.V.; Spigai, J.S. 1968. A preliminary investigation of the heavy mineral suites of the coastal rivers and beaches of Oregon and northern California. The Ore Bin (OSU Dept. of Geology and Mineral Industries) 30: 165-180.

Lang, E.W. et al. 1947. Report of the sub-committee on sediment terminology. Trans. Am. Geophys. Union 28: 936-938.

Leeder, M.R. 1982. Sedimentology - process and product. London: George Allen and Unwin.

Lockett, J.B. 1959. Interim considerations of the Columbia River entrance. Paper 1902, Proc. A.S.C.E. Journal of the Hydraulics Division 85 HY-1: 17-40.

Lockett, J.B. 1962. Phenomena affecting improvement of the lower Columbia Estuary and entrance. Presented at 8th Conference on Coastal Engineering, Mexico City, Mexico. Portland: U. S. Army Engr. Division.

Lockett, J.B. 1963. Phenomena affecting improvement of the lower Columbia River Estuary and entrance. Prepared for Federal Interagency Sedimentation. Jackson: I.C.W.R.

Lockett, J.R. 1967. Sediment transport and diffusion: Columbia Estuary and entrance. WW-4, Proc. A.S.C.E., J. Waterways and Harbors Div. 93: 167-175.

Lockett, J.B.; Kidby, A.A. 1961. Prototype measurements of the C.R.E. Proc. Amer. Soc. Civil Engineers Hydraulics Division Journal 87: 57-83.

Lutz, G.A.; Hubbell, D.W.; Stevens, H.H. Jr. 1975. Discharge and flow distribution, Columbia River Estuary. Geological Survey Prof. Paper 433-P. Washington, D.C.: U.S. Govt. Printing Office.

McAnally, W.H. Jr.; Brogdon, N.J. Jr.; Letter, J.V. Jr.; Stewart, J.P.; Thomas, W.A. 1983a. Columbia River Estuary Hybrid Model Studies, Report 1. Verification of hybrid modeling of the Columbia River mouth. Hydraulic Laboratory Tech. Report HL-83-16. Vicksburg, MS: U.S. Army Engineer Waterways Experiment Station.

McAnally, W.H. Jr.; Brogdon, N.S.; Stewart, J.P. 1983b. Columbia River Estuary Hybrid Model Studies, Report 4. Entrance channel tests. Hydraulics Laboratory Tech. Report HL-83-16. Vicksburg, MS: U.S. Army Engineer Waterways Experiment Station.

McAnally, W.H. Jr.; Thomas, W.A., Letter, J.V. Jr. 1980. Physical and numerical modelling of estuarine sedimentation. Paper presented at the International Symposium on River Sedimentation, Beijing, China.

McKee, B. 1972. Cascadia. New York: McGraw Hill.

McLaren, P. 1981. An interpretation of trends in grain size measures. J. Sed. Pet. 51: 611-624.

McLaren, P. 1982. Discussion: hydraulic control of grains-size distributions in a macrotidal estuary. Sedimentology 29: 437-439.

McLaren, P.; Bowles, D. 1983. The effects of sediment transport on grain-size distributions. Manuscript in preparation.

McLaughlin, W.T.; Brown, R.L. 1942. Controlling coastal sand dunes in the Pacific Northwest. U.S. Dept. Agriculture Circular 660, 46 pp.

McManus, D.A. 1982. Phi and sediment size analysis: discussion. J. Sed. Pet. 52: 1011-1014.

Meade, R.H. 1967. Relations between suspended matter and salinity in estuaries of the Atlantic seaboard, U.S.A. Int. Assoc. Sci. Hydrol. Gen. Ass. Bern, v. 4.

Middleton, G.V. 1962. On sorting, sorting coefficients, and the lognormality of the grain-size distribution of sandstone: a discussion. J. Geology 70: 754-756.

Middleton, G.V. 1976. Hydraulic interpretation of sand-size distributions. J. Geol. 84: 405-426.

Moore, C.R. and R.E. Hickson. 1939. The Lower Columbia River. Military Engineer 31: 19-23.

Morse, B.A.; Gross, M.G.; Barnes, C.A. 1968. Movement of seabed drifters near the Columbia River. WW1, Proc. A.S.C.E., J. Waterways and Harbors Div. 94: 93-103.

National Marine Consultants 1961. Wave statistics for the three deep water stations along the Oregon-Washington coast. Santa Barbara.

National Ocean Survey 1978. Tide tables 1979. West coast of North and South America including the Hawaiian Islands. Rockville: National Oceanographic and Atmospheric Administration, U. S. Department of Commerce.

National Ocean Survey 1979. Tide tables 1980. West coast of North and South America including the Hawaiian Islands. Rockville: National Oceanographic and Atmospheric Administration, U. S. Department of Commerce.

Neal, V.T. 1972. Physical aspects of the Columbia River and its estuary. Pruter, A.T.; Alverson, P.L. eds. The Columbia River Estuary and adjacent ocean waters. Seattle: University of Washington Press.

Nittrouer, C. A. 1978. The process of detrital sediment accumulation in a continental shelf environment: an examination of the Washington shelf. Ph.D. dissertation. Seattle: University of Washington.

Norberg, J.R. 1980. Black sand occurrences in the Columbia River estuary and vicinity. Tech. Assistance Report. Spokane: U.S. Bureau of Mines, Western Field Operations Center.

Northwest Cartography, Inc. 1984. Calculations of volume and area changes in the Columbia River Estuary. Seattle: unpublished data.

O'Brien, M.P. 1936. Mouth of the Columbia River--beach erosion investigations. Tech. Mem. No. 20. Berkeley, CA: U.S. Tidal Model Laboratory.

O'Brien, M.P. 1971. Field and laboratory studies of navigation channels of the Columbia River Estuary. Hydraulic Eng. Lab. Report HEL-24-4. Berkeley, CA: University of California.

Officer, C.B. 1980. Discussion of the turbidity maximum in partially mixed estuaries. Estuarine Coastal Marine Science 10: 239-246.

Oregon Historical Society. 1980. Columbia's Gateway, A History of the Columbia River Estuary to 1920. Pacific Northwest River Basins Commission, Vancouver, WA.

Pacific Northwest River Basins Commission 1972. Historical hourly project operations 1970-71, Columbia River and lower Snake River dams. Power Planning Committee Report, Pacific Northwest River Basins Committee, Vancouver, Washington.

Pacific Northwest River Basins Commission 1980. Columbia River Estuary Data Development Program. Procedures Manual. Vancouver.

Passega, R. 1957. Texture as characteristic of clastic deposition. Am. Assoc. of Petrol. Geolog. Bull. 41: 1952-1984.

Passega, R. 1964. Grain size representation by CM patterns as a geological tool. J. Sed. Pet. 34: 830-847.

Passega, R. 1977. Significance of CM diagrams of sediments deposited by suspensions. Sedimentology 24: 723-733.

Peterson, C.; Scheiddegger, K.; Komar, P. 1982. Sand dispersal patterns in an active margin estuary of the Northwestern United States as indicated by sand composition, texture and bedforms. Mar. Geology 50: 77-96.

Peterson, C.; Scheiddegger, K.; Komar, P.; Niem, W. 1984. Sediment composition and hydrography in six high-gradient estuaries of the northwest United States. J. Sed. Pet. 54: 86-97.

Pierce, J.W.; Grauss, R.R. 1981. Use and misuses of the phi-scale: discussion. J. Sed. Pet. 51: 1348-1350.

Postma, H. 1967. Sediment transport and sedimentation in the estuarine environment. Lauff, G.E. ed. Estuaries. v. 83. Am. Assoc. Adv. Sci. Publ.

Pritchard, D.W. 1955. Estuarine circulation patterns. Proc. Amer. Soc. Civil Eng. 81: 1-11.

Pruter, A.T.; Alverson, D.L. eds. 1972. The Columbia River Estuary and adjacent ocean waters -- bioenvironmental studies. Seattle: University of Washington Press.

Reading, H.G. 1978. Sedimentary environments and facies. New York: Elsevier.

Reineck, H.E.; Singh, I.B. 1980. Depositional sedimentary environments. 2nd ed.. New York: Springer-Verlag.

Roy, E.H.; Creager, J.S.; Walter, S.R.; Borgeld, J.C. 1979. An investigation to determine the bedload and suspended sediment transport over the outer tidal delta and monitor the sedimentary environment of sites E and D near the mouth of the Columbia River. Final report, December 1979. Portland: Department of the Army, Corps of Engineers, Portland District.

Roy, E.H.; Creager, J.S.; Gelfenbaum, G.R.; Sherwood, C.R.; Stewart, R.J. 1982. An investigation to determine sedimentary environments near the entrance to the Columbia River Estuary. Final Report, June 1982. Portland: Department of the Army, Corps of Engineers, Portland District.

Rubin, D.M.; McCulloch, D.S. 1980. Single and superimposed bedforms: a synthesis of San Francisco Bay and flume observations. Sed. Geology 26: 207-231.

Runge, E.J. Jr. 1966. Continental shelf sediments, Columbia River to Cape Blanco, Oregon. Ph.D. dissertation. Corvallis: Oregon State University.

Scheidegger, K.F.; Kulm, L.D.; Runge, E.J. 1971. Sediment source sand dispersal patterns of Oregon continental shelf sands. J. Sed. Pet. 41: 1112-1120.

Scheidegger, K.F.; Phipps, J.P. 1976. Dispersal patterns of sand in Grays Harbor Estuary, Washington. J. Sed. Pet. 46: 163-166.

Schubel, J.R.; Wilson, R.E.; Okubo, A. 1978. Vertical transport of suspended sediment in upper Chesapeake Bay. Kjerfve, B. ed., Estuarine Transport Processes, Belle G. Baruch Library in Marine Sci. #7. Columbia, SC: University of South Carolina Press.

Sedimentation Seminar 1981. Comparison of methods of size analysis for sands of the Amazon-Solimes rivers, Brazil and Peru. Sedimentology 28: 123-128.

Senate Document 49. 1881. 46th Congress, 3rd Session. 8 pp.

Senate Document 57. 1917. 65th Congress, 1st Session. 5 pp.

Shalowitz, A.L. 1964. Shore and Sea Boundaries, Vol. II. U.S. Coast and Geodetic Survey and Government Printing Office, Washington, D.C. 749 pp.

Shepard, F.P. 1954. Nomenclature based on sand-silt-clay ratios. J. Sed. Pet. 24: 151-158.

Shideler, G.L. 1976. A comparison of electronic particle counting and pipette techniques in routine and analysis. J. Sed. Pet. 46: 1017-1025.

Shields, A. 1936. Application of similarity principles and turbulence research to bedload movement (trans. by W. P. Ott and J. C. Van Uchelen). U.S. Dept. of Agriculture Soil Conservation Service, Coop. Laboratory. Pasadena: California Institute of Technology.

Simenstad, C.A.; Jay, D.A.; McIntire, C.D.; Nehlsen, W.; Sherwood, C.R.; Small, L.F. 1984. The dynamics of the Columbia River estuarine ecosystem, volumes I and II. Astoria, OR: Columbia River Estuary Data Development Program.

Simmons, H.B. 1966. Field experiences in estuaries. In: A.J. Ippen and D.B. Harteman (eds.), Estuary and Coastline Hydrodynamics. McGraw-Hill, N.Y. pp. 673-690.

Simmons, H.B.; Hermann, F.A. Jr. 1972. Effects of man-made works on the hydraulic, salinity, and shoaling regimes of estuaries. G.S.A. Memoir 133: 555-570.

Simons, D.B.; Richardson, E.V.; Nordin, C.F. 1965. Sedimentary structures generated by flow in alluvial channels. Soc. of Econ. Paleon. and Min. Spec. Publ. 12: 34-52.

Slotta, L.S. 1975. Physical characteristics of the Youngs Bay estuarine environs. Final Report Alumax Pacific Aluminum Corp., Ocean Engineering Program. Corvallis: Oregon State University.

Sly, P.G.; Thomas, R.L.; Pelletier, B. R. 1983. Interpretation of moment measures derived from water-lain sediments. Sedimentology 30: 219-233.

Smith, J.D. 1970. Stability of a sand bed subjected to a shear flow of low froude number. J. Geophys. Res. 75: 5928-5940.

Smith, J.D. 1977. Modeling of sediment transport on continental shelves. The Sea, v. 6. New York: Wiley-Interscience.

Smith, J.D.; Hopkins, T.S. 1972. Sediment transport on the continental shelf off of Washington and Oregon in light of recent lowest measurements. Chap. 7. Swift, D.J.P.; Duane, D.B.; Pilkey, O.H. eds. Shelf sediment transport: processes and patterns. Stroudsburg, PA: Dowden, Hutchinson and Ross.

Smith, J.D.; McLean, S.R. 1977. Spatially averaged flow over a wavy surface. J. Geophys. Res. 82: 1735-1746.

Sternberg, R.W.; Creager, J.S.; Glassley, W.; Johnson, J. 1977. Aquatic disposal field investigations, Columbia River disposal site, Oregon. Appendix A: Investigation of the hydraulic regime and physical nature of bottom sedimentation. Final Report, December 1977. Vicksburg: U. S. Army Engineer Waterways Experiment Station.

Sternberg, R.W.; McManus, D.A. 1972. Implications of sediment dispersal from long-term, bottom current measurements on the continental shelf of Washington. Chapter 8. Swift, D.J.P.; Duane, D.B.; Pilkey, O.H. eds. Shelf sediment transport: processes and patterns. Stroudsburg, PA: Dowden, Hutchinson and Ross.

Stevens, H.H. Jr.; Hubbell, D.W.; Glenn, J.L. 1973. Model for sediment transport through an estuary cross section. 21st Ann. Hydr. Div. Spec. Conf., Bozeman, Montana State University. A.S.C.E.

Sundborg, Å 1956. The river Klarälven: a study of fluvial processes. Geografiska Annaler 38: 126-316.

Swift, D.J.P.; Schubel, J.C.; Sheldon, R.W. 1972. Size analysis of fine-grained suspended sediments: a review. J. Sed. Pet. 42: 122-134.

Tanner, W.F. 1959. Sample components obtained by the methods of differences. J. Sed. Pet. 29: 408-411.

Tennessee Valley Authority 1941. A study of methods used in measurements and analysis of sediment loads in streams. Rept. 5. Laboratory Investigation of Suspended Sediment Samplers. Iowa City: University of Iowa Hydraulic Laboratory.

Thomas, D.W. 1983. Changes in Columbia River Estuary habitat types over the past century. Astoria, OR: Columbia River Estuary Data Development Program.

Tucker, R.W.; Vacher, H.L. 1980. Effectiveness of discriminating beach, dune, and river sands by moments and the cumulative weight percentages. J. Sed. Pet. 50: 165-173.

Twenhofel, W.H. 1946. Mineralogical and physical composition of sands of the Oregon coast from Coos Bay to the mouth of the Columbia River. Oregon Department Geol. and Min. Ind. Bull. 30: 64 p.

U.S. Army Engineers. 1875. Report of Chief of Engineers, Appendix GG, pp. 730-759.

U.S. Army Engineers. 1903. Report of the Board of Engineers, Appendix XX of Annual Report, Chief of Engineers, U.S. Army. Part 3, Vol. 3.

U.S. Army Corps of Engineers 1933. Mouth of Columbia River current survey, 1932-1933. Report No. MCR 100/5.288. Portland.

Van Straaten, L.M.J.U.; Kuenen, Ph.H. 1958. Tidal action as a cause for clay accumulation. J. Sed. Pet. 28: 406-413.

Van Winkle, W. 1914a. Quality of the surface waters of Washington. U.S. Geological Survey Water Supply Paper 339.

Van Winkle, W. 1914b. Quality of the surface waters of Oregon. U.S. Geological Survey Water Supply Paper 363.

Visher, G.W. 1969. Grain-size distributions and depositional processes. J. Sed. Pet. 39: 1074-1106.

Walker, P.H.; Woodyer, D.D.; Hutka, J. 1974. Particle size measurements by Coulter counter of very small deposits and low suspended sediment concentrations in streams. J. Sed. Pet. 44: 673-679.

Walter, S.R. 1980. Mineralogy of sediments of the Columbia River Estuary: the discovery of a distinctive coastal mineral. M.S. thesis. Seattle, WA: University of Washington.

Walter, S.R.; Roy, E.H.; Creager, J.S.; Borgeld, J.C. 1979. An investigation to determine the bedload and suspended load transport over the outer tidal delta and monitor the sedimentary environment of sites A, E, and D near the mouth of the Columbia River. Annual Report, March 1979. Portland: Department of the Army Corps of Engineers, Portland District.

Whetten, J.T. 1966. Sediments from the lower Columbia River and origin of graywacke. Science 152: 1057-1058.

Whetten, J.T.; Kelley, J.C.; Hanson, L.G., 1969. Characteristics of Columbia River sediment and sediment transport. J. Sed. Pet. 39: 1149-1166.

White, S.M. 1967. The mineralogy and geochemistry of the sediments on the continental shelf off the Washington-Oregon coast. Ph.D. dissertation. Seattle: University of Washington.

White, S.M. 1970. Mineralogy and geochemistry of continental shelf sediments off the Washington-Oregon coast. J. Sed. Pet. 40: 38-54.

Yalin, M.S. 1964. Geometrical properties of sand waves. J. Hydrol. Div., Amer. Soc. Civil Eng. 90: 105.

APPENDIX A

Bottom Samples in the Columbia River Estuary and Adjacent Continental Shelf

The following tables and figures list and locate the bottom samples considered in this study. Table 9 summarizes the data collection conducted by the University of Washington in the vicinity of the Columbia River Estuary under several contracts with the Corps of Engineers and CREDDP. The subsequent tables list the cruise name (CRUISE), station number (STN), extra identification, date, latitude, longitude, depth, and Folk and Ward (1957) mean grain size (PHI) of the samples. The date is expressed as month/day/year. Latitude and longitude are written as degrees (north or west) and decimal minutes. Depth is in feet, corrected to mean lower low water (MLLW) on the basis of interpolated predicted tides. Most samples were acquired from one of several vessels with either a Van Veen or Shipek grab sampler; in a few instances, samples were scooped by hand from shallow or intertidal zones. Some of the earlier cruises included samples acquired with a tripod-mounted bedload sampler or from the foot of the tripod. The latter generally are identified by an "F" or "FS" in the six-character extra identification columns which follow the station number (STN). The other common notations in these columns include IN and OUT, which refer to inner and outer sample bags; TOP and BOT which refer to the top and bottom subsamples in an obviously stratified grab-sample; BAY, which indicates a sample obtained in one of the peripheral bays of the estuary; MBL, which refers to "mudballs", round or disc-shaped, silty sand rip-up clasts; VV indicates a Van Veen grab during some of the tripod cruises; BL indicates a Helland-Hansen bedload sampler sample, and FS represents a tripod-foot sample on the same cruises. The original ships' logs must be consulted for the significance of the other notations in these columns.

Tables 10, 11 and 12 and Figures 61 to 66 contain stations from the three CREDDP sampling efforts conducted in October 1979, February 1980, and June 1980. All of the samples obtained in February and June were subjected to grain size analysis, using the methods described in the report. Only about one-third (609/1800) of the samples obtained in October 1979 have been processed and only the processed samples are included in this tabulation. The locations and tide-corrected depths of the remaining samples may be obtained at the University of Washington. Locations are considered accurate to ± 100 ft (30 m), and depths are considered accurate to ± 1.0 ft (0.3 m). See text for details and procedures.

Tables 13, 14 and 15 and Figures 67, 68 and 69 contain data from several cruises conducted mostly near the entrance to the estuary for the Corps of Engineers. Table 9 provides a brief summary of these cruises. More information is available in Sternberg et al. (1977), Borgeld et al. (1978), Walter et al. (1979), Roy et al. (1979), Creager et al. (1980) and Roy et al. (1982). These are grouped by river

discharge season (see text) into fall, winter and spring. Depths were not encoded for a number of these samples.

Table 16 and Figures 70 and 71 contain data collected during a fourth seasonal sampling effort in October 1980 as part of the CREDDP studies. The locations and corrected depths of these samples have been encoded, but none of these samples have been analyzed.

With the exception of some samples which were utilized completely during analysis, splits of the samples are archived and stored under refrigeration at the University of Washington. Complete tabulation of the raw data and calculated granulometric parameters from the SEDAN program are available on magnetic tape from the National Environmental Data Referral System (NEDRES) repository or through the Corps of Engineers, Portland District.

Table 9. Summary of bottom sample data collection.

Cruise	File Name	Equipment	Dates	Number of Stations	Positioning Technique	Discharge[1] (cfs)	Season
WN7701	SWN701*	Grab Sampler	1/22/77	42	SX,LR	132,000	Winter
DF7707	SDF7707	Grab Sampler	7/15/77	37	SX	116,000	Fall
DF7707A	SD7707A*	Grab Sampler	7/21/77	42	MR,SX	85,800	Summer
DF7708A	SDF7708A	Grab Sampler	8/30/77	49	MR	83,500	Fall
DF7709	SD7709*	Grab Sampler	9/6/77	46	MR	107,000	Summer
UW7803	SUW7803*		3/16/78	7	SX	157,900	Winter
FR7804	SFR7804	Grab Sampler	4/21/78	40	RD	228,100	Spring
FR7804A	SFR7804A	Grab Sampler	4/28/78	42	SX	243,200	Spring
WN7805A	SWN7805A	Tripod	5/31/78	12	SX,RD	238,800	Spring
DF7806	SDF7806	Grab Sampler	6/12/78	19	SX	298,800	Spring
WN7807	SWN7807	Tripod	7/15/78	12	SX	182,900	Fall
WN7807A	SWN7807A	Tripod	7/16/78	10	SX	145,000	Fall
DF7808	SDF7808	Grab Sampler	8/3,4,5/78	123	SX	144,100	Fall
WN7808A	SWN7808A	Tripod	8/24/78	10	MR	134,000	Fall
WN7808B	SWN7808B	Tripod	8/25/78	7	MR	126,500	Fall
WN7810	SWN7810	Tripod	10/28/78	9	MR	103,800	Fall
WN7810A	SWN7810A	Tripod	10/30/78	9	SX	103,300	Fall
UW7810B	----*		10/29/78	16	SX	103,300	Summer
FR7811	SFR7811	Grab Sampler	11/15/78	24	LR	181,400	Winter
FR7811A	SFR7811A	Grab Sampler	11/22/78	35	MR	182,400	Winter
FR7812	SFR7812	Grab Sampler	12/7/78	71	MR	197,800	Winter
FR7904	SFR7904	Grab Sampler	4/20,21, 22/79	137	LR,RD	189,800	Spring

Z7907	SZ7907*	Grab Sampler	7/2,3,4/79	70	MR		Summer
A7910			10/26-29/79				
C7910	S7910CPS	Grab Sampler	10/11-19/79	623	MR	147,100[2]	Fall
Z7910			10/2-23/79				
J8002	SJ8002	Grab Sampler	2/12-29/80	435	MR	213,600[2]	Winter
J8006	SJ8006	Grab Sampler 7/11/80	6/10-	431	MR	321,000[2]	Spring
J8010[3]	S8010	Grab Sampler	10/2-13/80	400	MR	130,500[2]	Fall
NB8106	SWB8106	Grab Sampler	6/25/81	18	MR	427,200[2]	Spring

* Not included in this study.

[1] River discharge at the Dalles.

[2] Monthly mean discharge, based on calculations of Jay, 1984.

[3] Not analyzed.

LF = Loran-C, SX = horizontal sextant fixes, RD = radar, MR = Miniranger or Del Norte.

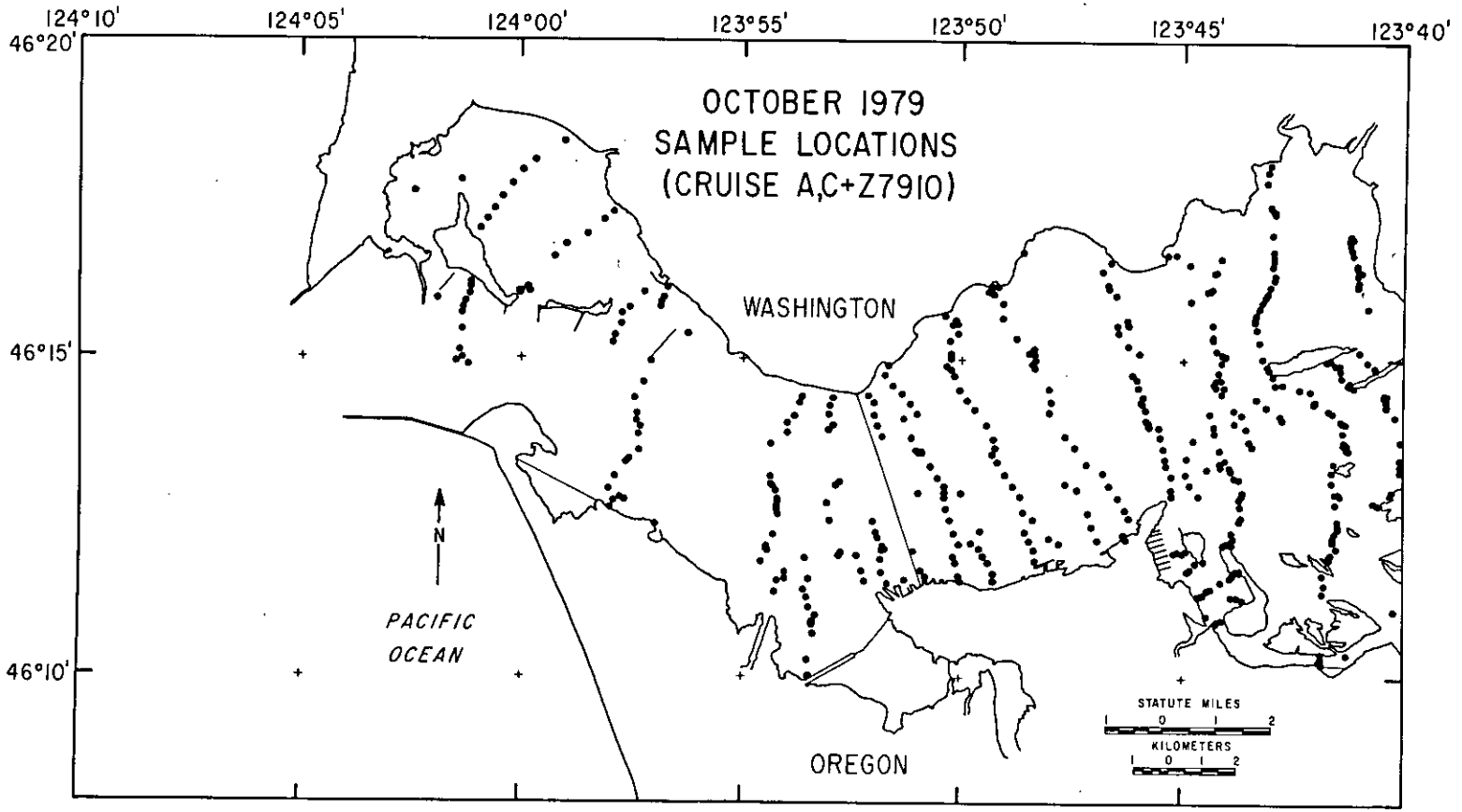

Figure 61. CREDDP bottom sample locations, October 1979.

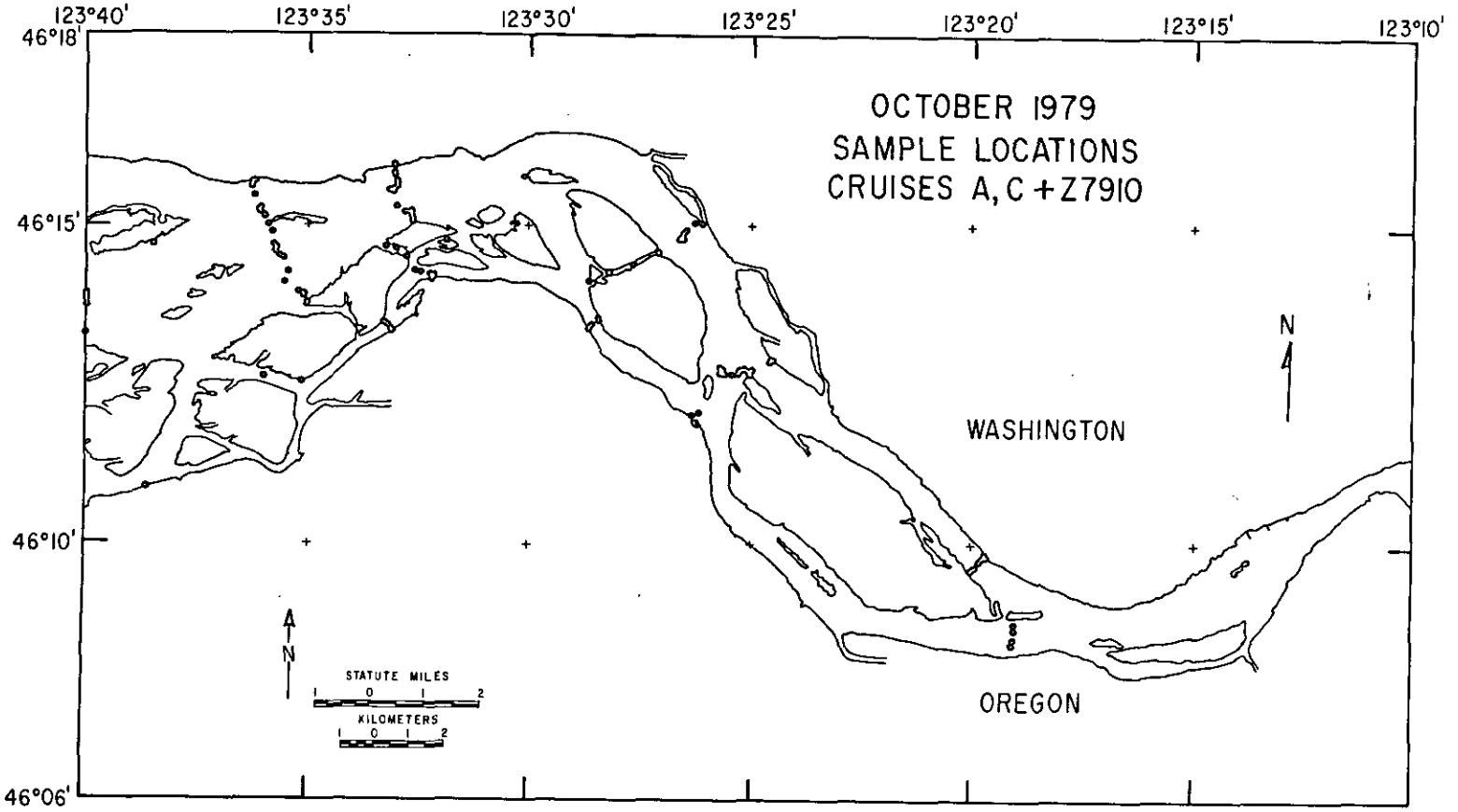

Figure 62. CREDDP bottom sample locations, October 1979.

TABLE 10.
OCTOBER 1979 BOTTOM SAMPLE LOCATIONS
CRUISES A7910, C7910, Z7910
(FIGURES 61, 62)

CRUISE	STN	DATE	LATITUDE	LONGITUDE	DEPTH	PHI
A7910	5	102679	46 9.88	123 19.70	4.2	0.69
A7910	6	102679	46 9.84	123 19.64	13.2	-0.49
A7910	7	102679	46 9.81	123 19.77	11.3	0.81
A7910	8	102679	46 9.77	123 19.82	6.3	0.22
A7910	9	102679	46 9.69	123 19.91	12.3	1.10
A7910	10	102679	46 9.67	123 19.93	21.3	1.05
A7910	11	102679	46 9.65	123 19.97	34.3	0.90
A7910	12	102679	46 9.62	123 20.01	22.3	1.24
A7910	13	102679	46 9.61	123 20.02	12.4	1.70
A7910	14	102679	46 9.61	123 20.02	6.4	1.90
A7910	15	102679	46 9.61	123 20.03	-0.6	2.44
A7910	69	102679	46 12.91	123 24.54	-1.0	3.28
A7910	70	102679	46 12.92	123 24.56	5.0	1.92
A7910	71	102679	46 12.92	123 24.56	17.9	0.87
A7910	72	102679	46 12.88	123 24.63	10.9	1.03
A7910	73	102679	46 12.82	123 24.76	0.8	1.05
A7910	74	102679	46 12.75	123 25.02	34.8	1.88
A7910	75	102679	46 12.74	123 25.03	20.7	2.35
A7910	76	102679	46 12.73	123 25.03	12.7	2.50
A7910	77	102679	46 12.72	123 25.05	4.6	2.55
A7910	78	102679	46 12.70	123 25.06	-2.4	2.50
A7910	201	102879	46 15.25	123 32.66	15.5	3.08
A7910	202	102879	46 15.17	123 32.65	9.5	3.08
A7910	203	102879	46 15.16	123 32.64	16.5	3.02
A7910	204	102879	46 15.15	123 32.65	28.6	2.77
A7910	205	102879	46 15.12	123 32.64	38.6	2.22
A7910	206	102879	46 15.09	123 32.64	29.6	2.65
A7910	207	102879	46 15.06	123 32.64	14.7	2.35
A7910	208	102879	46 15.06	123 32.62	8.7	1.58
A7910	209	102879	46 15.06	123 32.63	0.7	1.03
A7910	210	102879	46 15.62	123 32.98	29.8	1.56
A7910	211	102879	46 15.67	123 32.98	14.8	1.83
A7910	212	102879	46 15.69	123 32.97	10.8	1.80
A7910	213	102879	46 15.71	123 32.98	14.9	2.69
A7910	214	102879	46 15.79	123 33.04	28.9	1.34
A7910	215	102879	46 15.84	123 33.06	16.0	1.57
A7910	216	102879	46 15.96	123 33.05	0.0	4.24
A7910	217	102879	46 15.97	123 33.04	8.0	3.27
A7910	234	102879	46 15.16	123 34.98	1.3	1.57
A7910	237	102879	46 15.69	123 36.24	19.2	1.58
A7910	238	102879	46 15.69	123 36.22	9.1	1.34
A7910	239	102879	46 15.69	123 36.23	3.1	1.44
A7910	240	102879	46 15.23	123 36.07	11.1	2.77
A7910	241	102879	46 15.21	123 36.05	20.1	3.50
A7910	242	102879	46 15.16	123 35.98	9.0	2.08
A7910	243	102879	46 15.14	123 35.98	0.0	1.47
A7910	254	102979	46 13.81	123 35.04	1.1	2.57

A7910	255	102979	46	13.90	123 35.12	6.1	2.19
A7910	256	102979	46	13.94	123 35.12	12.2	1.99
A7910	257	102971	46	13.98	123 35.25	24.2	1.74
A7910	258	102979	46	14.12	123 35.54	14.3	2.28
A7910	259	102979	46	14.28	123 35.47	6.3	2.37
A7910	260	102979	46	14.48	123 35.58	4.4	2.54
A7910	261	102979	46	14.53	123 35.67	12.4	2.73
A7910	262	102979	46	14.59	123 35.74	16.9	2.50
A7910	263	102979	46	14.66	123 35.73	12.5	3.08
A7910	264	102979	46	14.70	123 35.77	7.0	2.79
A7910	265	102979	46	14.90	123 35.81	0.6	2.07
A7910	266	102979	46	15.02	123 35.90	-2.4	1.87
A7910	316	102979	46	14.70	123 38.50	-0.5	2.38
C7910	18	101179	46	16.00	124 1.22	18.3	2.06
C7910	19	101179	46	15.89	124 1.30	28.3	2.28
C7910	20	101179	46	15.79	124 1.37	42.1	2.35
C7910	21	101179	46	15.70	124 1.40	58.1	2.14
C7910	22	101179	46	15.44	124 1.39	79.0	1.34
C7910	23	101179	46	15.12	124 1.43	68.8	1.76
C7910	24	101179	46	15.01	124 1.40	46.7	1.96
C7910	25	101179	46	14.90	124 1.24	26.6	2.29
C7910	26	101179	46	14.95	124 1.52	38.4	2.20
C7910	54	101279	46	14.39	123 52.96	20.3	2.89
C7910	55	101279	46	14.28	123 53.02	42.4	1.76
C7910	56	101279	46	14.13	123 53.03	57.5	1.66
C7910	57	101279	46	13.96	123 52.96	67.6	1.47
C7910	58	101279	46	13.89	123 53.04	67.6	1.49
C7910	59	101279	46	13.85	123 53.97	46.9	1.40
C7910	60	101279	46	14.00	123 53.98	53.9	1.73
C7910	61	101279	46	14.12	123 53.80	57.0	1.62
C7910	62	101279	46	14.33	123 53.71	24.0	2.16
C7910	63	101279	46	14.41	123 53.64	18.1	2.08
C7910	77	101279	46	14.97	123 57.10	79.3	1.13
C7910	78	101279	46	14.65	123 57.25	39.5	1.35
C7910	79	101279	46	14.38	123 57.48	40.1	1.98
C7910	80	101279	46	14.15	123 57.42	33.3	2.55
C7910	81	101279	46	14.04	123 57.43	18.2	1.26
C7910	82	101279	46	13.93	123 57.34	19.1	1.25
C7910	83	101279	46	13.81	123 57.39	21.0	1.79
C7910	84	101279	46	13.56	123 57.37	19.3	2.58
C7910	85	101279	46	13.44	123 57.60	33.5	2.29
C7910	86	101279	46	13.37	123 57.68	45.9	2.19
C7910	87	101279	46	13.16	123 57.92	31.3	1.58
C7910	88	101279	46	12.95	123 58.07	18.2	3.15
C7910	89	101279	46	12.80	123 57.71	19.1	2.27
C7910	102	101279	46	11.82	123 54.58	10.3	3.72
C7910	106	101379	46	11.98	123 54.45	13.2	2.42
C7910	107	101379	46	11.66	123 54.02	26.3	1.82
C7910	108	101379	46	11.56	123 54.02	31.3	3.22
C7910	109	101379	46	11.35	123 54.27	43.4	2.27
C7910	110	101379	46	11.53	123 54.20	41.5	2.06
C7910	112	101379	46	10.98	123 53.32	20.7	2.20
C7910	113	101379	46	11.10	123 53.48	29.7	2.17
C7910	114	101379	46	11.25	123 53.52	39.8	1.96

C7910	115		101379	46	11.38	123	53.58	41.9	2.18
C7910	116		101379	46	11.55	123	53.47	27.9	2.10
C7910	117		101379	46	11.88	123	53.57	17.0	2.53
C7910	125		101379	46	11.51	123	52.23	40.8	1.69
C7910	126		101379	46	11.68	123	52.29	31.8	1.37
C7910	127		101379	46	11.92	123	52.40	16.9	4.59
C7910	128		101379	46	11.85	123	51.88	29.1	2.10
C7910	129		101379	46	11.65	123	51.85	39.2	1.75
C7910	130		101379	46	11.54	123	51.31	46.3	1.53
C7910	131		101379	46	11.48	123	51.73	31.4	2.61
C7910	132		101379	46	11.59	123	50.81	42.0	6.60
C7910	133		101379	46	11.69	123	50.93	12.0	1.49
C7910	134		101379	46	12.89	123	51.00	40.0	1.94
C7910	135		101379	46	11.99	123	51.11	15.1	2.02
C7910	136		101379	46	11.90	123	50.21	23.1	1.91
C7910	137		101379	46	11.80	123	50.14	38.1	1.68
C7910	138		101379	46	11.60	123	50.07	70.1	2.66
C7910	139		101379	46	11.53	123	50.04	64.1	6.06
C7910	140		101379	46	11.51	123	49.32	23.1	3.25
C7910	141		101379	46	11.63	123	49.33	40.1	2.65
C7910	1421		101379	46	11.80	123	49.44	45.1	1.32
C7910	143	INTOP	101379	46	11.92	123	49.55	33.1	3.58
C7910	143	OUTBOT	101379	46	11.92	123	49.55	33.1	1.33
C7910	144		101379	46	12.02	123	49.62	23.1	2.04
C7910	145		101379	46	12.30	123	49.61	22.0	1.75
C7910	146		101379	46	12.16	123	48.52	43.0	1.69
C7910	147		101379	46	12.01	123	48.40	45.9	1.93
C7910	148		101379	46	11.84	123	48.38	24.9	-0.34
C7910	150		101379	46	12.11	123	47.83	31.7	1.96
C7910	151		101379	46	12.19	123	48.06	41.7	1.20
C7910	152		101379	46	12.48	123	48.42	25.6	2.04
C7910	153		101379	46	13.04	123	47.67	19.4	1.93
C7910	154		101379	46	12.95	123	47.41	28.3	2.24
C7910	155		101379	46	12.60	123	47.15	44.2	1.45
C7910	156		101379	46	12.37	123	47.07	32.2	1.78
C7910	157		101379	46	12.17	123	46.94	19.2	1.98
C7910	158		101379	46	12.52	123	46.24	23.8	1.49
C7910	159		101379	46	12.65	123	46.33	41.8	1.73
C7910	160		101379	46	12.83	123	46.48	53.7	1.16
C7910	161		101379	46	13.01	123	46.69	39.7	1.62
C7910	162		101379	46	13.21	123	46.81	23.5	1.66
C7910	178	IN2TOP	101379	46	12.87	123	45.30	131.7	4.80
C7910	178	IN3TOP	101379	46	12.87	123	45.30	131.7	5.03
C7910	178	IN1TOP	101379	46	12.87	123	45.30	131.7	4.98
C7910	178	OUTBOT	101379	46	12.86	123	45.30	131.6	1.77
C7910	179		101379	46	12.96	123	45.30	69.5	2.08
C7910	180		101379	46	13.15	123	45.31	41.4	1.82
C7910	181		101379	46	13.35	123	45.43	23.3	1.72
C7910	190		101479	46	13.04	123	44.88	33.7	2.08
C7910	191		101479	46	13.20	123	44.98	41.7	1.55
C7910	192		101479	46	13.46	123	44.95	22.8	1.38
C7910	193		101479	46	13.74	123	44.80	12.8	1.31
C7910	194		101479	46	13.95	123	44.32	15.8	1.61
C7910	195		101479	46	13.85	123	44.31	28.8	1.81

C7910	196		101479	46	13.58	123 44.18	47.8	1.21
C7910	197	1	101479	46	13.37	123 44.17	30.8	2.54
C7910	197	2	101479	46	13.37	123 44.17	30.8	2.54
C7910	197	3	101479	46	13.37	123 44.17	30.8	2.55
C7910	198		101479	46	13.32	123 44.17	12.8	2.72
C7910	199		101479	46	13.64	123 43.45	9.9	2.95
C7910	200		101279	46	13.72	123 43.50	40.9	2.47
C7910	201		101479	46	13.93	123 43.58	43.0	1.68
C7910	202		101479	46	14.15	123 43.67	27.0	1.09
C7910	203		101479	46	14.20	123 43.86	17.0	1.80
C7910	204		101479	46	14.08	123 42.77	10.2	1.66
C7910	205		101479	46	14.13	123 42.81	37.2	2.19
C7910	206		101479	46	14.27	123 43.13	44.2	1.84
C7910	207		101479	46	14.41	123 43.34	22.2	1.48
C7910	208		101479	46	14.63	123 42.92	23.2	1.60
C7910	209		101479	46	14.63	123 42.77	34.2	1.80
C7910	210		101479	46	14.55	123 42.37	41.4	1.34
C7910	211		101479	46	14.52	123 42.13	48.3	2.14
C7910	212		101479	46	14.35	123 42.04	25.4	1.57
C7910	213		101479	46	14.32	123 42.02	19.5	0.91
C7910	214		101479	46	14.63	123 41.25	13.7	3.02
C7910	215		101479	46	14.66	123 41.23	25.7	2.34
C7910	216		101479	46	14.74	123 41.42	33.8	1.22
C7910	217		101579	46	14.84	123 41.45	42.7	1.75
C7910	218		101579	46	14.93	123 41.47	36.7	1.22
C7910	219		101579	46	14.94	123 41.56	44.7	0.64
C7910	220		101579	46	15.00	123 41.70	14.7	1.88
C7910	221		101579	46	14.99	123 41.73	28.7	1.90
C7910	222		101579	46	14.87	123 40.65	25.9	1.58
C7910	223		101579	46	14.90	123 40.66	36.9	1.65
C7910	224		101579	46	14.99	123 40.81	45.9	0.66
C7910	225		101579	46	15.13	123 41.02	33.8	2.19
C7910	256		101579	46	15.19	123 36.09	17.6	2.52
C7910	257		101579	46	15.22	123 36.09	25.7	2.22
C7910	258		101579	46	15.27	123 36.07	35.7	1.71
C7910	259		101579	46	15.48	123 36.20	48.8	1.42
C7910	260		101579	46	15.60	123 36.28	35.8	1.28
C7910	261		101579	46	15.67	123 36.25	21.9	1.41
C7910	267		101579	46	15.57	123 33.06	55.5	1.27
C7910	268		101579	46	15.55	123 33.16	40.5	1.53
C7910	269		101579	46	15.53	123 33.04	47.6	1.94
C7910	270		101579	46	15.31	123 32.98	35.7	1.75
C7910	271		101579	46	15.22	123 32.80	25.7	2.34
C7910	312		101679	46	15.04	123 26.11	41.7	2.75
C7910	313		101679	46	15.06	123 26.29	64.8	0.90
C7910	314		101679	46	14.95	123 26.48	34.9	1.84
C7910	315		101679	46	14.90	123 26.54	26.0	2.13
C7910	316		101679	46	14.82	123 26.60	19.0	2.08
C7910	344		101779	46	8.80	123 19.01	21.1	1.01
C7910	345		101779	46	8.70	123 19.00	28.1	1.25
C7910	346		101779	46	8.55	123 19.03	43.0	1.71
C7910	347		101779	46	8.47	123 19.07	27.0	2.13
C7910	390		101879	46	12.70	123 25.31	45.8	2.34
C7910	391		101879	46	12.69	123 25.47	42.7	1.82

C7910	392	101879	46	12.72	123	25.73	16.4	2.67
C7910	393	101879	46	12.69	123	25.65	32.2	1.52
C7910	394	101979	46	13.78	123	51.85	8.6	2.06
C7910	395	101979	46	13.96	123	51.96	30.6	2.24
C7910	396	101979	46	14.12	123	52.03	42.4	1.91
C7910	397	101979	46	14.32	123	52.02	51.3	1.09
C7910	398	101979	46	14.44	123	52.17	70.2	1.77
C7910	399	101979	46	14.76	123	51.78	32.0	6.11
C7910	400	101979	46	14.58	123	51.60	43.9	2.25
C7910	401	101979	46	14.45	123	51.38	35.8	2.13
C7910	402	101979	46	14.30	123	51.20	20.6	1.92
C7910	407	101979	46	15.61	123	50.17	42.5	3.95
C7910	408	101979	46	15.56	123	50.24	51.3	5.77
C7910	409	101979	46	15.57	123	50.13	11.3	1.84
C7910	410 INTOP	101979	46	16.14	123	49.37	27.8	4.78
C7910	411OUTBOT	101979	46	16.04	123	49.32	28.7	1.55
C7910	411IN TOP	101979	46	16.04	123	49.32	28.7	3.34
C7910	418	101979	46	15.18	123	48.40	22.0	1.13
C7910	419	101979	46	15.10	123	48.40	33.0	1.24
C7910	420	101979	46	14.98	123	48.38	18.0	2.34
Z7910	1	100279	46	15.93	124	1.96	29.1	4.44
Z7910	18BAY	100279	46	17.61	124	2.48	12.5	6.34
Z7910	24BAY	100279	46	17.79	124	1.42	-0.6	5.17
Z7910	28BAY	100279	46	18.40	123	59.10	-3.4	2.13
Z7910	32BAY	100279	46	17.30	123	57.98	-4.0	2.26
Z7910	33BAY	100279	46	17.18	123	58.20	-0.8	3.92
Z7910	34BAY	100279	46	16.96	123	58.58	1.4	5.52
Z7910	35BAY	100279	46	16.78	123	59.04	-3.1	2.40
Z7910	36BAY	100279	46	16.60	123	59.30	0.0	2.74
Z7910	39BAY	100279	46	16.12	123	59.90	11.8	2.52
Z7910	40BAY	100279	46	16.05	124	0.05	33.8	3.37
Z7910	41BAY	100279	46	16.04	124	0.08	18.9	4.33
Z7910	42BAY	100279	46	16.04	124	0.13	7.0	2.18
Z7910	43BAY	100279	46	16.03	124	0.13	-1.0	2.15
Z7910	56BAY	100279	46	17.03	124	0.98	1.7	2.47
Z7910	57 INBOT	100279	46	17.17	124	0.82	8.7	3.84
Z7910	57OUTTOP	100279	46	17.17	124	0.82	8.7	5.52
Z7910	58BAYTOP	100279	46	17.35	124	0.65	3.7	5.02
Z7910	59BAY	100279	46	17.53	124	0.47	1.7	2.45
Z7910	60BAY	100279	46	17.74	124	0.24	1.7	6.56
Z7910	61BAY	100279	46	17.95	124	0.00	1.7	4.53
Z7910	62BAY	100279	46	18.11	123	59.75	1.1	4.42
Z7910	71BAY	100379	46	16.05	123	57.25	10.9	5.53
Z7910	96BAY	100379	46	15.40	123	56.27	-3.0	2.27
Z7910	104BAY	100379	46	16.11	123	56.76	-0.5	2.98
Z7910	105BAY	100379	46	15.97	123	56.83	0.7	2.55
Z7910	106BAY	100379	46	15.90	123	56.88	1.9	2.71
Z7910	107BAY	100379	46	15.82	123	56.88	-0.9	2.70
Z7910	108BAY	100379	46	15.80	123	57.61	12.4	6.49
Z7910	109BAY	100379	46	15.72	123	57.79	0.0	2.47
Z7910	110BAY	100379	46	15.56	123	57.80	2.4	2.60
Z7910	111BAY	100379	46	15.36	123	57.94	-99.0	2.15
Z7910	112BAY	100379	46	15.25	123	58.01	16.0	2.13
Z7910	128	100379	46	16.13	124	1.20	11.3	2.09

Z7910	129		100379	46	16.18	124	1.19	6.3	2.13
Z7910	137		100479	46	13.44	123	45.43	11.2	1.53
Z7910	138		100479	46	13.61	123	45.48	7.1	1.87
Z7910	139		100479	46	13.79	123	45.57	2.9	2.34
Z7910	140		100479	46	13.94	123	45.57	2.7	1.73
Z7910	141		100479	46	13.95	123	45.81	9.5	1.34
Z7910	142		100479	46	14.03	123	45.84	15.9	2.03
Z7910	143		100479	46	14.05	123	45.87	9.8	1.88
Z7910	144		100479	46	14.21	123	45.88	23.5	2.52
Z7910	145		100479	46	14.30	123	45.96	10.4	2.05
Z7910	146		100479	46	14.34	123	45.98	3.3	1.83
Z7910	147		100479	46	14.43	123	45.94	14.1	2.64
Z7910	148		100479	46	14.56	123	46.04	11.1	1.55
Z7910	149		100479	46	14.70	123	46.10	4.0	2.90
Z7910	150		100479	46	14.77	123	46.19	-0.2	2.83
Z7910	151		100479	46	15.21	123	46.26	15.5	2.63
Z7910	152		100479	46	15.10	123	46.03	0.4	2.80
Z7910	153		100479	46	15.42	123	46.50	8.2	2.21
Z7910	155	1	100479	46	15.54	123	46.52	15.0	1.40
Z7910	155	2	100479	46	15.54	123	46.52	15.0	1.39
Z7910	156		100479	46	15.55	123	46.28	7.8	2.29
Z7910	157		100479	46	15.63	123	46.31	2.7	1.52
Z7910	159		100479	46	12.20	123	46.32	1.6	1.87
Z7910	160		100479	46	12.27	123	46.35	11.6	3.11
Z7910	161		100479	46	13.36	123	47.22	11.8	2.15
Z7910	162		100479	46	13.63	123	47.48	6.8	2.69
Z7910	163		100479	46	13.78	123	47.69	5.0	2.63
Z7910	164		100479	46	14.17	123	48.05	12.0	2.75
Z7910	165		100479	46	14.33	123	48.03	4.1	1.72
Z7910	166		100479	46	14.53	123	48.08	12.1	1.34
Z7910	167		100479	46	14.87	123	48.39	32.2	2.71
Z7910	168		100479	46	14.94	123	48.47	32.3	1.63
Z7910	169		100479	46	15.10	123	48.54	27.5	1.76
Z7910	170		100479	46	15.34	123	48.81	4.6	1.99
Z7910	171		100479	46	15.64	123	49.12	14.8	1.70
Z7910	172		100479	46	15.89	123	49.12	130.0	0.87
Z7910	173		100479	46	16.07	123	49.43	28.3	1.71
Z7910	174		100479	46	16.16	123	49.26	28.8	2.83
Z7910	175		100479	46	16.18	123	49.31	12.9	2.49
Z7910	176		100479	46	16.02	123	46.56	22.5	2.51
Z7910	177		100479	46	16.11	123	46.70	25.6	1.71
Z7910	178		100479	46	16.19	123	46.73	39.7	2.35
Z7910	179		100479	46	16.40	123	46.87	13.9	1.60
Z7910	180		100479	46	16.53	123	46.69	1.5	2.67
Z7910	183		100479	46	15.68	123	50.40	7.7	0.75
Z7910	184		100479	46	15.41	123	50.11	28.6	1.63
Z7910	185		100479	46	15.30	123	50.30	23.8	1.51
Z7910	186		100479	46	15.09	123	50.28	7.0	2.02
Z7910	187		100479	46	15.03	123	50.27	7.1	2.06
Z7910	188		100479	46	14.85	123	50.26	44.2	1.22
Z7910	189		100479	46	14.90	123	50.38	24.2	1.31
Z7910	190		100479	46	14.74	123	50.19	28.5	1.49
Z7910	191		100479	46	14.52	123	50.07	23.6	2.41
Z7910	192		100479	46	14.35	123	49.92	18.7	2.05

Z7910 193	100479	46 14.20	123 49.74	18.8	3.39
Z7910 194	100479	46 13.97	123 49.47	5.4	2.45
Z7910 195	100479	46 13.74	123 49.33	16.0	3.05
Z7910 196	100479	46 13.62	123 49.28	1.0	2.50
Z7910 197	100479	46 13.50	123 49.35	12.2	1.51
Z7910 198	100479	46 13.38	123 49.23	17.3	1.47
Z7910 199	100479	46 13.19	123 49.06	9.3	1.75
Z7910 200	100479	46 13.00	123 48.88	9.4	1.87
Z7910 201	100479	46 12.85	123 48.72	12.5	1.64
Z7910 202	100479	46 12.60	123 48.64	14.6	1.59
Z7910 203	100479	46 12.29	123 48.61	31.6	1.74
Z7910 205	100579	46 16.68	123 48.69	2.5	3.65
Z7910 207	100579	46 14.89	123 51.73	9.9	3.49
Z7910 208	100579	46 14.14	123 51.04	15.1	2.63
Z7910 209	100579	46 14.07	123 51.34	5.9	1.93
Z7910 210	100579	46 13.76	123 51.18	14.7	1.74
Z7910 211	100579	46 13.57	123 51.06	5.2	2.54
Z7910 212	100579	46 13.53	123 51.02	-0.5	2.43
Z7910 213	100579	46 13.54	123 50.96	5.4	3.05
Z7910 214	100579	46 13.55	123 50.92	13.2	2.98
Z7910 215	100579	46 13.31	123 50.70	6.3	1.86
Z7910 216	100579	46 13.14	123 50.56	12.1	1.19
Z7910 217	100579	46 13.00	123 50.40	5.9	2.15
Z7910 218	100579	46 12.91	123 50.40	1.6	1.77
Z7910 219	100579	46 12.89	123 50.03	7.6	2.11
Z7910 220	100579	46 12.83	123 50.40	13.6	2.11
Z7910 221	100579	46 12.66	123 50.36	7.5	1.92
Z7910 222	100579	46 12.47	123 50.28	3.4	2.08
Z7910 223	100579	46 12.27	123 50.18	1.3	2.11
Z7910 224	100579	46 12.10	123 50.08	10.2	1.98
Z7910 225	100579	46 12.02	123 51.79	11.4	2.16
Z7910 226	100579	46 12.02	123 51.86	7.5	2.20
Z7910 227	100579	46 12.06	123 51.84	-0.5	2.26
Z7910 228	100579	46 12.21	123 51.93	-2.4	2.31
Z7910 229	100579	46 12.28	123 51.98	3.6	2.77
Z7910 230	100579	46 12.45	123 52.04	-2.3	1.97
Z7910 234	100579	46 13.07	123 52.80	11.8	3.44
Z7910 235	100579	46 13.03	123 52.89	6.8	2.01
Z7910 241	100579	46 12.75	123 53.08	-2.8	2.21
Z7910 242	100579	46 12.46	123 53.02	-1.6	2.05
Z7910 244	100579	46 11.97	123 52.77	5.7	2.25
Z7910 245	100579	46 11.91	123 52.81	13.7	4.62
Z7910 246	100579	46 12.04	123 54.45	11.9	2.28
Z7910 247	100579	46 12.06	123 54.45	6.0	2.37
Z7910 248	100579	46 12.07	123 54.47	0.1	2.42
Z7910 249	100579	46 12.25	123 54.30	-3.8	2.64
Z7910 250	100579	46 12.56	123 54.18	6.4	2.76
Z7910 251	100579	46 12.63	123 54.23	11.5	2.63
Z7910 252	100579	46 12.70	123 54.22	0.5	2.65
Z7910 253	100579	46 12.77	123 54.21	6.6	2.48
Z7910 254	100579	46 12.80	123 54.20	14.8	2.38
Z7910 255	100579	46 12.94	123 54.25	12.9	2.38
Z7910 256	100579	46 13.01	123 54.31	7.0	2.80
Z7910 257	100579	46 13.04	123 54.35	1.1	1.80

Z7910	258		100579	46	13.16	123	54.37	7.2	1.74
Z7910	259		100579	46	13.68	123	54.35	11.7	1.45
Z7910	273		100679	46	14.00	123	43.85	17.1	1.35
Z7910	274		100679	46	14.21	123	43.97	9.9	1.53
Z7910	276BAY		100679	46	14.47	123	44.13	2.1	1.96
Z7910	277BAY		100679	46	14.60	123	44.30	7.7	2.05
Z7910	278BAY		100679	46	14.65	123	44.33	13.7	2.17
Z7910	279BAY		100679	46	14.68	123	44.26	7.6	1.54
Z7910	280BAY		100679	46	14.69	123	44.15	9.5	1.89
Z7910	281BAY		100679	46	14.80	123	44.20	4.4	2.14
Z7910	282BAY		100679	46	14.96	123	44.13	1.3	2.16
Z7910	283BAY		100679	46	15.07	123	44.06	8.9	2.14
Z7910	284BAY		100679	46	15.08	123	44.14	11.8	2.72
Z7910	285BAY		100679	46	15.15	123	44.27	6.6	2.07
Z7910	286BAY		100679	46	15.34	123	44.36	-1.8	2.23
Z7910	287BAY	1	100679	46	15.40	123	44.36	2.1	2.76
Z7910	288BAY		100679	46	15.55	123	44.35	9.8	2.00
Z7910	289BAY		100679	46	14.62	123	44.33	11.7	2.40
Z7910	290BAY		100679	46	15.93	123	44.87	5.6	2.53
Z7910	291BAY		100679	46	16.08	123	44.47	0.3	2.63
Z7910	292BAY		101679	46	16.13	123	44.38	5.2	2.84
Z7910	293BAY		100679	46	16.10	123	44.36	13.1	2.80
Z7910	294BAY		100679	46	16.39	123	44.29	2.7	2.44
Z7910	295BAY		101679	46	16.50	123	44.91	12.4	2.75
Z7910	296BAY		100679	46	16.39	123	44.32	10.9	2.56
Z7910	297BAY		101679	46	16.60	123	44.15	12.0	2.53
Z7910	298BAY		101679	46	16.65	123	45.22	4.9	3.76
Z7910	299BAY		101679	46	16.65	123	45.39	-2.1	1.14
Z7910	301BAY		100679	46	18.06	123	43.05	-2.4	2.06
Z7910	302BAY		100679	46	18.02	123	43.11	4.8	2.24
Z7910	303BAY		100679	46	17.97	123	43.12	11.7	2.04
Z7910	304BAY		100679	46	17.80	123	43.15	3.7	3.30
Z7910	305BAY		100679	46	17.42	123	43.05	3.6	2.18
Z7910	306BAY		100679	46	17.37	123	43.02	9.6	1.44
Z7910	307BAY		100679	46	17.32	123	42.98	26.5	4.71
Z7910	308BAY		100679	46	17.31	123	42.95	8.5	1.49
Z7910	309BAY		100679	46	16.97	123	43.02	3.5	2.20
Z7910	310BAY		100679	46	16.72	123	42.98	8.5	2.23
Z7910	311BAY		100679	46	16.63	123	42.98	19.5	1.39
Z7910	312BAY		100679	46	16.57	123	42.98	10.5	1.45
Z7910	313BAY		100679	46	16.48	123	43.02	5.5	2.71
Z7910	314BAY		100679	46	16.33	123	42.96	9.6	1.90
Z7910	315BAY		100679	46	16.29	123	42.97	16.6	1.75
Z7910	316BAY		100679	46	16.27	123	42.98	9.6	2.41
Z7910	317BAY		100679	46	16.16	123	43.06	3.7	1.79
Z7910	318BAY		100679	46	16.06	123	43.13	2.7	1.52
Z7910	319BAY		100679	46	15.92	123	43.23	9.2	2.40
Z7910	320BAY		100679	46	15.99	123	43.14	17.9	1.46
Z7910	321BAY		100679	46	15.82	123	43.30	3.9	2.32
Z7910	322BAY		100679	46	15.73	123	43.36	7.3	1.84
Z7910	323BAY		100679	46	15.65	123	43.38	10.3	2.09
Z7910	324BAY		100679	46	15.60	123	43.38	16.5	2.51
Z7910	325BAY		100679	46	15.49	123	43.37	8.6	2.05
Z7910	326BAY		100679	46	15.27	123	43.29	0.7	2.70

Z7910	327BAY	130679	46 15.03	123 43.21	10.8	3.72
Z7910	328BAY	100679	46 15.02	123 43.21	4.9	2.66
Z7910	329BAY	100679	46 14.93	123 43.12	-1.0	1.76
Z7910	330BAY	100679	46 14.84	123 43.07	4.9	2.25
Z7910	331	100679	46 14.75	123 43.00	13.2	1.34
Z7910	338BAY	100779	46 15.83	123 40.82	4.8	1.51
Z7910	340BAY	100779	46 16.18	123 41.06	6.7	1.83
Z7910	341BAY	100779	46 16.20	123 41.05	1.7	2.12
Z7910	342BAY	100779	46 16.23	123 41.04	-0.4	1.91
Z7910	343BAY	100779	46 16.35	123 41.07	0.4	2.44
Z7910	344BAY	100779	46 16.39	123 40.97	3.4	1.71
Z7910	345BAY	100779	46 16.47	123 41.08	6.3	1.63
Z7910	346BAY	100779	46 16.51	123 41.08	1.2	2.10
Z7910	347BAY	100779	46 16.87	123 41.26	13.7	1.46
Z7910	348BAY	100779	46 16.82	123 41.23	6.6	2.10
Z7910	349BAY	100779	46 16.76	123 41.21	2.6	3.13
Z7910	350BAY	100779	46 16.67	123 41.18	0.5	2.21
Z7910	351BAY	100779	46 16.92	123 41.25	26.3	1.35
Z7910	353BAY	100779	46 16.92	123 41.19	12.6	3.20
Z7910	355BAY	100779	46 16.96	123 41.24	-1.7	2.48
Z7910	378BAY	100779	46 14.20	123 41.71	8.9	2.53
Z7910	379BAY	100779	46 14.17	123 41.62	2.9	2.91
Z7910	380BAY	100779	46 14.05	123 41.45	8.3	3.04
Z7910	381	100779	46 14.03	123 41.38	20.3	3.19
Z7910	382BAY	100779	46 14.01	123 41.34	6.8	2.97
Z7910	383BAY	100779	46 13.87	123 41.38	0.8	2.56
Z7910	384BAY	100779	46 13.72	123 41.37	0.7	2.76
Z7910	385BAY	100779	46 13.67	123 41.36	10.7	2.51
Z7910	386BAY	100779	46 13.67	123 41.32	14.7	2.01
Z7910	387BAY	100779	46 13.60	123 41.28	20.7	2.00
Z7910	388BAY	100779	46 13.61	123 41.30	16.7	1.84
Z7910	389BAY	100779	46 13.38	123 41.60	0.8	2.06
Z7910	390BAY	100779	46 13.24	123 41.66	4.7	2.56
Z7910	391BAY	100779	46 13.08	123 41.65	10.7	2.17
Z7910	392BAY	100779	46 12.89	123 41.59	11.7	1.91
Z7910	393BAY	100779	46 12.89	123 41.55	25.7	2.44
Z7910	394BAY	100779	46 12.87	123 41.45	8.1	2.31
Z7910	395BAY	100779	46 12.73	123 41.56	0.8	2.25
Z7910	396BAY	100779	46 12.47	123 41.52	6.8	3.01
Z7910	397BAY	100779	46 12.40	123 41.49	2.8	2.80
Z7910	398BAY	100779	46 12.34	123 41.50	7.8	2.81
Z7910	399	100779	46 12.29	123 41.58	44.9	2.19
Z7910	400	100779	46 12.21	123 41.62	53.2	1.49
Z7910	401BAY	100779	46 12.16	123 41.63	15.9	1.87
Z7910	402BAY	100779	46 12.14	123 41.62	11.0	1.38
Z7910	403BAY	100779	46 12.04	123 41.54	3.0	2.81
Z7910	404BAY	100779	46 11.96	123 41.65	-1.0	2.89
Z7910	405BAY	100779	46 11.92	123 41.71	6.1	2.85
Z7910	406BAY	100779	46 11.88	123 41.72	-3.9	4.00
Z7910	410BAY	100879	46 14.58	123 41.15	11.1	2.12
Z7910	412BAY	100879	46 14.47	123 40.42	1.9	2.90
Z7910	413BAY	100879	46 14.42	123 40.34	5.4	2.22
Z7910	414BAY	100879	46 14.40	123 40.40	11.9	2.24
Z7910	415BAY	100879	46 14.43	123 40.39	20.4	2.68

Z7910	416BAY		100879	46	14.36	123	40.41	34.4	1.68
Z7910	417BAY		100879	46	14.32	123	40.37	17.4	2.18
Z7910	418BAY		100879	46	14.31	123	40.38	9.9	2.08
Z7910	419BAY		100879	46	14.28	123	40.41	5.4	2.78
Z7910	420BAY		100879	46	14.12	123	40.21	1.9	2.75
Z7910	421BAY		100879	46	13.91	123	39.97	5.9	2.66
Z7910	422BAY	R	100879	46	13.89	123	39.96	12.3	2.67
Z7910	422BAY	NR	100879	46	13.89	123	39.96	12.3	2.67
Z7910	423BAY		100879	46	13.85	123	39.98	19.3	2.08
Z7910	424BAY		100879	46	13.83	123	39.99	24.3	1.96
Z7910	425BAY		100879	46	13.74	123	40.01	17.3	1.72
Z7910	426BAY		100879	46	13.74	123	39.96	12.2	1.71
Z7910	427BAY		100879	46	13.45	123	40.01	13.1	1.73
Z7910	428BAY		100879	46	13.36	123	40.01	5.1	1.92
Z7910	429BAY		100879	46	13.30	123	39.99	5.1	1.96
Z7910	430BAY		100879	46	13.26	123	40.01	2.0	2.45
Z7910	432BAY		100879	46	12.94	123	40.29	1.5	2.96
Z7910	433BAY		100879	46	12.74	123	40.57	0.3	2.94
Z7910	434BAY		100879	46	12.76	123	40.70	8.7	3.20
Z7910	438BAY		100879	46	13.28	123	44.48	0.0	2.24
Z7910	440BAY		100879	46	14.18	123	44.43	6.8	2.43
Z7910	441BAY		100879	46	14.14	123	44.42	12.8	2.52
Z7910	442BAY		100879	46	13.42	123	44.06	12.6	2.77
Z7910	443BAY		100879	46	13.31	123	43.98	6.8	2.88
Z7910	444BAY		100879	46	13.27	123	43.94	1.2	2.66
Z7910	445BAY	2	100879	46	13.15	123	43.86	-2.5	1.57
Z7910	445BAY	1	100879	46	13.15	123	43.86	-2.5	1.59
Z7910	445BAY	3	100879	46	13.15	123	43.86	-2.5	1.57
Z7910	446BAY		100879	46	13.13	123	43.73	6.4	3.02
Z7910	447BAY	1	100879	46	12.90	123	43.68	2.1	2.97
Z7910	447BAY	2	100879	46	12.90	123	43.68	2.1	2.97
Z7910	447BAY	3	100879	46	12.90	123	43.68	2.1	2.97
Z7910	448BAY		100879	46	12.87	123	44.69	10.1	3.13
Z7910	449BAY		100879	46	12.85	123	43.70	21.0	2.68
Z7910	450BAY		100879	46	12.82	123	43.72	11.9	2.56
Z7910	451BAY		100879	46	12.80	123	43.72	5.8	2.24
Z7910	452BAY		100879	46	12.70	123	43.71	12.2	1.72
Z7910	453BAY		100879	46	12.54	123	43.70	28.5	2.15
Z7910	454BAY		100879	46	12.46	123	43.75	20.4	1.97
Z7910	455BAY		100879	46	12.29	123	43.91	14.2	2.20
Z7910	456BAY		100879	46	12.20	123	43.88	26.1	2.21
Z7910	457BAY		100879	46	12.20	123	43.88	43.0	1.56
Z7910	458BAY		100879	46	12.15	123	43.91	22.9	2.02
Z7910	459BAY		100879	46	12.13	123	43.98	11.9	2.05
Z7910	460BAY		100879	46	12.11	123	44.00	6.5	2.37
Z7910	461BAY		100879	46	12.11	123	44.06	-1.6	2.36
Z7910	462BAY		100879	46	12.05	123	44.13	-5.1	2.22
Z7910	472BAY		100879	46	11.34	123	41.86	-4.1	2.89
Z7910	473BAY		100879	46	11.46	123	41.81	1.2	2.47
Z7910	474BAY		100879	46	11.64	123	41.85	-5.1	2.96
Z7910	508BAY		100979	46	11.84	123	44.56	4.1	2.56
Z7910	510BAY		100979	46	11.81	123	44.74	15.0	2.67
Z7910	512BAY		100979	46	11.71	123	44.87	26.8	3.48
Z7910	514BAY		100979	46	11.69	123	44.93	9.8	2.87

Z7910	517BAY	100979	46	12.00	123	44.98	4.5	3.51
Z7910	519BAY	100979	46	11.96	123	45.04	16.3	3.47
Z7910	521BAY	100979	46	11.99	123	45.14	16.2	3.45
Z7910	523BAY	100979	46	11.97	123	45.23	16.1	3.70
Z7910	528BAY	100979	46	11.69	123	43.81	7.2	2.21
Z7910	529BAY	100979	46	11.66	123	43.77	12.6	2.36
Z7910	530BAY	100979	46	11.58	123	43.93	29.0	5.74
Z7910	531BAY	100979	46	11.62	123	43.87	21.4	3.10
Z7910	532BAY	100979	46	11.61	123	43.91	28.3	4.38
Z7910	533BAY	100979	46	11.50	123	44.16	20.2	5.83
Z7910	534BAY	100979	46	11.38	123	44.46	22.0	3.33
Z7910	535 INTOP	100979	46	11.40	123	44.37	24.4	5.57
Z7910	535OUTBOT	100979	46	11.40	123	44.37	24.4	3.51
Z7910	536BAY	100979	46	11.30	123	44.55	22.8	5.14
Z7910	537BAY	100979	46	11.29	123	44.68	12.2	4.59
Z7910	538BAY	100979	46	11.29	123	44.64	-0.4	2.68
Z7910	542BAY	100979	46	10.89	123	44.24	12.2	1.98
Z7910	544BAY	100979	46	10.87	123	44.26	14.9	2.83
Z7910	546BAY	100979	46	10.91	123	44.13	-0.2	2.91
Z7910	548BAY	100979	46	10.98	123	44.50	4.6	2.77
Z7910	553BAY	100979	46	11.24	123	43.66	4.1	3.33
Z7910	555BAY	100979	46	11.17	123	43.65	-1.1	3.14
Z7910	556BAY	100979	46	11.19	123	43.69	5.4	3.06
Z7910	559BAY	100979	46	11.26	123	43.78	24.7	6.83
Z7910	573BAY	100979	46	10.28	123	41.88	-1.4	3.03
Z7910	574BAY	100979	46	10.32	123	41.90	5.6	5.68
Z7910	575BAY	100979	46	10.34	123	41.89	8.6	5.49
Z7910	576BAY	100979	46	10.37	123	41.89	11.1	2.15
Z7910	577BAY	100979	46	10.40	123	41.89	8.6	1.95
Z7910	583BAY	100979	46	10.38	123	41.29	7.7	3.31
Z7910	590BAY	100979	46	11.07	123	40.22	25.3	1.93
Z7910	599	101079	46	12.40	123	56.98	10.1	4.00
Z7910	622	101079	46	12.66	123	58.03	1.4	2.30
Z7910	623	101079	46	12.76	123	57.96	7.3	3.47
Z7910	624	101079	46	12.82	123	57.80	13.3	2.51
Z7910	647BAY	101079	46	10.90	123	53.42	10.0	2.34
Z7910	648BAY	101079	46	10.84	123	53.39	4.0	2.27
Z7910	649BAY	101079	46	10.69	123	53.38	3.0	2.77
Z7910	650BAY	101079	46	10.27	123	53.50	1.0	4.52
Z7910	651BAY	101079	46	10.00	123	53.62	-2.9	4.67
Z7910	695	102079	46	10.89	123	38.62	7.0	4.65
Z7910	780	102179	46	12.65	123	35.96	3.3	3.03
Z7910	784	102179	46	12.55	123	35.16	2.6	2.84
Z7910	785	102179	46	13.36	123	33.07	-1.2	1.63
Z7910	786	102179	46	13.38	123	33.10	8.9	1.57
Z7910	787	102179	46	13.40	123	33.12	12.9	3.16
Z7910	788	102179	46	13.45	123	33.19	22.0	2.63
Z7910	789	102179	46	13.47	123	33.24	12.0	0.68
Z7910	790	102179	46	13.49	123	33.27	4.1	2.95
Z7910	812	102279	46	14.18	123	32.22	-0.5	3.30
Z7910	813	102279	46	14.22	123	32.22	6.4	3.34
Z7910	814	102279	46	14.24	123	32.19	11.4	2.86
Z7910	815	102279	46	14.25	123	32.26	15.3	0.77
Z7910	816	102279	46	14.28	123	32.47	7.1	4.33

Z7910	817		102279	46	14.29	123	32.58	12.0	2.94
Z7910	818		102279	46	14.51	123	32.79	25.8	2.12
Z7910	819		102279	46	14.65	123	33.01	13.5	1.95
Z7910	820		102279	46	14.68	123	33.23	22.4	1.97
Z7910	822		102279	46	14.77	123	31.89	2.0	1.23
Z7910	843		102279	46	14.14	123	28.67	-4.2	2.84
Z7910	844		102279	46	14.41	123	27.69	-0.2	2.89
Z7910	845		102279	46	14.29	123	28.25	13.1	2.57
Z7910	856		102379	46	13.57	123	28.46	5.3	3.20
Z7910	857		102379	46	13.52	123	28.48	11.3	2.72
Z7910	859		102379	46	13.46	123	28.60	25.4	0.94
Z7910	860		102379	46	13.42	123	28.63	16.4	1.00
Z7910	861		102379	46	13.40	123	28.67	12.5	0.19
Z7910	862		102379	46	13.39	123	28.68	0.5	3.28
Z7910	865		102379	46	14.59	123	27.11	1.9	2.56
Z7910	866		102379	46	14.81	123	26.84	1.9	2.79
Z7910	867		102379	46	14.80	123	26.62	6.0	2.25
Z7910	868		102379	46	14.80	123	26.53	14.0	1.92
Z7910	869	INTOP	102379	46	15.05	123	26.14	14.0	7.47
Z7910	869	OUTBOT	102379	46	15.05	123	26.14	14.0	1.09
Z7910	870		102379	46	15.05	123	26.14	1.0	4.79
Z7910	871		102379	46	15.05	123	26.14	-2.0	7.66
Z7910	872	INTOP	102379	46	15.05	123	26.14	26.0	5.86
Z7910	872	OUTBOT	102379	46	15.05	123	26.14	26.0	1.42
Z7910	897		102379	46	12.78	123	25.17	0.0	2.56
Z7910	898		102379	46	12.76	123	25.25	5.9	2.39
Z7910	899		102379	46	12.75	123	25.29	14.8	2.85
Z7910	900		102379	46	12.75	123	25.29	24.7	2.77
Z7910	901		102379	46	12.77	123	25.68	1.6	2.11
Z7910	902		102379	46	12.77	123	25.67	7.1	2.51
Z7910	903		102379	46	12.80	123	25.73	-1.5	2.16
Z7910	916		102379	46	12.06	123	26.31	-1.2	1.87
Z7910	919		102379	46	12.09	123	26.17	16.6	0.20

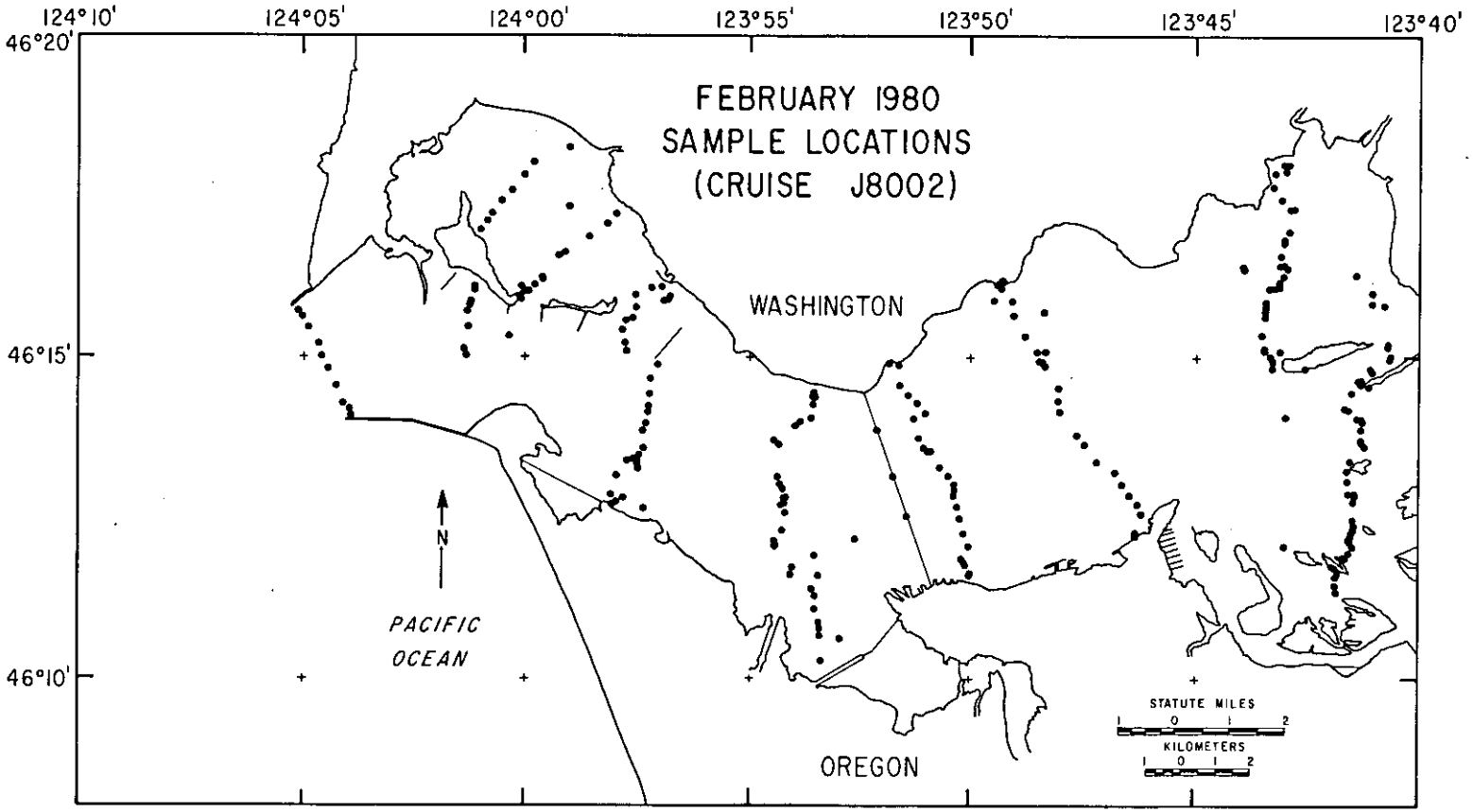

Figure 63. CREDDP bottom sample locations, February 1980.

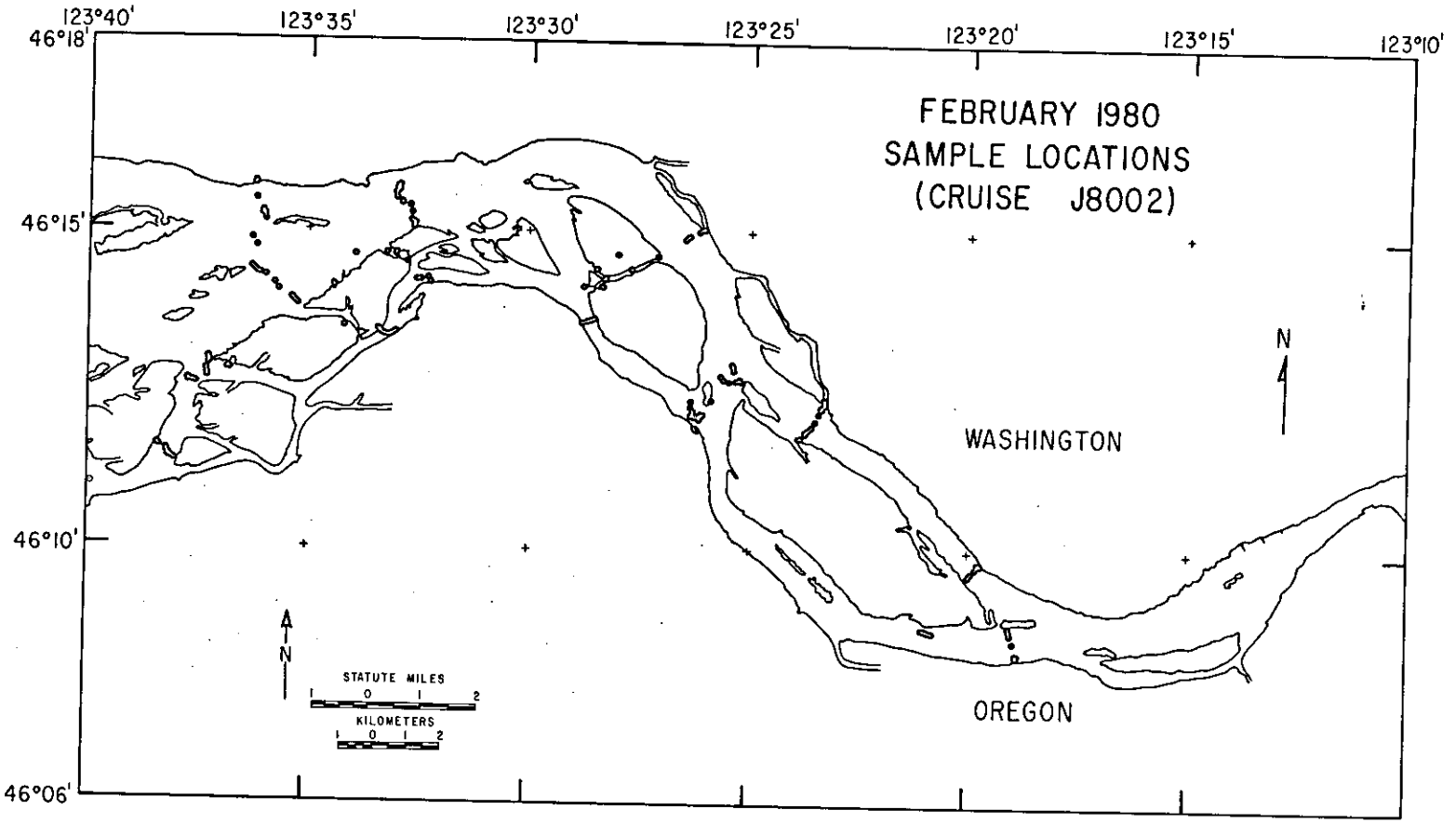

Figure 64. CREDDP bottom sample locations, February 1980.

TABLE 11.
FEBRUARY 1980 BOTTOM SAMPLE LOCATIONS
CRUISE J8002
(FIGURES 63, 64)

CRUISE	STN	DATE	LATITUDE	LONGITUDE	DEPTH	PHI
J8002	1	021280	46 14.40	123 53.55	26.0	2.00
J8002	2OUTBOT	021280	46 14.26	123 53.56	52.3	2.35
J8002	2IN TOP	021280	46 14.26	123 53.56	52.3	3.65
J8002	3	021280	46 13.99	123 53.85	43.2	1.36
J8002	4	021280	46 14.05	123 53.61	59.7	1.22
J8002	5	021280	46 13.93	123 53.96	35.4	1.54
J8002	6	021280	46 13.93	123 53.96	35.4	4.69
J8002	7	021280	46 13.70	123 54.45	12.8	1.49
J8002	8	021280	46 13.64	123 54.34	13.0	1.82
J8002	9	021280	46 13.14	123 54.37	4.4	1.85
J8002	10	021280	46 13.05	123 54.40	6.7	1.99
J8002	11	021280	46 13.02	123 54.34	8.8	2.10
J8002	12	021280	46 12.94	123 54.25	13.6	2.23
J8002	13	021280	46 12.82	123 54.21	17.8	2.26
J8002	14	021280	46 12.80	123 54.23	13.2	2.67
J8002	15	021280	46 12.72	123 54.22	6.4	2.58
J8002	16	021280	46 12.70	123 54.32	11.4	2.92
J8002	17	021280	46 12.57	123 54.21	-0.7	2.41
J8002	18	021280	46 16.03	124 1.12	23.4	2.16
J8002	19	021280	46 16.06	124 1.12	12.5	2.23
J8002	20	021280	46 16.09	124 1.12	8.5	2.23
J8002	21	021280	46 15.86	124 1.22	42.6	2.37
J8002	22	021280	46 15.81	124 1.25	50.7	2.26
J8002	23	021280	46 15.70	124 1.30	62.7	1.89
J8002	24	021280	46 15.47	124 1.29	79.8	1.42
J8002	25	021280	46 15.12	124 1.37	58.8	2.14
J8002	26	021280	46 15.02	124 1.32	36.8	2.37
J8002	27 TOP	021280	46 14.88	123 57.07	63.7	5.27
J8002	28OUTBOT	021280	46 14.88	123 57.07	63.7	1.80
J8002	29	021280	46 14.66	123 57.22	38.7	1.48
J8002	30	021280	46 14.42	123 57.24	30.7	2.00
J8002	31OUTBOT	021280	46 14.24	123 57.26	49.6	2.03
J8002	31IN TOP	021280	46 14.24	123 57.26	49.6	4.68
J8002	32	021280	46 14.13	123 57.28	28.6	1.36
J8002	33	021280	46 13.97	123 57.32	19.5	1.17
J8002	34	021280	46 13.85	123 57.39	17.5	1.65
J8002	35	021280	46 13.58	123 57.38	20.4	2.69
J8002	36	021280	46 13.47	123 57.49	31.4	2.10
J8002	37OUTBOT	021280	46 13.42	123 57.52	31.4	1.57
J8002	37IN MBL	021280	46 13.42	123 57.52	31.4	5.18
J8002	38	021280	46 13.34	123 57.53	34.3	2.14
J8002	39	021280	46 13.26	123 57.51	41.3	2.02
J8002	40	021280	46 12.64	123 57.39	20.1	2.40
J8002	41	021380	46 12.23	123 46.35	5.8	1.77
J8002	42	021380	46 12.26	123 46.33	-0.3	2.85
J8002	43	021380	46 12.56	123 46.21	27.5	1.93
J8002	44 BOT	021380	46 12.70	123 46.29	37.4	0.78

J8002	44SM MBL	021380	46	12.70	123	46.29	37.4	6.43
J8002	45	021380	46	12.85	123	46.46	53.3	0.86
J8002	46	021380	46	13.02	123	46.65	39.2	1.60
J8002	47	021380	46	13.22	123	46.80	27.1	2.02
J8002	48	021380	46	13.37	123	47.22	17.9	1.90
J8002	49	021380	46	13.64	123	47.48	9.8	2.03
J8002	50	021380	46	13.78	123	47.65	6.7	1.95
J8002	51	021380	46	14.15	123	48.04	12.6	2.66
J8002	52	021380	46	14.31	123	48.07	4.6	1.80
J8002	53	021380	46	14.51	123	48.07	12.5	4.26
J8002	54	021380	46	14.85	123	48.36	28.4	2.47
J8002	55	021380	46	14.93	123	48.47	48.4	1.54
J8002	56	021380	46	14.93	123	48.42	38.4	2.02
J8002	57	021380	46	15.08	123	48.35	28.4	1.84
J8002	58	021380	46	15.08	123	48.54	24.3	2.05
J8002	59	021380	46	15.15	123	48.38	22.3	2.09
J8002	60	021380	46	15.31	123	48.79	8.3	2.08
J8002	61	021380	46	15.69	123	48.38	13.3	1.34
J8002	62	021380	46	15.64	123	49.05	16.3	1.49
J8002	63	021380	46	15.86	123	49.09	17.5	0.94
J8002	64	021380	46	15.87	123	49.48	8.7	1.43
J8002	65OUTBOT	021380	46	16.07	123	49.33	27.8	1.58
J8002	65IN TOP	021380	46	16.07	123	49.33	27.8	5.12
J8002	66OUT	021380	46	16.10	123	49.37	32.9	1.42
J8002	67	021380	46	16.12	123	49.42	28.1	2.08
J8002	68	021380	46	16.09	123	49.35	31.0	2.79
J8002	69	021380	46	16.16	123	49.29	27.2	2.95
J8002	70	021380	46	12.05	123	50.05	14.6	1.96
J8002	71	021380	46	12.25	123	50.16	4.8	1.87
J8002	72	021380	46	12.48	123	50.24	2.1	1.88
J8002	73	021380	46	12.67	123	50.32	11.2	1.99
J8002	74	021380	46	12.82	123	50.39	11.3	2.12
J8002	75	021380	46	12.86	123	50.43	12.5	1.66
J8002	76	021380	46	12.92	123	50.38	4.7	1.67
J8002	77	021380	46	12.91	123	50.36	5.8	1.56
J8002	78	021380	46	13.01	123	50.39	3.9	1.89
J8002	79	021380	46	13.14	123	50.52	14.8	1.37
J8002	80	021380	46	13.28	123	50.70	9.9	1.74
J8002	81	021380	46	13.53	123	50.90	11.3	2.82
J8002	82	021380	46	13.52	123	50.99	3.4	2.36
J8002	83	021380	46	13.52	123	50.99	1.7	2.38
J8002	84	021380	46	13.57	123	51.08	21.0	2.66
J8002	85	021380	46	13.73	123	51.19	12.2	1.48
J8002	86	021380	46	14.03	123	51.30	4.4	2.14
J8002	87	021380	46	14.11	123	51.07	13.8	2.40
J8002	88	021380	46	14.28	123	51.23	21.0	1.51
J8002	89	021380	46	14.40	123	51.44	34.3	2.06
J8002	90OUTBOT	021380	46	14.55	123	51.62	45.4	2.20
J8002	90IN TOP	021380	46	14.55	123	51.62	45.5	2.82
J8002	91	021380	46	14.86	123	51.63	20.6	5.52
J8002	92	021380	46	14.89	123	51.85	3.9	2.91
J8002	93	021380	46	13.85	123	52.15	22.5	2.13
J8002	94	021380	46	13.14	123	51.76	26.8	2.12
J8002	95	021380	46	12.52	123	51.45	16.0	1.36

J8002	97	021380	46	11.60	123	50.04	68.2	5.16
J8002	98	021380	46	11.63	123	50.01	62.2	3.83
J8002	99	021380	46	11.77	123	50.13	46.3	1.56
J8002	100	021380	46	11.86	123	50.20	29.3	1.77
J8002	101	021380	46	11.80	123	50.15	41.3	1.70
J8002	102	021580	46	15.06	123	26.08	29.0	1.35
J8002	103	021580	46	15.02	123	26.20	47.8	2.01
J8002	104	021580	46	14.95	123	26.40	27.7	1.79
J8002	105	021580	46	14.92	123	26.47	26.7	1.87
J8002	106	021580	46	14.90	123	26.51	26.6	1.79
J8002	107	021580	46	12.83	123	25.38	49.1	1.21
J8002	108	021580	46	12.92	123	25.40	46.1	1.45
J8002	109	021380	46	12.94	123	25.42	52.1	1.72
J8002	114	021580	46	12.34	123	26.37	5.1	1.08
J8002	115	021580	46	12.25	123	26.36	14.2	1.04
J8002	116	021580	46	12.20	123	26.30	15.3	0.64
J8002	117	021580	46	12.13	123	26.35	9.3	1.61
J8002	118	021580	46	9.83	123	19.71	41.7	0.85
J8002	119	021580	46	9.65	123	19.98	32.8	-0.58
J8002	120	021580	46	9.68	123	19.95	28.8	0.71
J8002	121	021580	46	9.70	123	19.90	14.9	1.04
J8002	122	021580	46	9.75	123	19.82	8.0	0.62
J8002	123	021580	46	9.83	123	19.75	12.0	0.74
J8002	124	021680	46	15.93	124	0.12	9.1	2.23
J8002	125	021680	46	15.90	124	0.08	6.7	2.25
J8002	126	021680	46	16.09	124	0.07	32.5	2.38
J8002	127	021680	46	16.02	124	0.01	36.4	2.48
J8002	128	021680	46	16.02	123	59.92	15.9	2.56
J8002	129	021680	46	16.12	123	59.78	8.7	2.06
J8002	130	021680	46	16.22	123	59.62	7.6	2.45
J8002	131	021680	46	16.20	123	59.60	7.5	2.41
J8002	132	021680	46	16.57	123	59.25	3.4	2.47
J8002	133OUTBOT	021680	46	16.62	123	59.11	3.3	2.92
J8002	133 INMBL	021680	46	16.62	123	59.11	3.3	6.40
J8002	134	021680	46	16.87	123	58.57	3.2	3.28
J8002	135	021680	46	17.06	123	58.18	2.1	2.24
J8002	136	021680	46	17.21	123	57.98	2.0	2.32
J8002	137	021680	46	17.34	123	59.02	5.0	3.06
J8002	138	021680	46	18.26	123	59.01	1.0	4.85
J8002	139	021680	46	18.02	123	59.78	3.0	4.60
J8002	140	021680	46	17.82	124	0.00	3.1	4.11
J8002	141	021680	46	17.58	124	0.27	5.1	6.16
J8002	142	021680	46	17.42	124	0.52	7.1	5.13
J8002	143	021680	46	16.97	124	1.00	-2.6	2.06
J8002	144	021680	46	17.11	124	0.85	7.5	3.50
J8002	145	021680	46	17.22	124	0.74	11.7	2.78
J8002	146	021680	46	15.10	123	57.77	26.7	1.44
J8002	147	021680	46	15.22	123	57.79	20.9	1.80
J8002	148	021680	46	15.42	123	57.84	9.1	2.24
J8002	149	021680	46	15.57	123	57.78	5.6	5.09
J8002	150	021680	46	15.60	123	57.63	4.8	3.00
J8002	151	021680	46	15.77	123	57.54	-0.1	2.27
J8002	152	021680	46	15.86	123	56.94	0.5	3.26
J8002	153	021680	46	15.88	123	56.84	2.7	3.17

J8002 154	021680	46 15.93	123 56.80	2.9	2.48
J8002 155	021680	46 16.09	123 56.98	1.2	2.42
J8002 156	021680	46 16.07	123 57.19	4.0	4.56
J8002 157	021680	46 15.96	123 57.57	6.5	3.03
J8002 158	021880	46 14.24	123 32.57	13.4	1.22
J8002 159	021880	46 14.25	123 32.48	9.4	2.99
J8002 160	021880	46 14.26	123 32.30	12.3	1.68
J8002 161	021880	46 14.23	123 32.28	19.2	1.02
J8002 162	021880	46 14.21	123 32.26	15.2	0.14
J8002 163	021880	46 14.17	123 32.25	9.1	2.93
J8002 164	021880	46 13.40	123 33.03	8.7	4.30
J8002 165	021880	46 13.39	123 33.09	3.6	3.49
J8002 166	021880	46 13.37	123 33.13	9.5	3.84
J8002 167	021880	46 13.36	123 33.22	28.4	1.56
J8002 168	021880	46 13.37	123 33.30	12.2	1.21
J8002 169	021880	46 13.40	123 33.35	8.0	1.90
J8002 170	021880	46 13.45	123 33.44	-3.6	6.01
J8002 171	021880	46 13.50	123 34.21	5.9	4.87
J8002 172	021880	46 13.63	123 28.51	-0.6	4.82
J8002 173	021880	46 13.61	123 28.60	20.3	1.14
J8002 174	021880	46 13.61	123 28.62	5.2	1.14
J8002 175	021880	46 13.61	123 28.69	27.2	0.33
J8002 176	021880	46 13.59	123 28.70	27.1	0.74
J8002 177	021880	46 13.58	123 28.75	28.9	0.96
J8002 178	021880	46 13.57	123 28.80	-1.2	1.05
J8002 179	021880	46 14.14	123 28.77	-4.5	3.93
J8002 180	021880	46 14.12	123 28.40	20.5	4.64
J8002 181	021880	46 14.15	123 28.36	-0.6	3.19
J8002 182	021880	46 14.29	123 28.27	22.4	3.01
J8002 183	021880	46 14.42	123 27.73	1.6	2.75
J8002 184	021880	46 14.61	123 27.14	3.7	2.28
J8002 185	021880	46 14.40	123 28.47	8.6	2.61
J8002 186	21980	46 14.82	123 42.54	4.9	1.76
J8002 187	21980	46 14.82	123 43.30	6.9	1.31
J8002 188	21980	46 12.17	123 52.61	3.8	2.42
J8002 189	21980	46 12.30	123 54.28	-0.3	2.58
J8002 190	21980	46 12.13	123 54.45	2.7	2.45
J8002 191	21980	46 12.08	123 54.43	3.8	2.50
J8002 192	21980	46 12.06	123 54.45	6.8	2.39
J8002 193	21980	46 11.91	123 53.55	21.0	2.43
J8002 194	21980	46 11.72	123 54.04	28.1	2.15
J8002 195	21980	46 11.62	123 54.07	33.2	2.01
J8002 196	21980	46 11.60	123 53.46	33.4	2.27
J8002 197	21980	46 11.40	123 53.60	41.5	1.74
J8002 198	21980	46 11.27	123 53.53	43.6	1.84
J8002 199	21980	46 11.08	123 53.53	34.7	2.29
J8002 200	21980	46 10.87	123 53.44	12.9	2.26
J8002 201	21980	46 10.78	123 53.42	6.1	2.25
J8002 202	21980	46 10.67	123 53.42	5.3	2.63
J8002 203	21980	46 10.28	123 53.38	1.6	4.40
J8002 205	21980	46 10.62	123 52.95	0.2	3.14
J8002 206	22080	46 14.94	123 43.30	5.6	1.88
J8002 207	22080	46 15.08	123 43.13	1.6	2.92
J8002 208	22080	46 15.00	123 43.34	3.5	1.65

J8002 209	22080	46 15.09	123 43.48	5.5	2.25
J8002 210	22080	46 15.12	123 43.47	12.4	4.45
J8002 211	22080	46 15.33	123 43.55	2.4	2.62
J8002 212	22080	46 15.61	123 43.48	12.3	1.57
J8002 213	22080	46 15.72	123 43.47	7.3	1.69
J8002 214	22080	46 15.78	123 43.46	6.2	1.72
J8002 215	22080	46 15.83	123 43.45	4.1	1.59
J8002 216	22080	46 16.05	123 43.37	10.5	1.92
J8002 217	22080	46 16.07	123 43.27	13.4	2.76
J8002 218	22080	46 16.09	123 43.15	6.3	1.77
J8002 219	22080	46 16.15	123 43.15	4.2	1.82
J8002 220	22080	46 16.25	123 43.06	12.2	2.90
J8002 221	22080	46 16.36	123 43.93	4.1	1.93
J8002 222	22080	46 16.38	123 42.96	4.1	2.22
J8002 223	22080	46 16.42	123 43.04	5.0	3.04
J8002 224	22080	46 16.42	123 43.13	5.9	2.37
J8002 225	22080	46 16.40	123 43.97	9.6	2.89
J8002 226	22080	46 16.56	123 43.13	11.4	1.57
J8002 227	22080	46 16.77	123 43.03	17.3	1.98
J8002 228	22080	46 16.82	123 43.03	20.2	1.14
J8002 229	22080	46 16.95	123 42.93	4.0	1.67
J8002 230	22080	46 17.30	123 42.85	14.9	3.75
J8002 231	22080	46 17.30	123 42.90	15.8	3.98
J8002 232	22080	46 17.44	123 43.11	1.7	1.83
J8002 233	22080	46 17.64	123 43.28	18.5	1.60
J8002 234	22080	46 17.85	123 43.24	1.3	4.08
J8002 235	22080	46 17.99	123 43.05	-1.1	2.33
J8002 236	22080	46 17.89	123 43.00	4.7	2.30
J8002 237	22080	46 18.00	123 42.94	0.5	1.88
J8002 238	22080	46 16.27	123 41.44	4.5	2.23
J8002 239	22080	46 16.00	123 41.07	15.2	1.17
J8002 240	22080	46 15.83	123 41.07	9.1	1.67
J8002 241	22080	46 15.81	123 40.80	15.0	2.26
J8002 242	22080	46 11.35	123 41.84	-2.3	2.82
J8002 243	22080	46 11.46	123 41.88	-0.6	2.83
J8002 244	22080	46 11.63	123 41.83	1.2	2.47
J8002 245	22080	46 11.58	123 41.87	4.2	2.10
J8002 246	22080	46 11.73	123 41.88	5.1	2.18
J8002 247	22080	46 11.74	123 41.94	4.0	2.65
J8002 248	22080	46 11.88	123 41.65	5.9	1.63
J8002 249	22080	46 11.90	123 41.72	17.9	1.72
J8002 250	22080	46 11.96	123 41.59	17.8	1.46
J8002 251	22080	46 12.05	123 41.50	22.8	1.45
J8002 252	22080	46 12.13	123 41.58	69.7	2.98
J8002 253A	TOP022080	46 12.17	123 41.58	50.7	5.15
J8002 253B	BOT022080	46 12.17	123 41.58	50.8	2.46
J8002 254	22080	46 12.21	123 41.57	2.6	2.53
J8002 255	22080	46 12.27	123 41.53	-0.6	2.82
J8002 256	22080	46 12.33	123 41.47	-1.3	2.97
J8002 257	22080	46 12.39	123 41.47	-1.3	2.80
J8002 258	22080	46 12.47	123 41.50	2.7	3.04
J8002 259	22080	46 12.75	123 41.50	-0.3	2.38
J8002 260	22080	46 12.85	123 41.43	5.7	3.49
J8002 261	22080	46 12.87	123 41.48	6.6	3.19

J8002	262		22080	46	12.87	123	41.58	7.7	2.44
J8002	263		22080	46	13.06	123	41.62	0.8	2.12
J8002	264		22080	46	13.23	123	41.63	0.0	2.71
J8002	265		22180	46	14.45	123	41.53	39.8	2.44
J8002	266		22180	46	14.55	123	41.14	-0.4	1.90
J8002	268		22180	46	14.58	123	41.32	7.5	1.96
J8002	269		22180	46	14.63	123	41.37	30.3	1.21
J8002	270A	MBL	022180	46	14.64	123	41.29	31.2	5.02
J8002	270B	BOT	022180	46	14.64	123	41.29	31.2	3.04
J8002	271		22180	46	14.77	123	41.07	39.9	1.93
J8002	272		22180	46	14.82	123	41.10	40.7	1.84
J8002	273		22180	46	14.96	123	40.68	52.5	1.57
J8002	274		22180	46	15.01	123	40.65	51.2	0.42
J8002	275		22180	46	15.16	123	40.73	16.1	1.55
J8002	276		22180	46	15.20	123	40.73	9.1	0.53
J8002	277		22180	46	14.20	123	41.67	0.4	2.85
J8002	278		22180	46	14.18	123	41.58	1.2	2.85
J8002	279		22180	46	14.05	123	41.41	1.0	2.12
J8002	280		22180	46	14.03	123	41.31	-0.1	2.43
J8002	281		22180	46	14.00	123	41.28	0.8	1.99
J8002	282		22180	46	13.87	123	41.33	2.2	1.99
J8002	283		22180	46	13.71	123	41.33	22.1	1.83
J8002	284		22180	46	13.67	123	41.30	23.3	2.22
J8002	285		22180	46	13.61	123	41.27	16.9	2.62
J8002	286		22180	46	13.60	123	41.23	16.9	2.46
J8002	287		22180	46	13.38	123	41.56	13.5	2.82
J8002	288		22180	46	14.07	123	43.00	45.4	2.25
J8002	290		22180	46	12.05	123	43.03	-1.7	2.98
J8002	291	OUTBOT	022280	46	14.51	123	32.78	39.3	1.76
J8002	291	INTOP	022280	46	14.51	123	32.78	39.3	5.94
J8002	292		022280	46	14.62	123	33.05	14.8	2.00
J8002	293		022280	46	14.65	123	33.25	12.9	1.70
J8002	294		022280	46	14.62	123	33.97	25.6	1.57
J8002	295		022280	46	14.14	123	34.43	3.0	3.11
J8002	296		022280	46	13.83	123	35.25	3.3	2.49
J8002	297		022280	46	13.85	123	35.31	3.4	2.67
J8002	298		022280	46	13.93	123	35.38	22.5	1.90
J8002	299		022280	46	14.15	123	35.77	14.8	1.79
J8002	300		022280	46	14.05	123	35.69	24.7	1.36
J8002	301		022280	46	14.27	123	35.98	5.9	2.42
J8002	302		022280	46	14.30	123	36.09	6.2	2.32
J8002	303		022280	46	14.33	123	36.17	5.3	2.45
J8002	304		022280	46	14.37	123	36.23	5.4	2.68
J8002	305		022280	46	14.39	123	36.30	7.5	2.33
J8002	306		022280	46	14.72	123	36.19	15.6	3.07
J8002	307		022280	46	14.85	123	36.30	15.8	1.87
J8002	308		022280	46	15.14	123	36.01	-1.5	1.67
J8002	309		022280	46	15.15	123	35.97	-0.9	1.73
J8002	310		022280	46	15.16	123	36.04	8.4	3.24
J8002	311		022280	46	15.20	123	36.03	20.4	3.69
J8002	312		022280	46	15.19	123	36.07	24.5	3.74
J8002	313		022280	46	15.19	123	36.07	22.6	3.29
J8002	314		022280	46	15.26	123	36.05	33.8	2.27
J8002	315		022280	46	15.47	123	36.21	56.9	1.12

J8002	316	022280	46	15.47	123	36.20	51.0	0.85
J8002	317	022280	46	15.66	123	36.27	39.1	1.62
J8002	318	022280	46	15.68	123	36.22	41.4	1.30
J8002	319	022280	46	15.70	123	36.24	24.3	2.11
J8002	320	022280	46	15.75	123	36.23	12.3	2.20
J8002	321	022280	46	15.70	123	32.97	22.2	1.00
J8002	322	022280	46	15.67	123	33.00	15.3	1.25
J8002	323	022280	46	15.63	123	32.98	12.3	1.28
J8002	324	022280	46	15.58	123	33.06	13.4	1.46
J8002	325	022280	46	15.55	123	33.14	33.4	1.34
J8002	326	022280	46	15.52	123	33.03	49.5	1.27
J8002	327	022280	46	15.43	123	32.91	48.8	0.80
J8002	328	022280	46	15.41	123	32.73	48.9	2.15
J8002	329	022280	46	15.27	123	32.67	13.9	2.66
J8002	330	022280	46	15.16	123	32.67	30.9	2.73
J8002	331	022280	46	15.13	123	32.62	50.0	2.08
J8002	332	022280	46	15.13	123	32.69	52.0	2.61
J8002	333	022280	46	15.10	123	32.65	45.0	2.38
J8002	334	022280	46	15.05	123	32.63	4.0	1.64
J8002	335	022280	46	15.03	123	32.61	-11.0	1.13
J8002	336	022280	46	14.65	123	28.02	1.5	0.86
J8002	337	022380	46	8.80	123	19.03	26.0	1.04
J8002	338	022380	46	8.85	123	19.01	9.1	1.51
J8002	339	022380	46	8.85	123	19.01	14.2	1.64
J8002	340	022380	46	8.86	123	19.01	3.2	1.28
J8002	341	022380	46	8.73	123	18.97	26.4	1.34
J8002	342	022380	46	8.61	123	18.92	38.5	0.13
J8002	343	022380	46	8.43	123	18.85	24.6	1.63
J8002	344	022380	46	8.40	123	18.85	0.8	1.50
J8002	345	022380	46	8.40	123	18.85	2.8	1.30
J8002	346	022380	46	8.40	123	18.85	9.9	1.43
J8002	347	022380	46	8.40	123	18.82	11.0	1.25
J8002	348	022380	46	8.40	123	18.82	20.0	1.36
J8002	349	022380	46	12.37	123	25.86	6.7	0.12
J8002	350	022380	46	12.30	123	25.92	7.8	1.21
J8002	351	022380	46	12.25	123	25.97	3.8	2.02
J8002	352	022380	46	12.20	123	26.00	11.8	2.46
J8002	353	022380	46	12.15	123	26.13	19.9	0.18
J8002	354	022380	46	12.13	123	26.07	24.0	0.44
J8002	355	022380	46	12.10	123	26.12	22.1	0.52
J8002	356	022380	46	12.07	123	26.16	18.1	0.72
J8002	357	022380	46	12.09	123	26.26	12.2	1.73
J8002	358	022380	46	12.76	123	25.76	0.5	2.13
J8002	359	022380	46	12.75	123	25.66	33.6	1.02
J8002	360	022380	46	12.70	123	25.62	39.6	1.50
J8002	361	022380	46	12.67	123	25.48	44.7	1.95
J8002	362	022380	46	12.68	123	25.33	53.7	1.83
J8002	363	022380	46	12.68	123	25.25	15.7	2.56
J8002	364	022380	46	12.70	123	25.20	2.7	4.86
J8002	365	022380	46	12.73	123	25.25	12.7	2.66
J8002	366	022380	46	12.40	123	23.32	14.5	1.46
J8002	367	022380	46	12.23	123	23.40	38.5	1.41
J8002	368	022380	46	12.28	123	23.39	26.4	1.11
J8002	369OUTBOT	022380	46	12.30	123	23.34	14.4	1.71

J8002	369IN TOP	022380	46	12.30	123	23.34	14.4	3.13
J8002	370	022380	46	12.17	123	23.44	47.3	1.19
J8002	371	022380	46	12.05	123	23.50	17.2	1.53
J8002	372	022380	46	12.06	123	23.52	17.2	1.49
J8002	373	022380	46	11.97	123	23.61	7.1	0.98
J8002	374	022380	46	11.92	123	23.71	10.0	1.45
J8002	375	022380	46	11.89	123	23.74	9.9	1.92
J8002	376	022380	46	11.86	123	23.76	5.9	1.92
J8002	377	022380	46	11.78	123	23.85	3.8	2.09
J8002	378	022380	46	11.78	123	23.90	5.7	2.17
J8002	379	022880	46	11.21	123	40.12	3.7	3.93
J8002	380	022880	46	10.97	123	39.91	2.5	3.77
J8002	381	022880	46	11.35	123	38.02	38.8	1.52
J8002	382	022880	46	11.38	123	38.06	28.7	2.15
J8002	383	022880	46	11.42	123	38.13	9.6	2.25
J8002	384	022880	46	11.39	123	38.17	12.6	2.23
J8002	385	022880	46	11.47	123	38.18	7.5	2.15
J8002	386	022880	46	11.50	123	38.18	8.4	2.34
J8002	387	022880	46	11.56	123	38.35	6.2	2.65
J8002	388	022880	46	11.59	123	38.40	-2.8	6.45
J8002	389	022880	46	12.61	123	37.73	27.6	1.95
J8002	390	022880	46	12.58	123	37.70	23.5	1.40
J8002	391	022880	46	12.58	123	37.59	5.5	2.73
J8002	392	022880	46	12.56	123	37.54	6.4	3.33
J8002	393	022880	46	12.58	123	37.57	5.4	3.22
J8002	394	022880	46	12.67	123	37.30	5.3	2.34
J8002	395	022880	46	12.71	123	37.30	6.3	2.65
J8002	396	022880	46	12.67	123	37.31	5.2	2.33
J8002	397	022880	46	12.78	123	37.33	10.2	2.67
J8002	398	022880	46	12.87	123	37.28	27.2	3.08
J8002	399	022880	46	12.92	123	37.26	9.1	2.63
J8002	400	022880	46	12.96	123	37.28	19.0	2.68
J8002	401	022880	46	12.80	123	36.79	27.5	1.26
J8002	402	022880	46	12.80	123	36.81	19.6	1.04
J8002	403	022880	46	12.80	123	36.86	21.8	1.75
J8002	404	022880	46	12.80	123	36.85	25.9	2.06
J8002	405	022980	46	12.75	123	57.99	5.9	3.95
J8002	406	022980	46	12.81	123	57.84	10.9	2.44
J8002	407OUTBOT	022980	46	12.86	123	58.09	12.0	2.52
J8002	407IN TOP	022980	46	12.86	123	58.09	12.0	5.82
J8002	408	022980	46	13.16	123	57.99	28.1	1.59
J8002	409	022980	46	13.39	123	57.75	46.2	1.97
J8002	410	022980	46	13.41	123	57.62	34.2	3.28
J8002	411	022980	46	12.70	123	58.10	0.9	2.14
J8002	412	022980	46	14.40	123	53.60	20.9	1.74
J8002	413	022980	46	14.45	123	53.55	16.2	2.17
J8002	414	022980	46	15.71	124	5.08	67.9	2.02
J8002	415	022980	46	15.63	124	5.01	48.9	2.13
J8002	416	022980	46	15.46	124	4.87	56.7	1.85
J8002	417	022980	46	15.20	124	4.64	53.7	2.08
J8002	418	022980	46	15.01	124	4.57	44.6	2.36
J8002	419	022980	46	14.82	124	4.43	35.6	2.40
J8002	420	022980	46	14.54	124	4.25	27.5	2.48
J8002	421	022980	46	14.27	124	4.10	27.4	2.68

J8002	422	022980	46	14.07	124	3.93	23.4	2.70
J8002	423	022980	46	14.09	124	3.94	39.3	1.89
J8002	424	022980	46	14.19	124	3.95	27.3	2.69
J8002	425	022980	46	15.32	124	0.36	76.9	2.09
J8002	426	022980	46	8.78	123	20.91	34.4	-0.04
J8002	427	022980	46	8.76	123	20.88	29.4	1.11
J8002	428	022980	46	8.75	123	20.83	29.5	1.36
J8002	429	022980	46	8.75	123	20.78	27.5	1.65
J8002	430	022980	46	8.80	123	21.01	32.6	-1.12

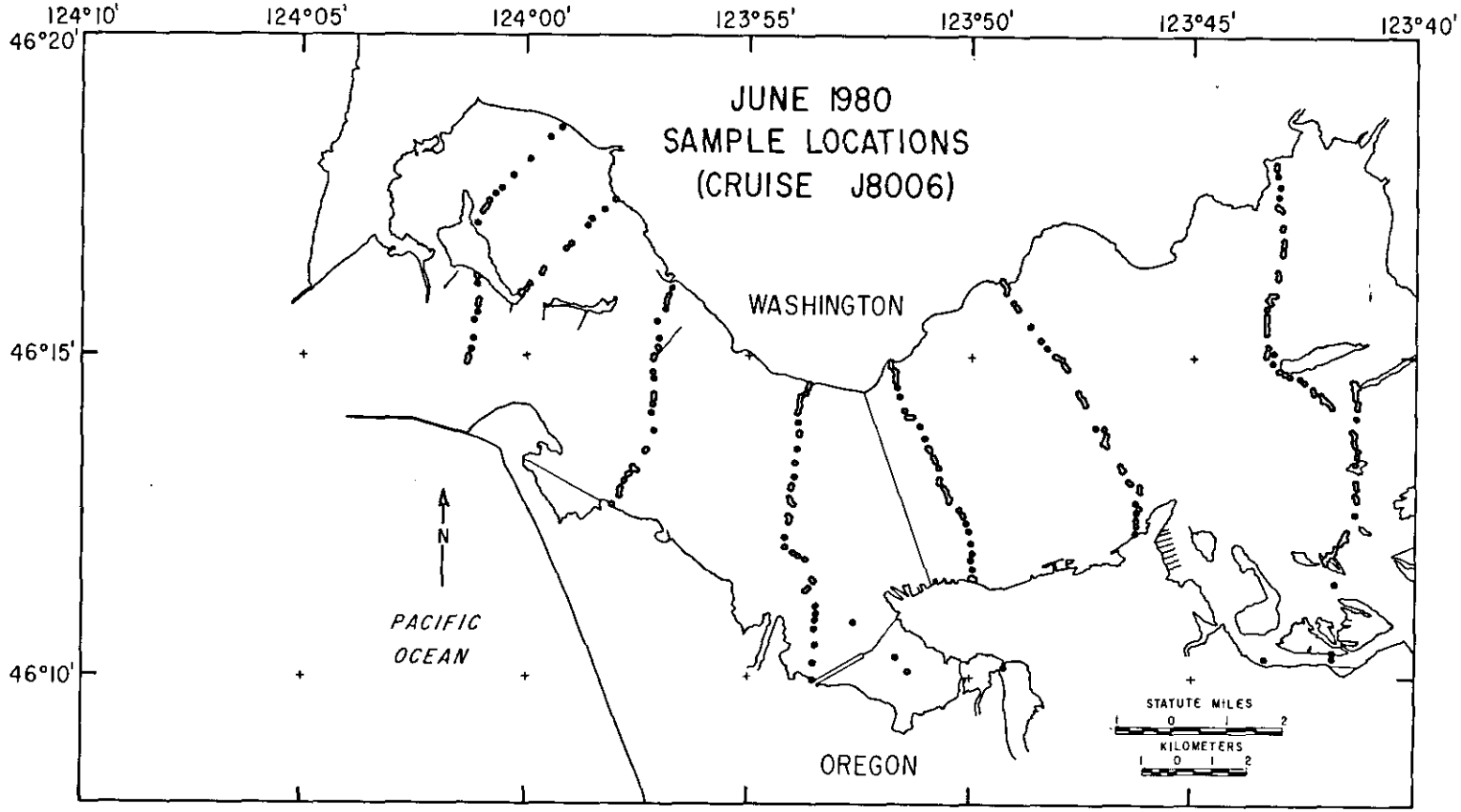

Figure 65. CREDDP bottom sample location, June 1980.

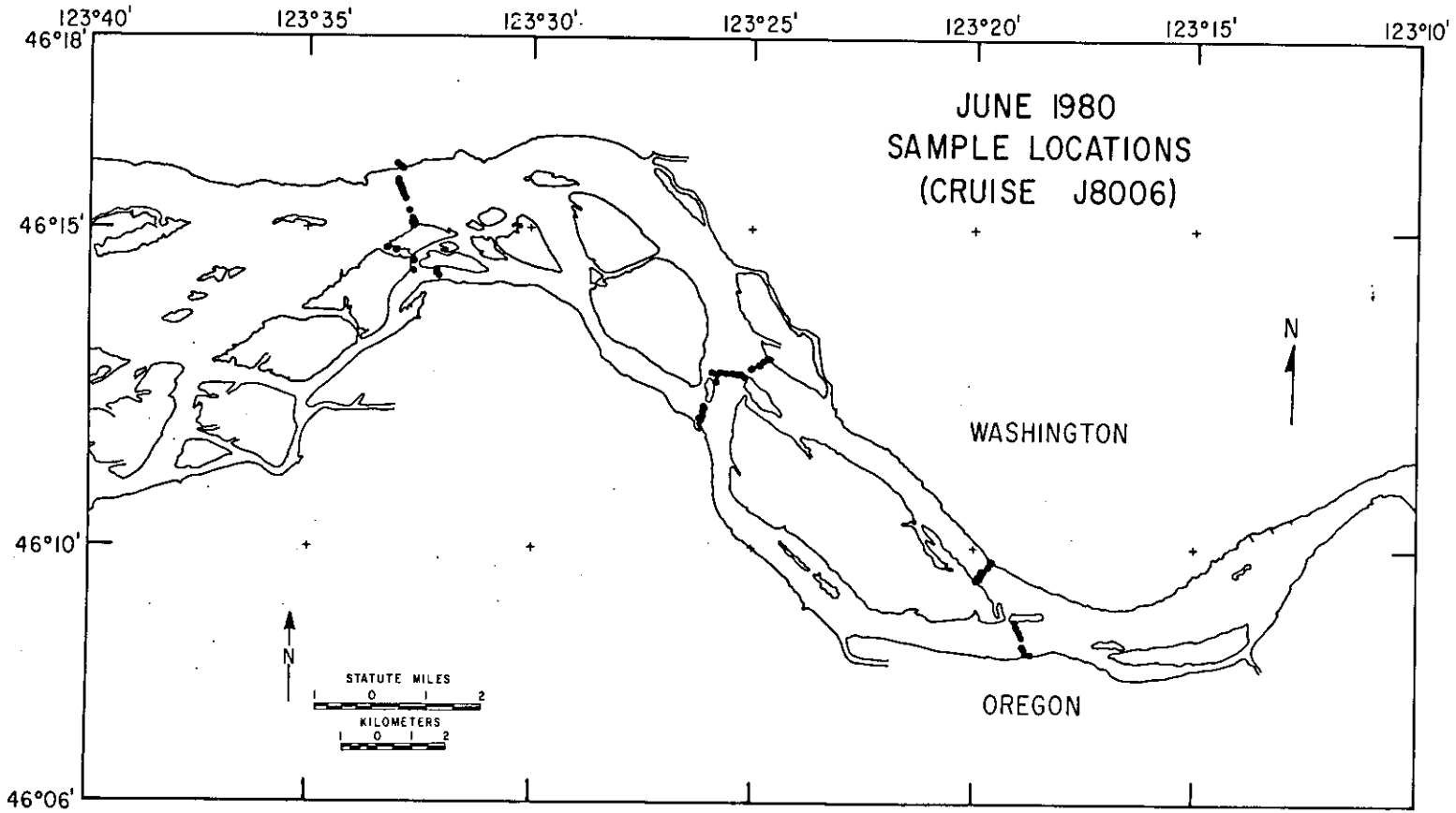

Figure 66. CREDDP bottom sample location, June 1980.

TABLE 12.
JUNE 1980 BOTTOM SAMPLE LOCATIONS
CRUISE J8006
(FIGURES 65, 66)

CRUISE	STN	DATE	LATITUDE	LONGITUDE	DEPTH	PHI
J8006	10UTBOT	061080	46 18.02	123 43.20	0.2	2.32
J8006	1 INTOP	061080	46 18.02	123 43.20	0.2	4.78
J8006	20UTBOT	061080	46 17.95	123 43.20	8.3	2.87
J8006	2 INTOPLD	1080	46 17.95	123 43.20	8.3	3.91
J8006	3BAY	061080	46 17.84	123 43.16	-0.6	3.85
J8006	4BAY	061080	46 17.67	123 43.10	-0.5	2.62
J8006	5BAY	061080	46 17.50	123 43.12	-0.4	2.35
J8006	60UTBOT	061080	46 17.38	123 43.17	4.8	4.29
J8006	6 INTOP	061080	46 17.38	123 43.17	4.8	6.33
J8006	70UTBOT	061080	46 17.35	123 43.19	12.0	2.92
J8006	7 INTOP	061080	46 17.35	123 43.19	12.0	6.15
J8006	8BAY	061080	46 17.36	123 43.15	19.1	3.65
J8006	9BAY	061080	46 17.33	123 43.08	12.2	4.36
J8006	10BAY	061080	46 17.31	123 43.05	5.4	2.25
J8006	11BAY	061080	46 17.05	123 43.03	10.5	2.63
J8006	12BAY	061080	46 17.00	123 43.06	15.6	2.26
J8006	13BAY	061080	46 16.84	123 43.02	14.8	1.77
J8006	14BAY	061080	46 16.76	123 43.02	12.5	2.32
J8006	15BAY	061080	46 16.66	123 43.03	5.5	1.80
J8006	16BAY	061080	46 16.61	123 43.04	0.1	1.68
J8006	17BAY	061080	46 16.35	123 43.13	6.2	2.95
J8006	18BAY	061080	46 16.27	123 43.14	12.3	3.96
J8006	19BAY	061080	46 16.24	123 43.14	6.4	3.35
J8006	20BAY	061080	46 15.99	123 43.21	1.1	1.50
J8006	21BAY	061080	46 15.98	123 43.25	9.7	1.81
J8006	22BAY	061080	46 15.98	123 43.25	14.7	2.43
J8006	23BAY	061080	46 15.98	123 43.30	10.3	3.45
J8006	24BAY	061080	46 15.86	123 43.29	1.9	2.82
J8006	25BAY	061080	46 15.91	123 43.37	5.4	3.20
J8006	26BAY	061080	46 15.77	123 43.38	2.0	2.09
J8006	27BAY	061080	46 15.67	123 43.39	6.0	1.64
J8006	28BAY	061080	46 15.63	123 43.39	6.0	2.11
J8006	290UTBOT	061080	46 15.57	123 43.39	13.6	3.18
J8006	29 INTOP	061080	46 15.57	123 43.39	13.6	6.61
J8006	30BAY	061080	46 15.50	123 43.40	8.1	2.37
J8006	31BAY	061080	46 15.46	123 43.37	2.1	2.62
J8006	32BAY	061080	46 15.37	123 43.39	1.2	2.77
J8006	33BAY	061080	46 15.17	123 43.34	0.7	2.85
J8006	34BAY	061080	46 15.10	123 43.38	8.2	5.17
J8006	35BAY	061080	46 15.07	123 43.24	12.2	7.08
J8006	36BAY	061080	46 15.02	123 43.40	5.7	2.31
J8006	37BAY	061080	46 15.06	123 43.38	3.2	1.79
J8006	38	061380	46 14.65	123 41.38	23.8	2.38
J8006	39	061380	46 14.63	123 41.40	17.7	2.77
J8006	40	061380	46 14.62	123 41.38	11.4	1.97
J8006	41	061380	46 14.60	123 41.37	13.2	2.19
J8006	42	061380	46 14.58	123 41.31	3.1	2.31

J8006	43	061380	46	14.57	123	41.35	10.8	2.16
J8006	44	061380	46	14.57	123	41.40	18.5	1.98
J8006	45	061380	46	14.55	123	41.40	24.2	1.49
J8006	46	061380	46	14.47	123	41.36	33.0	0.58
J8006	47	061380	46	14.39	123	41.34	23.9	1.75
J8006	48	061380	46	14.31	123	41.30	17.8	2.00
J8006	49	061380	46	14.27	123	41.30	5.6	2.42
J8006	50BAY	061380	46	14.24	123	41.31	0.4	2.36
J8006	51BAY	061380	46	14.07	123	41.35	0.3	2.28
J8006	52BAY	061380	46	13.87	123	41.40	0.4	2.31
J8006	53BAY	061380	46	13.82	123	41.38	5.9	1.85
J8006	54BAY	061380	46	13.80	123	41.37	10.7	2.03
J8006	55BAY	061380	46	13.78	123	41.36	14.6	2.08
J8006	56BAY	061380	46	13.72	123	41.38	22.5	1.81
J8006	57BAY	061380	46	13.72	123	41.38	25.2	2.08
J8006	58BAY	061380	46	13.66	123	41.37	15.9	2.47
J8006	59BAY	061380	46	13.57	123	41.31	7.7	2.15
J8006	60BAY	061380	46	13.48	123	41.33	3.5	2.04
J8006	61BAY	061380	46	13.36	123	41.35	2.4	2.61
J8006	62BAY	061380	46	13.08	123	41.34	1.1	2.70
J8006	63BAY	061380	46	12.98	123	41.32	3.7	2.90
J8006	64BAY	061380	46	12.87	123	41.36	11.5	3.35
J8006	65BAY	061380	46	12.86	123	41.34	13.3	3.57
J8006	66BAY	061380	46	12.85	123	41.36	11.1	3.04
J8006	67BAY	061380	46	12.84	123	41.32	6.9	3.16
J8006	68BAY	061380	46	12.79	123	41.32	-1.2	2.49
J8006	69BAY	061380	46	12.57	123	41.37	2.6	3.52
J8006	70BAY	061380	46	12.30	123	41.55	-0.6	2.83
J8006	71BAY	061380	46	12.27	123	41.55	7.3	3.37
J8006	72BAY	061380	46	12.27	123	41.57	12.1	2.64
J8006	73BAY	061380	46	12.26	123	41.56	16.1	3.39
J8006	74BAY	061380	46	12.24	123	41.56	23.0	2.25
J8006	75BAY	061380	46	12.24	123	41.57	29.9	5.53
J8006	76BAY	061380	46	12.24	123	41.57	44.8	2.99
J8006	77BAY	061380	46	12.18	123	41.55	61.7	2.49
J8006	78BAY	061380	46	12.18	123	41.65	34.6	1.82
J8006	79BAY	061380	46	12.17	123	41.63	29.6	1.72
J8006	80BAY	061380	46	12.16	123	41.64	22.6	2.31
J8006	81BAY	061380	46	12.15	123	41.65	15.6	1.55
J8006	82BAY	061380	46	12.12	123	41.67	10.6	1.59
J8006	83BAY	061380	46	12.06	123	41.78	1.6	1.89
J8006	84BAY	061380	46	11.99	123	41.80	-2.4	2.65
J8006	85BAY	061380	46	11.95	123	41.94	1.7	2.89
J8006	86BAY	061380	46	11.89	123	41.97	-2.3	4.80
J8006	87BAY	061380	46	11.84	123	42.04	-2.3	5.33
J8006	88BAY	061380	46	11.81	123	42.03	5.8	2.52
J8006	89BAY	061380	46	11.48	123	41.81	-1.2	2.88
J8006	90BAY	061380	46	10.41	123	41.88	7.1	3.59
J8006	91BAY	061380	46	10.33	123	41.87	10.0	2.06
J8006	92BAY	061380	46	10.31	123	43.42	5.2	2.93
J8006	93	061480	46	14.91	123	51.83	0.5	3.87
J8006	94	061480	46	14.86	123	51.80	3.5	4.79
J8006	95OUTBOT	061480	46	14.81	123	51.74	13.5	4.87
J8006	95 INTOP	061480	46	14.81	123	51.74	13.5	5.00

J8006	96OUTBOT	061480	46	14.80	123	51.75	18.6	5.15
J8006	96 INTOP	061480	46	14.80	123	51.75	18.6	6.10
J8006	97OUTBOT	061480	46	14.79	123	51.73	24.6	5.83
J8006	97 INTOP	061480	46	14.79	123	51.73	24.6	5.75
J8006	98OUTBOT	061480	46	14.78	123	51.73	30.6	5.32
J8006	98 INTOP	061480	46	14.78	123	51.73	30.6	4.74
J8006	99	061480	46	14.69	123	51.71	43.7	8.17
J8006	100	061480	46	14.62	123	51.69	39.8	1.15
J8006	101	061480	46	14.52	123	51.65	42.8	1.65
J8006	102	061480	46	14.38	123	51.60	35.9	2.14
J8006	103	061480	46	14.17	123	51.47	24.9	2.20
J8006	104	061480	46	14.06	123	51.38	20.0	2.58
J8006	105	061480	46	14.07	123	51.34	15.1	4.64
J8006	106	061480	46	14.07	123	51.32	4.2	2.25
J8006	107	061480	46	14.07	123	51.29	2.2	1.92
J8006	108	061480	46	13.93	123	51.17	6.4	2.06
J8006	109	061480	46	13.74	123	51.05	14.5	1.49
J8006	110	061480	46	13.60	123	50.99	17.4	2.96
J8006	111	061480	46	13.58	123	50.95	15.6	5.76
J8006	112	061480	46	13.56	123	50.94	5.6	3.83
J8006	113	061480	46	13.52	123	50.90	-1.3	2.33
J8006	114	061480	46	13.43	123	50.85	-1.2	2.18
J8006	115	061480	46	13.37	123	50.79	1.9	2.16
J8006	116	061480	46	13.28	123	50.73	6.0	1.69
J8006	117	061480	46	13.10	123	50.70	11.1	1.34
J8006	118	061480	46	13.04	123	50.71	9.3	1.35
J8006	119	061480	46	12.96	123	50.63	10.6	3.52
J8006	120	061480	46	12.92	123	50.56	10.7	3.00
J8006	121	061480	46	12.85	123	50.53	8.8	2.00
J8006	122	061480	46	12.79	123	50.48	15.9	2.05
J8006	123	061480	46	12.75	123	50.52	21.1	5.42
J8006	124	061480	46	12.62	123	50.28	8.2	1.99
J8006	125	061480	46	12.55	123	50.21	3.4	1.81
J8006	126	061480	46	12.51	123	50.19	1.5	1.94
J8006	127	061480	46	12.41	123	50.12	0.6	2.00
J8006	128	061480	46	12.30	123	50.04	1.8	1.93
J8006	129	061480	46	12.09	123	50.00	11.0	1.80
J8006	130	061480	46	11.93	123	49.96	23.1	1.73
J8006	131BAY	061680	46	16.00	124	0.16	1.2	2.13
J8006	132BAY	061680	46	15.97	124	0.12	6.6	2.14
J8006	133BAY	061680	46	15.98	124	0.14	11.5	2.13
J8006	134BAY	061680	46	16.00	124	0.12	18.4	5.39
J8006	135OUTBOT	061680	46	16.00	124	0.11	25.8	5.40
J8006	135 INTOP	061680	46	16.00	124	0.11	25.8	6.12
J8006	136BAY	061680	46	16.04	124	0.03	33.2	5.19
J8006	137BAY	061680	46	16.12	123	59.95	9.9	2.52
J8006	139BAY	061680	46	16.35	123	59.62	3.1	2.66
J8006	140BAY	061680	46	16.28	123	59.65	4.0	4.17
J8006	141OUTBOT	061680	46	16.67	123	59.11	1.9	3.27
J8006	141 INTOP	061680	46	16.67	123	59.11	1.9	4.76
J8006	142BAY	061680	46	16.76	123	58.97	-1.6	2.39
J8006	143OUTBOT	061680	46	17.05	123	58.63	2.2	5.83
J8006	143 INTOP	061680	46	17.05	123	58.63	2.2	6.39
J8006	144BAY	061680	46	17.15	123	58.52	-0.3	2.43

J8006	145BAY	061680	46	17.29	123	58.24	0.3	4.01
J8006	146BAY	061680	46	17.44	123	58.01	-1.8	2.25
J8006	147BAY	061680	46	18.57	123	59.20	-3.9	2.54
J8006	148OUTBOT	061680	46	18.41	123	59.44	0.6	5.25
J8006	148 INTOP	061680	46	18.41	123	59.44	0.6	5.81
J8006	149BAY	061680	46	18.06	123	59.94	0.6	4.65
J8006	150BAY	061680	46	17.81	124	0.32	2.1	5.44
J8006	151BAY	061680	46	17.62	124	0.57	-0.4	2.26
J8006	152OUTBOT	061680	46	17.52	124	0.71	1.6	3.35
J8006	152 INTOP	061680	46	17.52	124	0.71	1.6	4.39
J8006	153OUTBOT	061680	46	17.41	124	0.85	3.7	4.07
J8006	153 INTOP	061680	46	17.41	124	0.85	3.7	4.59
J8006	154BAY	061680	46	17.34	124	0.89	8.2	4.98
J8006	155OUTBOT	061680	46	17.31	124	0.92	11.2	6.09
J8006	155 INTOP	061680	46	17.31	124	0.92	11.2	6.45
J8006	156OUTBOT	061680	46	17.29	124	0.97	8.7	3.24
J8006	156 INTOP	061680	46	17.29	124	0.97	8.7	4.64
J8006	157BAY	061680	46	17.24	124	1.00	1.3	2.12
J8006	158BAY	061680	46	17.06	124	1.11	-2.1	2.13
J8006	159	061680	46	15.12	123	57.05	21.8	5.88
J8006	160	061680	46	15.14	123	57.06	13.4	3.54
J8006	161	061680	46	15.28	123	57.01	7.0	2.10
J8006	162BAY	061680	46	15.55	123	57.08	3.1	2.53
J8006	163BAY	061680	46	15.74	123	56.90	-4.0	2.37
J8006	164BAY	061680	46	15.82	123	56.86	-3.8	2.40
J8006	165BAY	061680	46	15.87	123	56.87	-4.2	2.38
J8006	166BAY	061680	46	15.91	123	56.87	1.8	2.58
J8006	167BAY	061680	46	15.96	123	56.82	1.9	2.76
J8006	168BAY	061680	46	16.06	123	56.75	-0.6	4.53
J8006	169	061780	46	14.58	123	53.65	3.3	5.94
J8006	170	061780	46	14.52	123	53.67	12.1	4.71
J8006	171	061780	46	14.43	123	53.75	17.5	2.06
J8006	172	061780	46	13.83	123	53.87	26.7	1.66
J8006	173	061780	46	13.77	123	53.87	19.0	1.32
J8006	174	061780	46	13.57	123	53.91	10.9	1.49
J8006	175	061780	46	13.34	123	53.96	12.2	1.81
J8006	176	061780	46	13.13	123	53.97	6.1	2.00
J8006	177	061780	46	12.98	123	54.02	3.4	2.43
J8006	178	061780	46	12.95	123	54.06	6.3	3.66
J8006	179	061780	46	12.80	123	54.08	14.6	1.69
J8006	180	061780	46	12.74	123	54.07	5.9	2.51
J8006	181	061780	46	12.70	123	54.00	1.8	2.37
J8006	182	061780	46	12.53	123	54.12	10.4	1.58
J8006	183	061780	46	12.48	123	54.07	5.3	2.53
J8006	184	061780	46	12.43	123	54.09	-0.4	2.39
J8006	185	061780	46	12.18	123	54.19	-0.7	2.56
J8006	186	061780	46	12.03	123	54.19	-1.3	2.37
J8006	187	061780	46	11.95	123	54.00	5.8	3.63
J8006	188	061780	46	11.90	123	53.90	11.7	1.72
J8006	189	061780	46	11.85	123	53.72	20.1	2.43
J8006	190BAY	061780	46	11.11	123	53.51	25.3	5.46
J8006	191BAY	061780	46	10.99	123	53.49	15.2	2.20
J8006	192BAY	061780	46	10.90	123	53.51	8.1	2.55
J8006	193BAY	061780	46	10.76	123	53.52	1.4	2.44

J8006	194BAY	061780	46	10.51	123	53.52	2.3	4.95
J8006	195OUTBOT	061780	46	10.23	123	53.56	0.7	4.81
J8006	195 INTOP	061780	46	10.23	123	53.56	0.7	6.18
J8006	196OUTBOT	061780	46	9.97	123	53.57	-1.9	4.61
J8006	196 INTOP	061780	46	9.97	123	53.57	-1.9	5.08
J8006	198 1	061880	46	16.20	123	49.29	1.8	5.59
J8006	198 2	061880	46	16.20	123	49.29	1.8	5.59
J8006	199	061880	46	16.19	123	49.30	12.6	5.95
J8006	200	061880	46	16.18	123	49.28	17.6	6.40
J8006	202	061880	46	16.10	123	49.22	29.2	3.26
J8006	203	061880	46	16.10	123	49.19	28.1	5.14
J8006	204	061880	46	16.07	123	49.19	20.0	1.57
J8006	205	061880	46	16.06	123	49.20	13.9	1.36
J8006	206	061880	46	16.00	123	49.22	9.3	1.71
J8006	207	061880	46	15.85	123	49.03	13.6	0.98
J8006	208	061880	46	15.80	123	48.98	17.1	1.53
J8006	209	061880	46	15.76	123	48.92	15.5	1.51
J8006	210	061880	46	15.47	123	48.66	4.9	1.79
J8006	211	061880	46	15.26	123	48.41	8.7	1.58
J8006	212	061880	46	15.15	123	48.26	19.6	1.81
J8006	213	061880	46	15.02	123	48.09	27.5	0.85
J8006	214	061880	46	15.00	123	48.04	29.3	3.16
J8006	215	061880	46	14.95	123	47.95	24.9	6.10
J8006	216	061880	46	14.89	123	47.89	19.3	4.93
J8006	217	061880	46	14.87	123	47.90	13.2	4.66
J8006	218	061880	46	14.82	123	47.83	8.0	2.22
J8006	219	061880	46	14.45	123	47.58	12.3	1.55
J8006	220	061880	46	14.40	123	47.55	14.2	1.83
J8006	221	061880	46	14.36	123	47.48	8.0	2.09
J8006	222	061880	46	14.32	123	47.46	4.4	1.86
J8006	223	061880	46	14.26	123	47.41	-0.7	1.72
J8006	224	061880	46	13.90	123	47.21	-1.3	2.28
J8006	225	061880	46	13.89	123	47.02	-0.9	2.00
J8006	226	061880	46	13.78	123	46.95	6.4	2.16
J8006	227	061880	46	13.74	123	46.97	12.3	2.11
J8006	228	061880	46	13.68	123	47.03	20.8	2.34
J8006	229	061880	46	13.66	123	46.98	10.7	2.53
J8006	230	061880	46	13.65	123	46.97	6.7	2.49
J8006	231	061880	46	13.63	123	46.95	-0.4	2.33
J8006	232	061880	46	13.31	123	46.63	11.5	1.76
J8006	233	061880	46	13.23	123	46.59	23.5	1.48
J8006	234	061880	46	12.59	123	46.26	24.4	1.55
J8006	235	061880	46	12.48	123	46.27	17.8	2.23
J8006	236OUTBOT	061880	46	12.38	123	46.27	11.8	5.34
J8006	236 INTOP	061880	46	12.38	123	46.27	11.8	4.17
J8006	237	061880	46	12.27	123	46.28	1.8	1.83
J8006	238	061880	46	12.27	123	46.28	-0.2	1.97
J8006	239	070780	46	16.24	124	1.12	0.8	2.08
J8006	240	070780	46	16.22	124	1.11	5.9	2.16
J8006	241	070780	46	16.11	124	1.11	12.5	2.17
J8006	242	070780	46	15.87	124	1.08	28.5	2.02
J8006	243	070780	46	15.78	124	1.12	42.2	2.19
J8006	244	070780	46	15.68	124	1.10	56.8	2.17
J8006	245	070780	46	15.55	124	1.18	68.0	1.88

J8006	246	070780	46	15.27	124	1.19	84.1	1.66
J8006	247	070780	46	15.10	124	1.23	67.1	2.85
J8006	248	070780	46	15.00	124	1.29	45.2	2.16
J8006	249	070780	46	14.97	124	1.30	39.8	2.19
J8006	250	070780	46	14.94	124	1.31	27.3	2.21
J8006	251	070780	46	14.92	124	1.32	18.3	2.32
J8006	252	070780	46	14.89	124	1.34	8.8	2.32
J8006	253	070780	46	12.67	123	58.08	2.6	2.52
J8006	254	070780	46	12.83	123	57.90	7.1	4.25
J8006	255	070780	46	12.91	123	57.88	13.1	4.26
J8006	256	070780	46	12.95	123	57.85	19.1	2.15
J8006	257	070780	46	13.06	123	57.79	27.0	1.88
J8006	258	070780	46	13.16	123	57.73	37.5	1.57
J8006	259	070780	46	13.18	123	57.65	44.0	1.32
J8006	260	070780	46	13.28	123	57.59	48.9	2.07
J8006	261	070780	46	13.23	123	57.50	34.8	2.77
J8006	262	070780	46	13.52	123	57.35	24.2	1.76
J8006	263	070780	46	13.57	123	57.29	19.1	2.73
J8006	264	070780	46	13.85	123	57.15	14.5	1.93
J8006	265	070780	46	14.12	123	57.19	28.4	3.24
J8006	266	070780	46	14.25	123	57.18	52.3	5.50
J8006	267	070780	46	14.35	123	57.14	39.1	2.42
J8006	268	070780	46	14.41	123	57.16	32.0	1.93
J8006	269	070780	46	14.66	123	57.15	38.3	1.25
J8006	270OUTBOT	070780	46	14.76	123	57.18	51.7	3.27
J8006	270 INTOP	070780	46	14.76	123	57.18	51.7	6.47
J8006	271	070780	46	14.96	123	57.17	85.3	1.34
J8006	272	070780	46	15.02	123	57.14	41.1	3.68
J8006	273	070880	46	11.35	123	53.74	37.3	1.57
J8006	274	070880	46	11.39	123	53.65	41.5	4.46
J8006	275	070880	46	11.50	123	53.57	34.8	5.44
J8006	276	070880	46	11.55	123	53.60	28.5	1.92
J8006	277OUTBOT	070880	46	14.38	123	53.83	22.7	2.89
J8006	277 INTOP	070880	46	14.38	123	53.83	22.7	4.43
J8006	278	070880	46	14.31	123	53.87	34.2	2.29
J8006	279	070880	46	14.24	123	53.86	44.7	4.09
J8006	280MBLBOT	070880	46	14.15	123	53.89	56.7	2.93
J8006	280 INTOP	070880	46	14.15	123	53.89	56.7	1.21
J8006	281	070880	46	14.12	123	53.92	52.7	1.16
J8006	282OUTBOT	070880	46	13.98	123	53.87	48.1	1.10
J8006	282 INMBL	070880	46	13.98	123	53.87	48.1	3.92
J8006	284	070880	46	11.83	123	50.00	37.2	1.44
J8006	285	070880	46	11.55	123	49.94	28.6	3.58
J8006	286	070880	46	11.55	123	49.94	42.6	5.21
J8006	287	070880	46	11.55	123	49.96	61.6	6.36
J8006	288OUTTOP	070880	46	11.57	123	50.01	68.8	6.33
J8006	288 INBOT	070880	46	11.57	123	50.01	68.8	5.97
J8006	289	070880	46	11.70	123	49.96	60.4	1.49
J8006	290	070980	46	12.66	123	46.20	36.1	1.63
J8006	291	070980	46	12.73	123	46.30	42.0	0.78
J8006	292	070980	46	12.91	123	46.18	58.9	0.90
J8006	293	070980	46	13.00	123	46.19	60.8	1.68
J8006	294	070980	46	13.04	123	46.37	46.7	1.57
J8006	295	070980	46	13.07	123	46.45	40.6	1.93

J8006	296	070980	46	13.24	123 46.54	33.5	1.59
J8006	297BAY	070980	46	15.07	123 43.40	11.8	4.65
J8006	298BAY	070980	46	15.06	123 43.39	3.6	2.91
J8006	299BAY	070980	46	15.03	123 43.39	2.3	1.80
J8006	300BAY	070980	46	14.79	123 43.12	4.9	1.77
J8006	301	070980	46	14.76	123 43.00	12.7	1.49
J8006	302	070980	46	14.72	123 42.87	21.8	1.09
J8006	303	070980	46	14.69	123 42.63	36.7	1.28
J8006	304	070980	46	14.63	123 42.52	34.5	0.93
J8006	306	070980	46	14.52	123 42.34	45.3	2.13
J8006	307	070980	46	14.47	123 42.28	49.3	1.98
J8006	308	070980	46	14.43	123 42.14	41.2	1.56
J8006	309	070980	46	14.38	123 42.08	31.1	1.99
J8006	310	070980	46	14.35	123 42.10	24.0	1.85
J8006	311	070980	46	14.35	123 42.02	14.9	1.93
J8006	312	070980	46	14.32	123 41.98	8.9	2.69
J8006	313	070980	46	14.28	123 41.92	2.9	2.66
J8006	314	070980	46	14.26	123 41.87	0.2	2.80
J8006	315	070980	46	14.36	123 32.25	4.9	1.37
J8006	316	070980	46	14.30	123 32.14	6.8	0.07
J8006	317	070980	46	14.25	123 32.10	17.8	1.14
J8006	319	070980	46	14.34	123 32.15	1.7	1.96
J8006	320	070980	46	14.33	123 32.67	8.7	5.24
J8006	321	070980	46	14.47	123 32.67	21.7	3.53
J8006	322	070980	46	14.51	123 32.72	33.7	4.00
J8006	323	070980	46	14.64	123 33.06	13.9	1.91
J8006	324	070980	46	14.68	123 33.27	26.9	2.17
J8006	325	070980	46	16.00	123 33.06	-2.0	4.75
J8006	326OUTBOT	070980	46	15.94	123 33.10	0.0	3.94
J8006	326 IN IN	070980	46	15.94	123 33.10	0.0	5.32
J8006	327	070980	46	15.92	123 33.08	14.0	4.18
J8006	328	070980	46	15.71	123 33.04	35.0	1.18
J8006	329	070980	46	15.74	123 33.03	24.1	1.56
J8006	330	070980	46	15.70	123 33.02	25.1	1.45
J8006	331	070980	46	15.67	123 32.98	15.1	1.42
J8006	332	070980	46	15.64	123 33.01	11.2	1.55
J8006	333	070980	46	15.60	123 32.97	15.2	1.34
J8006	334	070980	46	15.58	123 32.95	31.2	1.78
J8006	335	070980	46	15.57	123 32.93	38.2	1.38
J8006	336	070980	46	15.51	123 32.91	39.3	0.62
J8006	337	070980	46	15.54	123 32.94	42.3	1.54
J8006	338	070980	46	15.45	123 32.87	49.4	1.52
J8006	339	070980	46	15.27	123 32.77	28.5	2.36
J8006	340OUTBOT	070980	46	15.14	123 32.72	21.5	4.92
J8006	340 INTOP	070980	46	15.14	123 32.72	21.5	5.40
J8006	341	070980	46	15.09	123 32.69	13.6	4.55
J8006	342	070980	46	15.09	123 32.69	16.7	4.38
J8006	343	070980	46	15.06	123 32.69	30.7	4.41
J8006	344	070980	46	15.05	123 32.68	42.8	2.36
J8006	345	070980	46	15.03	123 32.65	29.9	2.56
J8006	346	070980	46	15.03	123 32.65	15.9	2.41
J8006	347	070980	46	15.00	123 32.68	9.0	2.49
J8006	348	070980	46	15.00	123 32.68	1.0	1.91
J8006	349	070980	46	15.05	123 32.71	46.1	2.37

J8006	350OUTBOT	071080	46	8.43	123	18.81	-0.3	5.12
J8006	350 INTOP	071080	46	8.43	123	18.81	-0.3	1.33
J8006	351	071080	46	8.42	123	18.76	9.2	1.73
J8006	352	071080	46	8.42	123	18.74	19.2	5.01
J8006	353	071080	46	8.46	123	18.85	36.2	4.46
J8006	354	071080	46	8.49	123	18.87	52.2	2.04
J8006	355	071080	46	8.64	123	18.90	37.2	0.59
J8006	356	071080	46	8.72	123	18.95	28.2	1.18
J8006	357	071080	46	8.79	123	19.01	26.2	1.29
J8006	358	071080	46	8.86	123	19.04	13.1	1.73
J8006	359	071080	46	8.89	123	19.04	1.6	1.63
J8006	360	071080	46	9.53	123	19.88	36.8	1.16
J8006	361	071080	46	9.57	123	19.86	29.7	0.23
J8006	362	071080	46	9.57	123	19.82	20.7	0.98
J8006	363	071080	46	9.59	123	19.83	16.6	0.83
J8006	364	071080	46	9.67	123	19.77	8.5	0.68
J8006	365	071080	46	9.67	123	19.80	13.4	1.12
J8006	366	071080	46	9.74	123	19.65	17.2	0.30
J8006	367	071080	46	9.83	123	19.61	17.1	0.07
J8006	368	071080	46	9.83	123	19.63	22.1	-0.05
J8006	369	071080	46	12.82	123	25.04	-2.5	2.52
J8006	370	071080	46	12.82	123	25.04	5.9	2.57
J8006	371	071080	46	12.82	123	25.04	11.8	6.12
J8006	372	071080	46	12.82	123	25.04	19.8	2.53
J8006	373	071080	46	12.82	123	25.02	37.7	1.41
J8006	374	071080	46	12.84	123	24.99	26.6	1.45
J8006	375	071080	46	12.82	123	25.02	20.5	1.66
J8006	376	071080	46	12.90	123	24.87	12.2	0.86
J8006	377OUTBOT	071080	46	12.89	123	24.85	17.2	1.18
J8006	377 INTOP	071080	46	12.89	123	24.85	17.2	5.02
J8006	378	071080	46	12.93	123	24.76	18.9	1.15
J8006	379	071080	46	12.97	123	24.69	28.8	1.08
J8006	380	071080	46	12.99	123	24.63	2.7	2.96
J8006	381	071080	46	12.98	123	24.67	21.7	1.10
J8006	382	071080	46	12.69	123	25.18	1.1	5.05
J8006	383	071080	46	12.74	123	25.28	16.0	2.73
J8006	384	071080	46	12.73	123	25.32	55.0	1.52
J8006	385	071080	46	12.75	123	25.45	44.9	1.79
J8006	386	071080	46	12.75	123	25.60	38.8	0.91
J8006	387	071080	46	12.77	123	25.73	32.8	1.35
J8006	388	071080	46	12.75	123	25.80	12.8	4.76
J8006	389OUTBOT	071080	46	12.75	123	25.82	0.7	4.00
J8006	389 INTOP	071080	46	12.75	123	25.82	0.7	4.29
J8006	390	071080	46	12.77	123	25.90	-1.3	4.18
J8006	391	071080	46	12.48	123	26.02	-4.9	1.67
J8006	392	071080	46	12.23	123	26.11	2.6	2.74
J8006	393	071080	46	12.19	123	26.10	23.6	1.94
J8006	394	071080	46	12.18	123	26.09	31.5	0.55
J8006	395	071080	46	12.15	123	26.13	20.5	0.65
J8006	396	071080	46	12.06	123	26.13	22.5	0.40
J8006	397OUTBOT	071080	46	12.03	123	26.19	11.5	2.22
J8006	397 INTOP	071080	46	12.03	123	26.19	11.5	4.95
J8006	398	071080	46	12.00	123	26.20	-1.5	1.99
J8006	399BAY	071180	46	10.86	123	52.65	8.7	2.56

J8006	400BAY	071180	46	10.32	123	51.68	10.5	2.52
J8006	401BAY	071180	46	10.10	123	51.38	10.3	2.83
J8006	402OUTBOT	071180	46	10.17	123	49.24	47.1	5.91
J8006	402 INTOP	071180	46	10.17	123	49.24	47.1	3.73
J8006	404BAY	071180	46	14.92	123	43.25	8.9	6.84

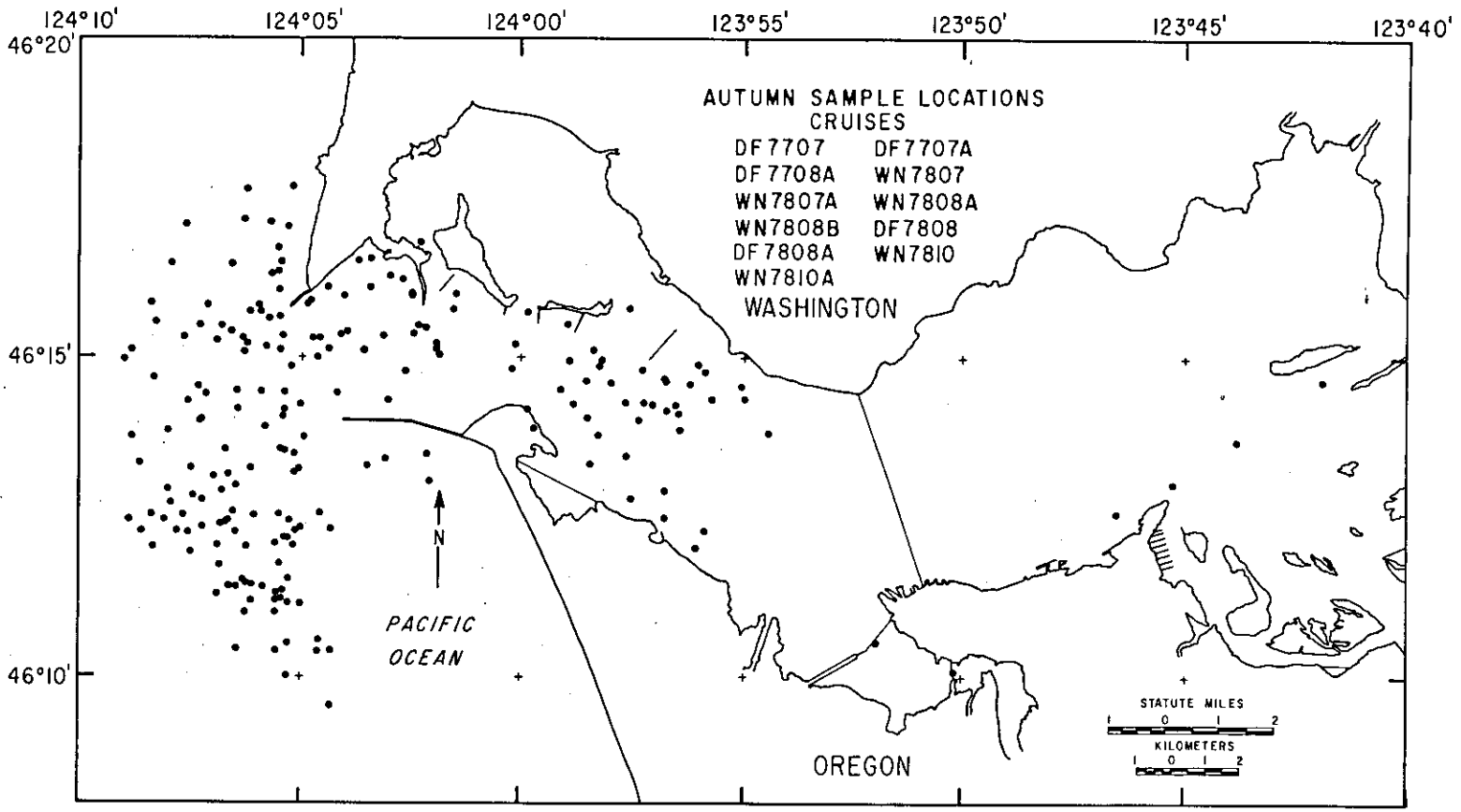

Figure 67. Seasonal fall bottom sample locations.

TABLE 13.
SEASONAL FALL BOTTOM SAMPLE LOCATIONS
CRUISES SDF7808, SDF77, SDF7708A, SWN7807,
SWN7807A, SWN7808A, SWN7808B, SWN7810A, SWN7810
(FIGURE 67)

CRUISE	STN		DATE	LATITUDE	LONGITUDE	DEPTH	PHI
DF808	01	7/F	080378	46 13.77	124 4.93	0.0	2.42
DF808	02		080378	46 13.57	124 6.70	0.0	2.83
DF808	03		080378	46 12.73	124 7.95	0.0	2.67
DF808	04		080378	46 16.23	124 2.72	0.0	2.45
DF808	05		080378	46 16.00	124 2.50	0.0	2.30
DF808	06		080378	46 16.12	124 3.42	0.0	2.57
DF808	07		080378	46 15.98	124 4.00	0.0	2.49
DF808	08		080378	46 16.52	124 3.67	0.0	2.04
DF808	09		080378	46 16.12	124 4.38	0.0	4.14
DF808	10		080378	46 15.35	124 3.12	0.0	1.73
DF808	11		080378	46 15.38	124 2.48	0.0	1.57
DF808	12		080378	46 14.80	124 2.65	0.0	2.28
DF808	13		080378	46 15.13	124 3.57	0.0	1.90
DF808	15	7/F	080378	46 15.15	124 1.97	0.0	1.71
DF808	16		080378	46 16.82	124 2.32	0.0	2.03
DF808	17		080378	46 16.00	124 1.50	0.0	3.93
DF808	18		080378	46 15.77	124 1.57	0.0	1.99
DF808	19		080378	46 15.23	124 1.97	0.0	1.81
DF808	20		080378	46 15.22	124 0.15	0.0	1.72
D7808	21	VV	080378	46 15.72	123 59.87	0.0	1.94
D7808	22	F/D	080378	46 15.53	123 59.00	0.0	2.14
D7808	23		080378	46 14.50	123 59.12	1.4	1.68
D7808	28		080378	46 13.28	124 6.12	0.0	2.50
D7808	29		080378	46 13.18	124 6.62	0.0	2.19
D7808	30		080378	46 13.15	124 6.95	0.0	2.20
D7808	31		080378	46 12.85	124 7.45	0.0	2.12
D7808	32		080378	46 12.55	124 7.67	0.0	2.25
D7808	33		080378	46 12.47	124 8.10	0.0	2.60
D7808	34		080378	46 12.30	124 8.60	0.0	2.46
D7808	35		080378	46 12.55	124 8.38	0.0	2.28
D7808	36		080378	46 12.05	124 8.35	0.0	2.71
D7808	37		080378	46 11.97	124 7.48	0.0	2.69
D7808	38		080378	46 12.30	124 7.80	0.0	2.32
D7808	39		080378	46 12.27	124 7.55	0.0	2.50
D7808	40		080378	46 12.35	124 7.22	0.0	2.10
D7808	41		080478	46 12.92	124 6.78	0.0	2.22
D7808	42		080478	46 12.78	124 7.23	0.0	2.26
D7808	43		080478	46 12.40	124 6.80	0.0	2.33
D7808	44		080478	46 12.07	124 6.87	0.0	2.64
D7808	45		080478	46 11.75	124 6.83	0.0	2.83
D7808	46		080478	46 11.30	124 6.87	0.0	2.84
D7808	47		080478	46 11.43	124 6.60	0.0	2.33
D7808	48		080478	46 11.53	124 6.30	0.0	2.33
D7808	49		080478	46 11.42	124 5.85	0.0	2.34
D7808	50		080478	46 11.05	124 5.75	0.0	2.89
D7808	51		080478	46 11.78	124 5.48	0.0	2.87

D7808	52		080478	46	12.47	124	8.87	0.0	2.59
D7808	53		080478	46	12.65	124	8.50	0.0	2.50
D7808	54		080478	46	12.95	124	8.00	0.0	2.75
D7808	55		080478	46	13.28	124	7.48	0.0	2.81
D7808	56		080478	46	13.87	124	8.00	0.0	2.90
D7808	57		080478	46	13.36	124	8.65	0.0	3.64
D7808	58		080478	46	13.78	124	8.82	0.0	3.40
D7808	60		080478	46	14.20	124	6.43	0.0	2.41
D7808	61		080478	46	14.48	124	5.90	0.0	2.32
D7808	62		080478	46	15.17	124	5.78	0.0	2.29
D7808	63		080478	46	15.65	124	5.48	0.0	2.13
D7808	064	VV	080478	46	15.73	124	5.90	1.4	2.34
D7808	065	VV	080478	46	15.02	124	4.62	1.3	2.24
D7808	066	VV	080478	46	14.83	124	0.23	2.2	1.91
D7808	067	VV	080478	46	14.98	123	58.23	0.9	1.47
D7808	068	VV	080478	46	15.13	123	58.42	0.7	1.64
D7808	069	VV	080478	46	14.88	123	58.27	1.3	1.14
D7808	070	VV	080478	46	14.62	123	58.02	1.1	1.58
D7808	071	VV	080478	46	14.30	123	57.67	1.5	1.65
D7808	072	VV	080478	46	14.03	123	57.40	0.5	1.01
D7808	073	VV	080478	46	15.78	123	57.62	2.1	4.04
D7808	074	VV	080478	46	14.82	123	57.30	1.6	2.75
D7808	075	VV	080478	46	14.68	123	56.80	1.1	0.56
D7808	076	VV	080478	46	14.60	123	56.22	1.1	1.41
D7808	077	VV	080478	46	14.78	123	55.90	1.0	1.92
D7808	078	VV	080478	46	14.55	123	55.10	1.2	1.16
D7808	079	VV	080478	46	13.82	123	54.48	0.5	1.24
D7808	080	VV	080478	46	14.36	123	55.03	1.1	1.08
D7808	081	VV	080478	46	14.36	123	55.03	1.3	1.42
D7808	082	VV	080478	46	14.27	123	56.55	1.2	1.41
D7808	083	VV	080478	46	13.88	123	56.45	0.5	2.35
D7808	084	VV	080478	46	14.17	123	56.75	0.9	1.38
D7808	085	VV	080478	46	15.62	124	5.72	1.1	2.01
D7808	086	VV	080478	46	16.07	124	5.50	0.6	1.98
D7808	087	VV	080478	46	16.35	124	5.53	0.7	2.37
D7808	088	VV	080478	46	16.72	124	5.52	0.6	2.22
D7808	089	VV	080478	46	17.05	124	5.30	0.6	2.43
D7808	090	VV	080478	46	17.12	124	5.70	1.0	2.54
D7808	91		080578	46	12.03	123	56.12	0.0	1.32
D7808	92		080578	46	12.30	123	55.92	0.0	1.97
D7808	93		080578	46	12.50	123	56.80	0.0	1.79
D7808	94		080578	46	12.92	123	56.78	0.0	1.72
D7808	95		080578	46	12.80	123	57.57	0.0	1.38
D7808	96		080578	46	13.47	123	57.65	0.0	1.92
D7808	97		080578	46	13.35	123	58.50	0.0	1.50
D7808	98		080578	46	14.07	123	58.53	0.0	4.40
D7808	100		080578	46	14.98	124	8.98	0.0	2.84
D7808	102		080578	46	15.13	124	8.83	0.0	3.04
D7808	104		080578	46	15.87	124	8.38	0.0	2.89
D7808	105		080578	46	16.48	124	7.92	0.0	2.71
D7808	106		080578	46	17.08	124	7.60	0.0	2.77
D7808	107		080578	46	17.63	124	6.20	0.0	2.87
D7808	108		080578	46	17.17	124	6.27	0.0	2.71
D7808	109		080578	46	16.47	124	6.55	0.0	2.42

D7808	110		080578	46	15.82	124	7.08	0.0	2.52
D7808	111		080578	46	15.33	124	7.63	0.0	2.51
D7808	112		080578	46	14.70	124	8.35	0.0	2.70
D7808	113		080578	46	15.27	124	6.88	0.0	2.18
D7808	114		080578	46	15.50	124	6.77	0.0	2.51
D7808	115		080578	46	15.73	124	6.15	0.0	2.47
D7808	116		080578	46	15.83	124	5.95	0.0	2.22
D7808	117		080578	46	16.32	124	5.65	0.0	2.36
D7808	118		080578	46	16.50	124	5.47	0.0	2.41
D7808	119		080578	46	17.67	124	5.20	0.0	2.70
D7808	A		080578	46	13.90	123	59.72	0.0	2.22
D7808	B		080578	46	14.20	123	59.87	0.0	2.26
D7808	C		080578	46	10.55	123	52.03	0.0	2.50
D7808	D		080578	46	10.10	123	50.22	0.0	3.50
DF707	006		071577	46	16.02	124	2.50	0.0	2.49
DF707	007		071577	46	16.29	124	3.00	0.0	2.47
DF707	008		071577	46	15.52	124	2.35	0.0	2.12
DF707	009		071577	46	14.35	124	3.02	0.0	2.47
DF707	010		071577	46	14.46	124	4.18	0.0	2.11
DF707	011		071577	46	14.28	124	5.03	0.0	2.34
DF707	012		071577	46	14.20	124	5.39	0.0	2.34
DF707	013		071577	46	14.09	124	5.42	0.0	2.46
DF707	014		071577	46	13.43	124	3.09	0.0	2.64
DF707	015		071577	46	12.59	124	6.51	0.0	2.82
DF707	016		071577	46	13.58	124	5.49	0.0	2.73
DF707	017		071577	46	14.02	124	7.31	0.0	2.63
DF707	018		071577	46	13.51	124	5.18	0.0	2.54
DF707	019		071577	46	13.55	124	5.37	0.0	2.31
DF707	020		071577	46	13.33	124	3.49	0.0	2.43
DF707	021		071577	46	13.27	124	5.06	0.0	2.47
DF707	022	7/F	071577	46	13.21	124	5.15	0.0	2.62
DF707	023	7/F	071577	46	12.54	124	6.05	0.0	2.82
DF707	024	7/F	071577	46	13.50	124	2.17	0.0	2.75
DF707	025	7/F	071577	46	13.08	124	2.10	0.0	2.72
DF707	026	7/F	071577	46	15.13	124	5.47	0.0	2.20
DF707	027	7/F	071577	46	15.09	124	6.28	0.0	2.26
DF707	028	7/F	071577	46	14.50	124	6.44	0.0	2.13
DF707	029	7/F	071577	46	14.43	124	7.15	0.0	2.26
DF707	030	7/F	071577	46	14.33	124	7.56	0.0	2.21
DF707	031		071577	46	14.04	124	7.25	0.0	2.61
DF707	032		071577	46	14.57	124	7.31	0.0	2.32
DF707	033		071577	46	15.51	124	7.27	0.0	2.57
DF707	034		071577	46	15.42	124	6.55	0.0	2.41
DF707	035		071577	46	15.23	124	6.22	0.0	2.08
DF707	036		071577	46	14.47	124	5.37	0.0	2.40
DF707	037		071577	46	15.15	124	4.37	0.0	2.04
D7708	001		083077	46	13.02	124	6.46	0.0	2.09
D7708	002		083077	46	12.28	124	6.48	0.0	2.36
D7708	003		083077	46	12.28	124	6.48	0.0	2.72
D7708	004		083077	46	11.42	124	6.44	0.0	2.99
D7708	007		083077	46	10.44	124	6.42	0.0	2.86
D7708	009		083077	46	11.02	124	6.23	0.0	2.82
D7708	011		083077	46	11.20	124	6.09	0.0	2.70
D7708	015		083077	46	11.45	124	6.09	0.0	2.39

D7708	016	083077	46	11.48	124	6.22	0.0	2.78
D7708	017	083077	46	12.04	124	6.21	0.0	2.78
D7708	018	083077	46	12.55	124	5.51	0.0	2.61
D7708	020	083077	46	12.18	124	5.38	0.0	2.90
D7708	021	083077	46	12.10	124	5.56	0.0	2.90
D7708	025	083077	46	11.36	124	5.42	0.0	2.64
D7708	026	083077	46	11.32	124	5.54	0.0	2.30
D7708	027	083077	46	11.23	124	5.43	0.0	2.92
D7708	028	083077	46	11.20	124	5.56	0.0	2.79
D7708	029	083077	46	11.02	124	5.56	0.0	2.95
D7708	030	083077	46	10.42	124	5.54	0.0	3.00
D7708	031	083077	46	10.53	124	5.28	0.0	2.94
D7708	032 7/8	083077	46	11.16	124	5.29	0.0	2.90
D7708	034	083077	46	11.54	124	5.28	0.0	2.90
D7708	035	083077	46	12.08	124	5.17	0.0	2.90
D7708	036	083077	46	12.18	124	5.30	0.0	2.88
D7708	037	083077	46	12.30	124	5.14	0.0	3.04
D7708	038	083077	46	12.46	124	5.26	0.0	3.01
D7708	039	083077	46	12.57	124	4.57	0.0	2.86
D7708	040	083077	46	12.33	124	4.29	0.0	2.80
D7708	041	083077	46	12.35	124	5.00	0.0	3.02
D7708	044	083077	46	11.17	124	5.00	0.0	2.84
D7708	45	083077	46	10.59	124	4.56	0.0	2.86
D7708	46	083077	46	10.43	124	4.30	0.0	2.94
D7708	47	083077	46	10.41	124	4.59	0.0	2.96
D7708	48	083077	46	9.57	124	4.29	0.0	2.86
D7708	49	083077	46	10.03	124	5.31	0.0	2.90
W7807	075	071578	46	15.98	124	4.00	0.0	2.53
W7807	09BL	071578	46	15.32	124	4.73	0.0	2.04
W7807	03FS	071578	46	15.85	124	4.83	0.0	2.39
W7807	04FS	071578	46	15.90	124	4.78	0.0	6.45
W7807	06FS	071578	46	15.85	124	4.85	0.0	5.02
W7807	11FS	071578	46	15.32	124	4.57	0.0	2.51
W808A	01BL1	082478	46	14.35	123	55.77	0.0	1.71
W808A	01BL2	082478	46	14.35	123	55.77	0.0	1.69
W808A	02 BL	082478	46	14.90	123	56.05	0.0	1.86
W808A	03 BL	082478	46	14.13	123	56.50	0.0	1.51
W808A	04 BL	082478	46	14.65	123	56.78	0.0	1.26
W808A	05 BL	082478	46	15.48	124	2.18	0.0	1.74
W808A	06 BL	082478	46	15.07	124	1.90	0.0	2.02
W808A	07 BL	082478	46	14.65	123	58.59	0.0	1.70
W808A	08 BL	082478	46	14.95	123	58.95	0.0	1.23
W808A	09 FS	082478	46	14.95	123	58.95	0.0	5.86
W808A	09 BL	082478	46	14.30	123	57.28	0.0	1.54
W808A	10 BL	082478	46	13.80	123	58.32	0.0	1.62
W808B	01 BL	082578	46	14.28	123	57.08	0.0	4.05
W808B	01 FS	082578	46	14.28	123	57.08	0.0	6.35
W808B	02 BL	082578	46	14.28	123	58.87	0.0	1.96
W808B	03 FS	082578	46	15.47	123	38.92	0.0	1.94
W808B	03 BL	082578	46	15.47	123	38.92	0.0	2.02
W808B	04 FS	082578	46	14.65	123	41.95	0.0	1.70
W808B	05 BL	082578	46	13.71	123	43.87	0.0	1.76
W808B	05 FS	082578	46	13.71	123	43.87	0.0	2.00
W808B	06 BL	082578	46	13.03	123	45.32	0.0	2.14

W808B	06	FS	082578	46	13.03	123	45.32	0.0	1.35
W808B	07	BL	082578	46	12.58	123	46.58	0.0	1.25
W810A	01	BL	103078	46	15.42	124	3.95	0.0	1.82
W810A	02	BL	103078	46	13.93	124	5.82	0.0	2.19
W810A	03	BL	103078	46	12.43	124	6.70	0.0	1.92
W810A	04	BL	103078	46	14.18	124	7.43	0.0	2.21
W810A	05	BL	103078	46	15.57	124	8.28	0.0	2.15
W810A	06	BL	103078	46	12.45	124	6.62	0.0	1.94
W810A	08	BL	103078	46	14.88	124	5.22	0.0	1.87
W810A	09	BL	103078	46	15.36	124	4.10	0.0	1.94
W7810	01	BL	102878	46	15.35	124	5.42	0.0	1.78
W7810	02	VV	102878	46	15.32	124	6.30	0.0	2.01

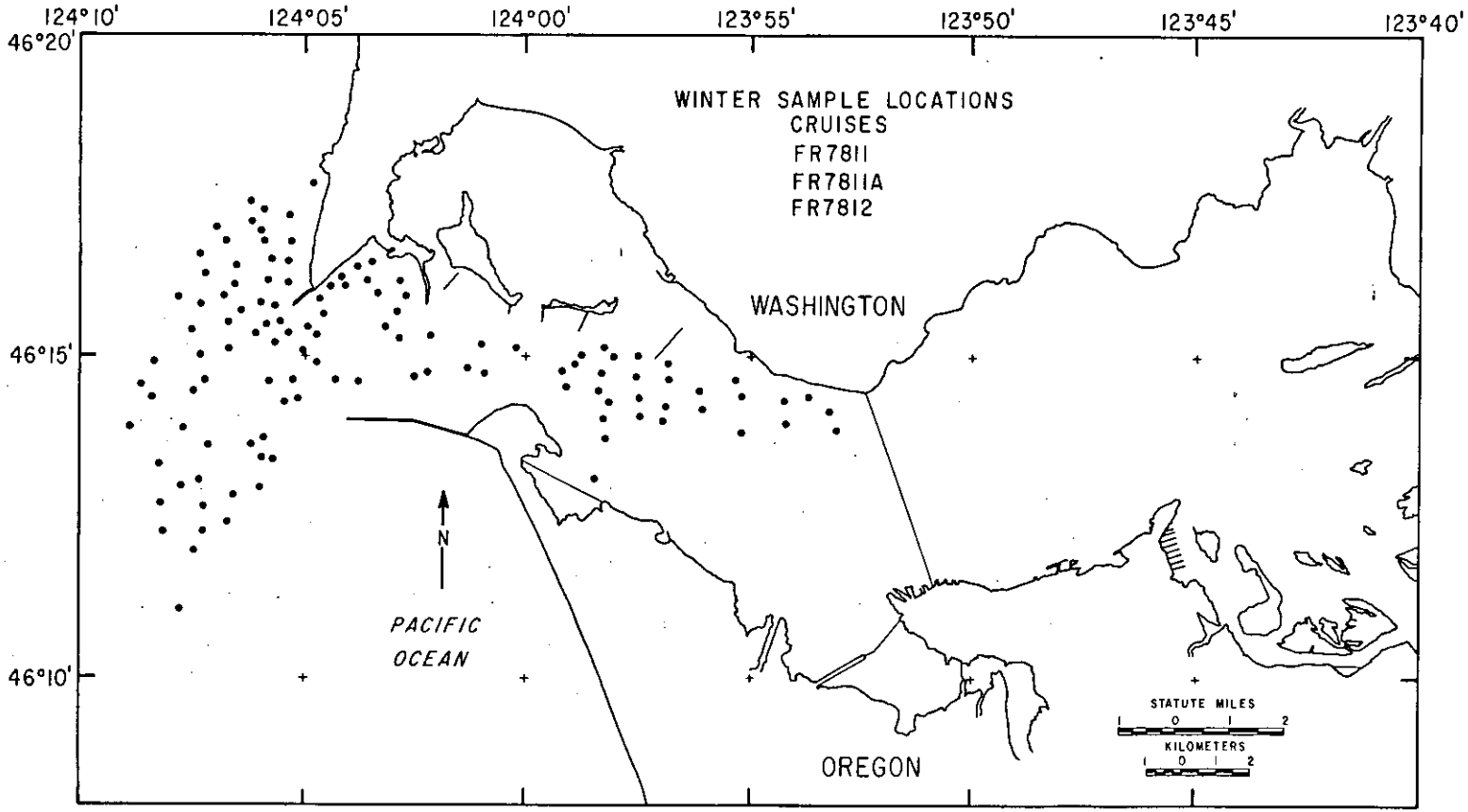

Figure 68. Seasonal winter bottom sample locations.

TABLE 14.
SEASONAL WINTER BOTTOM SAMPLE LOCATIONS
CRUISES F7812, F811A, F7811
(FIGURE 68)

CRUISE	STN	DATE	LATITUDE	LONGITUDE	DEPTH	PHI
F7812	01	120778	46 15.53	124 5.53	46.0	2.32
F7812	02	120778	46 15.47	124 5.83	38.0	2.26
F7812	03	120778	46 15.35	124 6.08	40.0	2.42
F7812	04	120778	46 15.10	124 6.67	39.0	2.28
F7812	05	120778	46 15.02	124 7.30	37.0	2.45
F7812	06	120778	46 14.62	124 7.22	43.0	2.40
F7812	07	120778	46 14.45	124 7.47	44.0	2.59
F7812	08	120778	46 14.92	124 8.35	42.0	2.80
F7812	09	120778	46 15.40	124 7.50	33.0	2.48
F7812	10	120778	46 15.52	124 6.67	30.0	2.43
F7812	11	120778	46 15.70	124 6.38	22.0	2.51
F7812	12	120778	46 15.82	124 5.97	19.0	2.42
F7812	13	120778	46 15.78	124 5.63	17.0	2.32
F7812	14	120778	46 16.13	124 5.35	19.0	2.74
F7812	15	120778	46 16.47	124 5.36	18.0	2.57
F7812	16	120778	46 16.77	124 5.28	17.0	2.79
F7812	17	120778	46 17.18	124 5.33	18.0	2.77
F7812	18	120778	46 17.68	124 4.80	18.0	2.82
F7812	19	120778	46 17.28	124 5.90	31.0	3.01
F7812	20	120778	46 17.40	124 6.18	35.0	2.91
F7812	21	120778	46 17.08	124 6.17	32.0	3.00
F7812	22	120778	46 16.95	124 5.97	30.0	2.88
F7812	23	120778	46 16.77	124 5.87	29.0	2.75
F7812	24	120778	46 16.50	124 5.72	25.0	2.63
F7812	25	120778	46 16.18	124 5.80	25.0	2.37
F7812	26	120778	46 16.10	124 6.53	25.0	2.51
F7812	27???	120778	46 16.40	124 6.50	26.0	7.60
F7812	28	120778	46 16.78	124 6.73	33.0	2.71
F7812	29	120778	46 17.00	124 6.95	35.0	2.94
F7812	30	120778	46 16.58	124 7.33	34.0	2.69
F7812	31	120778	46 16.27	124 7.20	31.0	2.54
F7812	32	120778	46 15.93	124 6.78	24.0	2.58
F7812	33	120778	46 15.80	124 7.30	29.0	2.51
F7812	34	120778	46 15.92	124 7.82	33.0	2.63
F7812	35	120778	46 14.60	124 5.77	49.0	2.40
F7812	36	120778	46 14.28	124 5.42	47.0	2.46
F7812	37	120778	46 14.33	124 5.13	43.0	2.40
F7812	38	120778	46 14.62	124 5.25	45.0	2.42
F7812	39	120778	46 14.63	124 4.30	25.0	2.32
F7812	40	120778	46 14.90	124 4.72	40.0	2.27
F7812	41	120778	46 15.08	124 5.03	54.0	2.43
F7812	42	120778	46 15.32	124 4.72	50.0	2.48
F7812	43	120778	46 15.97	124 3.32	20.0	2.19
F7812	44	120778	46 16.18	124 3.58	24.0	2.57
F7812	45	120778	46 16.38	124 3.80	28.0	2.06
F7812	46	120778	46 16.45	124 3.47	24.0	2.32
F7812	47	120778	46 16.15	124 2.83	21.0	2.49

F7812	48	120778	46	15.93	124	2.68	34.0	2.37
F7812	49	120778	46	15.13	123	58.27	24.0	1.63
F7812	50	120778	46	14.73	123	58.33	47.0	2.25
F7812	51	120778	46	14.28	123	58.17	33.0	2.75
F7812	52	120778	46	13.72	123	58.23	33.0	2.45
F7812	54	120778	46	14.07	123	57.48	17.0	1.17
F7812	55	120778	46	14.35	123	57.50	54.0	1.81
F7812	56	120778	46	14.67	123	57.57	39.0	1.34
F7812	57	120778	46	15.00	123	57.52	28.0	4.77
F7812	58	120778	46	14.88	123	56.85	35.0	1.19
F7812	59	120778	46	14.63	123	56.82	33.0	1.71
F7812	60	120778	46	14.20	123	56.88	38.0	2.32
F7812	61	120778	46	13.98	123	56.95	18.0	1.56
F7812	62	120778	46	14.17	123	56.08	42.0	1.88
F7812	63	120778	46	14.45	123	56.13	32.0	1.70
F7812	64	120778	46	14.62	123	55.36	35.0	3.62
F7812	65	120778	46	14.38	123	55.22	40.0	0.92
F7812	66	120778	46	13.80	123	55.22	14.0	1.78
F7812	67	120778	46	13.95	123	54.22	41.0	1.55
F7812	68	120778	46	14.30	123	54.27	47.0	1.33
F7812	69	120778	46	14.36	123	53.72	42.0	2.20
F7812	70	120778	46	14.13	123	53.25	64.0	1.04
F7812	71	120778	46	13.85	123	53.08	30.0	1.66
F811A	02	112278	46	12.42	124	6.68	72.0	2.16
F811A	03	112278	46	12.28	124	7.25	91.0	2.17
F811A	04	112278	46	11.98	124	7.45	101.0	2.62
F811A	05	112278	46	11.07	124	7.77	103.0	2.47
F811A	06	112278	46	12.27	124	8.15	106.0	2.54
F811A	07	112278	46	12.70	124	8.18	95.0	2.19
F811A	08	112278	46	12.65	124	7.25	76.0	2.20
F811A	09	112278	46	12.83	124	6.57	54.0	2.21
F811A	10	112278	46	12.95	124	5.97	55.0	2.42
F811A	11	112278	46	13.40	124	5.67	57.0	2.69
F811A	12	112278	46	13.42	124	5.93	47.0	2.41
F811A	13	112278	46	13.73	124	5.87	47.0	2.72
F811A	14	112278	46	13.62	124	6.17	46.0	2.63
F811A	16	112278	46	13.07	124	7.33	66.0	2.48
F811A	17	112278	46	12.97	124	7.75	77.0	2.64
F811A	18	112278	46	13.32	124	8.23	69.0	2.91
F811A	19	112278	46	13.90	124	8.87	60.0	2.90
F811A	20	112278	46	14.35	124	8.38	58.0	2.86
F811A	22	112278	46	14.57	124	8.62	48.0	2.74
F811A	23	112278	46	13.87	124	7.70	48.0	2.81
F811A	24	112278	46	13.62	124	7.13	50.0	2.90
F811A	28	112278	46	15.20	124	5.63	52.0	1.90
F811A	29	112278	46	15.35	124	5.35	68.0	1.89
F811A	30	112278	46	15.45	124	4.92	50.0	2.25
F811A	31	112278	46	15.65	124	4.57	37.0	2.44
F811A	32	112278	46	16.08	124	4.08	32.0	2.56
F811A	33	112278	46	16.22	124	4.17	38.0	1.96
F811A	34	112278	46	16.08	124	4.42	45.0	5.85
F811A	35	112278	46	15.88	124	4.65	49.0	2.35
F7811	01	111578	46	14.60	124	3.77	41.0	1.99
F7811	02	111578	46	14.74	124	2.20	54.0	2.00

F7811	03	111578	46	14.80	124	1.32	47.0	1.91
F7811	04	111578	46	15.17	124	1.01	79.0	1.77
F7811	05	111578	46	15.29	124	2.13	82.0	1.45
F7811	06	111578	46	15.26	124	2.85	54.0	1.91
F7811	07	111578	46	15.69	124	2.89	26.0	2.48
F7811	08	111578	46	15.45	124	3.16	36.0	2.18
F7811	09	111578	46	14.68	124	2.50	34.0	2.17
F7811	10	111578	46	14.73	124	0.93	46.0	2.05
F7811	11	111578	46	15.12	124	0.23	82.0	1.92
F7811	16	111578	46	15.01	123	58.78	53.0	1.65
F7811	17	111578	46	14.86	123	58.92	53.0	1.63
F7811	18	111578	46	14.77	123	59.20	60.0	1.56
F7811	19	111578	46	14.52	123	59.10	0.0	1.97
F7811	20	111578	46	14.98	123	58.08	50.0	1.96
F7811	21	111578	46	14.71	123	58.32	43.0	1.61
F7811	22	111578	46	14.45	123	58.40	47.0	1.78
F7811	23	111578	46	14.02	123	58.28	38.0	2.15
F7811	24	111578	46	13.09	123	58.47	47.0	2.21

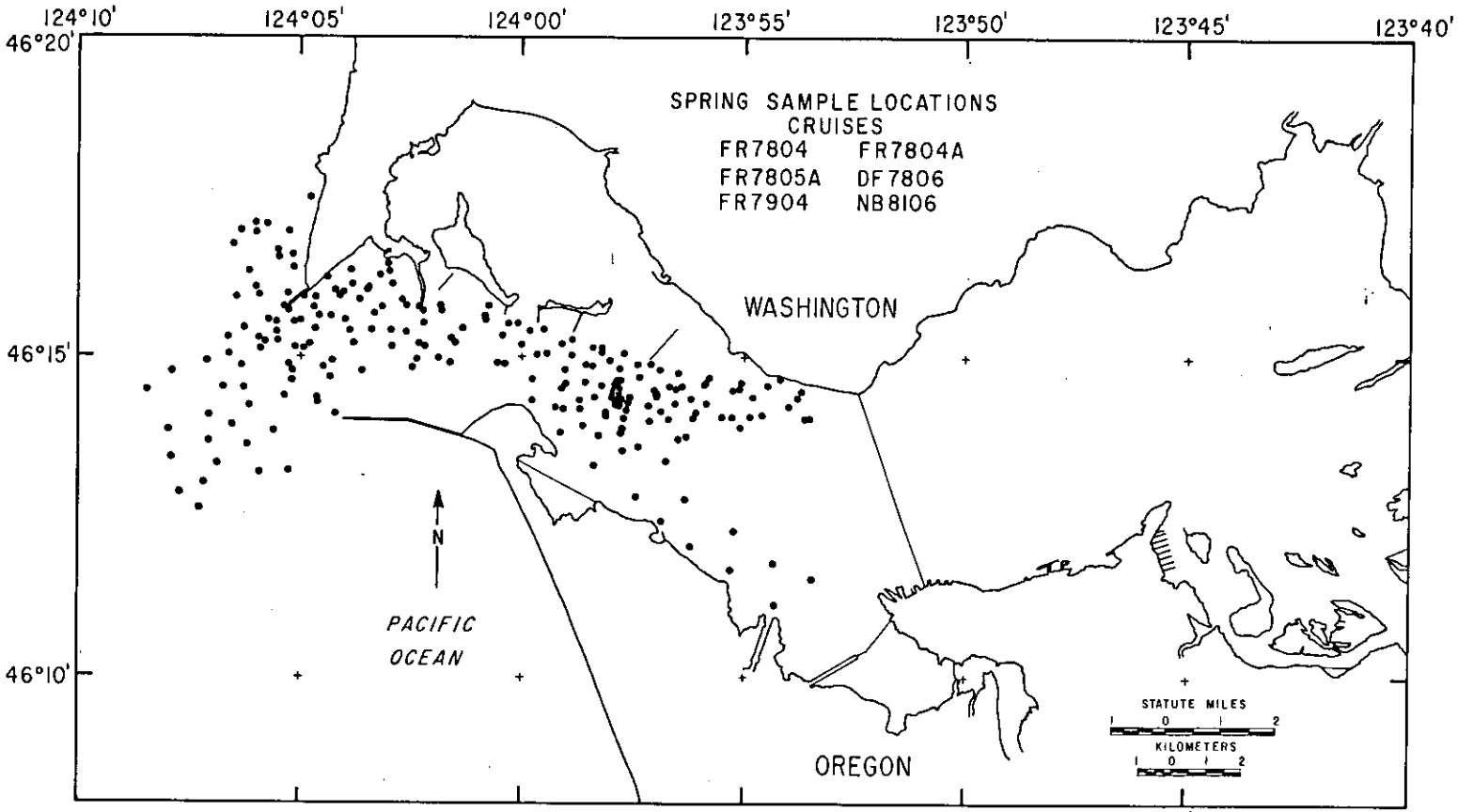

Figure 69. Seasonal spring bottom sample locations.

TABLE 15.
SEASONAL SPRING BOTTOM SAMPLE LOCATIONS
CRUISES SFR7804, SFR780, SDF7806, SFR7904, SNB8106, SWN7805A
(FIGURE 69)

CRUISE	STN	DATE	LATITUDE	LONGITUDE	DEPTH	PHI
F7804	1	042178	46 14.32	123 59.78	0.0	1.73
F7804	2	042178	46 14.65	123 59.78	0.0	1.64
F7804	3	042178	46 15.03	123 59.68	0.0	1.42
F7804	4	042178	46 15.42	123 59.53	0.0	1.76
F7804	5	042178	46 15.20	123 59.10	0.0	1.63
F7804	6	042178	46 14.80	123 59.05	0.0	1.21
F7804	7	042178	46 14.50	123 59.10	0.0	1.98
F7804	8	042178	46 14.18	123 59.07	0.0	1.87
F7804	9	042178	46 13.82	123 59.12	0.0	1.81
F7804	10	042178	46 14.32	123 58.70	0.0	4.85
F7804	11	042178	46 14.60	123 58.57	0.0	1.77
F7804	12	042178	46 14.85	123 58.42	0.0	1.20
F7804	13	042178	46 15.05	123 58.20	0.0	0.72
F7804	14	042178	46 15.05	123 57.72	0.0	0.94
F7804	15	042178	46 14.82	123 57.82	0.0	0.92
F7804	16	042178	46 14.62	123 57.88	0.0	1.98
F7804	17	042178	46 14.55	123 58.20	0.0	1.87
F7804	18	042178	46 14.38	123 58.00	0.0	1.61
F7804	19	042178	46 14.07	123 58.12	0.0	1.32
F7804	20	042178	46 13.75	123 58.27	0.0	2.47
F7804	21	042178	46 13.87	123 57.75	0.0	2.26
F7804	22	042178	46 14.03	123 57.72	0.0	2.44
F7804	22M	042178	46 14.03	123 57.72	0.0	6.38
F7804	23	042178	46 14.35	123 57.60	0.0	1.84
F7804	24	042178	46 14.47	123 57.50	0.0	2.60
F7804	25	042178	46 14.68	123 57.38	0.0	1.56
F7804	26	042178	46 14.80	123 56.93	0.0	1.71
F7804	27	042178	46 14.47	123 57.05	0.0	1.72
F7804	28	042178	46 14.23	123 57.17	0.0	1.59
F7804	29	042178	46 14.03	123 56.72	0.0	1.29
F7804	30	042178	46 14.25	123 56.57	0.0	1.87
F7804	31	042178	46 14.53	123 56.43	0.0	1.93
F7804	32	042178	46 14.85	123 56.02	0.0	1.91
F7804	33	042178	46 14.60	123 55.88	0.0	0.69
F7804	34	042178	46 14.27	123 55.88	0.0	1.59
F7804	35	042178	46 14.05	123 55.30	0.0	1.53
F7804	36	042178	46 14.47	123 55.27	0.0	1.68
F7804	37	042178	46 14.36	123 54.83	0.0	0.91
F7804	38	042178	46 14.08	123 54.63	0.0	1.35
F7804	39	042178	46 14.22	123 54.03	0.0	1.32
F7804	40	042178	46 14.03	123 53.57	0.0	1.58
F804A	04	042878	46 16.13	124 3.85	0.0	2.36
F804A	05	042878	46 16.08	124 3.48	0.0	2.29
F804A	06	042878	46 16.03	124 4.22	0.0	2.37
F804A	7	042878	46 16.22	124 4.42	0.0	2.40
F804A	08	042878	46 15.95	124 4.13	0.0	2.33
F804A	09	042878	46 15.63	124 4.60	0.0	2.51

F804A	10	042878	46	15.92	124	4.68	0.0	2.18
F804A	11	042878	46	15.93	124	4.93	0.0	1.95
F804A	12	042878	46	15.57	124	5.00	0.0	2.17
F804A	13	042878	46	15.72	124	5.27	0.0	2.08
F804A	14	042878	46	15.78	124	5.38	0.0	1.35
F804A	15	042878	46	14.83	124	2.50	0.0	2.09
F7904	01	042079	46	15.37	124	5.54	48.0	2.17
F7904	02	042079	46	15.28	124	5.94	42.0	2.15
F7904	03	042079	46	15.12	124	5.89	45.0	2.22
F7904	04	042079	46	15.03	124	6.62	42.0	2.19
F7904	05	042079	46	14.93	124	7.12	41.0	2.34
F7904	06	042079	46	16.66	124	5.51	34.0	2.49
F7904	07	042079	46	16.92	124	6.01	39.0	2.60
F7904	08	042079	46	17.08	124	6.03	41.0	2.66
F7904	09	042079	46	17.06	124	5.76	36.0	2.68
F7904	10	042079	46	17.47	124	4.79	21.0	2.47
F7904	11	042079	46	16.95	124	5.27	24.0	2.45
F7904	12	042079	46	16.58	124	5.17	18.0	2.16
F7904	13	042079	46	16.38	124	5.16	13.0	2.37
F7904	14	042079	46	15.98	124	5.28	16.0	2.31
F7904	15	042079	46	15.53	124	5.54	25.0	2.41
F7904	16	042079	46	15.58	124	5.73	24.0	2.48
F7904	17	042079	46	15.96	124	5.93	27.0	2.36
F7904	18	042079	46	16.54	124	5.49	29.0	2.52
F7904	19	042079	46	16.96	124	6.35	41.0	2.65
F7904	20	042079	46	16.75	124	6.53	36.0	2.55
F7904	21	042079	46	16.32	124	6.16	32.0	2.53
F7904	22	042079	46	16.07	124	6.01	31.0	2.52
F7904	23	042079	46	15.92	124	6.45	32.0	2.58
F7904	24	042079	46	15.44	124	6.28	31.0	2.48
F7904	25	042079	46	15.29	124	6.64	36.0	2.34
F7904	26	TOP042079	46	15.55	124	4.98	75.0	5.57
F7904	26	BOT042079	46	15.55	124	4.98	75.0	2.03
F7904	27	042079	46	15.77	124	4.72	60.0	2.28
F7904	28	042079	46	16.02	124	4.04	44.0	1.91
F7904	29	042079	46	16.34	124	3.89	31.0	2.09
F7904	30	042079	46	16.33	124	3.03	28.0	2.26
F7904	31	042079	46	16.13	124	2.95	23.0	2.58
F7904	32	042079	46	16.03	124	3.54	28.0	2.59
F7904	33	042079	46	15.89	124	3.71	31.0	2.47
F7904	34	042079	46	15.62	124	4.35	38.0	2.34
F7904	35	042079	46	15.42	124	4.69	44.0	2.28
F7904	36	042079	46	14.09	124	4.23	33.0	2.59
F7904	37	042079	46	14.77	124	3.64	36.0	2.32
F7904	38	042079	46	15.77	124	3.17	26.0	2.51
F7904	39	042079	46	15.71	124	2.24	34.0	2.43
F7904	40	042079	46	15.64	124	0.86	39.0	2.16
F7904	41	042079	46	15.40	123	59.85	63.0	2.01
F7904	42	042079	46	15.26	123	58.88	41.0	2.18
F7904	43	042079	46	15.12	123	58.21	61.0	2.18
F7904	44	042079	46	14.87	123	57.42	27.0	1.44
F7904	45	042079	46	14.74	123	56.52	45.0	2.43
F7904	46	042079	46	14.59	123	55.08	42.0	1.04
F7904	47	042079	46	14.33	123	56.23	37.0	1.85

F7904	48		042079	46	14.03	123	56.19	53.0	1.96
F7904	49		042079	46	13.75	123	56.31	18.0	1.25
F7904	50		042079	46	13.71	123	56.52	20.0	1.29
F7904	51		042079	46	14.15	123	56.90	56.0	1.71
F7904	52		042079	46	13.98	123	57.14	32.0	1.60
F7904	53		042079	46	14.13	123	58.11	33.0	1.98
F7904	54		042079	46	13.80	123	57.78	34.0	2.01
F7904	55		042079	46	13.58	123	57.39	31.0	2.47
F7904	56		042079	46	13.36	123	56.77	30.0	2.33
F7904	57		042079	46	12.78	123	56.35	30.0	2.04
F7904	58		042079	46	12.27	123	55.23	23.0	1.91
F7904	59		042079	46	11.78	123	54.36	24.0	1.86
F7904	60		042079	46	11.53	123	53.49	29.0	1.85
F7904	61		042179	46	14.47	124	8.42	54.0	2.71
F7904	62		042179	46	14.77	124	7.87	48.0	2.40
F7904	63		042179	46	13.85	124	7.95	61.0	2.76
F7904	64		042179	46	13.42	124	7.88	70.0	2.63
F7904	65		042179	46	12.87	124	7.70	87.0	2.57
F7904	66		042179	46	13.02	124	7.17	76.0	2.33
F7904	67		042179	46	13.33	124	6.88	64.0	2.16
F7904	68		042179	46	13.67	124	7.07	60.0	2.79
F7904	69		042179	46	14.08	124	7.07	58.0	2.82
F7904	70		042179	46	14.52	124	6.75	58.0	2.56
F7904	71		042179	46	14.85	124	6.33	56.0	2.44
F7904	72		042179	46	14.52	124	6.28	61.0	2.51
F7904	73		042179	46	14.23	124	6.15	60.0	2.59
F7904	74		042179	46	13.93	124	6.55	56.0	2.73
F7904	75		042179	46	13.62	124	6.20	50.0	2.74
F7904	76	;/F	042179	46	13.18	124	5.92	64.0	2.41
F7904	77		042179	46	13.22	124	5.27	65.0	2.67
F7904	78		042179	46	13.83	124	5.60	60.0	2.71
F7904	79		042179	46	14.38	124	5.36	55.0	2.24
F7904	80		042179	46	14.35	124	4.62	52.0	2.56
F7904	81		042179	46	14.67	124	4.33	36.0	2.52
F7904	82		042179	46	14.83	124	4.50	44.0	2.22
F7904	83		042179	46	14.77	124	5.18	50.0	2.45
F7904	84		042179	46	14.87	124	5.27	62.0	2.43
F7904	85		042179	46	15.12	124	4.93	64.0	2.51
F7904	86		042179	46	15.23	124	5.80	58.0	1.88
F7904	87		042179	46	15.23	124	5.50	68.0	1.84
F7904	88		042179	46	15.53	124	5.15	64.0	1.99
F7904	89		042179	46	15.18	124	4.80	60.0	2.58
F7904	90		042179	46	15.20	124	3.83	54.0	1.93
F7904	91		042179	46	15.40	124	3.43	61.0	1.87
F7904	92		042179	46	15.58	124	4.02	44.0	2.49
F7904	93		042178	46	15.67	124	3.36	48.0	2.26
F7904	94		042179	46	15.88	124	2.73	41.0	2.36
F7904	95		042179	46	15.80	124	2.62	68.0	2.44
F7904	96		042179	46	15.40	124	2.98	75.0	1.65
F7904	97		042179	46	15.38	124	2.63	94.0	1.57
F7904	98		042179	46	15.52	124	2.22	96.0	1.61
F7904	99		042179	46	15.15	124	2.20	59.0	1.98
F7904	100		042179	46	15.15	124	2.95	57.0	1.92
F7904	101		042179	46	14.95	124	2.38	34.0	2.27

F7904	102	042179	46	14.90	124	1.63	30.0	2.26
F7904	103	042179	46	15.28	124	1.60	84.0	1.50
F7904	104	042179	46	15.72	124	1.82	88.0	1.55
F7904	105	042179	46	15.80	124	1.85	58.0	2.07
F7904	106	042179	46	15.57	124	0.85	74.0	2.01
F7904	107	042179	46	14.88	124	0.42	72.0	2.34
F7904	108	042179	46	15.18	124	0.03	76.0	1.83
F7904	109	042179	46	15.52	124	0.13	65.0	2.90
F7904	110	042179	46	15.05	123	59.45	59.0	1.38
F7904	111	042179	46	15.02	123	58.88	48.0	1.40
F7904	112	042179	46	14.87	123	58.55	52.0	1.26
F7904	113	042179	46	14.93	123	58.03	32.0	1.93
F7904	114	042179	46	14.58	123	59.03	55.0	1.64
F7904	115	042179	46	14.20	123	59.23	39.0	1.94
F7904	116	042179	46	13.92	123	58.63	34.0	1.55
F7904	117	042179	46	13.30	123	58.38	34.0	1.54
F7904	118	042179	46	13.53	123	57.75	54.0	1.56
F7904	119	042179	46	14.58	123	57.73	44.0	1.55
F7904	120	042179	46	14.36	123	57.00	39.0	1.76
F7904	121	042179	46	14.13	123	56.90	38.0	1.85
F7904	122	042179	46	14.35	123	56.82	38.0	1.68
F7904	123	042179	46	14.50	123	56.55	44.0	1.49
F7904	124	042179	46	14.68	123	55.80	36.0	1.34
F7904	125	042179	46	14.57	123	55.92	42.0	0.91
F7904	126	042179	46	14.50	123	55.13	46.0	0.91
F7904	127	042179	46	14.65	123	54.23	28.0	2.21
F7904	128	042179	46	14.35	123	53.83	58.0	1.32
F7904	129	042179	46	14.45	123	53.75	32.0	1.58
F7904	130	042179	46	14.55	123	54.50	34.0	1.15
F7904	131	042179	46	13.88	123	55.10	24.0	1.54
F7904	132	042179	46	14.05	123	55.52	44.0	1.05
F7904	133	042179	46	12.80	123	57.43	28.0	1.65
F7904	134	042179	46	12.43	123	56.88	38.0	2.13
F7904	135	042179	46	12.03	123	56.23	55.0	1.42
F7904	136	042179	46	11.67	123	55.30	58.0	4.48
F7904	137	042179	46	11.13	123	54.32	37.0	0.24
D7806	1	061278	46	12.62	124	7.27	0.0	2.29
D7806	3	061278	46	16.45	124	3.05	0.0	2.46
D7806	4	061278	46	16.27	124	3.22	0.0	2.64
D7806	5	061278	46	15.77	124	2.33	0.0	2.70
D7806	6	061278	46	15.20	124	2.33	0.0	2.06
D7806	7	061278	46	14.97	124	1.90	0.0	2.34
D7806	8	061278	46	15.20	124	1.52	0.0	2.01
D7806	9	061278	46	15.45	124	1.37	0.0	1.49
D7806	10	061278	46	15.80	124	0.77	0.0	2.19
D7806	11	061278	46	15.52	124	0.33	0.0	1.96
D7806	12	061278	46	15.32	124	0.48	0.0	2.36
D7806	13	061278	46	14.90	124	0.57	0.0	1.91
D7806	14	061278	46	15.40	124	3.93	0.0	2.08
D7806	15	061278	46	14.93	124	4.30	0.0	2.06
D7806	16	061278	46	14.28	124	4.63	0.0	2.23
D7806	*16	061278	46	14.28	124	4.63	0.0	2.42
D7806	18	061278	46	14.63	124	5.20	0.0	2.49
D7806	19	061278	46	15.13	124	5.13	0.0	2.18

B8106	008	BOT	062581	46	14.23	123	57.83	35.4	3.10
B8106	012		062581	46	14.43	123	57.73	39.6	2.03
B8106	006		062581	46	14.46	123	57.47	31.2	1.96
B8106	018		062581	46	14.50	123	57.85	36.8	2.22
B8106	016		062581	46	14.63	123	57.77	45.0	5.14
B8106	013		062581	46	14.46	123	57.72	34.2	2.04
B8106	005MIX		062581	46	14.41	123	57.49	34.0	2.42
B8106	022MBA		062581	46	14.25	123	57.92	36.1	3.85
B8106	003		062581	46	14.33	123	57.51	49.1	4.94
B8106	005UPR		062581	46	14.41	123	57.49	34.0	3.69
B8106	004		062581	46	14.38	123	57.51	43.4	2.34
B8106	010		062581	46	14.27	123	57.83	45.1	1.84
B8106	009		062581	46	14.33	123	57.78	50.9	4.88
B8106	008SUR		062581	46	14.23	123	57.83	35.4	5.76
B8106	005LOWBOT		062581	46	14.41	123	57.49	34.0	2.17
B8106	011		062581	46	14.40	123	57.75	46.4	4.89
B8106	021		062581	46	14.37	123	57.87	51.2	5.21
B8106	017		062581	46	14.54	123	57.82	37.8	1.88
W805A	2	BL	053178	46	14.88	123	57.12	0.0	1.74
W805A	3	BL	053178	46	14.15	123	57.65	0.0	1.77
W805A	4	BL	053178	46	14.35	123	58.37	0.0	1.55
W805A	4B	F	053178	46	14.18	123	58.70	0.0	3.09
W805A	4B	BL	053178	46	14.18	123	58.70	0.0	1.39
W805A	7	BL	053178	46	15.13	123	58.40	0.0	1.41
W805A	8	BL	053178	46	14.03	123	53.67	0.0	1.28
W805A	9	BL	053178	46	14.05	123	54.88	0.0	0.85
W805A	10	F	053178	46	14.12	123	56.10	0.0	1.40
W805A	10	BLBOT	053178	46	14.12	123	56.10	0.0	1.51
W805A	11	F	053178	46	14.47	123	57.72	0.0	2.37
W805A	11	BLBOT	053178	46	14.47	123	57.72	0.0	1.94
W805A	12	F	053178	46	14.28	123	57.93	0.0	1.36
W805A	12+1		053178	46	14.28	123	57.93	0.0	1.74

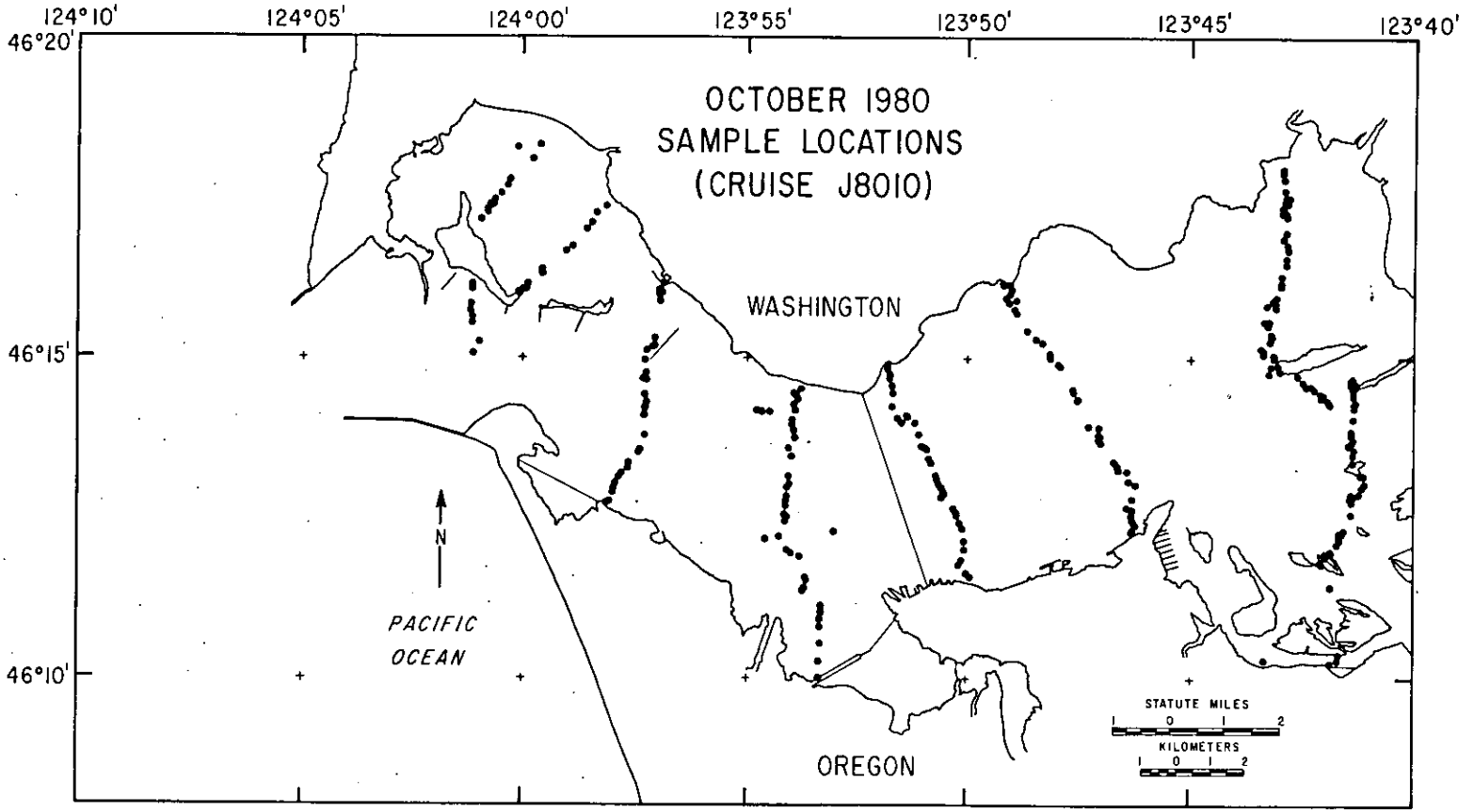

Figure 70. CREDDP bottom sample locations, October 1980 (not analyzed).

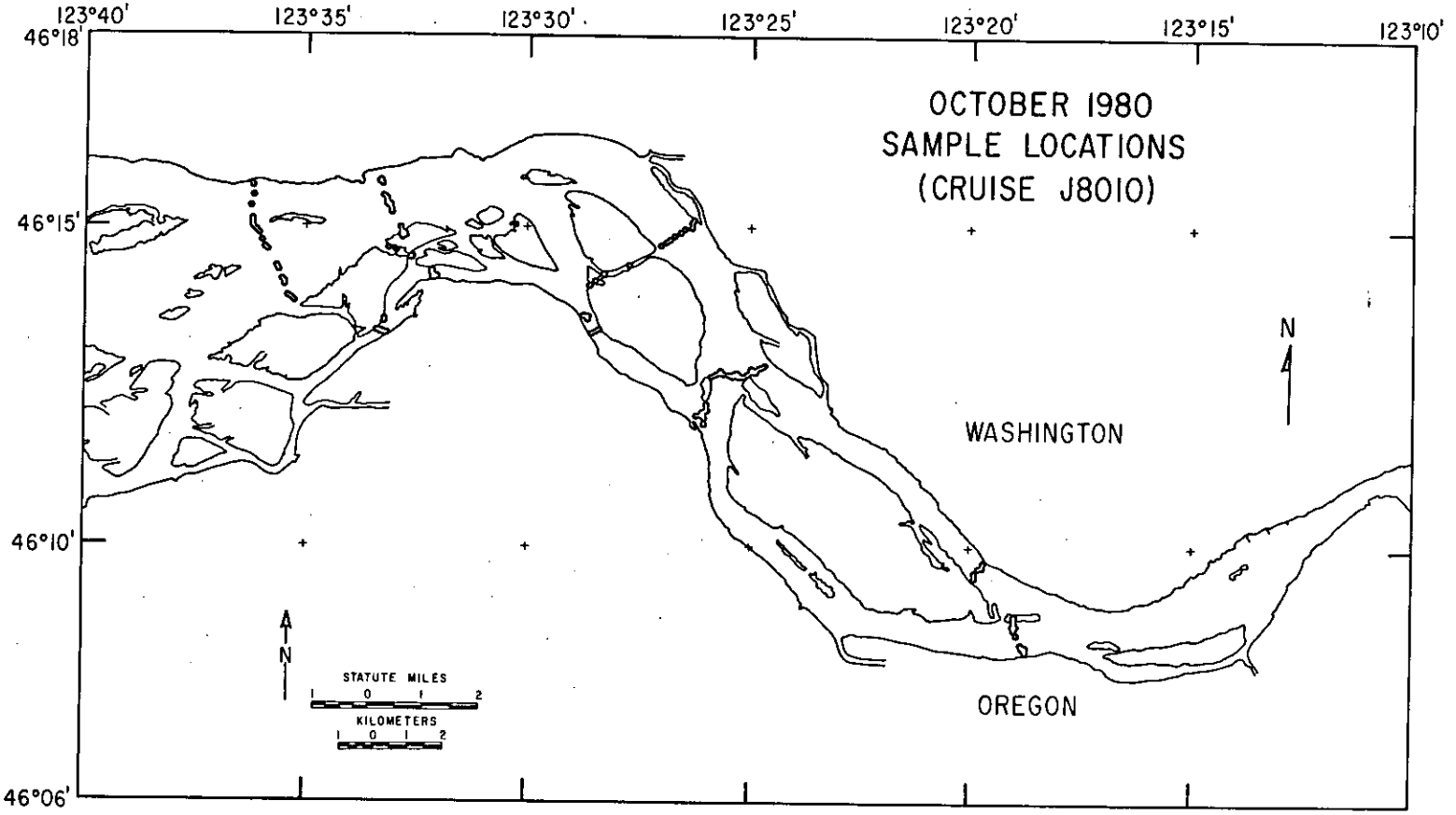

Figure 71. CREDDP bottom sample locations, October 1980 (not analyzed).

TABLE 16.
OCTOBER 1980 BOTTOM SAMPLE LOCATIONS
CRUISE J8010 (SAMPLES HAVE NOT BEEN ANALYZED)
(FIGURES 70, 71)

CRUISE	STN	DATE	LATITUDE	LONGITUDE	DEPTH
J8010	48	100280	46 16.18	123 49.19	1.3
J8010	47	100280	46 16.17	123 49.20	10.9
J8010	46	100280	46 16.17	123 49.18	16.0
J8010	45	100280	46 16.16	123 49.16	28.1
J8010	44	100280	46 16.14	123 49.08	32.7
J8010	43	100280	46 16.07	123 49.04	27.3
J8010	42	100280	46 16.03	123 49.06	17.0
J8010	41	100280	46 16.00	123 49.08	13.1
J8010	40	100280	46 15.94	123 49.18	8.7
J8010	39	100280	46 15.86	123 49.10	13.3
J8010	38	100280	46 15.75	123 48.98	19.8
J8010	37	100280	46 15.70	123 48.93	17.9
J8010	36	100280	46 15.42	123 48.69	6.0
J8010	35	100280	46 15.30	123 48.48	9.1
J8010	34	100280	46 15.24	123 48.33	18.7
J8010	33	100280	46 15.09	123 48.15	23.2
J8010	32	100280	46 15.01	123 48.13	35.3
J8010	29	100280	46 14.91	123 47.96	12.9
J8010	28	100280	46 14.88	123 47.91	8.9
J8010	27	100280	46 14.53	123 47.63	12.9
J8010	26	100280	46 14.47	123 47.61	16.4
J8010	25	100280	46 14.35	123 47.53	6.9
J8010	24	100280	46 14.36	123 47.51	6.9
J8010	23	100280	46 13.02	123 47.96	1.4
J8010	22	100280	46 13.95	123 47.25	-0.2
J8010	21	100280	46 13.93	123 47.04	2.3
J8010	20	100280	46 13.79	123 47.00	6.9
J8010	19	100280	46 13.78	123 47.02	12.8
J8010	18	100280	46 13.74	123 47.06	24.2
J8010	17	100280	46 13.72	123 47.01	11.7
J8010	16	100280	46 13.72	123 47.01	6.6
J8010	15	100280	46 13.69	123 47.00	1.0
J8010	14	100280	46 13.37	123 46.68	12.4
J8010	13	100280	46 13.32	123 46.63	23.3
J8010	12	100280	46 13.27	123 46.60	31.2
J8010	11	100280	46 13.24	123 46.39	38.7
J8010	10	100280	46 13.08	123 46.38	46.1
J8010	9	100280	46 13.03	123 46.22	59.1
J8010	8	100280	46 12.82	123 46.30	50.0
J8010	7	100280	46 12.69	123 46.39	42.0
J8010	6	100280	46 12.65	123 46.28	33.9
J8010	5	100280	46 12.56	123 46.32	23.9
J8010	4	100280	46 12.46	123 46.30	16.4
J8010	3	100280	46 12.41	123 46.23	10.9
J8010	2	100280	46 12.31	123 46.29	0.6
J8010	1	100280	46 12.29	123 46.30	-0.5
J8010	88	100380	46 14.78	123 43.25	2.7

J8010	87	100380	46	14.88	123	43.21	6.7
J8010	86	100380	46	15.00	123	43.15	12.2
J8010	85	100380	46	14.89	123	43.10	10.7
J8010	84	100380	46	15.06	123	43.15	2.0
J8010	83	100380	46	15.26	123	43.23	2.0
J8010	82	100380	46	15.36	123	43.20	2.9
J8010	81	100380	46	15.38	123	43.22	8.4
J8010	80	100380	46	15.53	123	43.28	19.3
J8010	79	100380	46	15.58	123	43.34	7.2
J8010	78	100380	46	15.58	123	43.25	3.2
J8010	77	100380	46	15.81	123	43.29	3.0
J8010	76	100380	46	15.78	123	43.20	8.9
J8010	75	100380	46	15.79	123	43.13	1.6
J8010	74	100380	46	15.87	123	43.15	8.5
J8010	73	100380	46	15.88	123	43.12	15.3
J8010	72	100380	46	15.89	123	43.12	12.2
J8010	71	100380	46	15.96	123	43.10	1.1
J8010	70	100380	46	16.15	123	42.99	7.0
J8010	69	100380	46	16.18	123	42.99	14.4
J8010	68	100380	46	16.28	123	42.97	7.8
J8010	67	100380	46	16.48	123	42.88	1.6
J8010	66	100380	46	16.57	123	42.89	6.6
J8010	65	100380	46	16.69	123	42.85	17.4
J8010	64	100380	46	16.76	123	42.86	19.1
J8010	63	100380	46	16.87	123	42.94	2.0
J8010	62	100380	46	16.97	123	42.88	13.4
J8010	61	100380	46	17.22	123	42.89	7.8
J8010	60	100380	46	17.25	123	42.91	9.6
J8010	59	100380	46	17.27	123	43.00	23.3
J8010	58	100380	46	17.30	123	42.97	12.2
J8010	57	100380	46	17.34	123	42.98	5.2
J8010	56	100380	46	17.45	123	42.92	2.1
J8010	55	100380	46	17.43	123	42.88	2.1
J8010	54	100380	46	17.45	123	42.89	4.6
J8010	53	100380	46	17.50	123	42.85	2.6
J8010	52	100380	46	17.62	123	42.92	0.7
J8010	51	100380	46	17.78	123	42.94	1.3
J8010	50	100380	46	17.90	123	42.97	11.9
J8010	49	100380	46	17.95	123	42.97	-0.4
J8010	89	100480	46	10.02	123	53.36	-0.1
J8010	90	100480	46	10.29	123	53.37	1.2
J8010	91	100480	46	10.56	123	53.33	3.6
J8010	92	100480	46	10.82	123	53.35	2.3
J8010	93	100480	46	10.95	123	53.34	11.1
J8010	94	100480	46	11.05	123	53.32	18.1
J8010	95	100480	46	11.15	123	53.32	27.9
J8010	96	100480	46	11.39	123	53.76	38.1
J8010	97	100480	46	11.42	123	53.71	41.9
J8010	98	100480	46	11.55	123	53.65	35.3
J8010	99	100480	46	11.59	123	53.67	29.7
J8010	100	100480	46	11.91	123	53.81	20.1
J8010	101	100480	46	11.96	123	54.01	11.5
J8010	102	100480	46	12.02	123	54.09	5.5
J8010	103	100480	46	12.19	123	54.61	-2.1

J8010	104	100480	46 12.29	123 53.06	-2.2
J8010	105	100580	46 12.23	123 54.26	-1.6
J8010	106	100580	46 12.47	123 54.17	0.4
J8010	107	100580	46 12.54	123 54.11	5.5
J8010	108	100580	46 12.57	123 54.15	11.1
J8010	109	100580	46 12.71	123 54.13	2.1
J8010	110	100580	46 12.77	123 54.14	6.2
J8010	111	100580	46 12.84	123 54.11	19.3
J8010	112	100580	46 13.00	123 54.12	6.3
J8010	113	100580	46 13.03	123 54.06	4.4
J8010	114	100580	46 13.15	123 54.08	7.0
J8010	115	100580	46 13.47	123 54.01	15.7
J8010	116	100580	46 13.60	123 54.07	12.4
J8010	117	100580	46 13.77	123 53.91	20.0
J8010	118	100580	46 13.87	123 53.95	25.0
J8010	119	100580	46 13.97	123 54.01	36.1
J8010	120	100580	46 14.04	123 53.98	48.7
J8010	121	100580	46 14.19	123 53.93	58.5
J8010	122	100580	46 14.27	123 53.95	52.6
J8010	123	100580	46 14.37	123 53.85	44.1
J8010	124	100580	46 14.43	123 53.89	35.5
J8010	125	100580	46 14.54	123 53.79	22.7
J8010	126	100580	46 14.17	123 54.52	18.7
J8010	127	100580	46 14.17	123 54.68	13.5
J8010	128	100580	46 14.18	123 54.79	2.9
J8010	129	100580	46 14.88	123 51.86	1.5
J8010	130	100580	46 14.83	123 51.86	3.8
J8010	131	100580	46 14.76	123 51.80	11.9
J8010	132	100580	46 14.74	123 51.79	17.9
J8010	133	100580	46 14.72	123 51.75	24.0
J8010	134	100580	46 14.70	123 51.81	32.1
J8010	135	100580	46 14.67	123 51.82	43.1
J8010	136	100580	46 14.56	123 51.74	43.2
J8010	137	100580	46 14.45	123 51.73	47.2
J8010	138	100580	46 14.24	123 51.74	34.3
J8010	139	100580	46 14.07	123 51.60	26.3
J8010	140	100580	46 14.00	123 51.51	19.3
J8010	141	100580	46 14.12	123 51.41	14.4
J8010	142	100580	46 14.11	123 51.38	5.9
J8010	143	100580	46 14.09	123 51.38	2.9
J8010	144	100580	46 14.01	123 51.21	6.4
J8010	145	100580	46 13.81	123 51.12	14.9
J8010	146	100580	46 13.63	123 51.06	20.4
J8010	164	100680	46 14.29	123 41.89	0.9
J8010	163	100680	46 14.32	123 41.91	2.5
J8010	162	100680	46 14.35	123 41.94	9.0
J8010	161	100680	46 14.39	123 42.02	14.7
J8010	160	100680	46 14.41	123 42.09	24.8
J8010	159	100680	46 14.43	123 42.05	30.0
J8010	158	100680	46 14.45	123 42.12	40.1
J8010	157	100680	46 14.53	123 42.25	55.2
J8010	156	100680	46 14.58	123 42.33	45.3
J8010	155	100680	46 14.57	123 42.42	40.0
J8010	154	100680	46 14.64	123 42.52	36.1

J8010	153	100680	46	14.73	123	42.62	37.7
J8010	152	100680	46	14.80	123	42.86	21.9
J8010	151	100680	46	14.84	123	43.03	13.6
J8010	150	100680	46	14.89	123	43.08	4.9
J8010	149	100680	46	15.09	123	43.37	3.1
J8010	148	100680	46	15.14	123	43.37	4.8
J8010	147	100680	46	15.16	123	43.40	10.4
J8010	165	100680	46	14.67	123	41.41	24.7
J8010	166	100680	46	14.68	123	41.37	17.0
J8010	167	100680	46	14.66	123	41.39	12.9
J8010	168	100680	46	14.62	123	41.34	0.2
J8010	169	100680	46	14.60	123	41.33	11.3
J8010	170	100680	46	14.61	123	41.41	16.7
J8010	171	100680	46	14.58	123	41.30	17.7
J8010	172	100680	46	14.51	123	41.36	37.1
J8010	173	100680	46	14.42	123	41.36	25.5
J8010	174	100680	46	14.31	123	41.30	18.5
J8010	175	100680	46	14.30	123	41.34	6.3
J8010	176	100680	46	14.26	123	41.35	0.4
J8010	177	100680	46	14.08	123	41.36	0.0
J8010	178	100680	46	13.88	123	41.42	0.4
J8010	179	100680	46	13.83	123	41.38	5.8
J8010	180	100680	46	13.82	123	41.39	10.2
J8010	181	100680	46	13.81	123	41.39	14.6
J8010	182	100680	46	13.76	123	41.41	20.5
J8010	183	100680	46	13.74	123	41.37	33.3
J8010	184	100680	46	13.69	123	41.41	16.7
J8010	185	100680	46	13.58	123	41.35	9.0
J8010	186	100680	46	13.50	123	41.37	3.9
J8010	187	100680	46	13.38	123	41.36	-2.8
J8010	188	100680	46	13.17	123	41.19	6.7
J8010	189	100680	46	13.17	123	41.13	-1.3
J8010	190	100680	46	12.93	123	41.25	0.6
J8010	191	100680	46	12.99	123	41.16	3.6
J8010	192	100680	46	13.07	123	41.11	9.6
J8010	193	100680	46	12.98	123	41.35	3.6
J8010	194	100680	46	12.88	123	41.42	11.1
J8010	195	100680	46	12.85	123	41.35	15.6
J8010	196	100680	46	12.85	123	41.41	12.7
J8010	197	100680	46	12.83	123	41.39	7.7
J8010	198	100680	46	12.77	123	41.40	-0.3
J8010	199	100680	46	12.57	123	41.42	3.7
J8010	200	100680	46	12.31	123	41.57	-0.2
J8010	201	100680	46	12.26	123	41.59	7.9
J8010	202	100680	46	12.27	123	41.63	11.4
J8010	203	100680	46	12.26	123	41.62	18.0
J8010	204	100680	46	12.25	123	41.62	23.0
J8010	205	100680	46	12.24	123	41.61	29.1
J8010	206	100680	46	12.24	123	41.62	45.2
J8010	207	100680	46	12.18	123	41.62	66.2
J8010	208	100680	46	12.18	123	41.69	50.8
J8010	209	100680	46	12.17	123	41.69	29.4
J8010	210	100680	46	12.16	123	41.68	23.5
J8010	211	100680	46	12.16	123	41.70	15.5

J8010	212	100680	46	12.13	123	41.72	12.1
J8010	213	100680	46	12.00	123	41.83	2.3
J8010	214	100680	46	11.98	123	41.85	-1.6
J8010	215	100680	46	11.96	123	41.98	4.0
J8010	216	100680	46	11.91	123	41.96	-1.4
J8010	217	100680	46	11.82	123	42.09	1.3
J8010	218	100680	46	11.81	123	42.08	7.0
J8010	219	100680	46	11.46	123	41.88	-1.3
J8010	220	100680	46	10.37	123	41.70	8.0
J8010	221	100680	46	10.30	123	41.72	11.1
J8010	222	100680	46	10.27	123	41.87	1.7
J8010	223	100680	46	10.31	123	43.33	8.9
J8010	224	100780	46	16.14	124	1.18	9.0
J8010	225	100780	46	16.07	124	1.18	12.9
J8010	226	100780	46	15.83	124	1.19	26.8
J8010	227	100780	46	15.73	124	1.21	41.7
J8010	228	100780	46	15.63	124	1.18	56.5
J8010	229	100780	46	15.53	124	1.18	66.7
J8010	230	100780	46	15.25	124	1.00	88.7
J8010	231	100780	46	15.06	124	1.13	68.6
J8010	232	100780	46	14.97	123	57.25	95.3
J8010	233	100780	46	14.77	123	57.23	49.3
J8010	234	100780	46	14.66	123	57.23	38.3
J8010	235	100780	46	14.43	123	57.26	29.3
J8010	236	100780	46	14.31	123	57.22	36.6
J8010	237	100780	46	14.22	123	57.27	50.3
J8010	238	100780	46	14.12	123	57.28	28.4
J8010	239	100780	46	13.80	123	57.25	14.5
J8010	240	100780	46	13.56	123	57.37	18.5
J8010	241	100780	46	13.52	123	57.42	19.6
J8010	242	100780	46	13.36	123	57.61	32.7
J8010	243	100780	46	13.27	123	57.65	48.8
J8010	244	100780	46	13.20	123	57.78	43.9
J8010	245	100780	46	13.14	123	57.86	36.9
J8010	246	100780	46	13.05	123	57.92	28.0
J8010	247	100780	46	12.95	123	57.97	19.1
J8010	248	100780	46	12.90	123	57.99	13.2
J8010	249	100780	46	12.76	123	58.06	7.8
J8010	250	100780	46	12.73	123	58.15	1.4
J8010	251	100780	46	13.61	123	50.97	14.3
J8010	252	100780	46	13.60	123	50.96	6.4
J8010	253	100780	46	13.59	123	50.92	-1.5
J8010	255	100780	46	13.44	123	50.88	0.7
J8010	256	100780	46	13.38	123	50.85	5.3
J8010	257	100780	46	13.17	123	50.73	12.5
J8010	258	100780	46	13.12	123	50.71	9.9
J8010	259	100780	46	13.04	123	50.67	15.2
J8010	260	100780	46	12.97	123	50.59	12.5
J8010	261	100780	46	12.92	123	50.56	11.7
J8010	262	100780	46	12.88	123	50.53	13.3
J8010	263	100780	46	12.83	123	50.58	19.5
J8010	264	100780	46	12.67	123	50.34	7.8
J8010	265	100780	46	12.61	123	50.25	3.4
J8010	266	100780	46	12.56	123	50.26	0.5

J8010	267	100780	46	12.44	123	50.19	1.2
J8010	268	100780	46	12.35	123	50.12	1.8
J8010	269	100780	46	12.16	123	50.08	9.9
J8010	270	100780	46	12.03	123	50.08	22.0
J8010	271	100780	46	11.86	123	50.13	37.2
J8010	272	100780	46	11.78	123	50.20	61.4
J8010	273	100780	46	11.65	123	50.02	78.5
J8010	274	100780	46	11.60	123	49.95	62.7
J8010	303	100880	46	16.17	123	56.85	-0.1
J8010	304	100880	46	16.02	123	56.88	1.9
J8010	305	100880	46	15.98	123	56.94	1.4
J8010	306	100880	46	15.88	123	56.93	-0.6
J8010	308	100880	46	15.17	123	57.08	20.1
J8010	309	100880	46	15.12	123	57.21	24.7
J8010	310	100880	46	15.19	123	57.04	13.8
J8010	311	100880	46	15.30	123	57.03	7.8
J8010	294	100880	46	17.75	124	0.31	2.3
J8010	291	100880	46	18.27	124	0.14	-1.6
J8010	292	100880	46	18.30	123	59.65	0.3
J8010	293	100880	46	18.08	123	59.81	1.1
J8010	295	100880	46	17.66	124	0.38	-0.4
J8010	296	100880	46	17.55	124	0.52	2.0
J8010	297	100880	46	17.44	124	0.67	3.9
J8010	298	100880	46	17.37	124	0.71	8.8
J8010	299	100880	46	17.36	124	0.76	13.2
J8010	300	100880	46	17.29	124	0.82	8.6
J8010	301	100880	46	17.25	124	0.83	1.6
J8010	302	100880	46	17.14	124	0.97	-2.5
J8010	290	100880	46	17.35	123	58.16	-1.2
J8010	289	100880	46	17.25	123	58.35	1.0
J8010	288	100880	46	17.09	123	58.49	0.3
J8010	287	100880	46	17.01	123	58.60	3.5
J8010	286	100880	46	16.73	123	58.91	-0.7
J8010	285	100880	46	16.65	123	59.07	2.1
J8010	284	100880	46	16.36	123	59.58	4.8
J8010	283	100880	46	16.30	123	59.60	5.9
J8010	282	100880	46	16.14	123	59.93	11.6
J8010	281	100880	46	16.07	123	59.95	22.3
J8010	280	100880	46	16.05	123	59.98	36.5
J8010	279	100880	46	16.01	124	0.07	26.2
J8010	278	100880	46	16.00	124	0.08	18.8
J8010	277	100880	46	15.99	124	0.08	11.9
J8010	276	100880	46	15.98	124	0.09	7.0
J8010	275	100880	46	16.00	124	0.11	1.1
J8010	354	101180	46	12.25	123	25.97	-3.2
J8010	355	101180	46	12.17	123	26.00	1.9
J8010	356	101180	46	12.15	123	25.98	20.9
J8010	357	101180	46	12.14	123	26.00	30.5
J8010	358	101180	46	12.13	123	26.04	20.5
J8010	359	101180	46	12.02	123	26.02	19.1
J8010	360	101180	46	12.06	123	26.18	13.2
J8010	361	101180	46	11.93	123	26.02	-2.8
J8010	345	101180	46	12.68	123	25.24	-1.4
J8010	347	101180	46	12.71	123	25.34	18.1

J8010	346	101180	46	12.71	123	25.29	10.6
J8010	348	101180	46	12.68	123	25.40	56.6
J8010	349	101180	46	12.70	123	25.47	44.6
J8010	350	101180	46	12.71	123	25.60	41.6
J8010	351	101180	46	12.75	123	25.67	36.7
J8010	352	101180	46	12.70	123	25.77	16.2
J8010	353	101180	46	12.67	123	25.86	-0.3
J8010	344	101180	46	12.70	123	25.09	-1.6
J8010	343	101180	46	12.71	123	25.06	2.6
J8010	342	101180	46	12.68	123	25.09	11.2
J8010	341	101180	46	12.66	123	25.10	22.3
J8010	340	101180	46	12.72	123	25.04	39.4
J8010	339	101180	46	12.79	123	24.97	25.5
J8010	338	101180	46	12.76	123	24.99	17.6
J8010	337	101180	46	12.74	123	24.90	19.9
J8010	336	101180	46	12.73	123	24.92	24.6
J8010	335	101180	46	12.83	123	24.80	17.6
J8010	334	101180	46	12.81	123	24.78	21.3
J8010	333	101180	46	12.85	123	24.71	16.2
J8010	332	101180	46	12.86	123	24.70	25.4
J8010	330	101180	46	9.79	123	19.70	20.7
J8010	329	101180	46	9.76	123	19.66	17.3
J8010	328	101180	46	9.70	123	19.77	11.9
J8010	327	101180	46	9.68	123	19.77	11.9
J8010	326	101180	46	9.63	123	19.82	13.9
J8010	325	101180	46	9.59	123	19.81	19.9
J8010	324	101180	46	9.61	123	19.82	21.9
J8010	323	101180	46	9.55	123	19.84	21.8
J8010	312	101180	46	8.43	123	18.75	2.6
J8010	313	101180	46	8.44	123	18.72	9.5
J8010	314	101180	46	8.44	123	18.70	21.6
J8010	315	101180	46	8.46	123	18.77	38.3
J8010	316	101180	46	8.50	123	18.81	52.0
J8010	317	101180	46	8.65	123	18.89	39.1
J8010	318	101180	46	8.80	123	18.92	31.3
J8010	319	101180	46	8.80	123	18.98	28.8
J8010	320	101180	46	8.82	123	18.94	27.9
J8010	321	101180	46	8.92	123	18.95	17.4
J8010	322	101180	46	8.95	123	18.94	0.5
J8010	363	101280	46	15.71	123	33.39	2.0
J8010	364	101280	46	15.70	123	33.40	6.5
J8010	365	101280	46	15.71	123	33.36	15.1
J8010	366	101280	46	15.67	123	33.30	34.1
J8010	367	101280	46	15.47	123	33.26	23.2
J8010	368	101280	46	15.45	123	33.24	23.7
J8010	369	101280	46	15.42	123	33.22	16.3
J8010	370	101280	46	15.36	123	33.21	11.3
J8010	371	101280	46	15.31	123	33.18	17.3
J8010	372	101280	46	15.32	123	33.14	33.3
J8010	373	101280	46	15.21	123	33.11	52.8
J8010	374	101280	46	15.25	123	33.11	48.4
J8010	376	101280	46	14.96	123	32.88	22.4
J8010	377	101280	46	14.90	123	32.83	13.4
J8010	378	101280	46	14.90	123	32.84	19.3

J8010	379	101280	46	14.89	123	32.84	30.3
J8010	381	101280	46	14.87	123	32.85	51.2
J8010	382	101280	46	14.86	123	32.81	40.7
J8010	383	101280	46	14.85	123	32.80	30.6
J8010	384	101280	46	14.83	123	32.79	16.1
J8010	385	101280	46	14.83	123	32.84	9.0
J8010	386	101280	46	14.82	123	32.82	1.9
J8010	380	101280	46	14.89	123	32.85	38.3
J8010	388	101280	46	15.63	123	36.21	10.0
J8010	389	101280	46	15.63	123	36.22	22.8
J8010	390	101280	46	15.62	123	36.20	32.7
J8010	391	101280	46	15.47	123	36.19	49.4
J8010	392	101280	46	15.29	123	36.24	33.8
J8010	393	101280	46	15.10	123	36.22	14.3
J8010	394	101280	46	15.04	123	36.20	0.1
J8010	395	101280	46	15.00	123	36.20	13.9
J8010	396	101280	46	14.96	123	36.17	4.3
J8010	397	101280	46	14.87	123	36.08	5.0
J8010	398	101280	46	14.85	123	36.05	11.9
J8010	399	101280	46	14.77	123	35.99	17.8
J8010	400	101280	46	14.66	123	35.92	11.2
J8010	401	101280	46	14.62	123	35.89	5.0
J8010	402	101280	46	14.36	123	35.68	7.3
J8010	403	101280	46	14.31	123	35.64	8.3
J8010	404	101280	46	14.17	123	35.55	16.7
J8010	405	101280	46	14.12	123	35.50	23.7
J8010	406	101280	46	14.09	123	35.51	28.5
J8010	407	101280	46	13.91	123	35.41	22.4
J8010	408	101280	46	13.87	123	35.36	16.3
J8010	409	101280	46	13.83	123	35.28	4.2
J8010	410	101280	46	14.67	123	33.33	28.3
J8010	411	101280	46	14.66	123	33.15	14.7
J8010	412	101280	46	14.53	123	32.80	30.6
J8010	413	101280	46	14.50	123	32.73	27.1
J8010	414	101280	46	14.52	123	32.63	24.5
J8010	415	101280	46	14.27	123	32.20	3.5
J8010	416	101280	46	14.31	123	32.20	6.5
J8010	417	101280	46	14.20	123	32.20	13.6
J8010	418	101280	46	14.19	123	32.18	20.1
J8010	419	101280	46	14.24	123	32.11	18.7
J8010	420	101380	46	15.05	123	26.18	8.1
J8010	421	101380	46	15.06	123	26.22	26.5
J8010	422	101380	46	15.09	123	26.25	47.4
J8010	423	101380	46	15.06	123	26.32	68.2
J8010	424	101380	46	14.97	123	26.45	53.1
J8010	425	101380	46	14.92	123	26.57	34.0
J8010	426	101380	46	14.85	123	26.70	26.9
J8010	427	101380	46	14.80	123	26.77	13.3
J8010	428	101380	46	14.77	123	26.87	7.7
J8010	429	101380	46	14.71	123	27.00	0.6
J8010	430	101380	46	14.59	123	27.15	8.2
J8010	431	101380	46	14.40	123	27.73	7.6
J8010	432	101380	46	14.28	123	28.30	20.9
J8010	433	101380	46	14.16	123	28.51	26.8

J8010 434	101380	46 14.09	123 28.63	16.6
J8010 435	101380	46 13.64	123 28.50	1.1
J8010 436	101380	46 13.57	123 28.68	16.9
J8010 437	101380	46 13.61	123 28.67	17.8
J8010 443	101380	46 13.30	123 33.17	0.6
J8010 444	101380	46 13.32	123 33.23	25.6
J8010 445	101380	46 13.35	123 33.28	5.6
J8010 446	101380	46 13.35	123 33.32	12.6
J8010 447	101380	46 13.37	123 33.38	7.2
J8010 448	101380	46 13.38	123 33.43	-1.3
J8010 442	101380	46 13.41	123 28.41	1.2
J8010 441	101380	46 13.41	123 28.42	12.3
J8010 440	101380	46 13.38	123 28.46	21.9
J8010 439	101380	46 13.35	123 28.54	32.9
J8010 438	101380	46 13.32	123 28.60	27.5

APPENDIX B

Summary of Computer Programs Modified or Developed for the CREDDP Program

A variety of programs were written to manipulate and analyze the Columbia River Estuary data. An overall picture of the relationships among the programs and data files is presented in a system flowchart (Figure 72). In the system flowchart, data files are represented by boxes and programs are represented by circles. Inputs and outputs are shown by means of arrows. An arrow that points from a file to a program indicates an input, and an arrow that points from a program to a file indicates an output. Final outputs, printed on paper, are shown at the bottom of the flowchart.

Each program was run with a "macro", a list of system commands that accepts arguments and assigns input and output files to the logical unit numbers specified in each program. As a convention, most macros were named "Gpname," where "pname" was the name of the program. Attaching a "G" to the beginning of each program name to create the macroname facilitated use of this system.

All programs were written in Fortran 66 on a Harris/6 computer (Vulcan Operating System). The programs were designed for a 24-bit word size. All of the programs involving computation were tested on data sets or hand-checked to detect programming errors. The plotting routines utilized pen-plotter emulation subroutines to make plots on a dot-matrix line printer. The emulation subroutines were contained in a library called FASTER/RASTER, written by Adam Schultz, a Harris/6 user. All plotting programs allow the user to specify the plot size. Complete documentation and code for any of these programs is on file with the principal investigator, Dr. Joe S. Creager.

A summary of each program follows:

FRACT -- Purpose: To convert keypunched data to a form readable by SEDAN, PHI, and SIDAN.

-- Input: keypunched data, file name "F_____".

-- Output: "Z_____" file, sediment weight per phi size for each sample.

-- Source: Originally programmed by Linda S. Olund in July 1972. Modified by Linda S. Green in October 1980. Modified by Thomas W. Dempsey in August 1983.

SEDAN -- Purpose: (1) To generate a complete set of commonly used grain-size distribution parameters from sediment fractional weights in the FRACT output file.

(2) (Optional:) To plot the average sediment-size distribution of the samples.

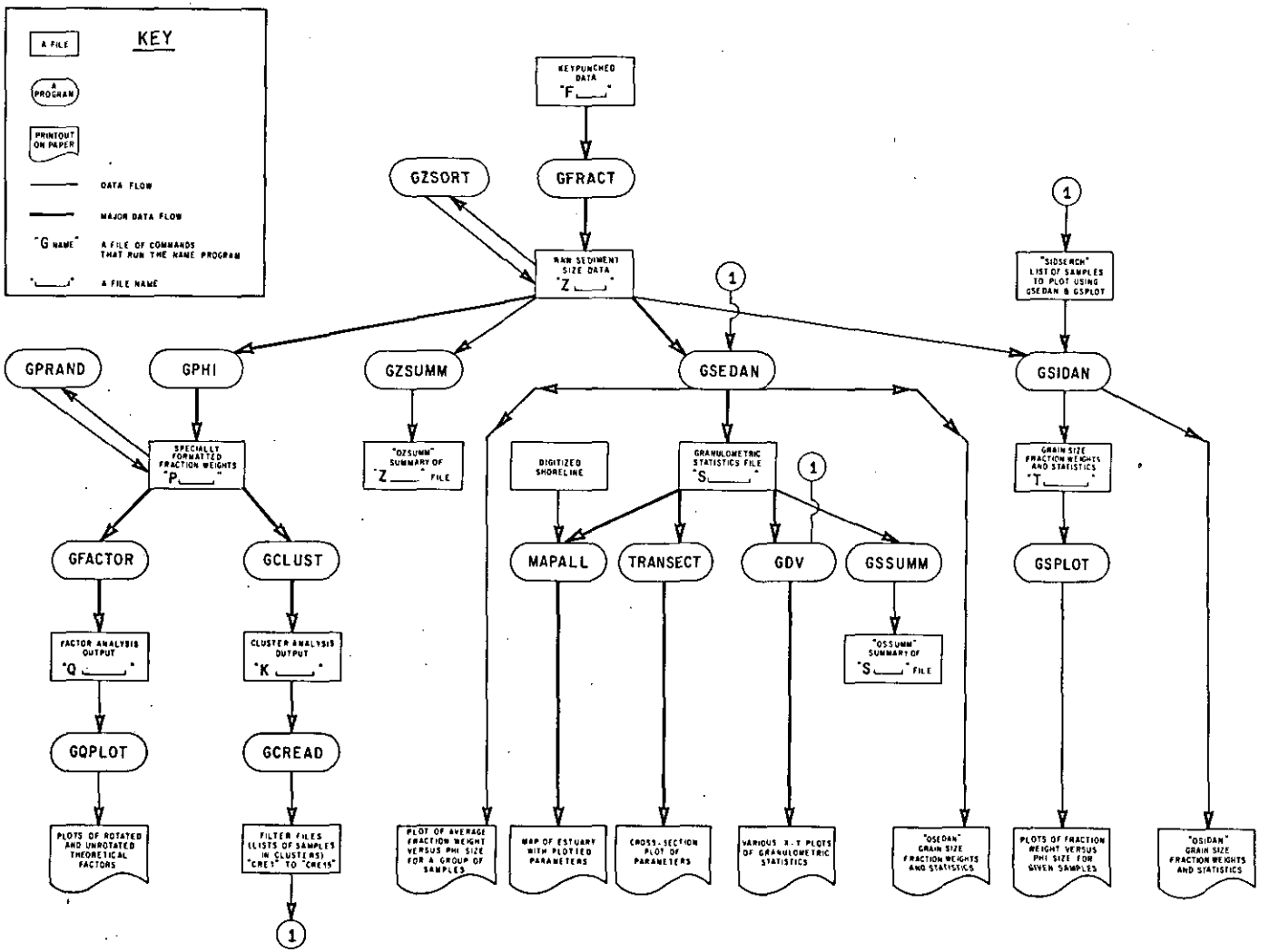

Figure 72. System flowchart of computer programs used in the CREDDP study.

-- Features: The standard SEDAN output contains all of the data pertaining to cruise, station number, extra identification, and location of the sample. It lists the fraction weight, fraction percent, and cumulative percent in each phi class, and prints the post-analytic weight. It further lists the percent of gravel sand, silt and clay in each sample and a number corresponding to Shepard (1954) class (Creager et al. 1962), as well as estimates the phi sizes of various percentiles. These estimates are obtained using either a linear interpolation or an Aitkens four-point interpolation, and the A or L beside the phi-size indicates which value was used (Creager et al. 1962). The computed grain-size parameters of Trask (Krumbein and Pettijohn, 1938), Inman (1952), and Folk and Ward (1957) are printed, as well as the computed moment measures (Krumbein and Pettijohn 1938; Blatt et al. 1972).

-- Input: (1) "Z_____" file from FRACT.

(2) (Optional:) A "filter file" (a list) of station identifiers to determine which stations to process. (Note that filter files of clusters from Cluster Analysis can be obtained by running the CREAD program.)

-- Output: (1) "S_____" file of grain size parameters.
(2) "OSEDAN" grain size parameters file that can be spooled to the printer for archiving.

(3) (Optional:) A plot of the average of the samples.

-- Source: Programmed by Paavo E. Kovala in December 1978. Modified by Linda S. Olund in October 1979 and October 1980. Modified by Thomas W. Dempsey in August 1983.

SIDAN -- Purpose: (1) To generate grain size parameters on selected samples and (2) to create a file of these samples which can be plotted using the SPLOT or SPLOTL programs.

-- Input: (1) "Z_____" file from FRACT.

(2) "SIDSERCH", a file of up to 100 station identifiers to search for in the "Z_____" file.

-- Output: (1) "T_____" file, which can be plotted with SPLOT or SPLOTL.

(2) "OSIDAN" grain size parameters file that can be spooled to the printer for achiving.

-- Source: Same as SEDAN.

SPLOT and
SPLOTL -- Purpose: To plot (1) Phi Size versus Sediment Fraction Weight and (2) Phi Size versus Cumulative Fraction Weight.

-- Comment: The GSPLOT macro runs both SPLOT and SPLOTL.

-- Input: "T_____" file output from SIDAN.

-- Output: Two plots per page, one page per sample. SPLOT plots the cumulative fraction according to the cumulative normal distribution; SPLOTL plots the cumulative fraction with a linear distribution.

-- Source: Written by Thomas W. Dempsey in August 1983.

DV -- Purpose: To print the following types of plots from "S_____" files:

(1) Mean phi size versus deviation.

(2) Modal phi size versus deviation.

(3) Median phi size versus phi size at 1% coarser.

(4) Mean phi versus phi value at 1% coarser.

(5) Depth versus mean and deviation.

(6) Depth versus mode and deviation.

(7) Depth versus median and deviation.

(8) Mean versus skewness and kurtosis.

(9) Skewness versus kurtosis and deviation.

(10) River mile versus mean and deviation.

(11) River mile versus mode and deviation.

(12) River mile versus median and deviation.

(13) River mile versus kurtosis and skewness.

-- Features: (1) Plots either Folk & Ward or Moment Statistics.

(2) Prints mean, variance, standard deviation, covariance, and correlation.

(3) Plots data within specified upper and lower depth limits and between river mile limits.

(4) Optionally plots a least-squares Nth-order polynomial curve fit to the data and prints the equation of the curve.

-- Input: (1) "S_____" file, output from SEDAN.

(2) "DVIN", or parameter file specified by the user: specifies plot label, depth range, river mile range, plot size factor, plot type, polynomial curve fit, etc.

(3) (Optional:) A filter file (a list) of sample identifiers to specify which samples to process.

-- Output: (1) Refer to the above output plot types.

(2) DVPRINT, contains plot statistics. This file is printed, and should be attached to the plot.

(3) DVREG, file containing statistics on the curve fit.

-- Source: Written by Thomas W. Dempsey and Christopher R. Sherwood, August 1983, utilizes some FORTRAN subroutines of Davis, 1973.

PHI -- Purpose: To convert "Z_____" file to fraction weights, and to specially format the resulting "P_____" file for input to the FACTOR or CLUST program.

-- Features: Optionally allows samples to be output only if they lie within a specified longitude window.

-- Input: "Z_____" file from FRACT.

-- Output: "P_____" file of sediment fraction weights, specially formatted for input to the FACTOR and CLUST programs.

-- Source: Written by Thomas W. Dempsey, August 1983.

PRAND -- Purpose: To randomly select a subset of PHI output files small enough to be FACTOR-analyzed or CLUSTER-analyzed.

-- Input: "P_____" file (output from PHI).

-- Output: Two "P_____" files, created by randomly sorting the input file into the two files.

-- Source: Written by Thomas W. Dempsey, August 1983.

FACTOR -- Purpose: To perform Q-mode Factor Analysis on a "P_____" file.

-- Input: "P_____" file, output from PHI or PRAND.

-- Output: "OFACTOR" or file specified by the user.

-- Source: Programmed by Jeffry C. Borgeld in March 1981, based upon Davis (1973, pp. 494-496). Modified by Thomas W. Dempsey, August 1983.

QPLOT -- Purpose: To plot a table of Factor Scores from the output of the FACTOR Analysis program.

-- Input: A table of Factor Scores extracted from the output of the FACTOR Analysis program.

-- Output: A plot of each theoretical factor on the Factor Scores table.

-- Source: Written by Thomas W. Dempsey, August 1983.

CLUST -- Purpose: To perform Cluster Analysis on a "P_____" file.

-- Features: Q- and R-mode analyses can both be performed, and three types of input similarity matrices can be specified: (1) Cosine Theta Coefficient, (2) Distance Coefficient, and (3) Correlation Coefficient Matrix.

-- Input: "P_____" file, output from PHI or PRAND.

-- Output: "OCLUST" or "K_____" file specified by the user.

-- Source: Programmed by Thomas W. Dempsey, based upon Davis (1973, pp. 467-473).

CREAD -- Purpose: To copy station identifiers from the CLUST Dendrogram into separate files based upon clusters correlated at less than a specified correlation. The resulting files can then be used as filter-files in SEDAN to plot the average of each cluster.

-- Input: "K_____" or "OCLUST" output file from CLUST.

-- Output: Up to 15 files containing station identifiers, where the files are numbered according to decreasing cluster size.

-- Source: Written by Thomas W. Dempsey, August 1983.

ZSUMM -- Purpose: To summarize the header records of FRACT output ("Z_____") files. Detects duplicate and non-ascending station numbers.

-- Input: "Z_____" file, output from FRACT.

-- Output: "OZSUMM" is default, user-defined output file names can be specified.

-- Source: Written by Thomas W. Dempsey, August 1983.

SSUMM -- Purpose: To summarize the header records of SEDAN output files.

-- Input: "S_____" file, output from SEDAN.

-- Output: "OSSUMM" is default, user-defined output file names can be specified.

-- Source: Written by Thomas W. Dempsey, August 1983.

ZSORT -- Purpose: To sort and reorder FRACT output ("Z_____") files by ascending cruise and station number.

-- Input: "Z_____" file, output from FRACT.

-- Output: "OZSORT" is default, but you can specify an output file name of your own.

-- Source: Written by Thomas W. Dempsey, August 1983.

MAPALL -- Purpose: General purpose mapping package designed for CREDDP and antecedent data. Plots data location symbols and associated text or numbers.

-- Features: (1) Permits plotting of any scale on a: a) Mercator projection, b) Oregon North state-plane projection, c) UTM projection.

(2) Includes 12,000 point digitized Columbia River Estuary shoreline.

(3) Plots any one of nine standard sub-areas of the estuary or any specified latitude/longitude box.

(4) Plots all standard SEDAN-generated sediment grain size parameters, and some combinations, with numbers, symbols, or both, as well as current-meter and tide gauge locations, depths, or other parameters.

(5) Produces files of stations plotted and their plotted parameters, as well as stations not plotted.

-- Input: (1) "S____" file of grain size parameters from SEDAN, or other suitably formated data file containing latitude, longitude, and various parameters.

(2) Digitized shoreline
(3) MAPIN file with requested map options.
-- Output: (1) Printer file with generated map.

(2) MAPOUT file with plotted stations, option information and error messages.

(3) MAPOZ file with stations not plotted.

-- Source: Written by Christopher R. Sherwood, June 1983.

TRANS -- Purpose: Collapses all sediment data between specified longitudes to a single transect and plots chosen sediment parameter at appropriate depth in cross-section format.

-- Features: (1) Plots at any scale and collapses data from any longitude range.

(2) Plots any of the parameters generated by SEDAN.

-- Input: "S____" file at grain size parameters.

-- Output: Cross-section plot.

-- Source: Programmed by Christopher R. Sherwood, August 1983.

File names on the HARRIS/6 computer can be from one to eight characters long. For convenience in file maintenance, certain types of files for the user "6DEMP" were named consistently with the same first letter.

The following data files have the indicated naming conventions:

"F_____" = FRACT input files (stored on tape as of 4/29/83)

"K_____" = CLUST (cluster analysis) output file.

"P_____" = PHI output file; FACTOR and CLUST input file.

"Q_____" = FACTOR analysis output file.

"S_____" = SEDAN output file (condensed form); DV, SSUMM, and MAPALL input file.

"T_____" = SIDAN output file; SPLOT or SPLOTL input file.

"Z_____" = FRACT output file; input file to PHI, SEDAN, SIDAN, ZSUMM, and ZSORT.

Below are some examples of the conventions used for filling "_____", the seven characters following the first letter:
_1234567 = "_" is first letter, as defined above; "1234567" is the remaining seven characters.

_A7910ST = cruise A7910, Settling Tube analysis
_A7910SV = cruise A7910, SieVe analysis
_Z7910R = cruise Z7910, sediments analyzed by Roy.
_Z7910L = cruise Z7910, sediments analyzed by Lee.
_Z7910C = cruise Z7910, sediments analyzed by Campbell.
_BIO83 = sediments analyzed in '83 for BIOlogists.
_BIOBAK = sediments analyzed by BAKer for BIOlogists.

The following non-data files have the indicated naming conventions:

"Cpname" = A macro that can be streamed (JS Cpname) to compile and vulcanize the Fortran program sourcecode "pname" into the executable code "Xpname".

"Epname" = The file assigned in the "OUT=Epname" statement in batch jobs, which are called "Ipname".

"Gpname" = A macro that can be invoked (Gpname arg1 arg2 ... argN) to run the Fortran program Xpname.

"Ipname" = A macro that can be inserted into the control point queue (IJ Ipname) to run a job in batch mode.

"Lpname" = Output file assigned to LFN 6 (AS 6=Lpname). Note that when a program is compiled with the FO.W (Walkback) option, LFN 6 should be assigned to receive Walkback error messages.

"Opname" = An output file of program "pname".

"Xpname" = The executable code of the sourcecode program "pname".

APPENDIX C

Analysis of Historical Changes in the Columbia River Estuary

C.1 HISTORICAL CHANGE IN THE COLUMBIA RIVER ESTUARY

Human influence on the physical environment of the Columbia River Estuary began about fifty years after the arrival of the first white settlers. Although native populations had lived and fished in the area for centuries, it was not until the construction of the salmon canneries and the beginning of lumber exports in the 1840's and 1850's that men and women began to shape the estuary to their own needs (Oregon Historical Society 1980). Until 1885, human influence on the morphology of the estuary was probably negligible; it was confined to the construction of pilings, weirs, and some sporadic scrape-dredging of the bars. In 1885, however, construction of the South Jetty began, and a new era in the evolution of the estuary was inaugurated.

Several surveys made previous to 1885 establish the dynamic nature of the entrance to the estuary before the construction of the entrance jetties. Shifting shoals and channels occupied the entrance regions. Early charts (collected by the Oregon Historical Society 1980) and descriptions of the entrance region (U.S. Army Corps of Engineers 1903; Moore and Hickson 1939; Lockett 1962, 1963; Borgeld et al. 1978) indicate that in various years, either one or two main channels crossed the tidal delta (the "bar"). The earliest survey by Vancouver in 1792 shows a single channel, but by the time of the 1839 survey by Belcher, two channels existed, separated by an intertidal sand body seaward of Clatsop Spit (Middle Sands) which was connected to the Sand Island immediately landward of the entrance. The entrance morphology changed continuously through 1880, but two channels existed across the tidal delta for the entire period. During this time, Clatsop Spit prograded north and west, forcing the South Channels and Sand Island north. In 1868, the South Channel was well suited for navigation, but by 1881, the continued northward migration of the South Channel had caused the two channels to merge, creating a single broad, shallow channel across the delta. Clatsop Spit was eroded and lost elevation during the same time. The end result of these changes was that the best channel across the delta provided only 5.8 m (19 ft) of depth at the time of the 1881 survey.

The Board of Engineers prepared the plans for an improvement project in 1882, and construction of the original South Jetty began in 1885. There was little effect on the entrance region in the first four years, but beginning in 1889, the channel across the tidal delta began to swing north and deepen until, in 1895, a depth of 10.6 m (35 ft) was obtained. However, the channel continued to swing north and began to shoal, and by 1902, the channel had broadened and bifurcated, again creating two channels across the outer tidal delta. At this point, the best channel into the estuary was only 6.7 m (22 ft) deep and plans for the

extension of the South Jetty and construction of the North Jetty were initiated.

Construction of the South jetty extension began in 1903 and was completed in 1914. The North Jetty was begun in 1913 and completed in 1917, and dredging of the entrance channels began in 1903. Rapid changes in the channel occurred as a result of the jetty construction and the dredging (Hickson 1922). Subsequent rehabilitation of the jetties, construction of Jetty A and the Sand Island dikes in 1939, and dredging associated with increases in the project depth of the entrance channel have resulted in further modifications to the morphology of the entrance region (Lockett 1962, 1963; Borgeld et al. 1978).

While these changes were occurring near the entrance as a result of jetty construction, the upriver channels were being modified by the construction of pile dikes and dredging. In the upper estuary, the complex channel system was gradually replaced by a single large channel. Previously important channels such as Cordell Channel and Cathlamet Channel were isolated from the main flow by pile dikes, and bars in the main channel were removed by dredging. The greatest changes occurred during the initial development of the river for navigation; by 1935 the 10.7 m (35 ft) river channel had been obtained. Concurrent with the channel modifications and continuing into the 1940's, extensive diking of marsh and swampland occurred in the estuary and lower reaches of the river. Thomas (1983) indicates that a total of 1.2×10^8 m^2 (30,000 acres) of estuarine wetland (tidal swamps and tidal marshes) has been lost by diking and filling activities.

Meanwhile, development was ongoing in the drainage basin and upper reaches of the Columbia River, affecting the river discharge and possibly the sediment load. Beginning in the 1840's, water was diverted for irrigation, and beginning with the construction of the first major dam on the main stem of the Columbia (the Rock Island Dam, in 1933) changes in the hydrology of the river were effected.

A chronology of many of the important developments in the river and estuary system is listed in Table 17. This table has been compiled from a variety of sources and is presented here as a brief history of the physical changes that have altered the form of the estuary.

Table 17

Chronology of important events affecting the physical evolution of the Columbia River Estuary

1792	Captain George Vancouver commanding sent Lt. Broughton to chart river and mouth: single entrance channel, controlling depth 8 m (27 ft); Robert Gray prepared harbor sketch.
1805	Lewis and Clark expedition arrived.
1811	Fort Astoria constructed by Pacific Fur Company.
1839	Sir Edward Belcher survey: two entrance channels, controlling depth 8 m (27 ft).
1840's	Irrigation began in Columbia River basin.
1841	Wilkes survey.
1844 to present	Log and lumber exports.
1849	Large June freshet.
1849 -1850	First USCGS bathymetric survey (Lt. Commander McArthur).
1850's	First salmon canneries.
1863	June freshet >26,900 m^3s^{-1} (950,000 cfs).
1867 -1877	USCGS survey of estuary and river.
1867	Dredging begun in Willamette River.
1868	First dikes in place in Youngs Bay.
1873 -1874	Dredging of the Hogsback bar, Cordell Channel.
1876	June freshet >27,180 m^3s^{-1} (960,000 cfs).
1877	Navigation channel from mouth to Vancouver/Portland approved by Congress.
1878	First current observations.
1880	June freshet >26,050 m^3s^{-1} (920,000 cfs); first scrape-dredging on bar.
1882	9 m (30 ft) entrance channel approved.
1883	Peak of cannery operations.

pre-1885	Only occasional dredging and a few training structures were employed to date.
mid-1880's	Minor dredging in Cordell Channel.
1885	South Jetty construction began.
1890	Cordell Channel no longer in use.
1890's	First pile dikes constructed in river channel.
1893	Snag Island dike (and Green Island and Marsh Island dikes?) built: Cordell Channel closed and flow diverted to North Channel.
1894	June freshet >33,980 m^3s^{-1} (1,2 kcfs); first extensive dredging (305,820 m^3, 400,000 yd^3) after freshet.
1895	6.8 km (4.25 mi) South Jetty completed with four groins; 9.5 m (31 ft) controlling depth in entrance channel; rock ledge near upper Astoria blasted.
1899	7.6 m (25 ft) river channel from mouth to Portland authorized.
1899-1902	Dredging across Upper Sands Shoal: navigation channel realigned.
1902	Three entrance channels, controlling depth 6.7 m (22 ft).
1903	Dredge Grant arrived.
1904	Dredge Chinook arrived.
1905	River and Harbor Act of 3 March 1905 approved 12.2 m (40 ft) Entrance Project, including extension of South Jetty.
1909	Grays River channel obstructions cleared.
1912	River and Harbor Act, 9.1 m (30 ft) channel authorized from Brookfield to Portland.
1913	North Jetty construction began; Cowlitz River channel dredged to 1.2 m (4 ft); Oregon slough dredged to 7.6 m (25 ft); Baker Bay (east) channel dredged to 3.4 m (11 ft).
1914	South Jetty extension completed; 7.3 m (24 ft) entrance channel obtained; extensive dredging and pile dike construction in Columbia River channel to Portland begins.
1917	North Jetty extension completed; 9.1 m (30 ft) channel authorized from mouth to Brookfield.
1918	Entrance channel controlling depth 12.2 m (40 ft).
1920	Skamokawa Creek channel cleared to 2 m (6.5 ft).

1924	Clatskanie River channel dredged to 1.8 m (6 ft).
1927	Entrance channel controlling depth 14.3 m (47 ft).
1928	Deep River channel cleared to 2.4 m (8 ft); 10.7 m (35 ft) river channel recommended.
1931	South Jetty rehabilitation begun; Lake River channel dredged to 1.8 m (6 ft).
1932	Chinook pile dike constructed; COE current survey at mouth.
1933	Rock Island Dam.
1934	Ilwaco (east) Channel completed (3.1 m, 10 ft).
1935	10.7 m (35 ft) Columbia River Channel completed; dikes along Columbia River completed, channel revision at Harrington Point completed; Multnomah channel completed (7.6 m, 25 f5); Cathlamet side channel (3.1 m, 10 ft) completed.
1935 -1939	USCGS bathymetric survey of estuary and river.
1936	Flood Control Act of 22 June 1936; extensive COE diking begun, largely completed by 1942; South Jetty rehabilitated (asphalt added); COE salinity measurements.
1938	Bonneville Dam; Youngs Bay channel cleared (3.1 m, 10 ft); North Jetty rehabilitation begun (concrete terminal and asphalt added).
1939	Jetty A completed; four Sand Island pile dikes completed; North Jetty rehabilitation completed; Skipanon channel dredged (9.1 m, 30 ft); Skipanon peninsula created with dredged material; Westport slough dredged (8.5 m, 28 ft); Elochoman slough dredged (3.1 m, 10 ft).
1939 -1955	Dredging at entrance confined to Clatsop Spit.
1940	Chinook Channel (3.1 m, 10 ft), mooring basin, and breakwaters completed.
1941	Grand Coulee Dam; concrete terminal added to South Jetty.
1942 -1945	Mott Basin dredged, Lois Island created/enlarged?
1944	Ilwaco (west) Channel mostly completed (3.1 m, 10 ft).
1945	Regular annual dredging (of outer bar?) initiated.
1947 -1958	USCGS bathymetric survey of estuary and river.

1948	June freshet >28,320 m^3s^{-1} (1 kcfs); Ilwaco (west) Channel (2.4 m, 8 ft) and three pile dikes (on larger Sand Island) completed.
1950	Flood Control Act of 17 May 1950; Astoria east boat basin completed.
1951	Channel alignment on Desdemona shoal.
1953	McNary Dam; fourth pile dike on larger Sand Island completed.
1954	River and Harbor Act of 3 September 1954: 14.6 m (48 ft) entrance channel project approved.
1955	Chief Joseph Dam.
1956	Begin dredging 14.6 m (48 ft) entrance channel.
1957	The Dalles Dam; Warrenton mooring basin (3.7 m, 12 ft) completed; Ilwaco (west) Channel (3.1 m, 10 ft) completed; 14.6 m (48 ft) entrance channel obtained.
1958	Westport slough cleared (8.5 m, 28 ft); Chinook harbor breakwaters extended; dredge material disposal Sites A and C abandoned, Site B used extensively.
1959	Priest Rapids Dam; COE current meter study.
1960	Cowlitz River channel dredged to 2.7 m (9 ft).
1961	Rocky Reach Dam; South Jetty and Jetty A rehabilitated.
1962	12.2 m (40 ft) Columbia River channel to RK-169 (RM-105) and 18.5 km (11.5 mi) up Willamette River authorized; completion of WES physical model of Columbia River.
1963	Wanapum Dam; prototype physical measurements initiated by WES.
1965	Radionuclide studies of estuary sediments
1966	Astoria-Megler Bridge completed, radionuclide studies of Columbia River sediments.
1967	Wells Dam.
1968	Mica Lake, Arrow Lake Dams.
1975	COE current meter studies.
1976	12.2 m (40 ft) river channel completed from mouth to Portland/Vancouver; Oregon slough deepened to 12.2 m (40 ft).
1977	15.9 m (52 ft) entrance project initiated; COE current meter studies.
1978	COE current meter studies.
1979	Initiation of CREDDP field work.

1980	Mt. St. Helens eruption and associated mudflows into the Columbia River at Kelso/Longview.
1980 -1983	5-11 million m^3 of material dredged from the Cowlitz/Columbia confluence.
1981	NOS current meter survey.
1982	Coal port channel (16.7-18.3 m, 55-60 ft) to Tongue Point (RM-18) proposed.

Sources: U.S. Army Engineers (1875, 1903), various Congressional documents (House of Representatives Document, 1899, 1900, 1917, 1919, 1921, 1946; House of Representatives Report, 1906; Senate Documents 1881, 1917), U.S. Army Corps of Engineers (1960), Lockett (1963, 1967), Oregon Historical Society (1980), Roy et al. (1982), George Blomberg (pers. communication), David Jay (pers. communication).

The following sections will summarize historical changes in estuarine volume and surface area and discuss the historical changes in the processes that act in the estuary, beginning with changes in the circulation and continuing with the effects on sedimentation.

C.2 CHANGES IN THE MORPHOLOGY OF THE ESTUARY

C.2.1 Causes

The substantial changes that have taken place in the structure of the estuary in historical time are the result of natural processes, human activity, and sedimentological responses to human activity. The dredging of material from channels and the transfer of dredged material into shallow water or onto land may be the least important cause of structural change in the estuary in terms of quantity of sediment. The natural response to the construction of permeable pile dikes and jetties, especially the jetties at the entrance, has probably caused the largest changes in the location of sediment in the estuarine system. The accumulation of sediment behind these dikes, and the associated scour of the adjacent river channel, has resulted in deeper channels and broader, shallower expanses of shallow intertidal and supratidal areas. Many previously important channels, such as Cordell Channel, Prairie Channel, Cathlamet Channel, and the channels of eastern Grays Bay have been isolated from the main flow by pile dikes and have subsequently shoaled. The processes that have caused these changes were anticipated by the Corps of Engineers (COE) in designing their "training" structures. They have taken advantage of the fact that in order for the river to maintain a relatively constant discharge in the face of an artificially reduced channel width, velocities must increase. In the absence of salinity intrusion effects, the resulting increased shear stresses cause erosion of sediment from the channel bottom until the increased depth compensates for the reduced channel width. The displaced sediment will move down-current to a regime of lower shear stress, where it will be deposited. For this reason the system of permeable pile dikes is highly effective, for it narrows the channel cross section and provides a protected region of lower current velocities that receives the displaced sediment. By judicious location of the dikes, the Corps of Engineers has avoided the task of physically moving most of the sediment from the channels. Dredging efforts have been concentrated on obtaining new project depths, channel realignments, and maintenance dredging on a finite number of troublesome bars.

The natural movement of sediment down the river channel has probably been greatly affected by 1) changes in sediment supply from the drainage basin of the Columbia River and its tributaries, 2) changes in the hydrographic regime of the

river, 3) removal of material from the river bed by dredging and by storage behind pile dikes, and 4) transitory increases in the transport rates immediately following the construction of new pile dikes. The net result of these effects is unknown; to date insufficient progress has been made in developing a sediment budget for the lower reaches of the river, and the individual contribution of each of these changes is not well understood. While increased agricultural and logging activity has probably accelerated erosion rates in the drainage basin of the Columbia River, sediment supply to the lower Columbia River may not have increased because of storage behind dams, removal from the system by dredging, and reduction in transport rates due to the damping of the hydrographic curve. On the other hand, Fullam (1969) argues that during high flow periods the mainstem dams of the Columbia River permit sediment to pass freely and analysis of flow regulation indicates that substantial damping of the discharge curve did not occur until about 1969 (David Jay, pers. communication). In fact, the effect of pile dike construction along the lower reaches of the river may have been to hasten transport of bed sediment down the river, producing an artificial and transient increase in sediment supply to the estuary. Regardless of whether the rate of sediment supply to the estuary from the river has been altered substantially in historic times, the river has undoubtedly been the primary source of sediments in the estuary, and the sediment budget of the lower reaches of the river will need to be examined in the future to completely interpret the results of sediment budget estimates in the estuary.

C.2.2 Measurements of Structural Changes

In order to approach the changes in the estuary quantitatively, the digitized bathymetric information compiled by Northwest Cartography, Inc., in the preparation of the Bathymetric Atlas (CREDDP 1983) was used. These data represent the most comprehensive collection of bathymetric data available for the Columbia River Estuary in a format suitable for comparison. Surveys from four composite periods were chosen for analysis:

> 1868: includes U.S. Coast and Geodetic Survey (USCGS) charts made between 1867 and 1873, before any major influences of jetty construction;
>
> 1935: includes USCGS surveys made between 1926 and 1937, post-dating jetty construction and coincident with construction of numerous pile dikes and channel alignments;
>
> 1958: includes USCGS surveys made between 1949 and 1958, post-dating the completion of the 14.6 m (48 ft) entrance channel but pre-dating the initiation

of the 12.2 m (40 ft) river channel and much of the flow regulation;

1982: includes COE surveys made between 1979-1982 and represents the most recent available bathymetry.

Great effort was made by Northwest Cartography, Inc. to compile the various surveys at identical scale relative to the same datum. The resulting suite of charts and differencing maps and the Bathymetric Atlas (CREDDP 1983) form the basis for the discussions in this chapter. Shalowitz (1964) guidelines were used in interpreting the surveys.

Calculations of surface area in each of several depth regimes were made utilizing the digitized bathymetric data. The estuary was subdivided into thirteen subareas on the basis of physical, geological, and biological criteria (Figure 73). Computer programs developed by Northwest Cartography, Inc., calculated the areas within each of fourteen depth intervals for each of the subareas (Table 18) using two methods. The first of these methods provided an approximation of the surface area over the actual topography of the bottom, while the second calculated the surface area projected onto a level plane (the "normal" surface area). The actual surface area is most appropriate in biological analyses requiring surface area estimates, but the normal area is more convenient in that it conserves area within the surveyed region from year to year regardless of any bathymetric changes. The two areas differ by less than 1% in all cases. The bathymetric data used in the analysis were interpolated onto a latitude-longitude grid which contained one bathymetric data point every 29 m along the north-south axis and every 21 m along the east-west axis. Areas calculated from this grid should not be considered accurate to more than ± 1000 m^2 (generally much less than 0.1% of the total area of the depth interval). Greater inaccuracies may be present in the original data as a result of the difficulties encountered during compilation of the historical bathymetric series. Northwest Cartography, Inc., considers the contours and shoreline accurate to within ±51 m. Although errors of up to 30% in the measurement of a 100,000 m^2 area could occur with uncompensated boundary displacements of 50 m, this is considered the maximum error involved in the calculations, and the much larger area of many of the polygons and internally consistent comparisons are likely to produce fairly precise numbers. The vertical control on the bathymetric data is considered reliable to within several centimeters in the estuary proper but degrades to ±.5 m in the upriver sections due to datum inconsistencies and runoff effects on river height. A bias toward the shallowest soundings is probably included, as all of the data were collected for navigational purposes and

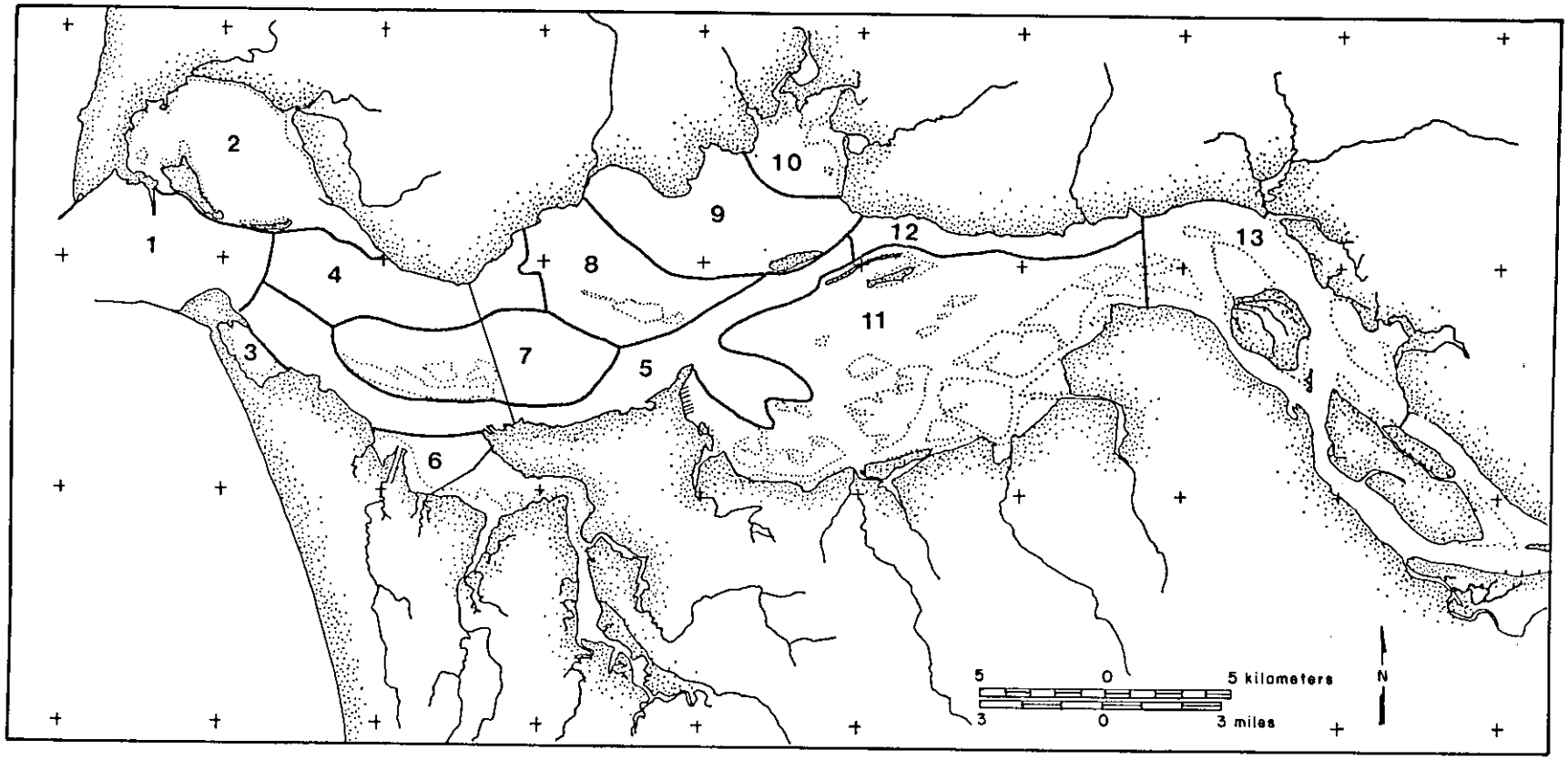

Figure 73. Map of the Columbia River Estuary showing 13 subareas used in volume and area calculations: 1) Entrance, 2) Baker Bay, 3) Trestle Bay, 4) North Channel, 5) South Channel, 6) Youngs Bay, 7) Desdemona Sands, 8) Mid-Estuary Shoals, 9) Grays Bay, 10) Brix Bay, 11) Cathlamet Bay, 12) Lower River Channel, 13) Upper River Channel.

more modern data were collected with acoustic echo-sounders. Small scale topographic features such as bed-forms, which are known to exist over much of the estuary, are not resolved, but as the areas are computed for relatively broad depth intervals, the error is negligible. In the upper intertidal regions more serious errors occur for two reasons: 1) bank to bank surveys were not performed in all four time periods, and shoreline locations are often uncertain, especially in marshes and swamps; 2) the digital scheme, designed for bathymetry, assigned all "land" the value of -2.1 m (-7 ft); therefore the depth interval -2.1 m (-7) includes not only intertidal areas, but in some cases upland areas with greater elevations. (Note that the depth intervals are discussed using the shallower of the bracketing depths; Table 18.) In these areas, the estimates provided by Thomas (1983) may prove more accurate and are used in portions of the discussion. In the subtidal depths, the digitized data allow fairly precise calculations for a number of depth intervals.

In addition to area calculations, the digital bathymetric data were used to calculate volume changes in the estuary between the four survey periods. For the overlapping regions of each survey, the change in volume of each triangular prism defined by three bathymetry data points was summed over the estuary subarea, providing an estimate of the change in sediment volume of that subarea between the survey periods. Many of the same sources of error discussed above are inherent in these calculations. In addition, the volume estimates are highly sensitive to area changes and more sensitive than the area calculations to errors in depth measurements. It is difficult to assign error estimates to the volume calculations: although a systematic error in depth could cause large errors if multipled over a large area, errors in depth are thought to be random. These errors should not bias the volume calculations. It is believed that the important errors are those of omission, rather than calcu-lation errors. Several dredged material disposal sites and broad expanses of beach near the entrance jetties grew rapidly from intertidal or subtidal depths to elevations in excess of 2.1 m (7 ft) between survey periods. In the subsequent survey these are considered land and are assigned maximum elevations of 2.1 m or omitted from the survey altogether. In the first instance, the volume differences presented underestimate the amount of shoaling occurring in the estuary. In the second case, no comparison between the two areas is made (only the intersecting regions of consecutive surveys is compared). Although in this case the error can fall in either direction, the accumulation of sediment is again usually underestimated. Therefore, the volume difference numbers presented in the following section are conservative in the sense that they provide a minimum estimate of the amount of material that has accumulated in the estuary since the 1868 survey period.

Table 18

Depth intervals used in area calculations
(relative to MLLW)

Interval (m)	Interval (ft)	Applicable depth range (ft)
-2.1	-7.0	-7.0 < z < -3.0
-.9	-3.0	-3.0 < z < 0.0
0.0	0.0	0.0 < z < 3.0
.9	3.0	3.0 < z < 6.0
1.8	6.0	6.0 < z < 12.0
3.7	12.0	12.0 < z < 18.0
5.5	18.0	18.0 < z < 24.0
7.3	24.0	24.0 < z < 30.0
9.1	30.0	30.0 < z < 36.0
11.0	36.0	36.0 < z < 42.0
12.8	42.0	42.0 < z < 60.0
18.3	60.0	60.0 < z < 80.0
24.4	80.0	80.0 < z < 100.0
36.5	100.0	100.0 < z

As another approach to the volume changes in the estuary, estimates of water volume were calculated from the area estimates. These volume figures are based on the midpoint of the depth interval over which the areas were obtained, and they tend to overestimate the water volume in the estuary because there is generally more shallow water area than deep water area in a given depth interval. Changes in the water volume between survey periods should equal the changes in sediment volume and be opposite in sign. In fact, the reductions in water volumes were generally comparable in magnitude and contrasted in sign, especially in areas with little upper intertidal area. Discrepancies were helpful in resolving problems in areas where particular biases of one technique or the other were encountered.

C.2.3 Area Changes

The results of the area calculations are presented, in part, as Tables 19 and 20. The entrance region areas, which have shown dramatic changes, have been omitted from the areas shown in Table 20 to emphasize the changes within the estuary proper. The normal surface area of the surveyed area (in 1958) of each of the thirteen subareas (labeled on Figure 73) is shown on Figure 74. The area included in the digital bathymetry is identical for each of the first three survey periods (1868, 1935, and 1958) in all of the areas except those showing a minus sign (-). The coverage of these three areas (with a minus sign) decreased over the 90-year period due mostly to extensive shoreline changes and, as a result, the areas are not strictly comparable. The effects of these omissions on the interpretation of the data are discussed before the final conclusions are presented. The results of the 1982 survey have been entirely omitted because the survey did not produce comparable coverage and excludes large areas, especially near shore, that were surveyed in the previous periods.

The area changes in each depth regime of the thirteen subareas were calculated and are presented as Tables 21 to 33. The following discussion relies on the changes observed in the individual depth intervals of the subareas, which may be found in these tables.

The largest area changes occurred in the entrance region as a result of jetty construction and shoaling. Area losses of 35 million m^2 in the 0.0 m interval between 1868 and 1935 represent 70% of the total area lost in the estuary for the entire 90-year period. Most of this area, which had been low intertidal shoal area in 1868, was transferred to supratidal environments on Clatsop Spit and Peacock Spit during beach accretion around the newly constructed jetties. Nearly 38 million m^2 were omitted from the 1935 surveys as a result of the land growth, creating

Table 19.

Areas, volumes, volume changes, and area changes by depth regime for 1868, 1935, and 1958

Depth regimes (m)	Depth regimes (ft)	Area (10^6 m^2) 1868	Area (10^6 m^2) 1935	Area (10^6 m^2) 1958	Water volume† (10^6 m^3) 1868	Water volume† (10^6 m^3) 1935	Water volume† (10^6 m^3) 1958	Volume changes (10^6 m^3) 1868–1935	Volume changes (10^6 m^3) 1935–1958	Volume changes (10^6 m^3) 1868–1958	Area changes (10^6 m^2) 1868–1935	Area changes (10^6 m^2) 1935–1958	Area changes (10^6 m^2) 1868–1958
-2.1	-7.00	294.22	339.33	326.31	-448.39	-517.14	-497.15	-68.75	19.99	-48.76	45.11	-13.12	31.99
-0.9	-3.00	38.05	54.46	50.91	-17.40	-24.90	-23.27	-7.50	1.62	-5.88	16.41	-3.55	12.86
0.0	0.00	113.85	69.48	65.11	52.05	31.77	29.77	-20.28	-2.00	-22.28	-44.36	-4.37	-48.74
0.9	3.00	47.65	50.23	48.66	65.36	68.90	676.75	3.54	-2.15	1.38	2.58	-1.57	1.01
-1.8	6.00	104.43	74.19	75.72	286.47	203.52	207.72	-82.95	4.20	-78.74	-30.24	1.53	-28.71
3.7	12.00	70.71	53.33	55.39	323.31	342.85	253.25	-79.46	9.40	-70.06	-17.38	2.06	-15.32
5.5	18.00	61.63	43.36	38.65	394.50	277.51	247.37	-116.98	-30.14	-147.13	-18.28	-4.71	-22.99
7.3	24.00	45.41	35.62	31.48	373.72	293.13	259.91	-80.59	-33.22	-113.81	-9.79	-4.04	-13.83
9.1	30.00	28.82	33.56	33.30	289.85	337.59	334.96	47.74	-2.63	45.11	4.75	-0.26	4.49
11.0	36.00	21.42	32.33	30.87	254.58	384.31	366.98	129.73	-17.33	112.41	10.91	-1.46	9.46
12.8	42.00	44.93	62.38	66.19	698.36	969.68	1028.94	271.32	59.26	330.59	17.45	3.81	21.27
18.3	60.00	24.63	22.16	25.86	525.51	472.88	551.83	-52.63	78.95	26.32	-2.47	3.70	1.23
24.4	80.00	17.98	13.79	11.51	493.16	378.33	315.79	-114.83	-62.54	-177.37	-4.19	-2.28	-6.47
36.5	100.00	8.52	9.19	7.81	285.71	308.27	261.90	22.56	-46.37	-23.81	0.67	-1.38	-0.71
	Total	922.24	893.43	867.78	4042.57	3969.74	3925.17	-72.83	-44.57	-117.40	-28.82	-25.64	-54.46
Summed depth regimes*													
-0.9≤ 0.9	-3≤3	151.89	123.94	116.01	69.45	56.66	53.04	-12.78	-3.62	-16.40	-27.96	-7.92	-35.88
0.9≤ 5.5	3≤18	222.80	177.76	179.78	675.13	516.26	527.71	-158.87	11.45	-147.42	-45.04	2.02	-43.02
5.5≤12.8	18≤42	157.28	144.87	134.40	1312.64	1292.54	1209.22	-20.10	-83.32	-103.42	-12.41	-10.46	-22.87
12.8≤	42≤	96.06	107.53	111.38	2002.75	2129.16	2158.47	126.42	29.30	155.72	11.47	3.85	15.32
Total below -3		628.02	554.09	541.57	4059.96	3994.63	3948.44	-65.33	-46.19	-111.52	-73.93	-12.52	-86.45

†Volumes above MLLW are expressed as negative.

*Volume sums do not include volume above 0.9 m (3 ft) above MLLW).

Table 20.

Areas, volumes, volume changes, and area changes by depth regime for 1868, 1935, and 1958 (excluding entrance)

Depth regimes (m)	Depth regimes (ft)	Area (10^6 m^2) 1868	1935	1958	Water volume† (10^6 m^3) 1868	1935	1958	Volume changes (10^6 m^3) 1868–1935	1935–1958	1868–1958	Area changes (10^6 m^2) 1868–1935	1935–1958	1868–1958
-2.1	-7.00	285.44	323.82	310.67	-435.01	0493.50	-473.45	-58.50	20.05	-38.45	38.39	-13.16	25.23
-0.9	-3.00	36.40	50.76	48.66	-16.64	-23.21	-22.25	-6.56	0.96	-5.60	14.35	-2.09	12.26
0.0	0.00	74.12	67.50	63.28	33.89	30.86	28.93	-3.02	-1.93	-4.96	-6.62	-4.22	-10.84
0.9	3.00	45.34	48.29	46.68	62.18	66.23	64.03	4.05	-2.20	1.85	2.95	-1.61	1.35
-1.8	6.00	88.21	69.56	70.56	241.97	190.81	193.57	-51.16	2.77	-48.39	-18.65	1.01	-17.64
3.7	12.00	58.19	48.18	49.22	266.06	220.27	225.05	-45.80	4.78	-41.01	-10.02	1.05	-8.97
5.5	18.00	45.04	35.88	31.43	288.28	229.66	201.20	-58.61	-28.47	-87.08	-9.16	-4.45	-13.60
7.3	24.00	29.30	26.61	22.09	241.15	219.00	181.78	-22.15	-37.22	-59.36	-2.69	-4.52	-7.21
9.1	30.00	17.12	21.42	21.79	172.18	215.41	219.17	43.23	3.76	46.99	4.30	0.37	4.67
11.0	36.00	10.35	14.17	16.18	123.07	168.39	192.38	45.32	23.99	69.31	3.81	2.02	5.83
12.8	42.00	17.79	11.25	12.89	276.55	174.88	200.44	-101.67	25.56	-76.11	-6.54	1.64	-4.90
18.3	60.00	2.17	1.83	1.68	46.25	39.07	35.88	-7.18	-3.19	-10.37	-0.34	-0.15	-0.49
24.4	80.00	0.41	0.11	0.19	11.28	3.08	5.13	-8.20	2.05	-6.15	-0.30	0.07	-0.22
36.5	100.00	0.04	0.11	0.00	1.25	3.76	0.00	2.51	-3.76	-1.25	0.07	-0.11	-0.04
	Total	709.91	719.48	695.33	1764.11	1561.42	1547.56	-202.69	-13.85	-216.54	9.57	-24.14	-14.58
Summed depth regimes*													
-0.9< 0.9	-3-3	110.52	118.26	111.94	50.53	54.07	51.18	3.54	-2.89	0.65	7.74	-6.32	1.42
0.9< 5.5	3-18	191.74	166.02	166.47	570.21	477.30	482.65	-92.91	5.35	-87.56	-25.71	0.45	-25.27
5.5<12.8	18-42	101.81	98.07	91.50	824.67	832.46	794.53	7.79	-37.93	-30.14	-3.74	-6.58	-10.32
12.8-	42-	20.41	13.31	14.76	335.34	220.79	241.45	-114.55	20.67	-93.88	-7.10	1.46	-5.64
Total below -3		424.47	395.66	384.67	1780.75	1584.62	1569.81	-196.13	-14.81	-210.94	-28.82	-10.99	-39.80

†Volumes above MLLW are expressed as negative.

*Volume sums do not include volume above 0.9 m (3 ft) above MLLW.

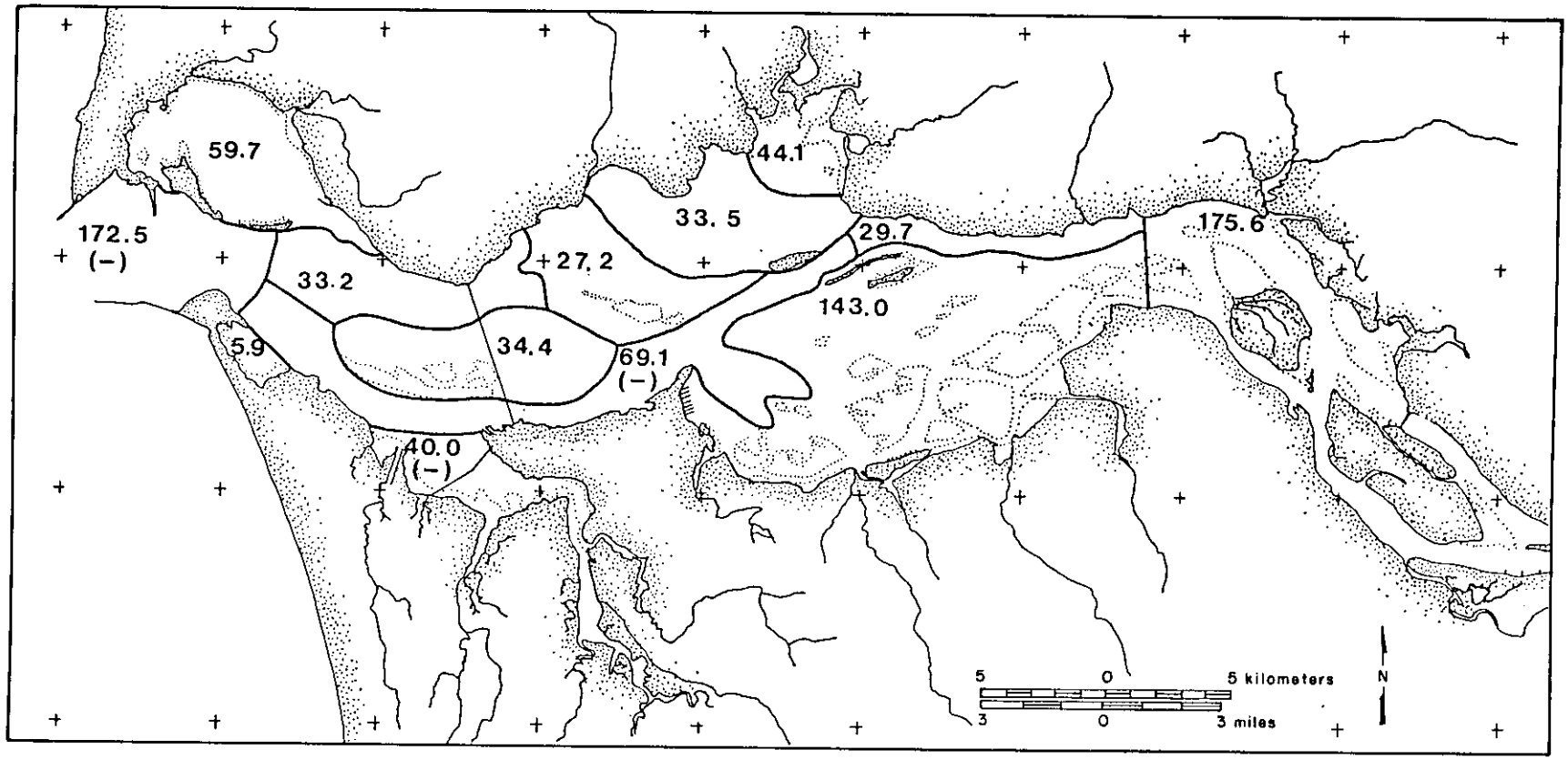

Figure 74. Map of the Columbia River Estuary showing the "normal" surveyed area (m^2 10^6) in each of the 13 subareas during the 1958 survey period. The (-) indicates a reduction in surveyed area since earlier surveys.

Table 21.

Area and area changes by depth regime
in the Upper River Channel

Depth interval (ft)	Area (million sq m)			Area Change (million sq m)	
	1868	1935	1958	1868/ 1935	1935/ 1958
-7.00	108.69	116.57	117.81	7.89	1.23
-3.00	6.13	6.69	6.88	0.56	0.19
0.00	16.59	6.39	5.42	-10.20	-0.97
3.00	4.67	4.93	5.27	0.26	0.34
6.00	9.27	10.02	10.76	0.75	0.75
12.00	7.03	8.07	8.04	1.05	-0.04
18.00	6.35	5.94	6.32	-0.41	0.37
24.00	5.49	5.98	4.34	0.49	-1.64
30.00	3.85	4.49	4.60	0.64	0.11
36.00	2.28	3.21	2.39	0.93	-0.82
42.00	4.49	2.58	3.33	-1.91	0.75
60.00	0.75	0.67	0.41	-0.07	-0.26
80.00	0.00	0.04	0.04	0.04	0.00
100.00	0.00	0.00	0.00	0.00	0.00
Area total	175.59	175.59	175.59	0.00	0.00

Table 22.

Area and area changes by depth regime in the Entrance

Depth interval (ft)	Area (million sq m)			Area Change (million sq m)	
	1868	1935	1958	1868/ 1935	1935/ 1958
-7.00	15.14	16.22	14.84	1.08	-1.38
-3.00	0.78	0.90	1.50	0.11	0.60
0.00	3.25	1.64	0.75	-1.61	-0.90
3.00	3.40	2.58	1.42	-0.82	-1.16
6.00	8.26	7.40	6.76	-0.86	-0.64
12.00	9.72	7.66	8.19	-2.06	0.52
18.00	8.41	8.86	7.92	0.45	-0.93
24.00	7.06	8.48	7.03	1.42	-1.46
30.00	5.42	8.26	9.12	2.84	0.86
36.00	3.25	5.12	7.62	1.87	2.50
42.00	5.27	3.18	3.59	-2.09	0.41
60.00	0.49	0.26	0.22	-0.22	-0.04
80.00	0.26	0.07	0.11	-0.19	0.04
100.00	0.04	0.11	0.00	0.07	-0.11
Area total	70.75	70.75	69.07	0.00	-1.68

Table 23.

Area and area changes by depth regime in Cathlamet Bay

Depth interval (ft)	Area (million sq m)			Area Change (million sq m)	
	1868	1935	1958	1868/ 1935	1935/ 1958
-7.00	51.54	55.54	59.76	4.00	4.22
-3.00	19.17	17.72	17.64	-1.46	-0.07
0.00	12.78	16.03	17.12	3.25	1.08
3.00	13.60	15.02	14.17	1.42	-0.86
6.00	20.07	19.25	15.62	-0.82	-3.63
12.00	11.74	9.57	9.87	-2.17	0.30
18.00	7.36	5.79	5.08	-1.57	-0.71
24.00	4.75	2.77	2.24	-1.98	-0.52
30.00	1.53	0.82	1.05	-0.71	0.22
36.00	0.34	0.22	0.19	-0.11	-0.04
42.00	0.11	0.19	0.22	0.07	0.04
60.00	0.00	0.07	0.04	0.07	-0.04
80.00	0.00	0.00	0.00	0.00	0.00
100.00	0.00	0.00	0.00	0.00	0.00
Area total	143.00	143.00	143.00	0.00	0.00

Table 24.

Area and area changes by depth regime in Youngs Bay

Depth interval (ft)	Area (million sq m)			Area Change (million sq m)	
	1868	1935	1958	1868/ 1935	1935/ 1958
-7.00	24.97	45.52	27.77	20.56	-17.75
-3.00	2.62	4.11	2.39	1.50	-1.72
0.00	16.63	4.67	4.22	-11.96	-0.45
3.00	2.21	3.03	2.69	0.82	-0.34
6.00	4.19	3.85	2.32	-0.34	-1.53
12.00	1.83	1.20	0.64	-0.64	-0.56
18.00	0.37	0.15	0.04	-0.22	-0.11
24.00	0.07	0.00	0.00	-0.07	0.00
30.00	0.07	0.00	0.00	-0.07	0.00
36.00	0.00	0.00	0.00	0.00	0.00
42.00	0.00	0.00	0.00	0.00	0.00
60.00	0.00	0.00	0.00	0.00	0.00
80.00	0.00	0.00	0.00	0.00	0.00
100.00	0.00	0.00	0.00	0.00	0.00
Area total	52.96	62.53	40.07	9.57	-22.46

Table 25.

Area and area changes by depth regime in Baker Bay

Depth interval (ft)	Area (million sq m)			Area Change (million sq m)	
	1868	1935	1958	1868/ 1935	1935/ 1958
-7.00	25.34	29.53	29.27	4.19	-0.26
-3.00	2.95	9.57	8.97	6.62	-0.60
0.00	4.04	13.68	12.97	9.64	-0.71
3.00	5.72	4.71	5.31	-1.01	0.60
6.00	13.34	2.09	2.84	-11.25	0.75
12.00	3.48	0.11	0.19	-3.36	0.07
18.00	1.94	0.00	0.11	-1.94	0.11
24.00	1.98	0.00	0.00	-1.98	0.00
30.00	0.49	0.00	0.04	-0.49	0.04
36.00	0.11	0.00	0.00	-0.11	0.00
42.00	0.30	0.00	0.00	-0.30	0.00
60.00	0.00	0.00	0.00	0.00	0.00
80.00	0.00	0.00	0.00	0.00	0.00
100.00	0.00	0.00	0.00	0.00	0.00
Area total	59.69	59.69	59.69	0.00	0.00

Table 26.

Area and area changes by depth regime in Brix Bay

Depth interval (ft)	Area (million sq m)			Area Change (million sq m)	
	1868	1935	1958	1868/1935	1935/1958
-7.00	28.78	28.52	28.33	-0.26	-0.19
-3.00	1.72	3.59	4.75	1.87	1.16
0.00	6.50	5.76	4.34	-0.75	-1.42
3.00	2.54	3.10	2.73	0.56	-0.37
6.00	2.73	1.98	2.84	-0.75	0.86
12.00	1.12	0.86	0.90	-0.26	0.04
18.00	0.52	0.19	0.15	-0.34	-0.04
24.00	0.07	0.04	0.04	-0.04	0.00
30.00	0.07	0.04	0.00	-0.04	-0.04
36.00	0.00	0.00	0.00	0.00	0.00
42.00	0.00	0.00	0.00	0.00	0.00
60.00	0.00	0.00	0.00	0.00	0.00
80.00	0.00	0.00	0.00	0.00	0.00
100.00	0.00	0.00	0.00	0.00	0.00
Area total	44.07	44.07	44.07	0.00	0.00

Table 27.

Area and area changes by depth regime in the South Channel

Depth interval (ft)	Area (million sq m)			Area Change (million sq m)	
	1868	1935	1958	1868/ 1935	1935/ 1958
-7.00	15.14	16.22	14.84	1.08	-1.38
-3.00	0.78	0.90	1.50	0.11	0.60
0.00	3.25	1.64	0.75	-1.61	-0.90
3.00	3.40	2.58	1.42	-0.82	-1.16
6.00	8.26	7.40	6.76	-0.86	-0.64
12.00	9.72	7.66	8.19	-2.06	0.52
18.00	8.41	8.86	7.92	0.45	-0.93
24.00	7.06	8.48	7.03	1.42	-1.46
30.00	5.42	8.26	9.12	2.84	0.86
36.00	3.25	5.12	7.62	1.87	2.50
42.00	5.27	3.18	3.59	-2.09	0.41
60.00	0.49	0.26	0.22	-0.22	-0.04
80.00	0.26	0.07	0.11	-0.19	0.04
100.00	0.04	0.11	0.00	0.07	-0.11
Area total	70.75	70.75	69.07	0.00	-1.68

Table 28.

Area and area changes by depth regime
in the Lower River Channel

Depth interval (ft)	Area (million sq m)			Area Change (million sq m)	
	1868	1935	1958	1868/ 1935	1935/ 1958
-7.00	15.51	15.17	15.06	-0.34	-0.11
-3.00	0.45	0.37	0.41	-0.07	0.04
0.00	0.67	0.34	0.45	-0.34	0.11
3.00	0.86	0.78	0.82	-0.07	0.04
6.00	1.68	2.35	1.87	0.67	-0.49
12.00	2.21	1.23	1.79	-0.97	0.56
18.00	2.77	2.13	1.98	-0.64	-0.15
24.00	1.50	1.91	2.39	0.41	0.49
30.00	1.27	2.88	2.35	1.61	-0.52
36.00	1.05	1.08	1.38	0.04	0.30
42.00	1.46	1.27	1.01	-0.19	-0.26
60.00	0.19	0.19	0.15	0.00	-0.04
80.00	0.11	0.00	0.04	-0.11	0.04
100.00	0.00	0.00	0.00	0.00	0.00
Area total	29.71	29.71	29.71	0.00	0.00

Table 29.

Area and area changes by depth regime in Desdemona Sands

Depth interval (ft)	Area (million sq m)			Area Change (million sq m)	
	1868	1935	1958	1868/ 1935	1935/ 1958
-7.00	0.00	0.00	0.00	0.00	0.00
-3.00	0.19	2.47	1.61	2.28	-0.86
0.00	1.76	4.82	6.02	3.06	1.20
3.00	3.29	4.07	4.71	0.78	0.64
6.00	10.88	7.55	9.87	-3.33	2.32
12.00	7.36	8.78	8.60	1.42	-0.19
18.00	5.87	5.12	2.58	-0.75	-2.54
24.00	2.88	1.46	0.97	-1.42	-0.49
30.00	0.45	0.07	0.00	-0.37	-0.07
36.00	0.34	0.00	0.00	-0.34	0.00
42.00	1.35	0.00	0.00	-1.35	0.00
60.00	0.00	0.00	0.00	0.00	0.00
80.00	0.00	0.00	0.00	0.00	0.00
100.00	0.00	0.00	0.00	0.00	0.00
Area total	34.35	34.35	34.35	0.00	0.00

Table 30.

Area and area changes by depth regime in Grays Bay

Depth interval (ft)	Area (million sq m)			Area Change (million sq m)	
	1868	1935	1958	1868/ 1935	1935/ 1958
-7.00	4.22	4.49	4.56	0.26	0.07
-3.00	1.35	1.98	1.53	0.64	-0.45
0.00	6.13	9.12	8.30	2.99	-0.82
3.00	3.55	5.57	4.97	2.02	-0.60
6.00	7.74	5.31	7.14	-2.43	1.83
12.00	5.72	3.85	4.04	-1.87	0.19
18.00	3.18	1.61	1.35	-1.57	-0.26
24.00	0.90	0.64	0.71	-0.26	0.07
30.00	0.30	0.49	0.52	0.19	0.04
36.00	0.07	0.15	0.15	0.07	0.00
42.00	0.34	0.30	0.22	-0.04	-0.07
60.00	0.00	0.00	0.00	0.00	0.00
80.00	0.00	0.00	0.00	0.00	0.00
100.00	0.00	0.00	0.00	0.00	0.00
Area total	33.49	33.49	33.49	0.00	0.00

Table 31.

Area and area changes by depth regime in the North Channel

Depth interval (ft)	Area (million sq m)			Area Change (million sq m)	
	1868	1935	1958	1868/ 1935	1935/ 1958
-7.00	8.04	7.74	7.62	-0.30	-0.11
-3.00	0.37	0.71	0.75	0.34	0.04
0.00	0.45	0.64	0.86	0.19	0.22
3.00	0.64	1.27	1.16	0.64	-0.11
6.00	1.53	1.38	1.23	-0.15	-0.15
12.00	2.24	1.53	1.87	-0.71	0.34
18.00	5.76	3.51	3.03	-2.24	-0.49
24.00	3.25	4.04	3.03	0.78	-1.01
30.00	3.14	3.85	3.81	0.71	-0.04
36.00	2.80	4.15	4.45	1.35	0.30
42.00	4.19	3.74	4.52	-0.45	0.78
60.00	0.75	0.64	0.86	-0.11	0.22
80.00	0.04	0.00	0.00	-0.04	0.00
100.00	0.00	0.00	0.00	0.00	0.00
Area total	33.19	33.19	33.19	0.00	0.00

Table 32.

Area and area changes by depth regime in the Mid-estuary Shoals

Depth interval (ft)	Area (million sq m)			Area Change (million sq m)	
	1868	1935	1958	1868/ 1935	1935/ 1958
-7.00	2.06	2.09	2.09	0.04	0.00
-3.00	0.56	1.31	0.67	0.75	-0.64
0.00	3.63	2.95	2.35	-0.67	-0.60
3.00	4.30	2.92	3.25	-1.38	0.34
6.00	6.73	8.11	9.16	1.38	1.05
12.00	5.31	5.23	5.12	-0.07	-0.11
18.00	2.32	2.50	2.88	0.19	0.37
24.00	1.35	1.31	1.35	-0.04	0.04
30.00	0.52	0.52	0.30	0.00	-0.22
36.00	0.11	0.22	0.00	0.11	-0.22
42.00	0.30	0.00	0.00	-0.30	0.00
60.00	0.00	0.00	0.00	0.00	0.00
80.00	0.00	0.00	0.00	0.00	0.00
100.00	0.00	0.00	0.00	0.00	0.00
Area total	27.17	27.17	27.17	0.00	0.00

Table 33.

Area and area changes by depth regime in Trestle Bay

Depth interval (ft)	Area (million sq m)			Area Change (million sq m)	
	1868	1935	1958	1868/ 1935	1935/ 1958
-7.00	1.16	2.43	3.55	1.27	1.12
-3.00	0.11	1.35	1.57	1.23	0.22
0.00	1.68	1.46	0.49	-0.22	-0.97
3.00	0.56	0.30	0.19	-0.26	-0.11
6.00	1.79	0.26	0.15	-1.53	-0.11
12.00	0.45	0.07	0.00	-0.37	-0.07
18.00	0.19	0.07	0.00	-0.11	-0.07
24.00	0.00	0.00	0.00	0.00	0.00
30.00	0.00	0.00	0.00	0.00	0.00
36.00	0.00	0.00	0.00	0.00	0.00
42.00	0.00	0.00	0.00	0.00	0.00
60.00	0.00	0.00	0.00	0.00	0.00
80.00	0.00	0.00	0.00	0.00	0.00
100.00	0.00	0.00	0.00	0.00	0.00
Area total	5.94	5.94	5.94	0.00	0.00

discrepancies in the surveyed areas. The 1868 survey included 212.33 million m^2, the 1935 survey included 173.95 million m^2, and the 1958 survey covered 172.45 million m^2. In addition to these changes, large gains in the area above MLLW were noted between the 1868 and 1935 surveys, also reflecting the spit growth. Area was lost during the same period in the 0.9, 1.8, 3.7, 5.5, and 7.3 m intervals (36 million m^2) but a nearly equal area was gained in the deeper 9.1, 11.0, and 12.8 m intervals (32 million m^2). Areas of the deepest water were somewhat reduced as the outer tidal delta was forced seaward. Changes in the entrance region were much less dramatic in the period between 1935 and 1958, suggesting that an equilibrium had been reached. Area was lost in the 9.1 and 11.0 m intervals and gained in the 12.8 and 24.4 m intervals, probably reflecting dredging of the 14.6 m (48 ft) entrance channel which was begun in 1956.

The relative changes among the depth regimes in the entrance are apparent in the hypsometric curve of the entrance region, presented as Figure 75. The hypsometric curve plots the cumulative area beneath a particular depth in the estuary. Integration of the area to the left of the curve provides a water volume estimate. The shape of the hypsometric curve and the amount of water stored in various water depths has changed dramatically since 1868. Large water volumes have been removed from the shallow intertidal and subtidal ares. Smaller volume losses have occurred in the deepest areas, and large increases of water volumes in the mid-dpeth ranges has nearly offset the volume losses in shallower and deeper water. Figure 75 also indicates that most of the changes occurred in the 1868-1935 period, following jetty construction.

Changes have also occurred in two other subareas that have affected the area calculations to some extent. The Youngs Bay subarea has been modifed greatly in historic time by the dredging of the Skipanon waterway and the filling of the surrounding marsh. Thomas (1983) estimates that 40% of the original estuarine area has been converted to developed floodplain by diking and filling which began prior to even the 1868 survey. Survey coverage of the Youngs Bay area is inconsistent as a result of the changes, and more area was included in the 1935 survey than either the earlier or later survey. As a result, a large gain in the -2.1 m interval of 20 million m^2 was noted between 1868 and 1935. A loss of 12 million m^2 occurred in the same period from the 0.0 m interval. The latter number probably more accurately reflects the loss of intertidal area to diking and filling. In the subsequent period (from 1935 to 1958), an additional loss of 18 million m^2 from the -2.1 m interval was calculated: at least some of this loss is the result of reduced coverage in the 1958 survey. These calculations underestimate the change in intertidal area measured by Thomas (1983) in the same regions of the estuary.

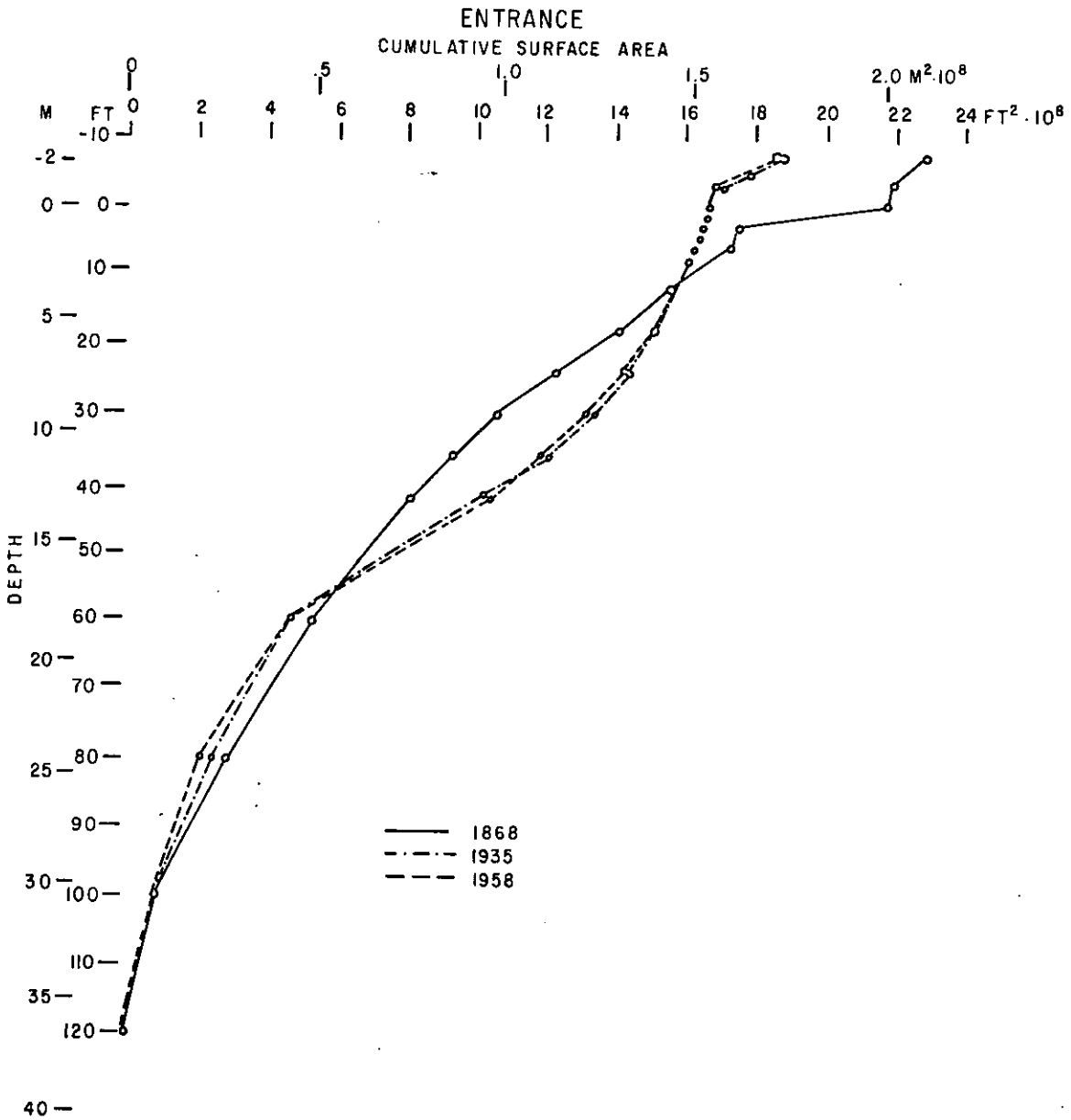

Figure 75. Hypsometric curve relating cumulative surface area with depth in the entrance region for 1868, 1935, and 1958.

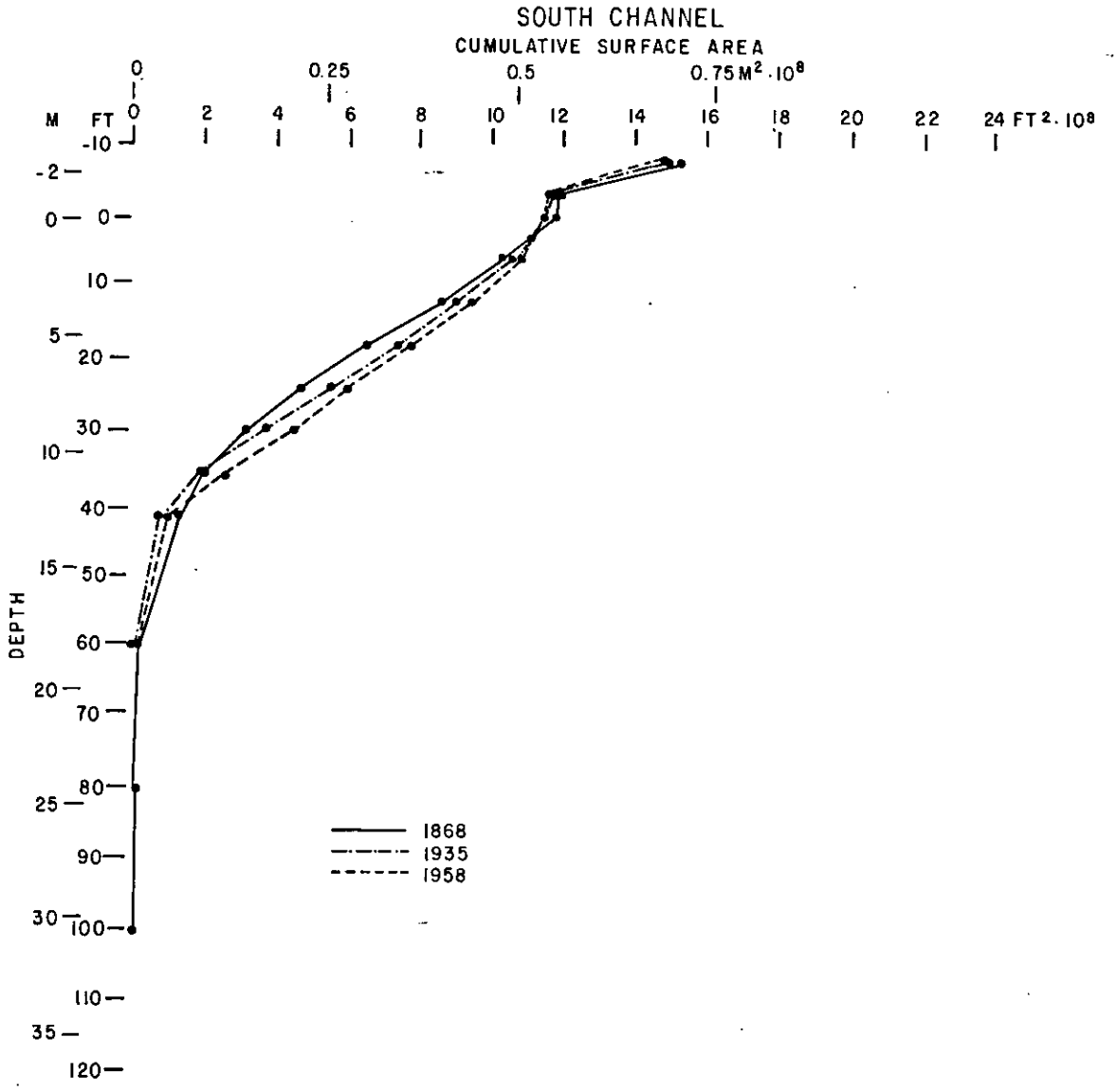

Figure 76. Hypsometric curve relating cumulative surface area with depth in the South Channel in 1868, 1935, and 1958.

There are also minor differences in the area covered by the 1935 and 1958 surveys in the South Channel. The total area covered in 1868 and 1935 is 70.75 million m^2, but it decreases to 69.07 million m^2 in 1958. Most of this probably appears in the difference calculations as a loss of 1.38 million m^2 in the -2.1 m interval over the period 1935 to 1958. It is likely that the decrease in the survey coverage was related to the dredging of Mott Basin for use as a seaplane base during WW II and the construction of Mott and Lois Islands with the dredged materials.

The hypsometric curve for the South Channel subarea is included as Figure 76. The changes are similar in trend to those of the entrance but involve smaller areas and volumes. Area and water volume in the shallow intervals has decreased since 1968, while large increases in area and water volume have occurred in the mid-depths. Examination of the specific area data reveals that the areas in the 5.5 to 11.0 m intervals increased between 1868 and 1935 (Table 27). In the subsequent period (1935 to 1958) area was lost in the 5.5 and 7.3 m intervals and gained in the 12.8 m interval. This trend probably reflects the increased navigation channel depths maintained in the more recent period. It is interesting to note that there has been a loss of deeper water since 1868 in the South Channel subarea (Figure 76).

With the exception of the survey discrepancies that have been discussed, the numbers from each of the time periods provide accurate estimates of the area changes in the estuary. Some exchange between upper intertidal elevations and "dry" land may occur in the -2.1 m interval, and for many calculations, the area below in the -0.9 m interval and below should be used as the most accurate estimate of estuary areas. Area totals below MLLW are considered very reliable.

Tables 19 and 20 summarize the area changes that have occurred in the estuary since 1868. Water volumes approximated by multiplying the area of each depth regime by the mid-point of the depth interval are also shown on the tables. The changes in both areas and volumes have been computed and summations of the volume below MLLW and the area (total; i.e., complete survey area) appear at the bottom of each column. A breakdown of the totals into depth regimes compatible with Thomas (1983) is appended at the bottom of each column, as well as totals of the areas and volumes below -0.9 m. The volumes above MLLW are flagged as negative volumes, but in calculating the volume sums, the volume of the -0.9 interval has been subtracted, effectively adding to the volume total.

Several trends in the long-term changes are apparent from Table 20 (which does not include the large changes that

have occurred in the entrance region). An overall loss in the area of the estuary has occurred since 1868. Nearly 40 million m^2 of area below -0.9 m (3 feet above MLLW) have been lost, representing a decrease of 9% relative to the 1868 area of 424.47 million m^2. Most of the loss has been from the shallow subtidal depths in the intervals from 0.9 to 3.7 m (64% of the total loss), but significant losses from the deeper intervals (5.5 to 11.0 m, 26%; and 12.8 on, 14%) have also occurred. Most of the change occurred during the longer early period (1868 to 1935); it was during this period that most of the relatively shallow area was lost (loss of 26 million m^2 from the 0.9 to 3.7 m intervals). In the more recent period (1935 to 1958) there has been a slight increase in the area of this shallow interval; the losses in the intervals between 5.5 and 11.0 m are twice the losses in the same intervals for the preceding period. A slight gain in the area deeper than 12.8 m occurred during the more recent period, probably reflecting increased depths in the navigation channel.

It is difficult to estimate the changes in the upper intertidal area from the figures shown in Tables 19 and 20 because of the survey inconsistencies. Thomas (1983) estimates that 121.6 million m^2 of area (30,050 acres) has been lost in the tidal marshes and swamps. This amounts to a loss of approximately 20% of the original estuary area. The loss of some of this area has been important in decreasing the tidal prism of the estuary; however, the diked and filled areas were originally high and many were upriver, where the tidal prism was small.

The effects of these area changes on the water volumes of the estuary are depicted graphically in Figure 77, which shows a hypsometric curve for the estuary as a whole and for four of the subareas. Curves for both 1868 area and 1958 areas are shown. The shift in area from the shallow subtidal depths to deeper depths between 1868 and 1958 is readily apparent. Much of the shift can be attributed to changes in the entrance, but separate examination of the South Channel (also shown in Figure 76) and the upper river channel (Figure 78) show similar trends. The subareas of Baker Bay and Cathlamet Bay are filling in more uniformly, with no marked shift to relatively more deep water (Figures 76 and 79).

The same trends observed on the hypsometric curves may also be seen in the volume figures of Tables 19, 20, and 34. It should be noted that the choice of the depth interval midpoint results in an overestimate of the water volume associated with each area, so these numbers should be used mostly for comparison. They indicate that there has been little change in the intertidal intervals (between -0.9 and 0.0 m) and large volume losses in all of the deeper intervals. The greatest volume losses have apparently

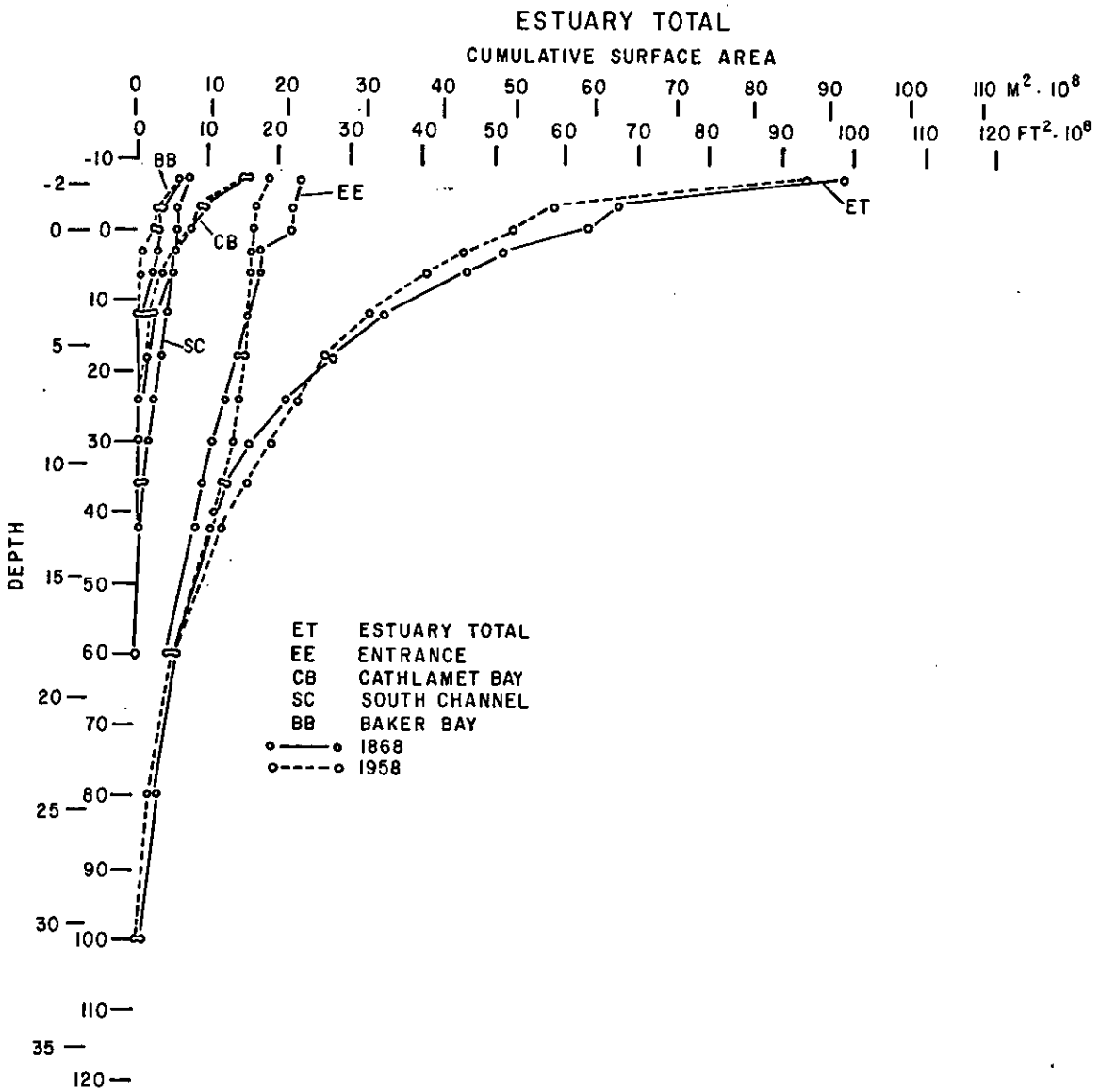

Figure 77. Hypsometric curve relating cumulative surface area to depth for the estuary as a whole and several subareas in 1868 and 1958.

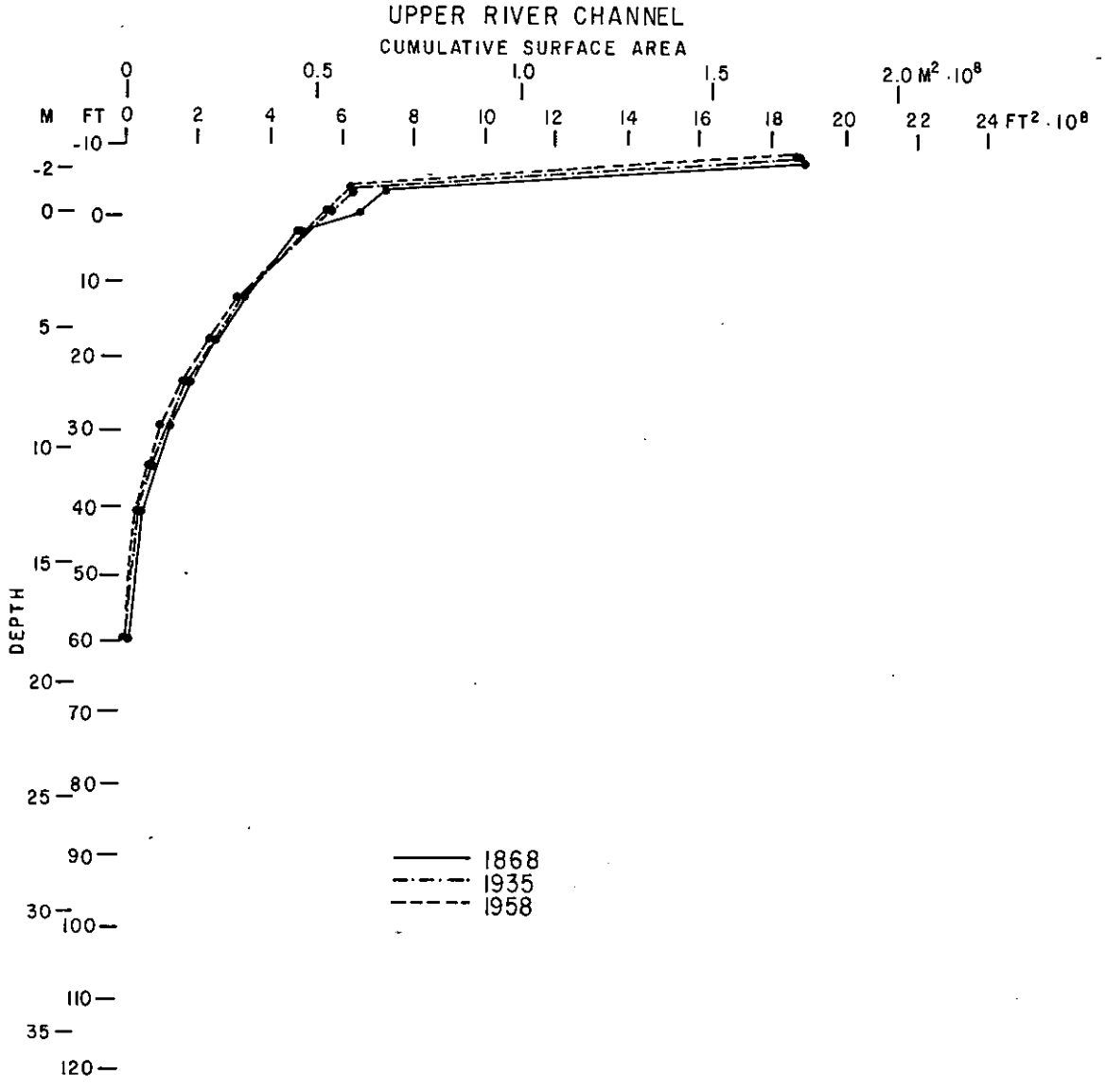

Figure 78. Hypsometric curve relating cumulative surface area to depth in the upper river channel in 1868, 1935, and 1958.

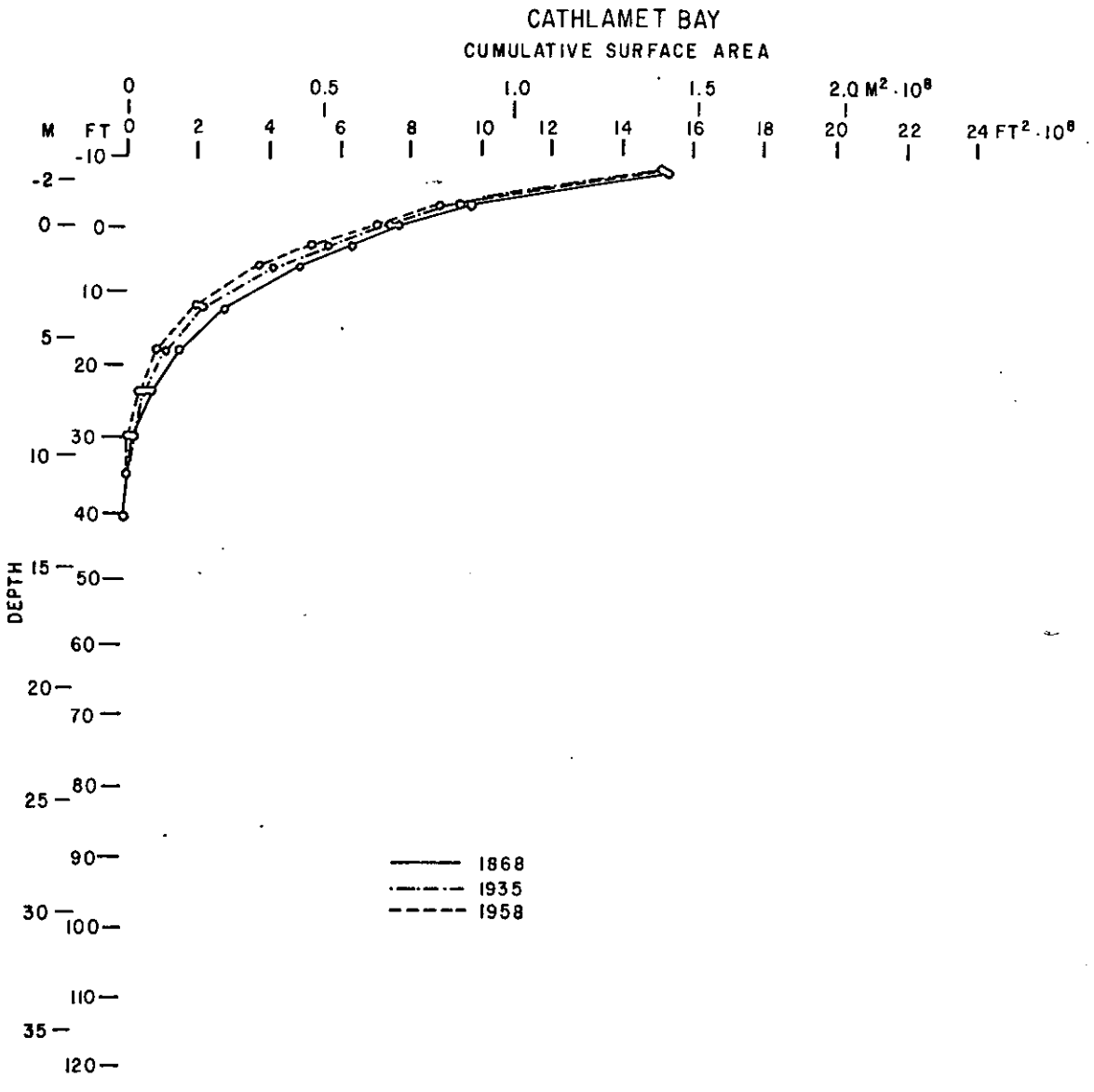

Figure 79. Hypsometric curve relating cumulative surface area to depth in Cathlamet Bay in 1868, 1935, and 1958.

Table 34

Volumes, volume changes, and sedimentation by subarea

Estuary subarea	Volumes[1] (10^6 m^3)			Volume changes (10^6 m^3)					
				1868-1935		1935-1958		1868-1958	
	1868	1935	1958	(1)	(2)	(1)	(2)	(1)	(2)
1 Entrance	2279.23	2410.03	2378.64	130.80*	-212.86	-31.39*	-33.87	99.41*	-246.73
2 Baker Bay	103.14	23.34	27.05	-79.80	90.89	3.71	-4.76	-76.09	86.13
3 Trestle Bay	9.76	3.23	1.61	-6.53	9.03	-1.62	3.96	-8.15	12.99
4 North Channel	226.25	228.56	238.40	2.31	-3.42	9.84	-5.63	12.15	-9.05
5 South Channel	379.44	391.28	413.50	11.84*	-9.96	22.22	17.64	34.06*	7.68
6 Youngs Bay	35.44	25.15	16.22	-10.29*	31.43	-8.93*	3.88	-19.22*	35.31
7 Desdemona Sands	159.57	115.31	100.82	-44.26	45.93	-14.49	12.92	-58.75	58.85
8 Mid-estuary Shoals	87.68	86.84	86.88	-0.84	1.26	0.04	-0.29	-0.80	0.97
9 Grays Bay	92.50	71.70	74.33	-20.80	23.13	2.63	-4.00	-18.17	19.13
10 Brix Bay	8.40	6.40	6.67	-2.00	6.18	0.27	-0.58	-1.73	5.60
11 Cathlamet Bay	249.33	207.87	191.31	-41.46	49.34	-16.56	26.86	-58.02	76.20
12 Lower River Channel	101.34	108.40	107.24	7.06	-7.11	-1.16	0.88	5.90	-6.23
13 Upper River Channel	311.73	303.18	291.41	-8.55	19.32	-11.77	8.24	-20.32	27.56
Estuary w/o entrance	1764.58	1571.26	1555.44	-193.32	256.02	-15.82	59.12	-209.14	315.14
Estuary total	4043.81	3981.29	3934.08	-62.52	43.16	-47.21	25.25	-109.73	68.41

[1]Based on water volume estimates.

[2]Based on bathymetric differencing; negative n umbers indicate erosion, positive indicate shoaling.

*Numbers biased by unequal survey coverage (see text).

occurred in the deepest intervals (>12.8 m) and nearly equivalent losses have occurred in all of the intervals. Somewhat less water volume has been lost from the intervals between 0.9 and 11.0 m. The intertidal water volume loss again can not be estimated from these numbers, but based on Thomas' (1983) figures it is apparent that a substantial loss in water volume has occurred in the shallow regions of the estuary.

The net effect of the area changes in the estuary have been to reduce the total area of the estuary, while shifting a larger percentage of the estuary area and water volume into deeper water. Both the total volume of the estuary and the intertidal volume of the estuary have been substantially decreased by the changes in the distribution of area among the depth regimes. One effect of the area loss has been to reduce the tidal prism significantly in historical time. A 12% loss of deep water area, coupled with additional changes in the intertidal areas (Thomas 1983), has resulted in a 10-15% reduction of the tidal prism of the estuary.

C.3.4 Volume Changes and Sedimentation Estimates

The digitized bathymetric data were used to directly calculate the volume changes in each of the subareas between the surveys. These calculations are not subject to the same kinds of errors discussed relative to the area calculations because only overlapping areas from consecutive surveys were used in the calculations. Thus, although volume differences were not computed for all of the area of the estuary among all of the surveys, those numbers that were calculated contain no particular biases. The subareas which do not overlap exactly between surveys are marked with a (-) on Figure 74: the entrance, the South Channel, and Youngs Bay. As discussed in the first part of the preceding section, the areas omitted from subsequent surveys were often newly developed land, so it is reasonable to assume that the figures generally underestimate shoaling in the estuary. The lumping of all elevations greater than 2.1 m (7 ft) above MLLW probably also serves to produce underestimates of the amount of shoaling. Furthermore, shoaling rates are calculated on the basis of the entire surveyed area in the individual subareas, rather than just the intertidal area, again underestimating the rate of shoaling. Therefore, these calculations are conservative estimates of the amount of sedimentation that has occurred in the estuary during historical time.

Table 34 presents the water volumes of the individual subareas for each of the three survey periods. These are the water volumes calculated as the product of the depth interval midpoint and the area, and they include the inherent limitations discussed in the last section. The volume changes based on these numbers are tabulated in the

successive columns, alternating with the estimates of shoaling calculated from the bathymetric differencing. Ideally, the changes in water volume and the volume of sediment accumulation or loss should be of equal magnitude and opposite sign. Except for the areas marked with an asterisk (*), which have survey coverage inconsistencies that have been discussed, there is reasonable agreement between the two methods of estimating the amount of shoaling in the estuary. The shoaling estimates based on the water volume changes are considered less reliable due to the overestimate of volume, especially in deep water, and the remainder of this discussion will focus on the sedimentation estimates derived from the differencing technique.

The largest volume change in sediments occurred in the entrance between 1868 and 1935, following jetty construction. Nearly 312 million m^3 of sediment was lost during this period, and another 34 million m^3 was lost in the subsequent period. However, the adjacent subareas of Trestle Bay and Baker Bay showed large gains during the early period; Trestle Bay showed an increase of 9 million m^3 and Baker Bay an increase of 91 million m^3. In the rest of the lower estuary, Desdemona Sands showed an increase of 46 million m^3 of sediment, while the North and South Channels exhibited a sediment loss of 3 and 10 million m^3, respectively. Youngs Bay gained approximately 31 million m^3, but overall, the losses in the entrance and the lower estuary exceeded the gains by nearly 50 million m^3. However, gains in the upper estuary, notably Grays Bay (23 million m^3) and Cathlamet Bay (49 million m^3), were more than sufficient to offset the loss in the lower estuary, and the system as a whole gained 43 million m^3. If the losses in the entrance region are ignored, over 256 million m^3 of sediment accumulated in the estuary.

In the subsequent period (1935 to 1958) the changes are less dramatic but nonetheless quite significant. Again, large losses of sediment occurred in the entrance region (34 million m^3). Slight losses occurred in the previously depositional subarea of Baker Bay and continued in the North Channel. Trestle Bay remained depositional, and substantial accumulation occurred on Desdemona Sands (13 million m^3). The South Channel became depositional, gaining nearly 18 million m^3. Cathlamet Bay remained depositional and accumulated 27 million m^3 of sediment. The system as a whole gained 25 million m^3; neglecting the losses at the entrance, the estuary gained 59 million m^3.

Over the 90-year period, net deposition in the entire system amounted to 68 million m^3; losses in the entrance region amounted to 247 million m^3; therefore, the accumulation in the estuary (neglecting the entrance) totaled 315 million m^3.

The normalized area of the various subareas has been used to calculate the rate of sediment deposition or erosion. The values appear in Tables 35 and Figures 80a, 80b, and 80c as shoaling rates in cm yr^{-1} and are presented for the periods between each of the two surveys and for the entire 90-year period. Shoaling rates vary from a maximum of 3.33 cm yr^{-1} (Trestle Bay between 1935 and 1958) to -1.84 cm yr^{-1} (erosion in the entrance between 1868 and 1935). The highest rate of accumulation over the 90-year period also occurred in Trestle Bay (2.43 cm yr^{-1}) and the highest erosion rate occurred in the entrance (-1.59 cm yr^{-1}). The averages do not depend greatly on whether the 1868 area for each of the subareas or the 1958 values are used (compare in Table 36). The grand average for the entire system is a shoaling rate of 0.08 cm yr^{-1}; when the erosion at the entrance is ignored, the average shoaling rate for the remainder of the estuary becomes 0.49 cm yr^{-1}.

C.4 LONG-TERM SHOALING PATTERNS AND THE SEDIMENT BUDGET

C.4.1 Sediment Budget

Some evidence regarding the historical shoaling patterns in the estuary can be derived from further examination of Table 34. The net accumulation in the system has totaled approximately 68 million m^3 since 1868. When adjusted for the loss of 247 million m^3 that occurred in the entrance region, it becomes clear that 315 million m^3 of sediment accumulated in the estuary proper in the 90-year period, an annual rate of 3.5 million m^3. However, several lines of evidence suggest that not all of this 315 million m^3 was derived from the fluvial supply. The history of change at the entrance, as related by Hickson (1922, 1930), Lockett (1963, 1967), the bathymetric differencing maps produced by Northwest Cartography, Inc. (CREDDP 1983), and sedimentological evidence (Borgeld et al. 1978; Walter et al. 1979; Roy et al. 1979, 1982) all suggest that much of the accumulation on Desdemona Sands, Baker Bay, and Trestle Bay is related to the displacement of sediment from the natural tidal delta as a result of the construction of the entrance jetties. Scouring of the entrance channel by the constrained tidal currents has transported sediment both offshore and into the estuary. Whereas the inner and outer tidal deltas were relatively close to each other in 1868, they are now separated by several miles of deep channel and by the spits formed around the jetties. The inner tidal delta in 1868 was a distinct, if dynamic, feature consisting of intertidal islands (the old Sand Islands) or shoals. The modern inner tidal delta has been forced further into the estuary and is no longer a distinct feature. The sandy sediment that made up the 1868 inner tidal delta is now found in the modern Sand Islands, Baker Bay, and Desdemona Sands.

Table 35

Shoaling rates

Estuary subarea	1958 area (10^6 m^2)	Shoaling (cm/yr) 1868-1935	1935-1958	1868-1958	1868 area (10^6 m^2)	Shoaling (cm/yr) 1868-1935	1935-1958	1868-1958
1 Entrance	-172.45	-1.84	-0.98	-1.59	212.33	-1.50	-0.80	-1.29
2 Baker Bay	-59.69	2.27	-0.40	1.60	59.69	2.27	-0.40	1.60
3 Trestle Bay	5.94	2.27	3.33	2.43	5.94	2.27	3.33	2.43
4 North Channel	33.19	-0.15	-0.85	-0.30	33.19	-0.15	-0.85	-0.30
5 South Channel	69.07	-0.22	1.28	0.12	70.75	-0.21	1.25	0.12
6 Youngs Bay	40.07	1.17	0.48	0.98	52.96	0.89	0.37	0.74
7 Desdemona Sands	34.35	2.00	1.88	1.90	34.35	2.00	1.88	1.90
8 Mid-estuary Shoals	27.17	0.07	-0.05	0.04	27.17	0.07	-0.05	0.04
9 Grays Bay	33.49	1.03	-0.60	0.63	33.49	1.03	-0.60	0.63
10 Brix Bay	44.07	0.21	-0.07	0.14	44.07	0.21	-0.07	0.14
11 Cathlamet Bay	143.00	0.51	0.94	0.59	143.00	0.51	0.94	0.59
12 Lower River Channel	29.71	-0.36	0.15	-0.23	29.71	-0.36	0.15	-0.23
13 Upper River Channel	175.59	0.16	0.23	0.17	175.59	0.16	0.23	0.17
	Area Totals	Average shoaling rates (unweighted)			Area Totals	Average shoaling rates (unweighted)		
Estuary w/o entrance	695.34	0.75	0.53	0.67	709.91	0.72	0.52	0.65
Estuary total	867.79	0.55	0.41	0.50	922.24	0.55	0.41	0.50

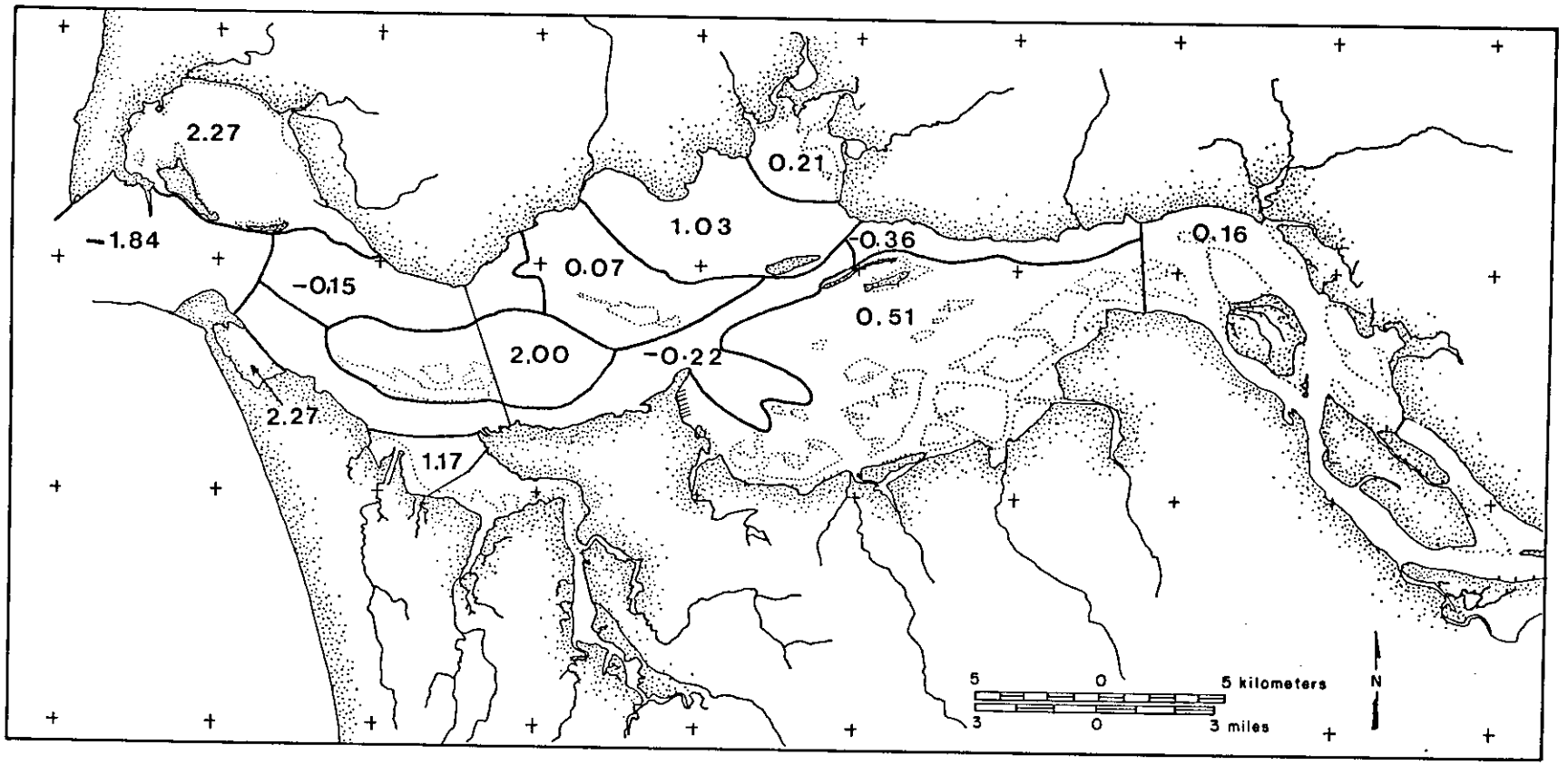

Figure 80a. Map of the Columbia River Estuary showing the rates of shoaling (+) or erosion (-) (cm/yr) in each of the 13 subareas for 1868-1935.

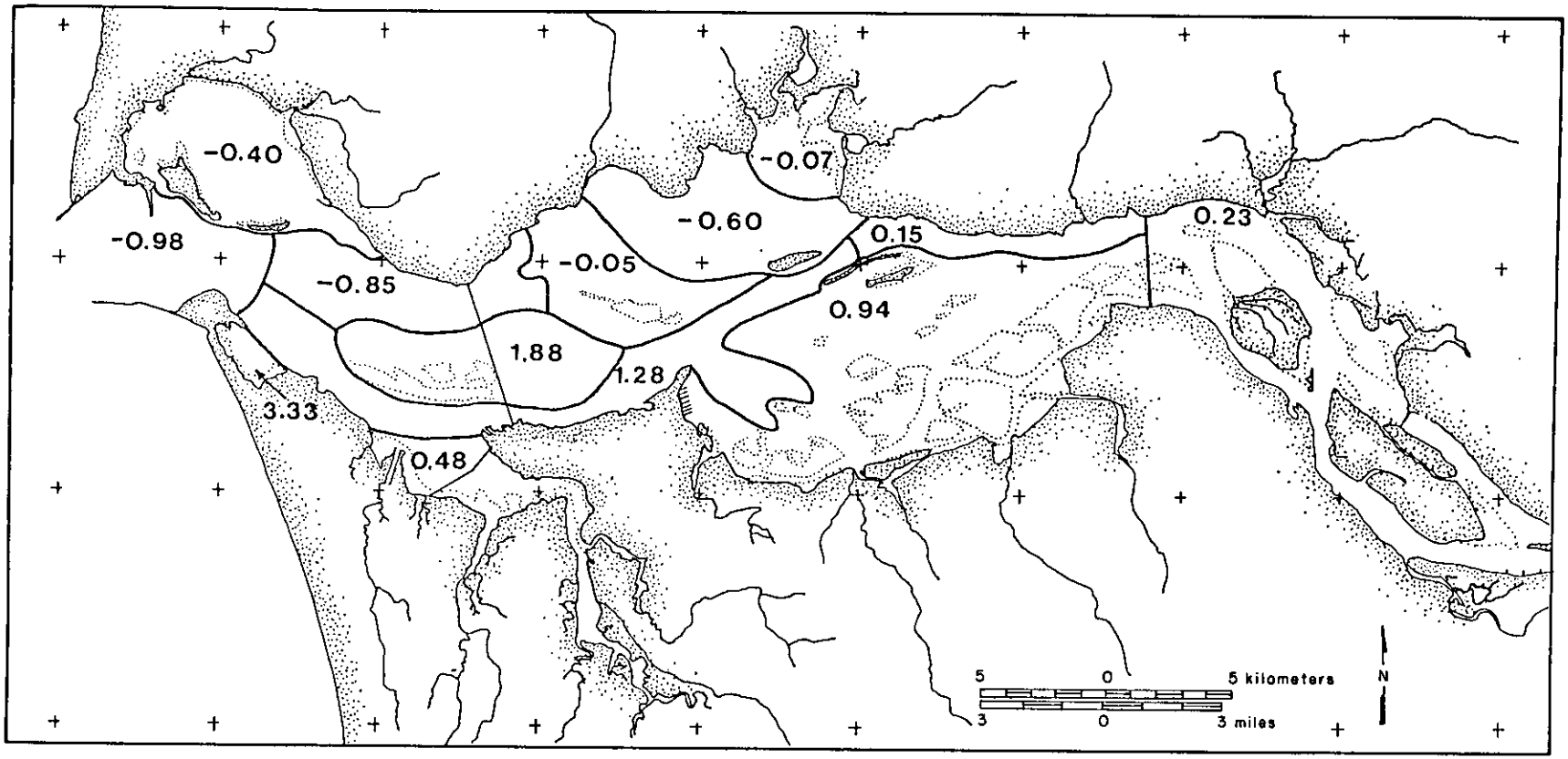

Figure 80b. Map of the Columbia River Estuary showing the rates of shoaling (+) or erosion (-) (cm/yr) in each of the 13 subareas for 1935-1958.

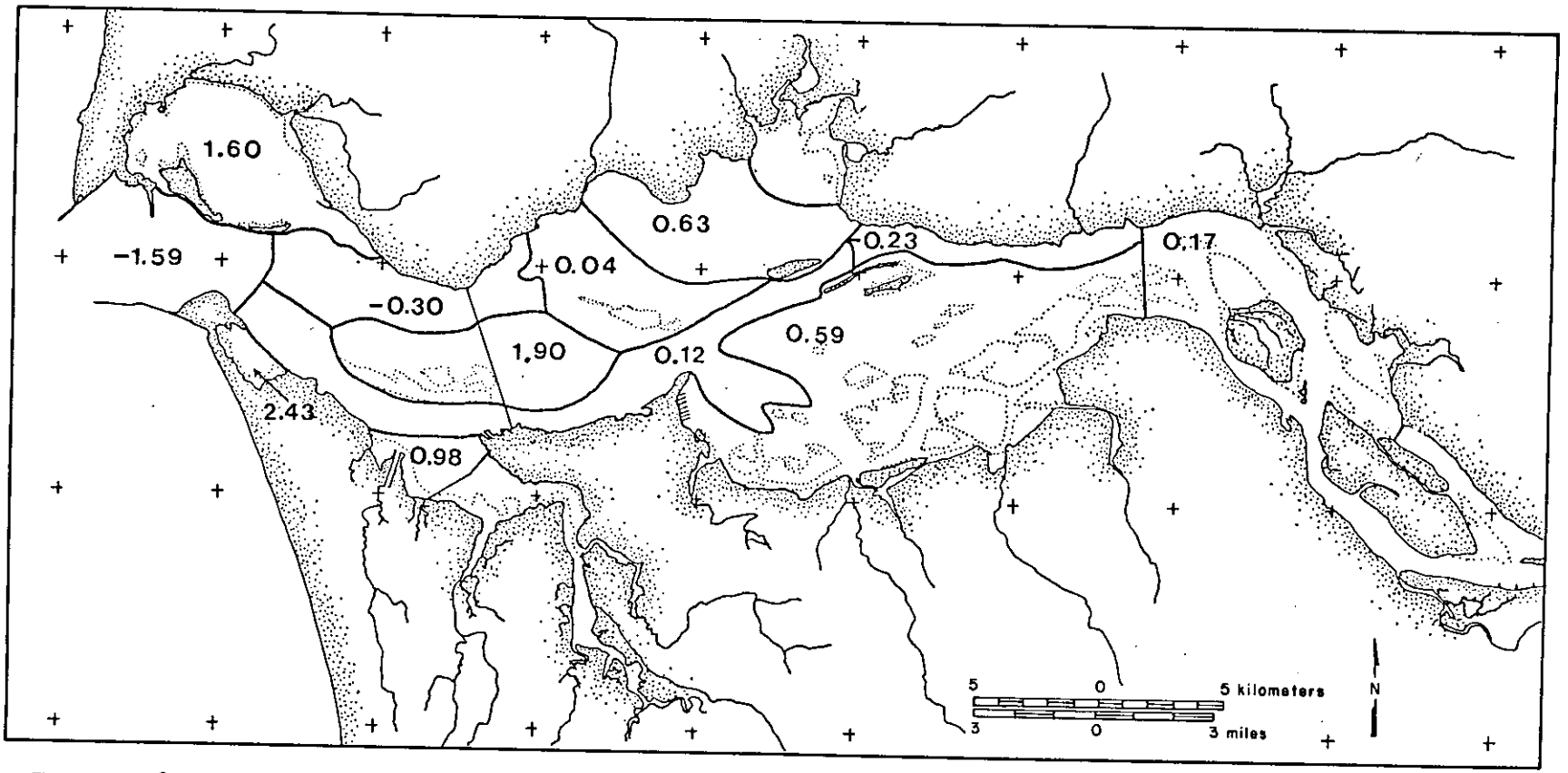

Figure 80c. Map of the Columbia River Estuary showing the rates of shoaling (+) or erosion (-) (cm yr^{-1}) in each of the 13 subareas for the entire period (1868-1958). Rates are normalized by the 1958 area.

In accordance with this scenario, sandy sediments deposited in the lower estuary, including Trestle Bay, Baker Bay, Desdemona Sands, and the North and South Channels, account for slighty more than half of the sediment lost from the entrance region (157 million m^3). The remainder of the 247 million m^3 lost from the entrance region (90 million m^3) has been either deposited on Clatsop or Peacock spits or has been lost entirely from the system. The portion that was lost from the system has been either pushed farther offshore or carried along the coast with the littoral drift. The patterns of erosion and deposition in the entrance region, discussed in Lockett (1963) and evident in the Bathymetric Atlas (CREDDP 1983) suggest that much of the displaced sediment has in fact moved seaward and north. This direction is consistent with studies of shelf sediment transport on the Oregon and Washington shelves and with the flux of winter wave energy. One possible implication is that the erosion of the outer tidal delta (since jetty construction was initiated in 1885) has provided sediment for the littoral drift system north of the Columbia River in unusually large quantities. In effect, a large pulse of sediment may have been introduced to the Washington beaches by jetty construction. The effects of the pulse, which may have been seen as beach accretion along Long Beach and sedimentation in Willapa Bay, may now be wearing off, and future littoral supply from the Columbia River will be dependent on the amount of bedload escaping from the mouth.

The 157 million m^3 that was deposited in the lower estuary accounts for half of the 315 million m^3 that accumulated in the estuary in the 90-year period. The remaining 158 million m^3 must represent the contribution from fluvial sources at an apparent rate of 1.76 million m^3/year. Using the accepted estimate of a total load amounting to 10 million metric tons yr^{-1} for the Columbia River (Whetten et al. 1969) and assuming that sediment deposits in the estuary have a porosity of 40% and a sediment density of 2.65 gm/cm^3, there is an annual sediment supply of 6.3 million m^3/year. If all of the bedload material is trapped in the estuary (10% of the total load, or 0.63 million m^3/year), 20% of the remaining supended load (1.13 million m^3/year) must also be deposited in the estuary to balance the sedimentation rate with the supply. The correctness of this estimate is subject to the correctness of the bedload supply estimate; it could be either high or low. However, even if no bedload was trapped in the estuary, an upper limit of 30% of the fine sediment could be retained. Clearly, most of the fine sediment escapes to the ocean. Our estimate of 20% retention of the fine sediment in the estuary is slightly lower than the value of approximately 30% retention calculated by Hubbell and Glenn (1973).

These budget estimates may be used to emphasize the

potential importance of infrequent catastrophic effects such as volcanic eruptions. Estimates of the volume of sediment in the mudflows from the May 18, 1980, eruption of Mt. St. Helens that reached the confluence of the Cowlitz and Toutle rivers approach 100 million m^3 (Fairchild and Wigmosta 1983). As much as 34 million m^3 of this sediment accumulated in the Columbia River adjacent to the mouth of the Cowlitz River (Schuster 1981). The Corps of Engineers has since removed more than 11.5 million m^3 of sediment from this reach, but the Cowlitz River continues to contribute 5 million tons of sediment to the Columbia River each year (Schuster 1981; Dunne and Leopold 1981). The amount of this sediment that has reached or will reach the estuary is unknown; much less will arrive, because of the land disposal of dredged material, than would have reached the estuary from an eruption 100 years ago. However, the magnitude of sediment involved clearly suggests that a few comparable eruptions over long periods of time would have a profound effect on the sediment budget of the estuary.

The major spring freshets that have been eliminated by flow regulation carried large total loads and may also have been of considerable importance to the sediment budget. U.S. Geological Survey data for 1963 to 1970 (summarized in Good and Jay 1978) show average, annual suspended load at Vancouver ranging from 4 to 28 million metric tons yr^{-1}, with the spring freshet of 1965 carrying 12 million metric tons and a winter freshet the same year carrying about 8 million tons. None of these freshets were truly major; much larger freshets occurred before 1963, e.g., in 1894 and 1948.

While the historical calculations show that most of the suspended sediment carried by such freshets was lost to the ocean, the effects of major floods on the bedload are harder to analyze. It is reasonable to suppose that large pulses of bedload were brought into the estuary by the major freshets (e.g., see Hickson 1930). It is improbable that even the largest freshets would have resulted in more transport of bedload out of the mouth of the estuary than entered from the river. Thus the larger freshets of the 1868-1958 period may have had a substantial impact on the total accumulation. Significant regulation of flow (post-1969) is too recent to be evaluated by the historical methodology, and we do not know whether the estuarine shoaling rate has been altered by elimination of large freshets. Further evaluation of historical data is required.

C.4.2 Equilibrium

The results presented in Section C.3 may be used to suggest that the estuary has not reached an equilibirum. Average shoaling rates and the hypothetical time required to

Table 36

Comparison of shoaling rates and estimated time required to fill the estuary

Average shoaling rates based on 1868 estuary area (cm yr^{-1})

	1868-1935	1935-1958	1868-1958
Excluding entrance	0.54	0.36	0.49
Total	0.07	0.12	0.08

Average shoaling rates based on 1958 estuary area (cm yr^{-1})

	1868-1935	1935-1958	1868-1958
Excluding entrance	0.55	0.37	0.50
Total	0.21	0.13	0.09

Estimated time (years) to fill the estuary, based on volume below MLLW in 1958 and above rates (1868/1958)

Excluding entrance	800	(average depth: ~4 m)
Total	7,778	(average depth: ~7 m)

fill the estuary at those rates are presented in Table 36. These estimates suggest that only 800 years would be required to fill the estuary entirely at the present rate. Because sea level reached its present height between 3,000 and 5,000 years ago, and the estuary is clearly still filling, it appears that the recent rate of 0.5 cm yr^{-1} is abnormally high for the Columbia River Estuary. This may be used as circumstantial evidence to suggest that the changes that have occurred in historical time have caused relatively rapid shoaling, compared to longer-term and more natural shoaling rates.